Targeting Androgen Receptor Splicing in Lethal Prostate Cancer

March 2021

Alec Kyriacos Paschalis

Division of Cancer Therapeutics

The Institute of Cancer Research

Thesis submitted to The University of London for the Degree of

Doctor of Philosophy

Declaration

I, Alec Kyriacos Paschalis, confirm that the work presented in this thesis has been performed by me unless otherwise stated in the relevant sections.

Alec Kyriacos Paschalis

Acknowledgements

First and foremost, I would like to thank Professor Johann S. de Bono, who supervised this project. I will always be grateful to him for giving me the opportunity to be a part of his enthusiastic team which has improved the care provided to men with lethal prostate cancer all over the world. I am privileged to have received his mentorship, and I am grateful for his ongoing support. Most of all, I am thankful for the time and advice he has given me over the past few years, which have been instrumental in both the completion of this thesis, and my development as a clinician-scientist. I would also like to thank the entire Cancer Biomarkers Team for making me feel so welcome during my time with the group, and for their help in the completion of this work, particularly Ines Figueiredo and Dr Wei Yuan. I am, however, especially grateful to Dr Adam Sharp, Dr Jon Welti, and Dr Antje Neeb who have all provided me with support and friendship throughout the duration of this project.

Importantly, this project has afforded me the opportunity to develop new collaborations with world-leading experts, and I would like to sincerely thank Professor Stephen Plymate (University of Washington) and Professor Christopher Schofield (University of Oxford) for their continuing and invaluable advice and guidance.

This work was supported by Cancer Research UK, and I would like to thank them and all their donors, for supporting my career and our research.

Finally, I would like to thank my family. To my mother and father, who have always been my strongest supporters, without you I would not be where I am today. To my wife, Mariana, without your unwavering love and support, none of this would have been possible. Thank you so much. And to my daughter, Lucia, who was born during my time at the Institute of Cancer Research, this, and everything I do, is for you.

Abstract

Over the past decade, androgen receptor (AR) directed therapies such as abiraterone and enzalutamide have become the standard of care for treating advanced prostate cancer, improving both progression-free and overall survival. Some patients, however, never respond to these agents, while all eventually acquire resistance, leading to invariably fatal disease progression. This resistance is in part due to the development of constitutively active alternatively spliced variants of the AR (AR-SVs) that are truncated and lack the regulatory AR ligand-binding domain; the target of current AR directed therapies. Of the many AR-SVs that have been reported, AR splice variant 7 (AR-V7) is the most prevalent and the best studied, and has been associated with resistance to AR targeting therapies and poorer overall survival.

In this thesis, I describe my work focused on identifying proteins that are key to the production of AR-V7, validate my findings using clinical samples and study splicing regulatory mechanisms in *in vitro* models of lethal prostate cancer. Through orthogonal studies I identify the 2-oxoglutarate-dependent dioxygenase JMJD6 as a key regulator of AR-V7, as evidenced by its: 1) upregulation with *in vitro* androgen-deprivation-resistance; 2) downregulation alongside AR-V7 by BET inhibition; 3) being the top hit of a targeted siRNA screen of spliceosome related genes. Furthermore, I demonstrate that JMJD6 protein levels increase significantly with castration-resistance *($p<0.001$)* and are associated with both higher levels of AR-V7 *($p=0.036$),* and shorter median survival from castration-resistant prostate cancer *($p=0.048$)*. *In vitro*, I show that JMJD6 knockdown reduces prostate cancer cell growth, AR-V7 levels, and recruitment of the splicing regulatory factor U2AF65 to AR pre-mRNA. Importantly, my mutagenesis studies indicate that JMJD6 enzymatic activity is key to JMJD6-mediated AR-V7 generation, with the JMJD6 catalytic machinery residing within a druggable pocket. Taken together, I conclude that JMJD6 is a druggable target for treating advanced prostate cancer.

Awards and Publications (2017 – 2020)

Awards

2019 Nizar M. Tannir, MD, Endowed Conquer Cancer ASCO Merit Award

2019 Institute of Cancer Research PhD Student Prize

Peer Reviewed Publications

- SG Ramanand, Y Chen, J Yuan, K Daescu, M Lambros, KE Houlahan, S Carreira, W Yuan, G Baek, A Sharp, A Paschalis, M Kanchwala, Y Gao, A Aslam, N Safdar, X Zhan, G Raj, C Xing, P Boutros, J de Bono, MQ Zhang, and R Mani. **The landscape of RNA polymerase II associated chromatin interactions in prostate cancer.** *J Clin Invest. 2020 Apr 28.*

- A Paschalis, B Sheehan, R Riisnaes, DN Rodrigues, B Gurel, C Bertan, A Ferreira, MBK Lambros, G Seed, W Yuan, D Dolling, JC Welti, A Neeb, S Sumanasuriya, P Rescigno, D Bianchini, N Tunariu, S Carreira, A Sharp, W Oyen, JS de Bono. **Prostate-specific Membrane Antigen Heterogeneity and DNA Repair Defects in Prostate Cancer.** *Eur Urol. 2019 Oct; 76(4): 469–478.*

- A Sharp, N Porta, MBK Lambros, JC Welti, A Paschalis, GV Raj, SP Plymate, JS de Bono. **Dissecting Prognostic From Predictive Utility: Circulating AR-V7 Biomarker Testing for Advanced Prostate Cancer.** *J Clin Oncol. 2019 Aug 20;37(24):2182-2184.*

- Z Zafeiriou, D Bianchini, R Chandler, P Rescigno, W Yuan, S Carreira, M Barrero, A Petremolo, S Miranda, R Riisnaes, DN Rodrigues, B Gurel, S Sumanasuriy, A Paschalis, A Sharp, J Mateo, N Tunariua, AM Chinnaiyan, CC Pritchard, K Kelly, and JS de Bono. **Genomic Analysis of Three Metastatic Prostate Cancer Patients with Exceptional Responses to Carboplatin Indicating Different Types of DNA Repair Deficiency.** *Eur Urol. 2019 Jan; 75(1): 184–192.*

- A Sharp, J Welti, MBK Lambros, D Dolling, DN Rodrigues, L Pope, C Aversa, I Figueiredo, J Fraser, Z Ahmad, C Lu, P Rescigno, M Kolinsky, C Bertan, G Seed, R Riisnaes, S Miranda, M Crespo, R Pereira, A Ferreira, G Fowler, B Ebbs, P Flohr, A Neeb, D Bianchini, A Petremolo, S Sumanasuriya, A Paschalis A, J Mateo, N Tunariu, W Yuan, S Carreira, SR Plymate, J Luo, JS de Bono. **Clinical Utility of Circulating Tumour Cell Androgen Receptor Splice Variant-7 Status in Metastatic Castration-resistant Prostate Cancer.** *Eur Urol. 2019 Apr 27.*

- A Paschalis, A Sharp, JC Welti, A Neeb, GV Raj, J Luo, SR Plymate, JS de Bono. **Alternative splicing in prostate cancer.** *Nat Rev Clin Oncol. 2018 Nov;15(11):663-675*

- J Welti, A Sharp, W Yuan, D Dolling, D.N Rodrigues, I Figueiredo, V Gil, A Neeb, M Clarke, G Seed, M Crespo, S Sumanasuriya, J Ning, E Knight, J Francis, A Hughes, W Halsey, A Paschalis, R Mani, G Raj, S Plymate, S Carreira, G Boysen, A Chinnaiyan, A Swain and JS de Bono. **Targeting bromodomain and extra-terminal (BET) family proteins in castration resistant prostate cancer (CRPC).** *Clin Cancer Res. 2018 Mar 19.*

Table of Contents

List of Figures

List of Tables

Abbreviation List

2, 4-PDCA	Pyridine-2,4-dicarboxylic Acid
2OG	2-oxoglutarate
ADC	Antibody-drug Conjugates
ADT	Androgen Deprivation Therapy
AF-1	Activation Function 1
AKT	AKT Serine/Threonine Kinase
AR	Androgen Receptor
AR-FL	Full-Length Androgen Receptor
AR-SV	Androgen Receptor Splice Variant
AR-V7	Androgen Receptor Splice Variant 7
AR-V9	Androgen Receptor Splice Variant 9
ARE	Androgen Response Element
ARID1A	AT-Rich Interaction Domain 1A
ARID2	AT-Rich Interaction Domain 2
ARID4A	AT-Rich Interaction Domain 4A
ATM	Ataxia Telangiectasia Mutated
BAG-1L	BCL-2-associated-athanogene-1L
BBC3	BCL2 Binding Component 3
BD2	Second Bromodomain of BET Protein
BET	Bromodomain and Extra-terminal
BRCA1	BRCA1 DNA Repair Associated
BRCA2	BRCA2 DNA Repair Associated
CBP	CREB-binding Protein
CCND1	Cyclin D1
cDNA	Copy DNA
CHEK2	Checkpoint Kinase 2
CHiP	chromatin immunoprecipitation
CRPC	Castration-Resistant Prostate Cancer
CSPC	Castration-Sensitive Prostate Cancer
CT	Computer Tomography
CTC	Circulating Tumour Cell
CXCR7	Atypical Chemokine Receptor 3
DBD	DNA Binding Domain
DHT	Dihydrotestosterone
DMEM	Dulbecco's Modified Eagle's Medium (DMEM)
DMSO	Dimethyl Sulfoxide

DNMT1	DNA Methyltransferase 1
DSBH	Double-Stranded b-Helix
ECL	Enhanced Chemiluminescence
EDTA	Ethylenediaminetetraacetic Acid
EPP	Erythropoietic Protoporphyria
ERK	Extracellular Signal-Regulated Kinase
ESI	Electrospray Ionisation
ETS	E26 Transformation-specific
EZH2	Enhancer Of Zeste 2 Polycomb Repressive Complex 2 Subunit
FAS	Ferrous Ammonium Sulphate
FBS	Foetal Bovine Serum
FECH	Ferrochelatase
FFPE	Formalin-fixed, Paraffin Embedded
FGF	Fibroblast Growth Factor
FGF8	Fibroblast Growth Factor 8
FGFR2	Fibroblast Growth Factor-2 Receptor
FLT1	Fms Related Receptor Tyrosine Kinase 1
FPKM	Fragments Per Kilobase of Transcript per Million Mapped Reads
GO	Gene Ontology
GSEA	Gene Set Enrichment Analyses
GSK3b	Glycogen Dynthase Kinase 3 Beta
H-Score	Modified Histochemical Score
HER2	erb-B2 Receptor Tyrosine Kinase 2
HERPUD1	Homocysteine Inducible ER Protein With Ubiquitin Like Domain 1
HIF1a	Hypoxia Inducible Factor 1-Alpha
hnRNP	Heterogeneous Nuclear Ribonuclear Protein
hnRNPA1	Heterogeneous Nuclear Ribonucleoprotein A1
hnRNPA2	Heterogeneous Nuclear Ribonucleoprotein A2
HNRNPF	Heterogeneous Nuclear Ribonucleoprotein F
HOTAIR	HOX Transcript Antisense Intergenic RNA
HSP	Heat Shock Protein
HSP27	Heat Shock Protein 27
HSP90	Heat Shock Protein 90
IGF	Insulin-like Growth Factor
IHC	Immunohistochemistry
JmjC	Jumonji C
KDM	Lysine Demethylase
KDM3A	Lysine Demethylase 3A
KDM4B	Lysine Demethylase 4B
KHDRBS1	KH RNA Binding Domain Containing, Signal Transduction Associated 1

KHDRBS1	KH domain-containing, RNA-binding, signal transduction-associated protein 1
KLF6	Kruppel-like Factor 6
KLF6SV1	KLF6 Splice Variant 1
LB	Luria-Bertani
LBD	Ligand Binding Domain
LC-MS	Liquid Chromatography Mass Spectrometry
LHRH	Luteinizing-Hormone-Releasing Hormone
LSD1	Lysine Demethylase 1A
LUC7L2	LUC7 Like 2, Pre-MRNA Splicing Factor
MALDI	Matrix-assisted Laser Desorption/Ionization
MAPK	Mitogen-activated Protein Kinase
miRNA	MicroRNA
MMP7	Matrix Metallopeptidase 7
MOPS	3-(N-morpholino)propanesulfonic Acid
MRI	Magnetic Resonance Imaging
MS	Mass Spectroscopy
MSidDB	Molecular Signatures Database
mTOR	Mammalian Target of Rapamycin
MYC	MYC Proto-Oncogene
NDRG1	N-Myc Downstream Regulated 1
NE	Neuroendocrine
NEPC	Neuroendocrine Prostate Cancer
NES	Nuclear Export Signal
NK-kB	Nuclear Factor-Kappa Beta
NLS	Nuclear Localisation Sequence
NMC	NUT-midline Carcinoma
NOVA	Neuro-oncological Ventral Antigen
NP-40	Nonidet P-40
NSCLC	Non-Small Cell Lung Cancer
NTD	N-terminal Transcriptional Domain
P-TEFb	Positive Transcription Elongation Factor Beta
p53	Tumour Protein p53
PAK1	Serine/threonine-protein Kinase
PAK4	p21 (RAC1) Activated Kinase 4
PARP	Poly (ADP-ribose) Polymerase
PBS	Phosphate Buffered Saline (PBS)
PCHD10	Protocadherin 10
PD	Pharmacodynamics
PET	Positron Emission Tomography
PI3K	Phosphoinositide 3-kinase

PIN	Prostate Intraepithelial Neoplasia
PK	Pharmacokinetics
Pol II	RNA Polymerase II
PolyS	Poly-serine
PSA	Prostate Specific Antigen
PSMA	Prostate-specific Membrane Antigen
PSR	Phosphatidylserine Receptor
PTEN	Phosphatase and Tensin Homolog
Q-TOF	Mass Quadrupole Time of Flight Mass Spectrometer
QC	Quality Control
qPCR	Quantitative Polymerase Chain Reaction
RB1	Retinoblastoma Protein 1
REST	RE1-silencing
RIP	RNA Immunoprecipitation
RMH	Royal Marsden Hospital
RNA-seq	RNA Sequencing
RPMI-1640	Roswell Park Memorial Institute 1640 Medium (RPMI-1640)
SCC	Small Cell Carcinoma
SDH	Succinate Dehydrogenase
SDS	Sodium Dodecyl Sulphate
SF1	Splicing Factor 1
SF3B1	Splicing Factor 3B Subunit 1
SF3B3	Splicing Factor 3b Subunit 3
SFSR3	Serine/arginine Rich Splicing Factor 3
shRNA	Short Hairpin RNA
siRNA	Small Interfering RNA
SMARCA1	SWI/SNF Related, Matrix Associated, Actin Dependent Regulator Of Chromatin, Subfamily A, Member 1
snRNA	Small Nuclear Ribonucleic Acids
snRNP	Small Nuclear Ribonucleoproteins
SOX2	SRY-Box Transcription Factor 2
SR	Serine-rich and/or Arginine-rich
SRE	Splicing Regulatory Element
SRRM4	Serine/arginine Repetitive Matrix Protein 4
SRSF1	Serine/arginine-rich Splicing Factor 1
SRSF2	SR Splicing Factor 2
SRSF5	Serine/arginine rich splicing factor 5
SRSF7	Serine/arginine rich splicing factor 7
SU2C/PCF	International Stand Up To Cancer/Prostate Cancer Foundation
SWI/SNF	Switch/sucrose Non-fermentable
SYP	Synaptophysin

Tau5	Transcription Activation Unit 5
TBS	10X Tris-Buffered Saline (TBS)
TBST	1X Tris-Buffered Saline, 0.1% Tween® 20 Detergent (TBST)
TCA cycle	The Citric Acid Cycle
TCF/LEF-1	T-Cell Factor/Lymphoid Enhancer Factor-1
TET1	Ten-eleven Translocation Methylcytosine Dioxygenase 1
TET2	Tet Methylcytosine Dioxygenase 2
TMPRSS2	Transmembrane Serine Protease 2
TWIST1	Twist Family bHLH Transcription Factor 1
U2AF1 (U2AF35)	U2 Auxiliary Factor 35 kDa subunit
U2AF65	U2 Auxiliary Factor 65 kDa subunit
UBE2C	Ubiquitin Conjugating Enzyme E2 C
UTR	Untranslated Region
V/V	% volume per volume
VEGF	Vascular Endothelial Growth Factor
VEGFR1	Vascular Endothelial Cell Growth Factor Receptor 1
VHL	Von Hippel-Lindau Tumour Suppressor
W/V	% weight per volume
WT	Wild-Type
ZRSR2	Zinc Finger CCCH-Type, RNA Binding Motif And Serine/Arginine Rich 2
β-TrCP	Beta-Transducin Repeats-Containing Protein

1

Introduction

Prostate cancer is the second most frequent malignancy in men worldwide [1], and is the second most common cause of male cancer death in the United Kingdom [2]. Since the pioneering work of Charles Huggins and Clarence Hodges, who first demonstrated the benefits of androgen deprivation therapy (ADT) in patients with metastatic prostate cancer [3], our understanding of its pathogenesis has increased substantially, particularly with regards to the fundamental importance of the androgen receptor (AR) in all stages of disease from tumorigenesis, to progression and ultimately treatment resistance and death [4, 5].

1.1 The androgen receptor and prostate cancer

The AR is a ligand-activated transcription factor that plays a central role in male sexual development. It is a member of the steroid and nuclear hormone receptor super-family and is encoded by the AR gene located on chromosome Xq12 [6], the transcriptional activity of which is modulated by its interactions with potentially more than 200 different transcriptional co-regulators [7]. In prostate cancer, in addition to these regulators, genomic aberrations such as AR copy number gains, mutations and rearrangements are also thought to have a major role in AR gene expression with AR overexpression, in particular, being key to the development and progression of castration-resistant prostate cancer (CRPC) [8].

The structure of the full-length product of AR transcription was first reported in 1988 [9, 10] and has a molecular weight of 110 kDa. The AR is comprised of four discrete functional domains ***(figure 1.1)*** namely, an N-terminal transcriptional domain (NTD) which is highly variable and inherently disordered [6], a DNA binding domain (DBD) which consists of a highly conserved 66-residue core made up of two zinc-nucleated modules [11], a hinge region and a carboxy-terminal ligand-binding domain (LBD) [12]. Of note, while the carboxy terminus and DBD have been crystallised, the crystal structure of the amino terminus remains elusive, hindering the development of amino-terminal-targeted agents.

In the absence of activating ligands, the AR is sequestered within the cytoplasm by a complex of heat shock protein (HSP) chaperones [13] and their co-chaperones such as BCL-2-associated-athanogene-1L (BAG-1L). In the presence of circulating androgens, namely dihydrotestosterone (DHT), and to a lesser degree, testosterone, the AR undergoes conformational change [12] and dimerises with other ligand-bound AR subunits to form homodimers. The nuclear localisation of the AR is dependent on the AR bipartite nuclear localisation sequence (NLS), which is highly conserved between many nuclear receptors and contains two clusters of basic amino acids [14]. The NLS is recognised by the transport adaptor proteins importin-α and importin-β, which regulate the shuttling of the AR homodimers into the cell nucleus. The NLS is also recognised and bound by dynein, a motor protein that

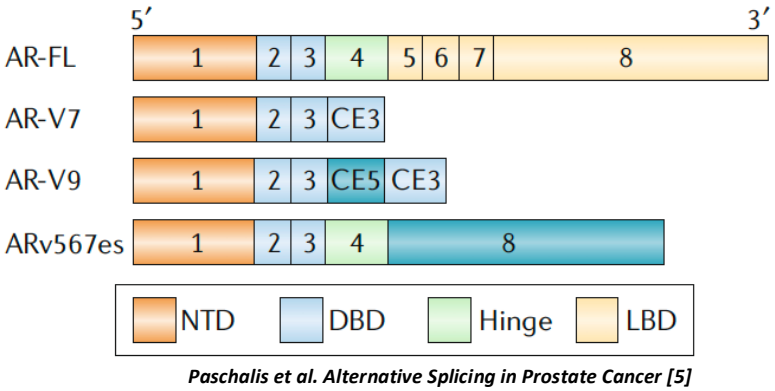

Paschalis et al. Alternative Splicing in Prostate Cancer [5]

Figure 1.1: AR splice variants. A schematic diagram depicting the full-length androgen receptor (AR-FL) alongside a selection of its truncated protein isoforms, the androgen receptor (AR) splice variants (AR-SVs) AR-V7, AR-V9, and ARv567es. These proteins share identical amino-terminal domains (NTDs) and DNA-binding domains (DBDs) but have unique carboxy-terminal extensions. AR-V7 and AR-V9 have a common 3'-terminal cryptic exon (CE), while ARv567es has a complete hinge region and nuclear localization signal, similar to that of the full-length protein, but lacks a ligand-binding domain (LBD).

interacts with cellular microtubules to enhance AR nuclear translocation via a cytoskeletal transport network [15]. Once in the nucleus, AR binds DNA at specific sites known as androgen-response elements (ARE) through its DBD. In this way, the AR can up- or down-regulate the transcription and activation of various genes, many of which are involved with regulating crucial cellular functions such as growth and proliferation. As a consequence of this ability to regulate cell survival, persistent activation of the AR has been shown to be a pivotal driving force in the development and progression of prostate cancer. Furthermore, inhibition of AR signalling with ADT (as achieved, for example, with luteinizing-hormone-releasing hormone (LHRH) agonists such as goserelin and leuprorelin acetate) remains the standard of care in the treatment of prostate cancer to this day [16, 17]. However, while nearly all patients initially respond to ADT, the duration of response varies from months to years, and ultimately all patients eventually acquire resistance and progress to CRPC, which is invariably lethal [18].

CRPC was long thought of as being an androgen-independent entity; however, over the past decade, in particular, the continuing importance of the AR in the progression of advanced-stage prostate cancer has become better appreciated, culminating in the introduction of abiraterone and enzalutamide into routine clinical practice, which have both provided additional improvements in survival for patients with CRPC [19, 20]. Despite the success of these second-generation AR-targeted therapies, treatment resistance continues to be a major challenge, leaving patients with only a limited number of meaningful treatment options following disease progression, namely taxane chemotherapy, which is not without its limitations such as cytopenia and neurotoxicity [21, 22], and targeted therapies that are only efficacious in a subgroup of patients, such as poly (ADP-ribose) polymerase (PARP) inhibitors or carboplatin (as yet unapproved) in homologous repair DNA repair defective prostate cancers, and anti-programmed cell death protein 1 (PD-1) antibodies for mismatch repair defective disease [23]. In addition, with clinical evidence emerging that use of abiraterone at diagnosis of castration sensitive prostate cancer (CSPC) improves outcomes [24, 25], it is foreseeable that, in the future, these agents will be used much earlier in the disease trajectory. Such a change could result in resistance to anti-androgens occurring at the time of progression from first-line therapy rather than as a later event, creating the possibility of new clinical dilemmas.

The full-length AR (AR-FL) has been well described in the literature [12, 26]; however, over the past 10 years, a variety of alternate versions of AR have been shown to exist. Evidence for this first emerged through the work of Dehm and colleagues who identified two truncated AR isoforms lacking the carboxy-terminal domain in the 22Rv1 prostate cancer cell line, which were encoded by mRNAs with a novel exon 2b at their 3' end [27]. In addition, they demonstrated that these AR isoforms remained constitutively active, and maintained the proliferation of 22Rv1 cells in the absence of exposure to androgen [27]. Subsequently, with the development of more advanced sequencing techniques, numerous other truncated forms of the AR have been reported, many of which are also constitutively active [26, 28, 29].

Expression of AR protein results from the transcription and translation of the AR gene. However, owing to the discontinuous nature of eukaryotic genes, featuring regions of non-coding DNA (introns) interspersed between stretches of coding DNA (exons), the resultant precursor mRNA (pre-mRNA) transcript typically contains both sequences when initially transcribed. Therefore, before translation, nascent pre-mRNA transcripts are edited through a process known as splicing, which removes introns and produces mature mRNAs that can be translated into functional proteins.

RNA splicing is performed by complex cellular machinery referred to generally as the spliceosome. The importance of this complex gained increased recognition with the discovery that, through the alternative inclusion and exclusion of exons and introns termed alternative splicing, a single gene can encode multiple different proteins [30]. Alternative splicing enables eukaryotic cells to transform a genome that contains only 20,000 genes into a substantially larger and more diverse proteome of approximately 95,000 unique proteins [31]. As such, awareness of the role of the spliceosome in numerous diseases, including cancer, is growing. However, our understanding of its underlying biological mechanisms remains incomplete, making it an important area of clinical research.

1.2 The Spliceosome

1.2.1 Spliceosome assembly

The spliceosome is a dynamic cellular machine composed of small nuclear ribonucleoproteins (snRNP) and associated protein co-factors [30, 32]. At the heart of this complex are a number of small nuclear ribonucleic acids (snRNAs) [33] that catalyse splicing in an ATP-dependent manner [34]. snRNAs are non-coding, non-polyadenylated transcripts that reside in the nucleoplasm, and can be broadly subdivided into Sm and Sm-like snRNA [35]. The major and minor Sm-class of spliceosomal snRNAs comprise of the snRNAs U1, U2, U4, U4atac, U5, U11 and U12, whereas the Sm-like snRNAs are U6 and U6atac [35]. The snRNAs which together make up the Sm-class of snRNAs are transcribed by RNA polymerase II (RNA Pol II) in a parallel manner to mRNA, although their transcription and processing relies on a distinct cellular system [35]. Of note, following transcription, these snRNAs are exported to the cytoplasm where they are processed, prior to returning to the cell nucleus, where they localise to nuclear speckles until required by the cell for splicing [36].

Although the full intricacy of the splicing process remains uncertain, with multiple models having been proposed, the current consensus regarding the process of splicing is that it occurs in a step-wise manner ***(figure 1.2)***. The first step in the process of splicing is the identification of the expressed exons and redundant introns within the nascent pre-mRNA by spliceosomal snRNA, which provides crucial fidelity to this complex choreography. To initiate splicing, the U1 snRNP recognises and couples with a short, conserved motif at the 5' end of the target mRNA, known as the 5' splice site, located at the junction between an exon and an intron [30, 32]. This reaction is ATP-independent and relatively weak, and is stabilised by the concomitant binding of two spliceosome associated proteins, splicing factor 1 (SF1) and the heterodimer U2 auxiliary factor 65 (U2AF65), to both an adenosine, usually 15-20 nucleotides upstream of the 3' splice site, known as the branch point, and the 3' splice site [30, 32, 37, 38]. Together these structures form the early-complex (complex E), which triggers the ATP-dependent recruitment of the U2 snRNP to the branch point [30, 32, 38]. The resultant interaction of U2 with U1 forms the pre-spliceosome (complex A) and defines the end of one exon and the beginning of the next, referred to as exon definition [30, 32]. In a subsequent poorly understood step, the U1 and U2 snRNPs are rearranged, bringing the 5' splice site,

branch point, and 3′ splice site into closer proximity; this is described as the intron definition complex [30, 39]. After the assembly of complex A, the pre-assembled U4-U6-U5 tri-snRNP is recruited to the pre-spliceosome to form complex B [30, 32]. This then undergoes a series of compositional and conformational changes, including the release of the U1 and U4 snRNPs, to form the catalytically active complex B (complex B*), which hosts the first catalytic step of splicing, generating complex C, which contains the free end of the first exon and the remaining intron–exon lariat intermediate [30, 32]. Complex C then undergoes further ATP-dependent rearrangements before performing the second catalytic step of splicing, resulting in a post-spliceosomal complex that contains the two liberated exons, now positioned sequentially and ligated, as well as the entire looped intron lariat [30, 32]. Finally, the post-

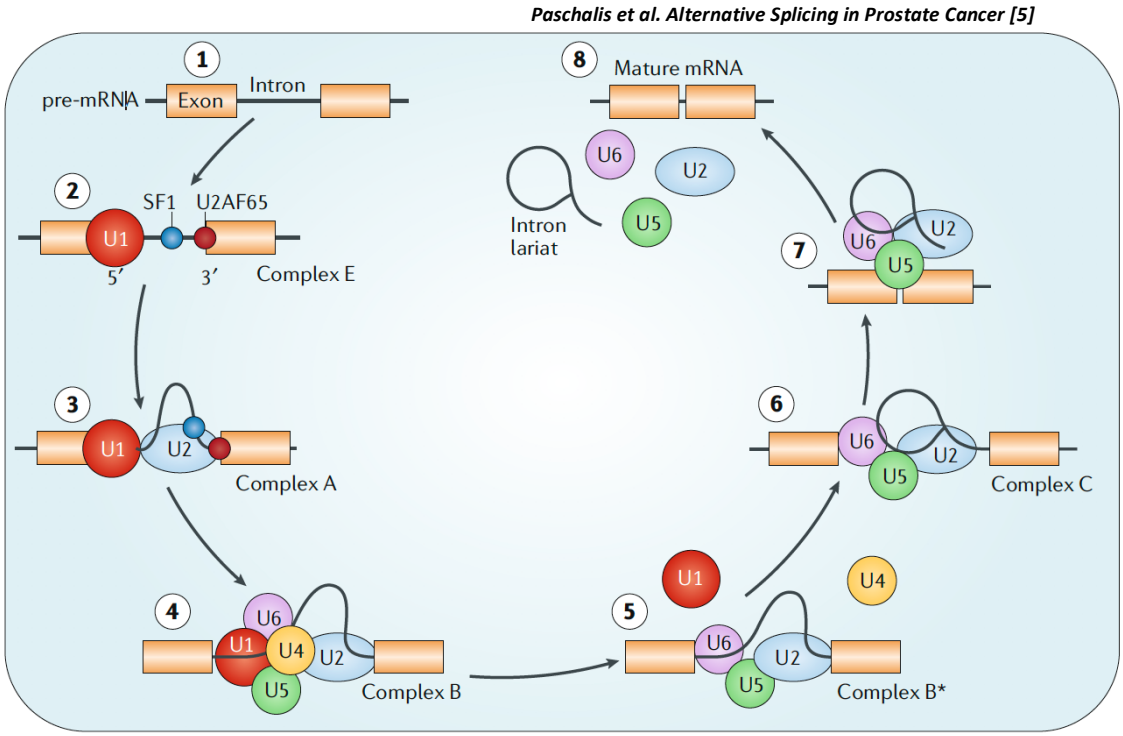

Figure 1.2: Spliceosome assembly. Splicing occurs in a stepwise manner beginning with coupling of the small nuclear ribonucleoprotein (snRNP) U1 with the intron 5′ splice site (step 1). This reaction is ATP-independent and results in a weak interaction, which is then stabilised by the binding of splicing factor 1 (SF1) and splicing factor U2 auxiliary factor 65 kDa subunit (U2AF65) to the 3′ splice site (step 2). Together these structures form the early complex (complex E) and trigger the ATP-dependent recruitment of the snRNP U2 to the intron branch point, thus forming the pre-spliceosome (complex A) and defining the end of one exon and the beginning of the next, a process referred to as exon definition (step 3). This also brings the 5′ splice site, branch point, and 3′ splice site, known as the intron definition complex, into closer proximity (step 4). Next, the pre-assembled U4–U6–U5 tri-snRNP is recruited to the pre-spliceosome to form complex B, which then undergoes a series of compositional and conformational changes including the release of U1 and U4, to form the catalytically active complex B (complex B*), which hosts the first catalytic step of splicing (step 5). The resultant complex, complex C, which contains the free end of the first exon and the remaining intron–exon lariat intermediate (step 6), then undergoes further ATP-dependent rearrangements before performing the second catalytic step of splicing to form the post-spliceosomal complex that contains the mature mRNA product, as well as the entire looped intron lariat (step 7). Finally, the U2, U5, and U6 snRNPs are released and recycled for subsequent splicing reactions (step 8).

catalytic spliceosome is disassembled in an ATP-dependent manner releasing the U2, U5 and U6 snRNPs from the mature mRNA product [30, 32].

Importantly, all the major steps in spliceosome formation are reversible, suggesting that a proof-reading mechanism is in operation during splicing [30, 40], with data from *in vitro* studies showing that partially assembled spliceosomes are able to disassemble and reassemble at alternative splicing sites [41]. This effect is particularly apparent during the early stages of spliceosome assembly because commitment to splicing increases as spliceosome assembly progresses [41].

1.2.2 Spliceosome regulation

The core constituents of the spliceosome complex, such as the snRNPs U1 and U2, are able to define exon–intron boundaries; however, splicing sequences within nascent mRNA precursors often contain too little information to unambiguously define specific splice sites [42]. In addition, human introns often contain sequences that are not canonical splice sites but have a high degree of similarity to authentic splice sites. As such, additional *cis* and *trans* regulatory factors are required to accurately define exon–intron junctions and maintain splicing fidelity. *Cis*-regulatory RNA elements are nucleotide sequences within pre-mRNA transcripts that can modify the splicing of the same pre-mRNA transcript in which they are located. As such, these sequences are referred to as splicing regulatory elements (SREs) and contribute to splicing in a context-dependent manner, whereby they can serve as either splicing enhancers or silencers depending on their position within the pre-mRNA transcript [43]. SREs exert their effects by recruiting *trans*-acting splicing factors, auxiliary proteins of the spliceosome such as serine-rich and/or arginine-rich (SR) proteins, and heterogeneous nuclear ribonuclear proteins (hnRNPs). These proteins interact with core components of the spliceosome, often the snRNPs U1 and U2, to either activate or suppress the splicing reaction during the early steps of spliceosome assembly. In addition, as with SREs, trans-acting splicing factors modify splicing in a context-dependent manner. For example, SR proteins can promote splicing when bound to SREs located within exons, but can also inhibit splicing when associated with SREs located in introns [44].

Other factors contributing to the regulation of splicing include 1) tissue-restricted protein splicing factors (such as the neuro-oncological ventral antigen (NOVA) [45] and the RNA-binding protein fox-1 [46]); 2) the rate of transcription elongation [47]; 3) tissue hypoxia [48, 49]; 4) heat stress [50, 51]; 5) genotoxic stress [52]; 6) chromatin structure; and 7) nucleosome positioning [53]. Knowledge of this complexity has been furthered by findings that indicate that not only can most splicing factors recognise multiple SREs, but also that each SRE is also often bound by multiple different factors. This observation suggests the presence of a complex network of protein–RNA interactions working alongside the spliceosome and regulating splicing to not only protect the proteome from error but also provide a level of cellular plasticity [54, 55].

1.2.3 Alternative splicing

Splice site selection is reported to depend on the 'strength' of a splice site. Sites that bear a close resemblance to recognisable consensus sequences, such as CAG/GUAAGU at the 5' splice site and NYAG/G at the 3' splice site, and that form stable interactions with core constituents of the spliceosome, such as snRNP U1, are referred to as strong splice sites. Strong splice sites are more efficiently recognised by the spliceosome and are selected over 'weaker' sites, with splicing consequently occurring more consistently at strong sites. However, the spliceosome regulatory network can modify the strength of these competing sites by silencing stronger splice sites and enhancing weaker ones, predominantly through *trans*-acting splicing factors. In this way, the interplay between these competing spliceosomal homing signals within a nascent pre-mRNA can lead to the preferential selection of non-canonical splice sites and result in alternative splicing [56].

High throughput RNA sequencing (RNA-seq) studies have shown that alternative splicing is a routine biological process, with 90-95% of human multi-exon gene transcripts demonstrating alternative splicing events, thereby generating a more diverse proteome [57]. Patterns of alternative splicing range from alternative 3' or 5' splice site recognition, to retained introns and mutually exclusive exons; however cassette exon skipping is the most common event in humans [58] ***(figure 1.3)***.

Despite the abundance of alternative splicing events, the functional roles of the many isoforms generated by alternative splicing remain largely uncertain. While this has led some authors to speculate that alternative splicing is a fundamental factor in the development of biodiversity, and thus evolution [59], others have implicated alternative splicing in the pathogenesis of a number of diseases, including cancer [58, 60, 61].

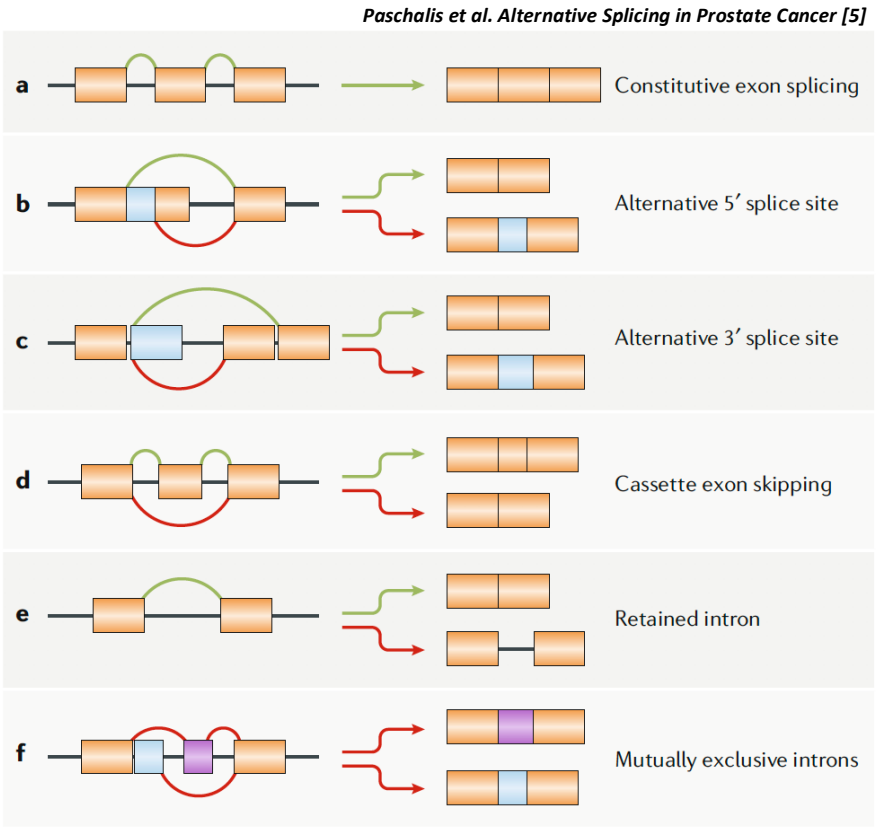

Figure 1.3: Summary of constitutive and alternative splicing events. (A) Graphic depiction of constitutive splicing where introns are removed and sequential exons are ligated to produce mature mRNA. **(B-C)** Alternative splicing, in which changes in 5' and 3' splice site selection can result in the generation of alternatively spliced protein variants. **(D)** Exon skipping, in which a cassette exon is spliced out of the nascent mRNA transcript altogether, along with its adjacent introns. **(E)** Intron retention; an intron that does not form part of the canonical mRNA transcript is not removed and remains within the mature mRNA. **(F)** Splicing, in which complex events give rise to mutually exclusive alternative splicing events, where only one of a set of two or more exons in a gene is included in the final transcript can also occur. Orange exons indicate those that are part of the canonical mRNA sequence; blue or purple exons indicate alternative sequences that might or might not be included in the mature mRNA. Black lines indicate introns, green lines indicate constitutive splicing patterns, and red lines indicate alternative splicing events.

1.2.4 The spliceosome in prostate cancer

The role of the spliceosome in prostate cancer is currently a major area of clinical research. While alternatively spliced variants of the AR that remain constitutively active in the absence of circulating androgen are the best-described splicing aberrations in prostate

cancer, the spliceosome has been implicated in the pathogenesis of prostate cancer in a number of other ways ***(figure 1.4)***.

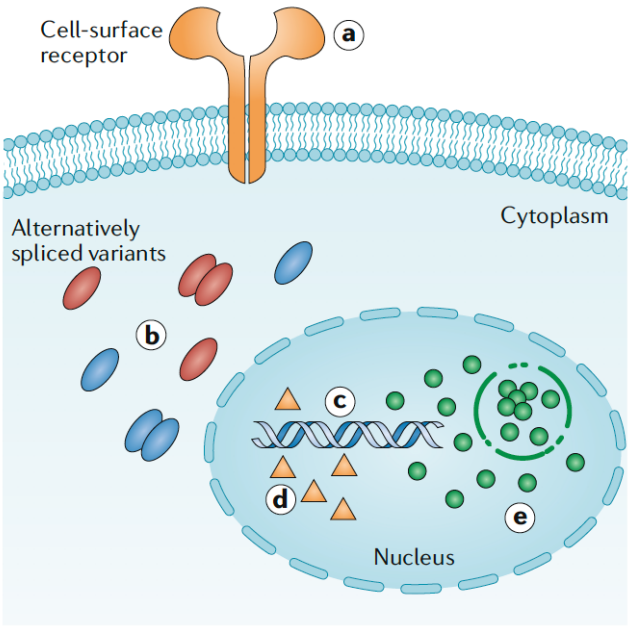

Paschalis et al. Alternative Splicing in Prostate Cancer [5]

Figure 1.4: Mechanisms through which the spliceosome contributes to disease progression in prostate cancer. **(A)** Alternative splicing of cell-surface receptors such as the FGFR have been reported to cause aberrant activation of key survival pathways in the absence of circulating androgens. **(B)** Constitutively active splice variants of intracellular transcription factors such as the androgen receptor (AR; red ovals) have been linked with disease progression in patients with castration-resistant prostate cancer and are correlated with inferior overall survival outcomes. **(C)** Gain-of-function mutations in *cis*-regulatory elements have been proposed to increase AR transcription in the absence of circulating androgens. **(D)** Alternative splicing of key cellular regulatory proteins (orange triangles) such as the G1-S-specific cyclin D1 (CCND1), a central component of cell cycle control, can promote the proliferation and survival of prostate cancer cells. **(E)** Upregulation, as well as alternative splicing, of nuclear splicing factors (green circles) such as Kruppel-like factor 6 (KLF6) is able to increase cell proliferation, colony formation, invasion, and epithelial–mesenchymal transition, which contributes to AR-independent treatment resistance.

1.2.4.1 Mutations of spliceosome regulators

Recurrent somatic mutations in genes encoding splicing factors have been identified in a variety of different cancers such as uveal melanoma [62], pancreatic ductal adenocarcinoma [63], lung adenocarcinoma [64], breast cancer [65] and prostate cancer [66]. Despite this diversity in tumour origin, most reported spliceosomal mutations occur in one of four genes, namely, those encoding splicing factor 3B subunit 1 (SF3B1), SR splicing factor 2 (SRSF2), splicing factor U2AF 35 kDa subunit (U2AF1), and CCCH-type zinc-finger RNA-binding motif and serine/arginine-rich protein 2 (ZRSR2) [67]. Of these, mutations in SF3B1 are the most common and have been observed in patients with both haematological and solid malignancies, reportedly occurring in 15% of chronic lymphocytic leukaemias, 15–20% of uveal melanomas, and 4% of pancreatic cancers [67]. The product of this gene, SF3B1, is a core spliceosomal protein that binds upstream of the pre-mRNA branch site and is thought to be required for the recognition of most 3‘ splice sites [30]. As such, SF3B1 mutations have been associated with improved recognition of cryptic 3‘ splice sites and the formation of alternatively spliced protein isoforms [68]. However, while alternatively spliced versions of

the AR spliced at cryptic exon 3 have been implicated in the development of treatment resistance and disease progression in patients with CRPC, with the reported incidence of SF3B1 mutations in patients with prostate cancer being in the region of 1% [66, 69], the contribution of SF3B1 mutations to treatment resistance through this mechanism is likely to be limited.

1.2.4.2 Alterations in spliceosome regulator activity

Changes in the activity of splicing factors have been reported to have direct implications for tumorigenesis and disease progression in prostate cancer. For example, KH domain-containing, RNA-binding, signal transduction-associated protein 1 (KHDRBS1) is a nuclear splicing factor involved in the regulation of G1–S-specific cyclin D1 (CCND1) splicing [70], which is a central component of cell cycle control. However, KHDRBS1 is activated through ERK-mediated phosphorylation [71], which is dysregulated in approximately a third of human cancers [72], including prostate cancer. As such, KHDRBS1 has been found to be frequently upregulated in prostate cancer and consequently has been associated with the increased expression of the truncated CCND1b isoform, rather than the canonical CCND1a protein, which promotes the proliferation and survival of prostate cancer cells *in vitro* [73].

Splicing factor upregulation has also been linked with epithelial-mesenchymal transition in the prostate, and disease progression in CRPC. Following androgen deprivation, upregulation of the splicing factor serine/arginine repetitive matrix protein 4 (SRRM4) has been shown to cause the alternative splicing of RE1-silencing (REST) [74], a neuronal master regulator that, in the absence of alternative splicing, prevents the expression of neuronal genes such as synaptophysin in non-neuronal cells [75]. Consequently, SRRM4 upregulation results in the expression of a truncated form of REST that lacks its canonical transcriptional repressor domain and gives rise to a more AR-independent, neuroendocrine phenotype, which confers a poorer prognosis [76].

As well as directly contributing to disease progression, the upregulation of canonical splicing factors has also been shown to be pivotal in the activation of other drivers of prostate cancer, such as oncogenes. The protooncogene MYC is reported to be overexpressed in up to

90% of all primary human prostate cancer lesions [77]. MYC hyperactivation amplifies pre-mRNA production, leading to stress on the spliceosome [78]. As such, these cancers are as equally dependent on the availability of splicing factors to sustain proliferation and survival as they are on MYC [78], as demonstrated by the upregulation of a number of splicing factors, such as serine/arginine-rich splicing factor 1 (SRSF1), heterogeneous nuclear ribonucleoprotein A1 (hnRNP A1) and heterogeneous nuclear ribonucleoprotein A2 (hnRNPs A2) in MYC-overexpressing tumours, and the disruption of many vital cellular processes, which occurs when they are inhibited [78-81].

1.2.4.3 Alternative splicing of cellular signal transduction pathways

The spliceosome and its associated proteins are involved in the routine operation of a wide range of cellular processes including DNA repair, transcription, and nonsense-mediated RNA decay. For example, the findings of chromatin immunoprecipitation (ChIP) studies demonstrate that SF3B1 and U2AF1 interact with breast cancer type 1 susceptibility protein (BRCA1) following DNA damage [82].

Kruppel-like factor 6 (KLF6) is a key tumour suppressor gene that is often mutated in prostate cancer. This gene encodes a member of the Kruppel-like family of transcription factors which binds DNA and regulates growth-related signal transduction pathways, cell proliferation, apoptosis, and angiogenesis [83]. Wild-type KLF6 has inhibitory effects on cell growth, although a common KLF6 germline single nucleotide polymorphism (IVS1−27 G>A/IVSΔA) results in the production of an alternatively spliced isoform, KLF6 splice variant 1 (KLF6 SV1), which increases cell proliferation, colony formation, and invasion. Furthermore, upregulation of KLF6 SV1 in prostate cancer is associated with worse prognosis [84, 85].

As well as impacting the function of several important protein signal transducers, the alternative splicing of cell-surface receptors, leading to aberrant activation of key survival pathways, is an equally important aspect of the contribution of the spliceosome to prostate cancer progression. For example, fibroblast growth factor-2 receptor (FGFR2) is a tyrosine kinase receptor, which, when activated by fibroblast growth factor (FGF), is involved in the regulation of numerous key cellular processes such as proliferation and differentiation that

contribute to cell survival [86]. Under non-malignant physiological conditions, FGFR2 exists as a number of alternatively spliced isoforms, which tend to be cell type-specific, with isoform IIIb predominantly expressed in epithelial cells and isoform IIIc predominantly expressed in mesenchymal cells. However, in prostate cancer this distribution has been reported to change, with isoform IIIc becoming more prevalent [87]. This increase in isoform IIIc expression favours the binding of FGF8b [87], which is the major FGF isoform expressed in prostate cancer and may have an important role in disease progression, as evidenced by the association of this isoform with higher tumour Gleason grade and clinical stage [88].

In summary, splicing influences prostate cancer carcinogenesis in a multitude of ways, and the breadth of these alterations suggests that endocrine therapy resistance is a multifactorial process. However, the most clinically relevant role of the spliceosome in the progression of prostate cancer is currently considered to be the generation of alternatively spliced AR isoforms.

1.3 Androgen receptor splice variants

To date, multiple AR splice variants (AR-SV) have been identified and evaluated in metastatic CRPC specimens [28, 89, 90] ***(figure 1.1)***; however, of these, the role of AR splice variant 7 (AR-V7) is the most widely studied and has been associated with resistance to AR-targeting therapies and poorer overall survival [91, 92]. In 2017, AR-V9 was shown not only to be co-expressed with AR-V7 but also to share a common 3‘ terminal cryptic exon [93]. Furthermore, AR-V9 might also lead to the ligand-independent growth of prostate cancer cells; high levels of AR-V9 mRNA are reported to be predictive of primary resistance to abiraterone in cellular models and in a small cohort of patients [93]; however, the clinical significance of this observation remains uncertain.

AR-V7 is a truncated isoform of the canonical AR-FL protein that lacks the LBD but retains both the DBD, which mediates AR dimerization and DNA interactions, and the NTD, which is responsible for the majority of AR transcriptional activity [92]. Crucially, the resulting conformational change maintains AR-V7 in a constitutively active state in the absence of

ligand, resulting in persistent AR activation and survival signalling in tumour cells [6]. Furthermore, this structural difference is also reported to enable AR-V7 to induce a distinctly different set of transcriptional programmes compared with those induced by AR-FL activation. For example, expression of AR-V7 but not AR-FL is positively correlated with the expression of UBE2C, which encodes ubiquitin-conjugating enzyme E2C, a protein required for the degradation of mitotic cyclins and for cell cycle progression in prostate cancer cells and in CRPC xenografts [94]. This observation suggests a shift towards AR-SV mediated signalling following anti-androgen therapy in a subset of patients with CRPC, although attempts to disentangle the functional role of AR-V7 from that of AR-FL have been challenging, and this area of investigation remains an active one. Further evidence is required before firm conclusions can be drawn on this possibility.

AR-V7 is to date considered the most commonly expressed AR-SV [28, 92] and the prevalence of this splice variant increases substantially as patients progress to CRPC [29, 95, 96]. This increased expression can, in part, be explained as a consequence of treatment with ADT. AR-V7 expression is intimately linked with AR transcription [97], which is increased by approximately tenfold in response to ADT [92], and, as such, AR-V7 expression is consequently also increased. In addition, as activation of AR signalling decreases transcription of AR-V7, inhibition of AR signalling with ADT results in the loss of this negative feedback and leads to further upregulation of AR-V7 [6, 92]. Ultimately, however, the processes determining AR-V7 expression, as opposed to those determining expression of the canonical AR-FL, remain unclear, although an increasing appreciation of the importance of the spliceosome in this process is beginning to emerge.

1.3.1 AR-V7 and the spliceosome

The AR-V7 protein arises from alternative splicing of AR mRNA at cryptic exon 3 as opposed to the 3‘ splice site of the canonical AR-FL ***(figure 1.1)***. AR gene copy number gain is considered an important determinant of AR-V7 mRNA levels in patients with CRPC metastases [98], although this observation alone does not explain why a proportion of encoded AR mRNAs become alternatively spliced. For example, in LNCaP95 cells, which are not reported to possess this AR copy number gain, AR-V7 RNA is expressed at levels comparable to those

of VCaP cells in which AR expression is amplified [97], whereas the parental cell line, LNCaP, does not express AR-V7. Therefore, rather than alternative splicing of AR mRNA occurring through random splicing error as a consequence of increased substrate concentration, these differences instead suggest the existence of regulatory mechanisms that are responsible for splice site selection.

In preclinical models of prostate cancer, Liu and colleagues reported that androgen deprivation leads to increased recruitment of the spliceosome to the AR transcript, thus facilitating both conventional and alternative splicing [97]. Furthermore, treatment with enzalutamide specifically enhanced the recruitment of a number of splicing factors to the AR pre-mRNA region containing the 3' splice site of AR-V7 [97]. This research group concluded that the splicing proteins splicing factor U2AF65 and SRSF1 acted as 'pioneer' factors, directing the recruitment of the spliceosome to SREs located adjacent to the 3' splice site of AR-V7, thus increasing the expression of AR-V7 mRNA [97]. Interestingly, while knockdown of these splicing factors resulted in a reduction in the levels of AR-V7 mRNA in both VCaP and LNCaP95 cell lines, levels of AR-FL mRNA remained unaffected [97], suggesting that these splicing factors play an important role specifically in AR-V7 splicing. hnRNP1 has also been proposed to be a regulator of AR-V7 splicing; however, the evidence for this is less conclusive than for U2AF65. Work by Nadiminty et al. has shown that overexpression of hnRNP1 results in AR-V7 upregulation, while downregulation of this protein both reduces AR-V7 expression and re-sensitises CRPC cell lines to enzalutamide [99]. However, hnRNP1 knockdown also reduces the level of AR-FL expression [97], suggesting that hnRNP1 is a general regulator of AR mRNA splicing rather than a specific regulator of AR-V7.

Importantly, and in keeping with the concept of a proofreading process within the spliceosomal network, AR-V7 splicing seems to be both a dynamic and a plastic process. For example, the re-introduction of androgens to androgen-deprived cell lines can repress AR-V7 mRNA levels, and this effect occurs within 24 hours of re-exposure in VCaP cells. Similarly, in primary cultures from enzalutamide-resistant VCaP xenograft models, both AR and AR-V7 mRNA levels decrease significantly upon exposure to DHT [97]. As an interesting aside, the rapidity of this plasticity might contribute to the antitumor activity demonstrated with bipolar androgen therapy, in which patients receive monthly doses of high-dose testosterone while

remaining on ADT, as demonstrated in a phase II clinical trial with results published in 2017. In this trial, 52% of patients with metastatic CRPC resistant to enzalutamide had a 50% reduction in serum prostate-specific antigen (PSA) level on enzalutamide re-challenge following bipolar androgen therapy [100]. This observation suggests that re-sensitization of treatment-resistant prostate cancer to enzalutamide through manipulation of AR-FL and AR-SV expression by modulating an individual's exposure to testosterone is feasible. However, definitive conclusions regarding this possibility are difficult to elucidate from this cohort alone given that patient's AR-V7 status in this study was determined through analysis of circulating tumour cells (CTCs) rather than tissue-based assessments. More than half of the patients included in this study were found to lack detectable CTCs, and, therefore, a large proportion of patients in this cohort could not be assessed for AR-V7 expression, and so a number of patients expressing AR-V7 could have been omitted from the analysis. Furthermore, preclinical evidence supporting the efficacy of this possible treatment approach remains inconclusive [101].

1.4 Alternative mechanisms of prostate cancer progression that impact splicing and transcriptional activity

While the restoration of AR signalling has been demonstrated to be one of the most important contributors to the development of CRPC, a variety of other genomic and epigenomic aberrations have also been proposed to drive prostate cancer cell survival and proliferation. Amongst these, a number have also been implicated in the regulation of transcription and alternative splicing.

1.4.1 Phosphoinositide 3-kinase (PI3K) Pathway

The PI3K/AKT Serine/Threonine Kinase 1 (AKT)/mammalian target of rapamycin (mTOR) pathway is hugely important in human cancer [102]. A number of different growth factors have been shown to regulate the PI3K signalling pathway including insulin-like growth factor (IGF) and fibroblast growth factor (FGF), leading to the activation of AKT [8]. Subsequently, AKT then regulates multiple molecules involved in cell survival, proliferation

and energy metabolism, including MDM2 proto-oncogene, c-MYC, glycogen synthase kinase 3 beta (GSK3b), nuclear factor-kB (NF-kB) and mTOR [8, 102]. The principle inhibitor of the PI3K pathway is the tumour suppressor phosphatase and tensin homolog (PTEN). Importantly, PTEN loss through deletion and mutation has been reported to occur in approximate 40% of prostate cancers [103], and associates with a poorer prognosis and resistance to AR directed therapy [104, 105]. These clinical observations have also been corroborated by a number of *in vivo* studies using Pten-knockout mice, showing them to develop invasive adenocarcinoma [106, 107], with this occurring more rapidly and more frequently when combined with knockout of tumour protein p53 (p53) [108]. Furthermore, these Pten null mice have also been found to develop castrate-resistant proliferative clones following castration [106]. Taken together therefore, these data highlight the importance of the PI3K pathway to the development of CRPC.

In addition to its role in these important cellular processes, the PI3K pathway has also been implicated in the regulation of alternative splicing events. AKT has been reported to phosphorylate serine and arginine rich splicing factor 1 (SRSF1) and 7 (SRSF7), and in doing so can regulate to alternative splicing of the fibronectin gene *in vitro* [109]. In keeping with these reports, another study has suggested that AKT may also similarly phosphorylate serine and arginine rich splicing factor 5 (SRSF5) [110].

1.4.2 MYC

MYC is a proto-oncogene and encodes a nuclear phosphoprotein which is involved in cell cycle progression, apoptosis and cellular transformation [111]. In a study by Gurel et al., c-MYC was found to be frequently overexpressed in prostate intraepithelial neoplasia (PIN) with an incremental increase from normal tissues to low-grade PIN and subsequently to high-grade PIN [112]. The MYC locus on chromosome 8q has also been observed to be frequently overexpressed in CRPC [103], with ADT having been suggested to increase the incidence of this amplification [113]. Consequently, MYC has been reported to contribute to both the initiation and progression or prostate cancer. These observations have been substantiated by reports that *in vivo* mouse models overexpressing MYC in the prostate develop PIN, with subsequent progression to invasive adenocarcinoma [114]. Furthermore, MYC has been

demonstrated to drive the development of metastatic disease in both *Pten* loss and *Pten/Trp53*-deficient genetically engineered mouse models [115, 116].

The mechanisms through which MYC contributes to prostate cancer progression remains incompletely understood. The role of MYC as a master regulator of transcription suggests however that this is likely multifactorial, including changes in alternative splicing. As discussed in **section 1.2.4.2**, MYC hyperactivation amplifies pre-mRNA production, leading to stress on the spliceosome [78]. Notably however, MYC has also been suggested to directly modulate alternative splicing events [117], with this having been proposed to contribute to its oncogenic role in prostate cancer given that changes in alternative splicing have been associated with more aggressive prostate cancer phenotypes, and the development of neuroendocrine prostate cancer (NEPC) [118, 119]. In a study by Phillips et al., MYC was determined to regulate the incorporation of 147 different cassette exons, with these being commonly enriched in genes encoding RNA binding proteins [117]. Importantly, many of these exons introduced frameshifts, or encoded premature stop codons, suggesting that MYC regulated RNA splicing by controlling nonsense mediated decay of RNA binding proteins [117]. MYC has also been more directly implicated in the production of AR and its alternatively spliced variants, although interestingly, despite reports linking MYC with the regulation of alternative splicing, a recent study by Bai et al. suggested that MYC-dependent regulation of AR and its splice variants did not occur through changes in AR splicing [120]. Instead, MYC was proposed to promote the transcription of the AR gene and enhance the protein stability of both AR-FL, and AR-SVs, without altering AR RNA splicing [120].

Taken together therefore, while it is generally accepted that MYC plays an important role in prostate cancer progression, further work is needed to better understand the mechanisms through which it does so. MYC overexpressing prostate cancers appear to be more aggressive, with wide-ranging changes in alternative splicing processes. These observations suggest that MYC overexpressing cancers may have a greater reliance of alternative splicing and the spliceosome for survival. Consequently, MYC may serve as a predictive biomarker for response to spliceosome-targeting therapies, as these agents may be more efficacious in MYC overexpressing cancers (Therapeutic targeting of alternative splicing in MYC overexpressing tumours is discussed further in **section 1.5.4**).

1.4.3 The Wnt/β-catenin pathway

The Wnt (Wingless/int1)/β-catenin pathway has been shown to be dysregulated in a number of different cancer types, including prostate cancer. Activation of the Wnt/β-catenin pathway has been associated with higher Gleason grade [121], higher prostate-specific antigen (PSA) levels [121], a younger age of prostate cancer onset [103], and higher risk of recurrence after radical prostatectomy [122]. In unstimulated cells, free cytoplasmic β-catenin is phosphorylated by glycogen synthase kinase 3 beta (GSK3β), after which it is ubiquitinated by the E3 ubiquitin ligase beta-transducin repeats-containing protein (β-TrCP), marking β-catenin for degradation via the proteasome [123]. Upon Wnt-ligand binding, GSK3β is inhibited, resulting in an accumulation of unphosphorylated β-catenin in the cell [123]. Consequently, β-catenin is then able to translocate to the nucleus and activate T-Cell factor/lymphoid enhancer factor-1 (TCF/ LEF-1) transcriptional activity, and upregulate genes such as MYC, matrix metallopeptidase 7 (MMP7) and vascular endothelial growth factor (VEGF) [123, 124]. Somatic mutations in genes that regulate the Wnt/β-catenin signalling pathway are present in approximately 10–20% of patients with metastatic CRPC [103, 125]. These include activating mutations in CTNNB1 and RSPO2, or inactivating mutations in APC, RNF43 and ZNRF3 [103, 126]. In addition to these genomic aberrations, inhibition of AR signalling has been proposed to activate the Wnt/β-catenin signalling pathway and contribute to androgen-independent prostate cancer growth [127, 128].

Further to these effects on transcription, the Wnt/β-catenin pathway has also been implicated in the regulation of alternative splicing decisions. In a study by Gonçalves et al. the Wnt/β-catenin pathway was demonstrated to directly activate the transcription of serine and arginine rich splicing factor 3 (SFSR3) [129]. Consequently, the resulting upregulation of SRSF3 protein levels was reported to be sufficient to modulate alternative splicing decisions in colorectal cancer cells [129]. Whether a similar role for the Wnt signalling pathway exists in prostate cancer remains to be confirmed, however, in keeping with these finding, the small molecule β-catenin inhibitor CWP232291 has recently been reported to downregulate the expression of both AR and its splice variants in prostate cancer cells [130].

1.4.4 The MAPK/ERK pathway

Another proposed driver of prostate cancer progression that has been implicated in the regulation of alternative splicing events is the mitogen-activated protein kinase (MAPK)/extracellular signal-regulated kinase (ERK) pathway. The downstream targets of the MAPK/ERK pathway regulate a number of important cellular process involved in cell cycle progression, proliferation and transcription, including c-MYC [131]. Aberrant activation of the MAPK/ERK signalling pathway in prostate cancer has been reported to be instigated by a variety of different ligands including neuregulin and fibroblast growth factors. More recently, in a study by Li et al., the transmembrane chemokine receptor atypical chemokine receptor 3 (CXCR7) was also reported to be capable of upregulating MAPK/ERK signalling, but through a ligand-independent, β-arrestin 2-dependent mechanism [132]. In this study, CXCR7 was identified as being directly repressed by AR, with its expression being restored with androgen deprivation [132]. As a consequence of this AR mediated regulation, levels of both CXCR7 and phosphorylated (activated) ERK in patient tissue biopsies were found to significantly increase as patients progressed from localised prostate cancer to CRPC, with levels increasing further still upon development of enzalutamide resistance [132]. In keeping with these results, the MEK inhibitor trametinib suppressed the growth of enzalutamide-resistant prostate cancer both *in vitro* and *in vivo* [132].

The MAPK/ERK pathway has also been proposed to serve as a link between extracellular cues and the regulation of splicing. CD44 is a non-kinase transmembrane glycoprotein that has been reported to be overexpressed in several cell types [133]. The principle ligand for CD44 is hyaluronic acid. Binding of hyaluronic acid to CD44 activates signalling pathways that promote cell survival, proliferation, and motility [133]. Interestingly, a number of alternatively spliced variants of CD44 have been identified, and have been proposed to play a role in cancer development and progression. Variant isoforms of CD44 frequently contain additional extracellular domains which influence the binding affinity of CD44 for ligands such as hyaluronic acid and growth factors [134]. Consequently, expression of different CD44 variants can impact the functional properties of their host cell.

Notably, the alternative splicing of CD44 on B and T lymphocytes can be triggered by their activation during an immune response [134]. In a study by Weg-Remers et al., the alternative splicing of CD44, and subsequent upregulation of variant CD44 mRNA species, upon T-cell activation was determined to require the MEK–ERK pathway [134]. In this study, activation of the Ras–Raf–MEK–ERK signalling cascade was shown to result in the retention of variant CD44 exon v5 in mature mRNA [134]. Importantly, the authors proposed that this change in CD44 increased the metastatic potential of lymphoma cells [134]. Further work is therefore now needed to determine whether a similar mechanism of alternative splicing regulation also plays a role in prostate cancer progression.

1.4.5 E26 transformation-specific (ETS) fusions

Translocations involving androgen-regulated promotors and members of the ETS family of transcription factors, leading to an overexpression of the ETS genes, have been found to be common in prostate cancer. The first such translocation, which is also the most common occurring in approximately 50% of localised prostate cancers [135], comprises of a fusion between the 5' untranslated region of the AR regulated gene transmembrane serine protease 2 (TMPRSS2) and the ETS transcription factor ERG (TMPRSS2:ERG) [136]. Knock-down of ERG has been reported to inhibit the growth of both prostate cancer cells and xenograft models [137, 138]. Notably however, ERG overexpression only has typically been shown to induce prostate cancer precursor-like lesions in mice [137, 139], or generate prostate cancers in elderly mice [140], suggesting that ERG-driven prostate cancers are likely relatively indolent and take years to develop. Consequently, it has been suggested that ETS fusions could instead serve as primers to tumorigenesis, with additional driver mutations being required to lead to cancer progression. For example, ERG overexpression combined with PTEN loss results in the development of prostatic intraepithelial neoplasia and subsequent progression to prostate adenocarcinoma [141, 142]. In addition to TMPRSS2, fusions between ERG and the androgen-responsive 5' partners SLC45A3 [143], HERPUD1 [144] and NDRG1 [145] have also been found.

Although not itself a known modulator of alternative splicing, it is noteworthy given its prevalence, that a number of functionally relevant alternatively spliced truncated versions

of the TMPRSS2:ERG gene have been identified [146]. Critically, the various TMPRSS2:ERG fusion isoforms have been reported to possess different biological functions, with some isoforms preferentially promoting tumour initiation and progression, and correlating with more aggressive disease [138]. These effects of TMPRSS2:ERG fusion isoforms may be in part due to an interaction with MYC, with an elevated TMPRSS2:ERG3/TMPRSS2:ERG8 ratio having been proposed to result in increased expression of c-MYC [147].

1.4.6 Neuroendocrine prostate cancer (NEPC)

AR-negative tumours constitute a complex spectrum of phenotypes ranging from NEPC and small-cell carcinomas (SCC), to mixed prostatic adenocarcinomas with neuroendocrine features, and anaplastic carcinomas [76]. While the histological features of these AR-negative prostate cancers have been well documented [148], their clinical significance remains controversial.

AR-negative phenotypes have been proposed to be a potentially important mechanism of treatment resistance due to the inherent inactivity of AR directed therapies on cells which do not depend on AR signalling for survival [76]. However, there remains a lack of consensus regarding the true prevalence of AR-negative prostate cancer. For example, in a study of 150 CRPC patients by Robinson et al, over 96% of patients were reported to have usual adenocarcinoma histology with only 2.9% exhibiting adenocarcinoma with neuroendocrine differentiation, and just 0.7% having SCC [103]. Contrary to this, in a study by Small et al., RNA-seq analyses performed on biopsies from 101 patients with CRPC resistant to abiraterone or enzalutamide revealed that only 33% of samples displayed the typical adenocarcinoma phenotype, whereas 12% had features of SCC and 27% were of an intermediate type distinct from either SCC or adenocarcinoma [149].

The origins of these AR-negative phenotypes are equally divisive, with uncertainty regarding whether these cells derive from the well-documented population of neuroendocrine cells scattered throughout the normal prostate gland [148], or if they arise as a result of transdifferentiation from AR-positive adenocarcinomas; a possibility exemplified

by the expression of neuroendocrine markers by LNCaP cells following prolonged androgen deprivation [150].

A better understanding of these histological subtypes is therefore becoming increasingly important, particularly as they appear to be associated with a more aggressive disease course and poorer prognosis [76]. A recent step forward in this regard has been the realisation that the genomic landscape of prostate cancer can change dramatically as patients progress from primary disease to CRPC. For example, concurrent alterations in p53 and retinoblastoma protein 1 (RB1), a transcriptional repressor that has been reported to function as a tumour-suppressor, are identifiable in only 5% of primary cancers, but are seen in 39% of metastatic CRPCs with adenocarcinoma histology, and 74% of metastatic CRPCs with neuroendocrine-like histology [151]. Critically, the combined loss of p53 and RB1 in mice has been shown to be sufficient to initiate tumour development in a variety of cancer types, including prostate, often with neuroendocrine histology [152]. In keeping with these reports, Sawyers et al. demonstrated that combined knockdown of p53 and RB1 resulted in sustained inhibition of AR target genes such TMPRSS2 while maintaining xenograft tumour growth, suggesting p53 and RB1 loss to enable AR-independent cancer cell proliferation [151]. Furthermore, combined p53 and RB1 loss conferred near complete enzalutamide resistance in both prostate cancer cell lines and xenograft models [151]. In addition, this study found that knockdown of both p53 and RB1 together, but not p53 or RB1 in isolation, resulted in a five to ten-fold increase in the expression of basal and neuroendocrine markers, as well as a reduction in luminal cell markers, at both a cellular and protein level. Taken together therefore, these data suggest that loss of p53 and RB1 function contributes to anti-androgen resistance by promoting 'lineage plasticity' and stimulating the expansion of tumour cells with basal epithelial features which are not dependent on AR for survival over luminal epithelial cells that are [151].

Mechanistically, inactivation of p53 and RB1 has been demonstrated to significantly upregulate the expression of SRY-box transcription factor 2 (SOX2), a transcription factor that is essential for maintaining the self-renewal of undifferentiated stem cells. Therefore, in keeping with p53 and RB1 alterations occurring commonly in NEPCs, SOX2 levels have been shown to be markedly increased in CRPC with neuroendocrine features [103]. Consequently,

SOX2 and has been implicated in both the development of squamous epithelial cancers, and as a marker of neuroendocrine differentiation in prostate cancer [153]. Importantly, knockdown of SOX2 has been shown to completely reverse the luminal to basal switch seen in LNCaP cells with inactivated p53 and RB1, and restore sensitivity to enzalutamide both *in vitro* and in mouse xenograft models [151]. Taken together therefore these results suggest that SOX2 is key driver of lineage plasticity, and that tumours with p53 and RB1 loss may gain resistance to treatment through the reprogramming capacity of SOX2, facilitating the transition from the typical AR-dependent luminal phenotype, to the AR-independent basal phenotype.

Alternative splicing events have been shown to be common in NEPC, and have been suggested to contribute to the development of the neuroendocrine phenotype [118, 119]. In support of this concept, E7107, an inhibitor of splicing factor 3B subunit 1 (SF3B1), has been reported to diminish cancer aggressiveness and reverse castration-resistance in xenograft and autochthonous prostate cancer models [119]. A possible contributing factor to the capability of SOX2 to regulate the pluripotency of cancer cells, and drive the transition towards NEPC, is therefore its proposed role in modulating alternative splicing. Interestingly, in addition to SOX2 having been reported to dictate alternative splicing events by regulating classical splicing factors, such as SRSF2 in lung carcinoma [154], it has also been suggested to serve as a splicing factor itself, for example in transitional cell carcinoma [155]. The mechanism underlying SOX2-associated regulation of alternative splicing in prostate cancer, however, remains incompletely understood, although it has been suggested that this occurs through its relationship with the splicing factor SRRM4 [156, 157]. This now merits further study because if better understood, targeting alternative splicing could represent a novel therapeutic strategy for the treatment of some of the most aggressive forms of lethal prostate cancer.

1.4.7 Epigenetic deregulation

As with the aforementioned genomic alterations, a number of epigenetic regulators have also been implicated in both the progression of prostate cancer, and the modulation of alternative splicing events.

1.4.7.1 DNA modification

DNA methyltransferase 1 (DNMT1) is a member of the DNA methyltransferase family of enzymes which are capable of methylating DNA by catalysing the transfer of methyl groups to specific CpG structures in DNA. DNMT1 has been proposed to act as an oncogene in late stage prostate cancer and contribute to the development of metastases [158]. Furthermore, increased DNMT1 expression has been associated with a more aggressive prostate cancer phenotype and biochemical recurrence following radical prostatectomy [159]. In contrast to DNMT1, the members of the TET family of enzymes, ten-eleven translocation methylcytosine dioxygenase 1 (TET1) and Tet methylcytosine dioxygenase 2 (TET2), which are capable of demethylating DNA, have been shown to play a tumour suppressive role in prostate cancer [160, 161]. Given the role of DNA methylation in regulating transcription, it is perhaps unsurprising that enzymes such as these, which modulate the methylation state of DNA, have been implicated in prostate cancer progression. Recently however, understanding of the role of DNA methylation in the regulation alternative splicing has improved, suggesting the mechanisms through which these enzymes contribute to disease progression are more complex. Exons have been found to have higher levels of DNA methylation than flanking introns, particularly at exon splice sites [162, 163]. It is thought, that these differences in methylation modulate both the elongation rate of RNA polymerase II (Pol II), and the recruitment of splicing factors onto transcribed alternative exons [162]. Further work is therefore now needed to better understand how DNA methylation impacts alternative splicing in prostate cancer, so as to determine if these processes represent therapeutic vulnerabilities in prostate cancer cells.

1.4.7.2 Histone modification

Mutations in epigenetic regulators and chromatin remodelers have been identified in up to 20% of prostate cancers, and have been reported to contribute to disease progression and treatment resistance [164]. Of particular note, such mutations have been identified amongst the constituents of the switch/sucrose non-fermentable (SWI/SNF) chromatin remodelling complex, including ARID1A, ARID4A, ARID2 and SMARCA1 [164-166]. While the functional significance of identified mutations in these genes remains incompletely

understood, the SWI/SNF complex as a whole has been reported to be critical for AR transcriptional activity and for prostate cancer progression [167]. Although epigenetic regulators and chromatin remodelling factors are more typically observed to be themselves alternatively spliced rather than be regulators of alternative splicing, as is the case with enhancer Of zeste 2 polycomb repressive complex 2 subunit (EZH2) [168] and lysine demethylase 1A (LSD1) [169, 170], in addition to contributing to prostate cancer progression the SWI/SNF complex has also been implicated in the regulation of alternative splicing [171]. The contribution of this function of the SWI/SNF complex to the development of prostate cancer however remains to be ascertained.

Other important epigenetic regulators that have been implicated in both prostate cancer progression and alternative splicing are the histone demethylases, and bromodomain-containing proteins, and these are discussed separately in **sections 1.6.2** and **1.7.1** respectively.

1.5 Treatment resistance in prostate cancer

There exist a number of mechanisms that have been proposed to contribute to treatment resistance in CRPC. These mechanisms of resistance include AR mutations, increased AR ligand availability, AR bypass signalling and complete AR independence. Likewise, alternative splicing has also been demonstrated to contribute to treatment resistance in a range of different cancers, including prostate cancer.

1.5.1 Alternative splicing and treatment resistance

Over the past 5–10 years, appreciation of the role of alternative splicing in the development of resistance to anticancer therapies has greatly increased. For example, alternative splicing of survivin, a member of the inhibitor of apoptosis protein family, has been reported to confer resistance to taxanes in preclinical models of ovarian cancer [172], while the alternative splicing of the B lymphocyte antigen CD19 may promote resistance to

immunotherapy involving adoptive T cells expressing anti-CD19 chimeric antigen receptors in preclinical models of B cell acute lymphoblastic leukaemia [173].

Similarly, even though the development of, and improvements in, genome sequencing have heralded the arrival of various new targeted anticancer therapies, evidence is emerging that patients receiving these agents are similarly vulnerable to the development of resistance as a consequence of alternative splicing. For example, a subset of BRAF-mutant melanomas have been reported to acquire resistance to vemurafenib through the expression of a variant $BRAF^{V600E}$ isoform, $p61BRAF^{V600E}$, that lacks exons 4–8, a region that encompasses the RAS-binding domain [174]. Furthermore, and perhaps more pertinently with regards to prostate cancer, alternative splicing has been suggested to contribute to acquired resistance to PARP inhibition [175].

The PARP inhibitor olaparib has a therapeutic impact on cancers harbouring DNA repair defects by inhibiting PARP, a protein that is important for repairing DNA damage, resulting in synthetic lethality. Inhibiting the repair of single-strand breaks in this way results in the generation of double-strand breaks during cell division, leading to the death of cells harbouring loss-of-function mutations in BRCA1 and/or BRCA2. Olaparib has been shown to improve overall survival in patients with DNA repair-deficient metastatic prostate cancer, with antitumor activity in biomarker-positive patients (defined as those with loss of function of BRCA1 and/or BRCA2, ATM, Fanconi anaemia-related genes, or CHEK2 [23]), thus marking a major step forward in the management of this patient group. PARP inhibition has also demonstrated efficacy in patients with other forms of cancer such as breast [176] and ovarian [177] cancers; however, evidence is emerging from these cancer types suggesting that alternative splicing contributes to resistance to olaparib. Wang et al. report that a proportion of patients possessing PARP-sensitising BRCA1 germline mutations either do not respond to, or eventually develop resistance to, PARP inhibition as a result of frameshift mutations in exon 11, leading to nonsense-mediated RNA decay of full-length BRCA1 mRNA transcripts and increased expression of an alternatively spliced BRCA1 isoform, BRCA1-Δ11q. The authors suggest that BRCA1-deficient cancer cells remove deleterious germline BRCA1 mutations by producing alternatively spliced protein isoforms that retain residual DNA repair activity and contribute to treatment resistance [175]. Notably, BRCA2 mutations are much more common

than BRCA1 mutations in patients with prostate cancer [178], although whether or not mechanisms of resistance similar to those seen in other cancers will emerge in patients with prostate cancer will be determined by clinical trials involving novel targeted therapies such as PARP inhibitors. However, these examples do serve to highlight the clinical implications of alternative splicing and add weight to the rationale of harnessing the spliceosome as a novel therapeutic target. Notwithstanding the growing body of literature in this area, with regards to prostate cancer, AR-SVs are currently the most well-established and clinically important mechanism through which alternative splicing is thought to contribute to treatment resistance in patients with CRPC.

1.5.2 AR splice variants and treatment resistance

The emergence of AR-SVs is proposed as a biologically credible mechanism of treatment resistance through the restoration of AR signalling. Data from preclinical studies have shown that inhibition of AR-V7 can re-sensitise enzalutamide-resistant prostate cancer cell lines to anti-androgen treatment [179-181]. AR-SVs have also been implicated in treatment failure in patients receiving combined ADT and radiotherapy, with aberrant AR-SV signalling bolstering the DNA damage response and increasing the clonogenic survival of prostate cancer cells following irradiation [182].

However, evidence supporting the role of AR-SVs in treatment resistance currently remains inconclusive. Despite the advantageous characteristics conferred by their structural properties, which hypothetically enable AR-SVs to remain constitutively active in the absence of androgens, only a minority of AR splice variant isoforms have demonstrated this ability in AR transactivation reporter assays [4], raising questions regarding the clinical significance of the majority of AR-SVs. A proposed explanation for this observation is that most AR-SVs are truncated after exon 3 and thus lack a complete NLS and therefore are expected to be predominantly sequestered within the cytoplasm [183]. AR-V7 is, however, an exception to this rule and despite having an incomplete NLS has been shown to reside in the nucleus for prolonged periods of time [6], where it has also been shown to be transcriptionally active [94].

An alternative theory exists that AR-SVs are a consequence of the physiological response to androgen deprivation. Support for this hypothesis is provided by the rapidity of increased AR-V7 expression following ADT. In xenograft models, expression of both AR-FL and AR-V7 has been shown to increase just two days following castration and reaches peak levels within two weeks, with AR-V7 mRNA being only a fraction of total AR-FL levels [183]. In addition, the re-introduction of androgens in these models restores the expression of both forms to baseline levels in only eight days [183]. Thus, if AR-SVs were to cause treatment resistance, one would expect this resistance to occur much sooner than is typically seen in clinical scenarios [19, 20]. In support of this argument, while data from a number of clinical studies corroborate reports that AR-V7 expression confers a worse prognosis and contributes to treatment resistance [89, 184-186], some research groups have failed to validate this relationship. For example, overexpression of AR-V7 in LNCaP cell lines, which do not produce AR-V7 protein, did not confer resistance to enzalutamide both *in vitro* and in *in vivo* mouse xenograft models of CRPC [183]. Furthermore, in a retrospective analysis of patient records, 6 out of 21 patients with detectable AR-V7 were found to have derived benefit from treatment with abiraterone or enzalutamide, suggesting that a subgroup of AR-V7-positive patients obtains benefit from novel anti-androgen therapies despite detection of AR-V7 in their CTCs [187]. Similarly, in a prospective study, investigators found no significant difference in either serum PSA response or median serum PSA-defined progression-free survival durations between patients with AR-V7-positive, AR-V9-positive or AR-V7-negative disease treated with abiraterone or enzalutamide, as defined using CTCs. The investigators concluded that AR-SV expression did not predict outcomes in patients with metastatic CRPC receiving either agent [188].

Recognising that nearly all studies with results currently reported rely on the determination of AR-V7 status using CTC analyses is an important point. Therefore, both positive and negative associations between AR-V7 expression and clinical outcomes of patients with CRPC have to be interpreted with careful consideration of the validity of the assays that were used, with multiple lines of evidence clearly indicating the limitations of these binary assays [89, 92, 93, 187, 188]. First, the ability of each assay to determine AR-V7 status (either mRNA or protein) only in patients with detectable CTCs needs to be considered; patients with detectable CTCs who lack AR-V7 expression are not the same as those with

undetectable CTCs, in whom AR-V7 status cannot be determined, although patients with undetectable CTCs have been shown to have the best prognosis, relative to those with detectable CTCs and either the presence or absence of AR-V7, after treatment with abiraterone or enzalutamide [91]. Second, although assays designed to measure AR-V7 protein expression overcome concerns regarding the stability of AR-V7 mRNA, such assays remain susceptible to off-target liabilities, specifically false positive results, as associated with use of the Abcam–Epitomics antibody previously described in the EPIC AR-V7 assay [189]. Moreover, consideration needs to be given to the possibility that despite detectable AR-V7 expression, large numbers of AR-V7-negative cells might also be present, which means that these patients could still benefit from abiraterone or enzalutamide. Finally, these molecular association studies will need to be supported by further understanding of AR-V7 biology and the development of novel therapies that abrogate AR-V7 signalling and induce robust responses in patients with CRPC. Only then will the biological and clinical significance of AR-V7 be truly confirmed; this remains a priority for the field and an unmet urgent clinical need.

1.6 Targeting alternative splicing to overcome treatment resistance

1.6.1 Targeting the core spliceosome complex

Several bacterial fermentation products with potent anticancer activity, owing to an ability to modulate the core spliceosome complex, have been identified using large-scale drug screens. The molecules can be broadly categorized into three classes, namely, pladienolides, herboxidienes, and spliceostatins ***(Table 1.1)***. These compounds are structurally distinct, although they also share a common mechanism of action whereby they bind with and inhibit SF3B1 [190]. Under non-malignant conditions, SF3B1 interacts with U2AF65 to recruit the snRNP U2 to the 3‘ splice site of the intron. However, by binding to SF3B1, these compounds interfere with the early stages of spliceosome assembly and therefore destabilise the interactions between U2 and its pre-mRNA target, thus modifying splice site selection [191]. This perturbation of U2 also causes an accumulation of unspliced pre-mRNA in the nucleus, of which a small proportion can ‘leak out’ into the cytoplasm and undergo translation, generating aberrant protein products, which themselves can be cytotoxic [192, 193]. In addition, several of these compounds have also been shown to decrease the expression of VEGF, thus inhibiting angiogenesis in chick chorioallantoic membrane assays [194].

Agent	Stage of Development	Mechanism of Action	Ref.
Targeting the core spliceosome complex			
Pladienolides A–G	Preclinical	*Bind to and inhibit SF3B1 to destabilise recruitment of snRNP U2; Decrease levels of VEGF; Cell cycle arrest in G1 and G2/M; Disrupts spliceosome assembly; Generate truncated form of cell cycle inhibitor p27 which is still functional but more robust; Reduce number of nuclear speckles; Reduced tumour angiogenesis*	*[195, 196]*
E7107	Phase I		*[197]*
Herboxidiene (GEX1A)	Preclinical		*[198]*
FR901463, FR901464 and FR901465	Preclinical		*[199]*
Meayamycin B	Preclinical		*[200]*
Spliceostatin A	Preclinical		*[192]*
H3B-8800	*Phase I clinical trial (NCT02841540)*	*Small molecule modulator of SF3B1; Preferential lethality toward spliceosome-mutant cancer cells due to retention of short, GC-rich introns*	*[201]*
Targeting spliceosomal regulatory proteins			
TG003	Preclinical	*Competitive antagonist of CLK binding of ATP; Inhibition of CLK enzymatic phosphorylation and activation of splicing factors e.g. SR proteins; Dissociation of nuclear speckles*	*[202]*
SRPIN340	Preclinical	*Competitive antagonist of SRPK1 and SRPK2 binding of ATP; Nicotinamide inhibitor; Inhibits SRPK phosphorylation and activation of splicing factors e.g. SR proteins; Modulates splicing of VEGF*	*[203]*
Cpd-1, Cpd-2 and Cpd-3	Preclinical	*Inhibition of both CLKs and SRPKs, components of the splicing machinery that are crucial for exon selection; CLK1, CLK2, SRPK1 and SRPK2; Reduced phosphorylation of SR proteins; Causes enlargement of nuclear speckles; Causes widespread splicing alterations*	*[204]*
GSK525762	Phase I (NCT03150056)	*Inhibitors of bromodomain and extra-terminal (BET) proteins BRD2, BRD3, BRD4 and BRDT; Downregulate expression of splicing factors; Decrease alternative splicing events in pre-clinical models*	*[205]*
ZEN003694	Phase I/II (NCT02711956)		*[206]*
OTX105/MK-8628	Phase I (NCT02259114)		*[207]*
Other small molecule inhibitors			
Isoginkgetin	Preclinical	*Biflavonoid natural plant product that interferes with the recruitment of the snRNP U4/U5/U6; Prevents transition from spliceosomal complex A to B*	*[208]*
NB-506	Preclinical	*Inhibits SRFS1 phosphorylation by topoisomerase I; In vitro disrupts early spliceosome assembly and produces a cytotoxic effect*	*[209]*

Table 1.1: Small molecules reported to target the process of splicing. snRNP = small nuclear ribonuclearprotein, CLK = CDC2-like kinase; SRPK = serine and arginine protein kinase; SRPIN340 = N-(2-(piperidin-1-yl)-5-(trifluoromethyl)phenyl; VEGF = vascular endothelial growth factor.

The potential clinical utility of bacterial fermentation products has been adequately demonstrated in preclinical studies, as observed, for example, in the dose-dependent inhibition of growth seen in experiments involving prostate cancer xenografts following treatment with pladienolide B [197]. However, the findings of early phase clinical trials have been less compelling. In two phase I, open-label, single-arm, dose-escalation studies, investigators assessed the safety and efficacy of pladienolide E7107 in patients with locally advanced or metastatic solid tumours. Data from both trials showed that E7107 was generally well tolerated and produced both dose-dependent and reversible inhibition of pre-mRNA processing in target genes *in vivo* [210], although both trials were suspended owing to unexpected incidences of bilateral optic neuritis [210, 211].

H3B-8800, a small-molecule modulator of SF3B1 [201], has also entered a phase I clinical trial (NCT02841540). This trial aims to determine the safety and recommended phase II dose in patients with myelodysplastic syndromes, acute myeloid leukaemia, or chronic myelomonocytic leukaemia, in which recurrent heterozygous mutations of SF3B1 are thought to have a pathological role. If found to be efficacious in subsequent phase II and phase III trials, H3B-8800 could provide proof of principle that targeting the spliceosome is a valid treatment strategy that could open a variety of new therapeutic avenues. However, the toxicity and tolerability of these agents will equally prove to be important factors that will dictate whether or not these agents will ever enter routine clinical use.

1.6.2 Targeting spliceosomal regulatory proteins

Rather than targeting the core spliceosome complex, an alternative approach is to modulate splicing by targeting one or more of the proteins that regulate it. For example, lysine demethylase 3A (KDM3A), also known as Jumonji domain-containing protein 1A (JMJD1A), has been reported to be an important regulator of AR splicing. In a report by Fan et al., knockdown of JMJD1A by short hairpin RNA (shRNA) reduced AR-V7 expression levels in prostate cancer cells, but had no effect on AR-FL [212]. This study reported that mechanistically, JMJD1A/KDM3A promoted alternative splicing of AR-V7 through recruitment of heterogeneous nuclear ribonucleoprotein F (HNRNPF), a splicing factor known to regulate exon inclusion, to cryptic exon 3b on AR pre-mRNA [212]. In light of these results, the authors

concluded that therapeutic targeting of JMJD1A, through its regulation of splicing factor HNRNPF, may inhibit the expression of AR-V7 and serve as a novel strategy in the treatment of CRPC. Interestingly, another Jumonji C (JmjC) domain containing lysine demethylase, lysine demethylase 4B (KDM4B), has also been implicated in the regulation of AR-V7. In a study by Duan et al., KDM4B was shown to be phosphorylated by protein kinase A under androgen-deprived conditions, eliciting its binding to both splicing factor 3b subunit 3 (SF3B3), and AR pre-mRNA near the 5' splice site of cryptic exon 3b [213]. In doing so, KDM4B was reported to serve as a *trans*-acting splicing factor and scaffold that recruits and stabilises the spliceosome near cryptic exon 3b on AR pre-mRNA, thus promoting its inclusion and the expression of AR-V7 [213]. Together, these examples highlight the potential utility of targeting spliceosome regulators as a therapeutic strategy that can overcome splice-variant mediated treatment resistance; however as yet no pharmacological inhibitors of these proteins have entered early phase trials for the purpose of overcoming oncogenic AR-V7 signalling.

In addition to these insightful preclinical data, a variety of compounds have been identified that can inhibit SR protein phosphorylation, and these have been shown to inhibit splicing *in vitro* [214]. TG-003, a benzothiazole, is one such agent and functions as an inhibitor of CLK1, CLK2, and CLK4, all of which are members of the CDC2-like (or LAMMER) family of dual-specificity protein kinases. These kinases are typically involved in the phosphorylation of SR proteins in the nucleus [202], the inhibition of which results in inhibition of splicing and dissociation of spliceosomal nuclear speckles [202]. More recently, bromodomain and extra-terminal (BET) protein inhibition, a promising therapeutic approach currently undergoing clinical evaluation in CRPC (NCT03150056, NCT02711956), has also been shown to effect alternative splicing by modulating spliceosomal regulators [207, 215], and are discussed in more detail in **section 1.6.1**.

1.6.3 Other small molecule inhibitors of the spliceosome

Several other small molecules have also been identified as being capable of modulating the spliceosome, some of which have been reported to have antitumor activity in preclinical cancer models. However, these studies have generally been limited by their use of

cell-free and non-mammalian models [216], and, as such, the therapeutic application of many of these agents is currently considered limited. Despite this lack of clinical implementation thus far, some interesting results have been seen with a number of these agents. For example, NB-506, a glycosylated indolocarbazole derivative that inhibits the capacity of topoisomerase I to phosphorylate SRFS1, has been shown to disrupt early spliceosome assembly and have a cytotoxic effect in murine P388 leukaemia cells [209]. In addition, preclinical antitumor activity of the biflavonoid natural plant product isoginkgetin has also been demonstrated, which occurs, at least in part, through the ability of this agent to interfere with the recruitment of the snRNPs U4, U5, and U6, thereby inhibiting splicing by precluding the transition from spliceosomal complex A to complex B [208].

1.6.4 Targeting the spliceosome in oncogene-driven cancers

As described previously, MYC overexpression places considerable oncogenic stress on the spliceosome, resulting in cells becoming equally dependent on the spliceosome for survival as they are on MYC. This observation has led to the hypothesis that, in these tumours, inhibition of the spliceosome might have an anticancer effect. In support of this view, spliceosome dysregulation through inhibition of SF3B1 using sudemycin D has been reported to increase survival and limit the formation of metastases in xenograft models of MYC-dependent breast cancer [78]. Ultimately, although intriguing, whether this principle will be applicable to other similarly important genomic aberrations, or whether the clinical utility of this approach will be limited to a subset of MYC-dependent cancers remains to be seen.

1.6.5 Targeting alternatively spliced variants

When devising therapeutic strategies to target pathological alternatively spliced variants, in addition to considering those generated through the action of the spliceosome, taking into account protein variants generated through alternative means, for example as a consequence of genomic fusions or rearrangements (which have been described in many cancers) is equally important. As such, while targeting the spliceosome remains a key consideration in this process, given the multiple routes through which alternatively spliced variants can arise, the concept of directly targeting these protein variants, rather than their mechanism of origin, seems logical. Efforts to target alternatively spliced proteins remain

attractive, but doing so directly with small-molecule inhibitors has to date proved challenging, often owing to the altered nature of these alternatively spliced variants. For example, because AR-SVs are truncated and generally lack the AR LBD, alternative target sites are required to facilitate their inhibition. However, the disordered nature of the AR NTD renders a consistent target site difficult to ascertain and has to date hindered drug discovery efforts, thus necessitating the development of novel therapeutic strategies. One such proposed approach involves the use of monoclonal antibodies such as GP369, which specifically blocks the IIIb splice variant of FGFR2 [217]. GP369 demonstrated antitumor activity in preclinical studies involving human cancer models driven by activated FGFR2 signalling [218]. A phase I trial involving patients with advanced-stage solid tumours known to express FGFR2 was opened (NCT02368951) on this basis, although the trial was terminated early owing to safety concerns regarding the development of nephrotic syndrome in two participants during dose-escalation, preventing the attainment of a therapeutic dose. Despite this setback, the ability to target alternatively spliced protein isoforms using monoclonal antibodies could yet help to circumvent the difficulties associated with directly inhibiting extracellular splice variants, which have hampered drug discovery efforts in this area to date.

1.6.6 Oligonucleotide therapy

Oligonucleotide-based therapies involve the use of engineered oligonucleotides designed to hybridise with RNA sequences that are known to be responsible for specific splicing events in order to prevent their alternative splicing and the production of erroneous protein products with pathological consequences. The potential of these therapeutic agents has so far been best realised in patients with neurodegenerative conditions, including those with Duchenne muscular dystrophy [219] or spinal muscular atrophy [220], in which late-stage clinical trials are underway. However, an important question remains as to whether oligonucleotide therapy is a viable treatment approach in cancer and particularly in cancers with more diverse splicing events. Evidence supporting the use of oligonucleotide therapy in patients with cancer stems from work by Smith et al. [221], who developed a novel RNA splice-switching oligonucleotide designed to induce skipping of exon 11 in BRCA1, which is crucial to the DNA damage repair functions of the protein. In doing so the authors successfully rendered wild-type BRCA1-expressing cell lines more susceptible to PARP inhibition [221].

This approach provides a fascinating potential therapeutic strategy for targeting cancers with wild-type BRCA1, although the challenge in this setting is to maintain BRCA1 function in non-malignant cells and thus minimize the potentially widespread risks of toxicity [222].

1.7 Targeting alternative splicing in prostate cancer

As outlined in **section 1.6**, a variety of different approaches have been investigated to identify novel strategies of overcoming the oncogenic effects of alternative splicing in cancer. Over the past decade, reports have similarly emerged of drugs in early phase clinical trials capable of impact the generation of AR-SV in prostate cancer; albeit with varying degrees of success.

TAS3681 is a novel AR antagonist that has recently entered into early phase clinical trials. TAS3681 has been reported to inhibit AR-FL transactivation and decrease the expression of both AR-FL and AR-SVs in preclinical models [223]. The current phase I, open-label study of TAS3681 in patients with metastatic CRPC (NCT02566772) is therefore of great interest to the field, and will be invaluable in elucidating the tolerability, efficacy and potential clinical utility of this agent for the treatment of lethal prostate cancer. While TAS3681 targets the intimate relationship between the AR and AR-SVs to inhibit the expression AR-SVs, EPI-001 and its analogues instead directly target AR-SVs. These agents bind to transcription activation unit 5 (Tau5; residues 370 to 494 [224]) of AF-1 (activation function 1) in the AR NTD and block protein-to-protein interactions critical for AR transcriptional activity, thereby inhibiting the growth of CRPC xenografts in mice [225]. In spite of the encourage preclinical data reported with EPI-001 and its analogues, concerns exist regarding the high concentrations of these drug that are required to elicit an antitumor effect. Consequently, a recent phase I/II trial of EPI-506 in patients with metastatic CRPC who have progressed on abiraterone and/or enzalutamide (NCT02606123) was terminated at the end of the phase I stage due to an excessively high pill burden (18 capsules/day). Interestingly, the antiparasitic agent ivermectin has also recently been shown to reduce AR-V7 levels in *in vitro* models of CRPC [226]. Ivermectin, has amongst other things [227], been shown to be an inhibitor of heat shock protein 27 (HSP27) [226]. In a study by Nappi et al., ivermectin reduced AR and AR-V7

protein levels, however this was not accompanied by a reduction in mRNA levels, suggesting that ivermectin interrupts in the protein stability of AR and AR-V7. Indeed, HSP27 has an established role in AR trafficking and stability [13]. Given the knowledge of its toxicology and pharmacology, ivermectin merits clinical evaluation for the treatment of lethal prostate cancer.

While neither TAS3861, ivermectin, nor EPI-001 (or its analogues) target the process of splicing, onalespib, a heat shock protein 90 (HSP90) inhibitor, has been shown to reduce AR-V7 expression *in vitro* by directly downregulating the frequency of alternative splicing events [228]. In a study by Ferraldeschi et al., onalespib reduced AR-V7, but not AR-FL, mRNA levels, indicating that HSP90 inhibition specifically disrupted AR-V7 splicing [228]; Although, in this study the specific splicing factors important to AR-V7 production were not ascertained. As with EPI-506 however, early phase clinical trials of onalespib have been disappointing, with the phase I/II study of onalespib in combination with abiraterone and prednisolone (NCT01685268) not showing sufficient clinical activity to justify further exploration in larger clinical trials. Encouragingly however, HSP90 inhibitors remain in development and recently the oral HSP90 inhibitor TAS-116 has shown promise in a first-in-human phase I study in patients with advanced solid tumours (NCT02965885). In addition to HSP90 inhibition, more recently, BET inhibition, a promising therapeutic approach that is currently undergoing clinical evaluation in patients with CRPC (NCT03150056 and NCT02711956), has also been shown to directly affect alternative splicing by modulating spliceosomal regulators [207, 215].

1.7.1 Therapeutic targeting of BET proteins in CRPC

The BET motif family of proteins, which include the proteins BRD2, BRD3, BRD4 and BRDT, serve as multi-functional chromatin effector proteins with critical roles in transcription and chromatin biology [229]. Importantly, BET proteins comprise two N-terminal bromodomains, and an extra-terminal domain. Bromodomains typically recognise and bind to acetylated lysine residues. While this has been most classically described to occur on histone H4, they have also been reported to recognise non-histone acetylated proteins including transcription factors such as twist family bHLH transcription factor 1 (TWIST1), and RelA, which is involved in nuclear factor kappa-light-chain-enhancer of activated B cells (NF-

kB) heterodimer formation. The characteristic BET extra-terminal domain meanwhile, facilitates protein-protein interactions such as the binding of BRD4 to p53 [230], and enables BET proteins to function as protein scaffolds at gene promotors and enhancers. Together, these properties enable BET proteins to bind to activated chromatin at acetylated lysine residues, and facilitate the initiation and elongation phases of transcription. While the mechanisms underlying this function have not yet been fully elucidated, it has been proposed that once bound to activated chromatin, BET proteins displace HEXIM1/7SK snRNP from the positive transcription elongation factor b (P-TEFb) complex, thereby enabling the phosphorylation and activation of RNA Pol II, and facilitating the progression of transcription. Consequently, the BET family of proteins have been implicated in the development and progression of cancer. In keeping with this, the competitive bromodomain inhibitors JQ1 and GSK1210151A (I-BET151) have been reported to cause early cell cycle arrest and apoptosis in haematological malignancies by displacing BRD4 from active chromatin and causing subsequent removal of RNA Pol II from key target genes [231, 232].

1.7.1.1 Development of BET inhibitors

The first compounds demonstrated to be capable of inhibiting bromodomains were not focused on the inhibition of the BET motif family of proteins, but rather the acetyltransferase CREB-binding protein (CBP) [233, 234]. These early compounds were however considered unsuitable for clinical development given their low level of binding affinity. Since these initial studies, more potent and selective inhibitors have been developed and have been shown to be able to inhibit BET proteins. In 2010, the thieno-triazolo-1,4-diazepine JQ1 was demonstrated to displace BRD4 from nuclear chromatin at nanomolar concentrations [235]. Importantly, JQ1 was found to inhibit the growth of NUT-midline carcinoma (NMC) cell lines and a xenograft model, thereby establishing MNC as the archetypal cancer amenable to treatment with BET inhibition [235]. Alongside this work, the novel benzodiazepine GSK525762A (I-BET762) was also shown to selectively bind BET proteins with nanomolar affinity [236, 237]. Subsequently, these reports were followed by preclinical data suggesting that I-BET762 demonstrated anticancer activity in myeloma, acute leukaemia and solid cancers, including NMC.

In light of these encouraging preclinical data, a number of BET inhibitors have been investigated within early phase clinical trials for activity against both haematological and solid-organ malignancies. Results from these clinical trials have however been mixed, although clinical trials in haematological malignancies have to date fared better than those focused on solid-organ cancers. For example, while the BET inhibitor OTX015 induced remissions in a phase I acute leukaemia study [238], including complete remission in two patients with refractory disease, treatment with OTX015 yielded only 4 partial responses amongst 46 patients with advanced solid malignancies, with three of these occurring in patients with NMC [239]. Consequently therefore, while there may be a role for BET inhibitors in the treatment of some haematological malignancies such as Multiple Myeloma and Acute Myeloid Leukaemia (AML), beyond the use of BET inhibitors for the treatment of NMC, treatment-related toxicities have thus far hampered the development of many novel BET inhibitors for the treatment of solid-organ cancers (further discussed in **section 1.7.1.2**).

A contributing factor to the adverse effects seen with the BET inhibitors that have been evaluated for the treatment of solid-organ malignancies to date is that these agents typically have a broad spectrum of activity, inhibiting all members of the BET motif family of proteins. Interestingly, unlike these agents, RVX-208, a quinazolone derivative of resveratrol that has been evaluated in phase II clinical trials for the treatment of atherosclerosis, has been shown to preferentially bind to the second bromodomain (BD2) of the BET proteins BRD2 and BRD3 [240]. RVX-208 therefore provides proof-of-concept that selective pharmacological inhibition within the BET family is feasible, which may assist in improving the toxicity profile associated with BET inhibitors. However, mechanisms of redundancy between the BET family of proteins may ultimately limit the efficacy of individual BET protein inhibition in the treatment of cancer [215]. Therefore, rather than inhibiting individual BET proteins, an alternative strategy for maximising the clinical utility of BET inhibitor therapy in solid-organ malignancies is instead to identify patients in whom BET inhibitor treatment is likely to be most efficacious; thereby shifting the risk vs benefit ratio in favour of their use.

As discussed above, BET proteins have been reported to play an important role in cancer biology through their role in the regulation of transcription elongation. In addition, however, BET proteins have also been reported to promote aberrant expression of the

transcription factor MYC, which has been implicated in the pathogenesis of a variety of human cancers. For example, the BET protein BRD4 has been shown to bind to both the promotor and enhancer regions of MYC, thereby regulating its expression [232, 241]. Furthermore, a number of preclinical studies have now demonstrated that BET inhibition downregulates MYC RNA and protein expression [207, 215, 232, 242, 243], with this being a key contributor to the anticancer activity observed with BET inhibition. Taken together, these findings have led to the hypothesis that MYC-driven cancers may be particularly sensitive to BET inhibitor therapy. In support of this theory, in a study by Bandopadhayay et al., the BET inhibitor JQ1 decreased the viability of MYC-amplified medulloblastoma cells by triggering G1 arrest and apoptosis [243]. Furthermore, JQ1 significantly prolonged the survival of MYC-amplified medulloblastoma xenograft models [243]. However, recent reports suggest that re-activation of MYC signalling, such as through upregulation of Wnt signalling pathways following BET inhibition, may serve as an acquired resistance mechanism to BET inhibitor therapy [244, 245]. Mechanisms of redundancy such as these may explain why clinical trials that have evaluated the activity of BET inhibitors in patients with MYC-amplified solid tumours have to date not yielded positive results. Such trials are however early phase trials, and are very limited in number. Consequently, further work is required to determine whether or not MYC-driven cancers represent a subset of cancers that may be more sensitive to BET inhibitor therapy. Encouragingly, such studies are currently underway, for example the study of the BET Inhibitor BMS-986158 in paediatric cancer, within which a specific inclusion criterion is the presence of MYC/MYCN amplification or high copy number gain (NCT03936465).

1.7.1.2 Utilisation of BET inhibitors in CRPC

BET inhibition has emerged as a potential novel therapeutic strategy in prostate cancer with the discovery that the BET protein BRD4 directly interacts with the AR NTD. Inhibition of BRD4 by JQ1 has been shown to not only disrupt AR recruitment to AR target gene loci, but also *in vivo* has been demonstrated to be more efficacious in inhibiting CRPC xenograft growth than direct AR antagonism. Furthermore, in a study by Asangani et al. JQ1 was reported to decrease the expression of AR-V7 in preclinical models of CRPC by down-regulating the activity of splicing factors SRSF1 and U2AF65, and in doing so, re-sensitised enzalutamide-resistant prostate cancer cells to AR-targeted therapy [207].

In light of these promising preclinical data, numerous BET inhibitors are being evaluated in early phase clinical trials for a variety of cancer types, including prostate cancer. In a phase Ib trial by Massard et al., 46 patients with advanced solid malignancies were treated with the BET inhibitor OTX015, of which 26 had a diagnosis of CRPC [239]. Four patients on this trial had a partial response, including a man with CRPC. However, alongside reports of the clinical activity of this new therapeutic strategy, concerns have also been raised regarding the adverse effects associated with BET inhibition. Reported adverse effects include thrombocytopenia, anaemia, neutropenia, nausea, diarrhoea, fatigue and hyperbilirubinemia [238, 246-248], with these toxicities being reversible with treatment interruption. Similar toxicities have also been reported with other BET inhibitors under clinical evaluation (CPI-0610 [249], GSK525762 [250] and TEN-010 [251]), however more concerningly, development of another BET inhibitor, BAY 1238097, was permanently interrupted due to severe adverse effects occurring below the predicted therapeutic dose [252]. In addition to these reports, preclinical models have also raised concerns of potentially serious adverse effects associated with BET inhibition including hyperinsulinemia [253] and neurological toxicity including impaired long-term memory [254], reduced exploratory motor activity and anxiety [255]. Overall, therefore, the long-term success of BET inhibition as a clinically useful therapeutic modality is likely to be limited by their poor tolerability.

1.8 Translating promising pre-clinical targets into clinically useful therapeutics

Despite the range of therapeutic targets and novel therapies outlined in **sections 1.6** and **1.7** that have been proposed to modulate the spliceosome, there remains a lack of medications capable of modulating alternative splicing events approved for clinical use. This is in part likely to be due to the difficulties in translating encouraging preclinical data into meaningful clinical benefit for patients. The validity of preclinical data is heavily dependent on the accuracy with which the models used preclinically replicate human disease, which is incredibly difficult given the complexity of cancer. Consequently, positive *in vitro* and *in vivo* results using novel therapies are often not replicated in early phase clinical trials [256]. The successful translation of preclinical developments into clinical trials therefore requires

consideration of a number of different factors, including the biology of the target, the biochemistry of the drug, and the relationship between the patient and the disease.

1.8.1 Understanding the biology of the target

A principle consideration regarding the development of a new therapy is the role of the proposed therapeutic target in both pathological and non-pathological states. The importance of a novel therapeutic target to a disease of interest is often determined preclinically in *in vitro* and *in vivo* studies. However, issues such as mechanisms of redundancy, particularly with regards to the speed with which these mechanisms compensate for target inhibition, and the importance of the target for the survival of normal/non-malignant cells, are harder to accurately evaluate. These considerations are however key to determining the clinical utility of a novel therapy as they can both contribute to treatment failure, either due to lack of efficacy or toxicity respectively. Consequently, there is an increasing drive to evaluate novel targets and therapies in multiple *in vitro* and *in vivo* models of disease with differing genomic backgrounds, and amalgamate these with additional data from patients, such as sequencing and patient clinical outcome data. Recently, these efforts have been aided by the development of patient-derived xenograft and organoid models [257].

Just as the design of rational hypothesis-driven preclinical studies is therefore fundamental in contributing to the success of translating preclinical findings into clinical trials, likewise understanding of the biology of a target enables investigators to most optimally evaluate the impact of a novel therapy within a clinical trial. Evaluating the pharmacodynamics (PD) of a novel therapeutic agent is critical to establishing its activity, toxicity, therapeutic window and duration of action. Assessments investigating the PD of a novel agent are typically incorporated into the design of a clinical trial before it is commenced, therefore understanding of the biology of the target is crucial for deciding when patient samples should be taken, where they should be taken from, and how often they should be taken. If these decisions are incorrect, therapies under evaluation in clinical trials could be erroneously considered to be ineffective, or worse still, potential toxicities could be missed.

1.8.2 Understanding the biochemistry of the drug

The biochemistry of a potential novel therapeutic agent is a fundamental consideration when developing a clinical trial, and this encompasses a range of factors such as on- and off-target activity, toxicity and drug pharmacokinetics (PK).

In a recently study by Lin et al., ten anti-cancer drugs under evaluation in clinical trials were investigated to confirm their proposed mechanism of action [258]. In this study, it was reported that none of the evaluated therapies acted through their intended targets [258]. This included the small molecule p21 (RAC1) activated kinase 4 (PAK4) inhibitor PF-03758309, for which a phase I trial in advanced solid tumours was discontinued early due to the lack of an observed dose-response relationship [258, 259]. While this may mean some anti-cancer therapies work because they are acting on unintended targets, it is perhaps more likely that clinical trials fail because the agents used are not achieving the desired on-target effect. By the same token, resultant off-target effects can lead to severe treatment-related toxicities. Stringent validation of the mechanism of action of cancer drugs in the preclinical setting is therefore an important step in translating a novel therapy into a clinical trial, however, issues such as funding/cost and clinical need may limit the extent to which more rigorous preclinical investigations are conducted, which is a limitation of the current model of drug development.

While it is therefore important to understand what impact a novel therapeutic agent has on a patient, it is equally important to appreciate what effect the patient's body has on the drug. In *in vitro* preclinical studies, therapeutic agents are typically directly applied to cell lines and/or patient-derived models. Consequently, issues such as the bioavailability of a drug are less consequential in these studies. This is in stark contrast to drug administration in patients, where the absorption, distribution, metabolism, and excretion of a therapeutic agent all have a direct impact on its clinical activity. Establishing the PK of a novel therapy is therefore vital in determining its optimal dosing and scheduling. For example, if the absorption of a drug is poor, or if its first-pass metabolism if high, the amount of drug a patient may need to take in order to achieve a therapeutic dose may be unacceptable for daily administration, detrimentally impacting patient compliance. Similarly, if a drug has a narrow therapeutic window, changes in rates of absorption and excretion can result in a drug either being ineffective, if the therapeutic dose is not reached, or toxic, if its levels accumulate. Such

is the importance of a drug PK in fact, that undesirable PK characteristics have been responsible for the abandonment of numerous drug development programmes [256, 259, 260], highlighting the importance of drug PK in translating preclinical developments into the clinical setting.

1.8.3 Understanding the relationship between the patient and the disease

As discussed above, understanding the relationship between the patient and the drug can greatly improve both the validity of preclinical studies, and the quality of clinical trial designs, which together can increase the likelihood of success when translating preclinical findings into the clinic. In addition however, an appreciation of the relationship between the patient and the disease is equally important. A key consideration in this regard is the risk verses benefit of a new treatment. If a novel therapy is being trialled for a condition that is not life threatening, and where recovery would otherwise occur without intervention, the threshold for acceptable toxicity, and the impact on patient quality of life, will be set very high. Conversely, if a patient is likely to die of their disease relatively quickly without intervention, especially in a condition when there are limited non-curative treatment options available, adverse effects of treatment may be more tolerable if they are manageable. An awareness of how a novel therapy may affect this balance therefore, is important in designing a clinical trial that is more likely to succeed. One strategy for minimising the detrimental impact a novel therapy may have on a patient is through the utilisation of patient selection methods, which aim to ensure that patients enrolled onto clinical trials are the most likely to receive a clinical benefit. The success of this approach however, again requires an understanding of the biology of both the target and the patient, and an understanding of the biochemistry of the drug. Recently, the development of clinical biomarkers have assisted investigators in overcoming this challenge.

1.8.3.1 Biomarkers

The World Health Organisation defines a biomarker is any measurable substance, structure or process that can influence or predict the incidence of an outcome or disease [261]. With the dawn of precision medicine, and the development of next-generation

sequencing technologies and improved imaging modalities, there has been a huge drive to identify novel predictive and prognostic biomarkers.

Predictive biomarkers predict response to specific therapeutic interventions such as erb-B2 receptor tyrosine kinase 2 (also known as HER2) expression, which predicts response to trastuzumab (Herceptin) in breast cancer [262]. In contrast, prognostic biomarkers inform physicians regarding the risk of clinical outcomes in the future, for example cancer recurrence or disease progression. In addition to these, diagnostic biomarkers are also in development, seeking to identify whether a patient has a specific disease condition. For example, diagnostic biomarkers have recently been implemented for colorectal cancer surveillance by testing for stool cancer DNA [263]. However, there remains a large gap between biomarker discovery, and the adoption of their clinical use.

A number of biomarkers have been shown to have clinical utility in prostate cancer, including one of the oldest and most widely used biomarkers, prostate specific antigen (PSA). PSA is a protein that is produced by both normal and malignant cells of the prostate gland, which has been shown to be elevated in the blood of men with prostate cancer [264]. Since its original FDA approval in 1986 [265], PSA has gone on to serve as a diagnostic biomarker of prostate cancer, and a prognostic biomarker indicative of prostate cancer recurrence and/or progression, which is still used clinically today [266]. PSA is not however without its limitations. PSA is produced by normal prostate epithelial cells, meaning its levels can fluctuate in the absence of underlying malignant disease. In addition, PSA levels can be increased by infection/inflammation of the prostate, and following digital rectal examination of the prostate [264]. Furthermore, more aggressive prostate cancers, such as those with a neuroendocrine-like phenotype that lose AR expression, may not express PSA and produce falsely reassuring PSA measurements [267]. As a consequence of these limitations, PSA measurement alone is not recommended for the diagnosis and/or monitoring of prostate cancer in patients, and is instead is considered alongside other investigations such as bone and soft tissue imaging, and histologically evaluation of patient tissue biopsies.

More recently, with the advent of next-generation sequencing technologies, other novel predictive biomarkers have also now been approved for use in patients with lethal

prostate cancer. Importantly, these biomarkers have been shown to predict response to specific targeted therapies. For example, the detection of deleterious genomic aberrations in DNA repair genes, such as BRCA2, has been shown to predict sensitivity to PARP inhibition in patients the metastatic CRPC [23]. Similarly, detection of micro-satellite instability in metastatic CRPC patient tissue samples has been shown to predict sensitivity to immune checkpoint inhibition [268]. Detection of these biomarkers, however, requires patient tissue sampling, which can be painful and inconvenient for patients. As such, work is currently ongoing to identify other, less invasive, clinically useful biomarkers.

Circulating tumour cells (CTCs) are cell released from primary tumours and metastases into the blood. Over the last 20 years, it has been discovered that CTCs can be detected and quantified in blood samples taken from patients with metastatic prostate cancer [269]. Moreover, prospective studies in patients with metastatic CRPC have shown a detectable CTC count of ≥5 CTC / 7.5 mL of blood to be associated with a significantly worse overall survival [269]. In addition to the presence of CTCs serving as a prognostic biomarker, recently it has been shown that single CTCs can be captured from circulating blood and sequenced, which has opened the door to numerous new avenues for clinical research. Notably, this has enabled the detection of AR-V7 mRNA from CTCs in the blood of patients with metastatic CRPC receiving AR-directed therapies. In a study by Antonarakis et al., the detection of AR-V7 in CTCs from men treated with abiraterone or enzalutamide was associated with a lower PSA response, a shorter progression-free survival, and a shorter overall survival compared with those patients without detectable circulating AR-V7 [89]. Although, as discussed in **section 1.5.2**, some groups have not replicated these findings. Nonetheless, in spite of these encouraging data, the complexities, cost and logistical challenges of successfully capturing and characterising single CTCs from samples containing millions of white cells has so far hindered the widespread use of CTCs clinically. Furthermore, the interpretation of detectable CTCs is dependent on the methods through which CTCs are analysed, which as discussed in **section 1.5.2**, is not standardised and still requires prospective validation. However, as technologies improve and become more cost-effective, the adoption of CTCs as clinical biomarkers may become more commonplace.

Alongside improvements in analysing patient blood and tissue samples, over the past two decades there has also been great improvement in the quality of radiological imaging. Although computer tomography (CT) and bone scans remain the standard of care for diagnosing metastatic prostate cancer and monitoring response to treatment, improvements in positron-emission tomography (PET) and magnetic resonance imaging (MRI) have seen these imaging modalities increase in popularity, demonstrating higher sensitivity and specificity [270], albeit when used in the right context. In addition to these, the development of prostate-specific membrane antigen (PSMA)-based imaging has provided a further step forward in the delineation of prostate cancer spread [271]. Importantly, PSMA has also emerged as predictive biomarker in prostate cancer. PSMA is overexpressed in prostate cancer and is the target of numerous radionuclides (antibody or small molecule), immunotherapies and antibody-drug conjugates (ADC). These therapies have been shown to improve survival in patients with metastatic CRPC [272, 273], however their efficacy is dependent on the expression of PSMA, with non-responder rates of approximately 30% have been reported [273-275]. This is likely, in part, due to the expression of PSMA being heterogenous [276]. Consequently, the use of PSMA-based imaging has emerged as an important tool in patient selection for PSMA-directed therapies, demonstrating it to be a predictive biomarker for these treatments.

Overall therefore, there are a number of challenges that hinder the successful translation of preclinical developments into clinical trials and their subsequent adoption into clinical practise. However, rigorous preclinical evaluation of novel therapeutic targets and therapies in hypothesis-driven studies that have been carefully designed to maximise understanding of the biology of the target and the biochemistry of the drug, in the context of both normal and pathological states, can mitigate against a number of these challenges. Although, this can be challenging within the current model of drug development, requiring the commitment of both investigators and funders alike. Furthermore, scientific and technological advances must also be subject to thorough prospective analytic and clinical validation with prespecified endpoints, predefined interventions, and adequate statistical power, before they can be considered for more widespread clinical use.

1.9 Conclusion

Despite the recent success of AR-directed therapies in treating metastatic CRPC, all these tumours eventually acquire resistance that invariably results in fatal disease progression. This resistance is in part due to the development of constitutively active AR-SVs that are truncated and lack the regulatory AR LBD which is the target of all currently available AR directed therapies. Of the many AR-SVs that have been reported, AR-V7 is the most prevalent, and the best studied, and has been associated with resistance to AR targeting therapies and poorer overall survival. Drug discovery efforts to target AR-V7 directly have, however, been challenging; thus, modulation of the spliceosome as a therapeutic tool represents an attractive alternative option, although, as yet, spliceosome inhibitors have not entered clinical practice in patients with prostate cancer, largely owing to the complexity of the spliceosome and a lack of understanding of its biology. Further research is required in order to identify the exact mechanisms underpinning the splicing abnormalities that are thought to contribute to the progression of CRPC, as well as the consequences of inhibiting these factors, before the true utility of these therapies can be realised.

2

Rationale for research

Despite the recent success of AR-directed therapies in treating advanced prostate cancer, all patients eventually acquire resistant disease, leading to invariably fatal disease progression [18]. This resistance is in part due to the development of constitutively active AR-SVs that are truncated and lack the regulatory AR LBD; the target of current AR-directed therapies [5, 27, 92]. Of the many AR-SVs that have been reported, AR-V7 is the most prevalent, and the best studied, and has been associated with resistance to AR targeting therapies and poorer overall survival [91, 92]. Efforts to target AR-V7 directly have, however, proved challenging due to the inherently disordered nature of the AR N-terminal domain [5]. As such, there remains an urgent unmet clinical need for novel therapeutic strategies to overcome AR-SVs and improve outcomes for patients with advanced prostate cancer.

One strategy to abrogate AR-V7-mediated resistance in metastatic CRPC is to target epigenetic processes that regulate proteins involved in AR-V7 generation and/or stabilization. In this regard members of the BET motif protein family are of particular interest as they have been shown to modulate AR signalling [215]. BET inhibition has been demonstrated to reduce AR-V7 protein levels, and the growth of enzalutamide-resistant patient-derived PC models, in part by blocking alternative splicing by the spliceosome [207, 215]. However, BET proteins have pleiotropic roles and regulate many signalling pathways, perhaps explaining why despite extensive efforts, no BET inhibitors have yet been approved for clinical use, with dose-limiting

toxicities restricting their clinical utility [277]. Nonetheless, the encouraging biochemical and antitumor activity seen with BET inhibition preclinically suggests that modulating alternative splicing to overcome oncogenic AR-V7 signalling is an attractive therapeutic strategy. Although, a better understanding of the mechanisms underlying the regulation of alternative splicing in CRPC is needed to facilitate the development of novel therapeutic strategies that can replicate the antitumor effects of BET inhibition, but also mitigate its associated adverse effects.

Interestingly, there is a growing body of evidence to suggest that despite the ubiquitous expression of the BET motif family of proteins, not all cancer cell types are sensitive to BET-inhibitors *in vitro* [242, 278]. One possible explanation for this lack of antitumor activity is that BET-mediated regulation of cellular processes may be tissue and context dependent. In keeping with this concept, Wu et al. demonstrated that BRD4 interacts with sequence-specific DNA-binding transcription factors in a gene-specific manner [279]. Given that tumour landscapes vary [103, 280], it is likely that different transcriptional regulators interact with the BET motif family of proteins in different cell types. Elucidation of the transcriptional regulators that are most significantly downregulated by BET-inhibition in prostate cancer cells may therefore identify the splicing regulatory genes/proteins that are most important for the regulation of alternative splicing in CRPC. Subsequently, therapeutic targeting of these genes/proteins, rather than the BET motif family of proteins, could replicate the antitumor effects demonstrated by BET-inhibitors (such as a reduction in AR-V7 levels), but potentially cause less toxicity, as these spliceosome regulators may be less critical to the survival of benign cells.

3

Hypotheses and specific aims

3.1 Hypotheses

I hypothesised that key spliceosome-related proteins that drive AR-V7 generation could be identified by a triangulation approach, analysing: 1) RNA-seq changes induced by BET inhibition, which downregulates AR-V7; 2) adaptations in prostate cancer cells as they become resistant to androgen deprivation by RNA-seq studies; 3) the top hits from a targeted siRNA screen of spliceosome-related genes. Furthermore, I hypothesised that by directly targeting identified key regulators driving AR-V7 splicing I could replicate the encouraging preclinical effects seen with BET inhibitors, while mitigating their associated adverse effects ***(figure 3.1)***.

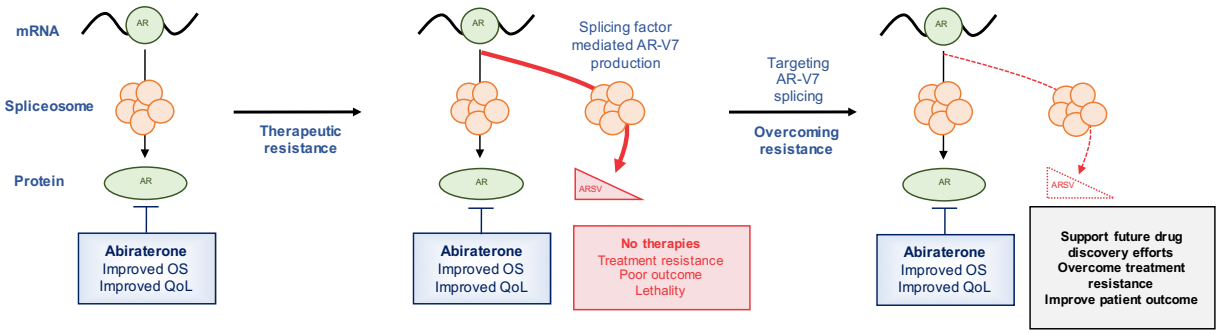

Figure 3.1: Schematic overview of hypothesis.

3.2 Specific Aims

The studies in my PhD aimed to identify and validate novel therapeutic targets capable of abrogating oncogenic AR-V7 signalling, to support future drug discovery efforts.

The specific aims of the project are:

1. To identify key spliceosome-related proteins that drive AR-V7 production *in vitro*.

2. To ascertain the clinical significance of identified regulators of AR-V7 production by evaluating their expression in metastatic CRPC tissue samples, and determining correlations with both AR-V7 expression, and patient clinical outcomes.

3. To determine the biological importance of identified regulators of AR-V7 production for prostate cancer cell growth and for AR-V7 production in preclinical models of prostate cancer.

4. To elucidate the underlying mechanisms through which identified spliceosome-related proteins regulate AR-V7 production.

5. To determine whether identified regulators of AR-V7 contain functionally important druggable pockets amenable to small-molecule pharmacological inhibition.

4

Materials and Methods

The work described herein has been conceptualised, performed and analysed by me unless otherwise stated in the relevant sections. I would, however, like to take this opportunity to formally acknowledge the contribution of the following people, without whom this work would not have been possible. I am truly grateful for their help and support.

- The siRNA screen described in this thesis was performed together with Dr Jonathan Welti, senior scientist in the de Bono research group (ICR). The raw data acquisition pertaining to the LNCaP95 portion of the siRNA screen was performed entirely by Dr Welti prior to commencement of my PhD. The interpretation of the results of this experiment involved multiple individuals in laboratory meetings that I attended, with my direct involvement.
- Raw data acquisition from the RNA sequencing studies described in this thesis was by Dr Jonathan Welti, with the subsequent bioinformatic analyses of these data being conducted with Dr Wei Yuan, bioinformatician in the de Bono research group (ICR).
- All bioinformatic analyses reported in this thesis were performed in collaboration with Dr Wei Yuan.

- The immunohistochemical studies of biopsies presented in this thesis were performed with the help of Ines Figueiredo (Higher Scientific Officer, ICR), Ana Ferreira (Higher Scientific Officer, ICR), and Ruth Riisnaes (Senior Scientific Officer, ICR).
- Immunohistochemical evaluation of cell pellets for antibody validation was performed with the help of Ines Figueiredo.
- Raw data acquisition from the RNA precipitation assay described in this thesis was by Soojin Kim, Research Scientist II, in collaboration with Prof. Stephen Plymate's research group (Department of Medicine, University of Washington School of Medicine and VAPSHCS-GRECC, Seattle, Washington, U.S.A.).
- Raw data acquisition and analysis of results from the Liquid Chromatography Mass Spectrometry (LC-MS) assay described in this thesis was performed by Dr Anthony Tumber, senior postdoctoral researcher in Prof. Christopher Schofield's research group (Chemistry Research Laboratory, Department of Chemistry, University of Oxford, Oxford, U.K.).
- The druggability assessments and associated figures presented in this thesis were done entirely by Patrizio di Micco, Structural Computational Biologist in Prof. Bissan Al-Lazikani's research group (ICR).

4.1 Reagents

4.1.1 General Reagents

Phosphate Buffered Saline (PBS)

Sodium Chloride	125 mM
Sodium Phosphate	16 mM
Sodium Hydrogen Phosphate	10 mM
pH 7.3	

10X Tris-Buffered Saline (TBS)

Sodium Chloride	1500 mM
Tris Base	200 mM
Adjust pH to 7.6 with 12 N Hydrochloride	
Deionized water to a final volume of 1 litre	

1X Tris-Buffered Saline, 0.1% Tween® 20 Detergent (TBST)

10X TBS Stock Solution	1000 mL
Tween® 20 detergent (Sigma Aldrich, Dorset, U.K.)	10 mL
Deionized water	9000 mL

4.1.2 Mammalian Cell Reagents

Thermo Fisher Scientific, U.K.

- Dulbecco's modified Eagle's medium (DMEM)
- Roswell Park Memorial Institute 1640 medium (RPMI-1640)
- RPMI-1640, no phenol red
- TrypLE™ Express Enzyme (1X), phenol red
- Penicillin/Streptomycin/L-Glutamine 100X concentrate

Penicillin G	10 mg/ml
Streptomycin	10 mg/ml
L-Glutamine	29.2 mg/ml

4.1.3 Protein Analysis Reagents

RIPA Lysis Buffer (Thermo Fisher Scientific, U.K)

Tris Hydrochloride Solution, pH 7.6	25 mM
Sodium Chloride	150 mM
Nonidet P-40 (NP-40)	1 % (v/v)
Sodium deoxycholate	1 % (v/v)
Sodium dodecyl sulphate (SDS)	0.1% (v/v)

NuPAGE™ MOPS SDS Running Buffer (20X)

3-(N-morpholino)propanesulfonic acid (MOPS)	50 mM
Tris Base	50 mM
SDS	0.1 %
Ethylenediaminetetraacetic acid (EDTA), pH 7.7	1 mM

Protein Transfer Buffer

20X NuPAGE™ Transfer Buffer (Thermo Fisher Scientific, U.K.)	100 mL
Methanol	200 mL
Deionized water	1700 mL

NuPAGE™ LDS Sample Buffer (4X)

(Thermo Fisher Scientific, U.K)

Invitrogen™ NuPAGE™ Sample Reducing Agent (10X)

(Thermo Fisher Scientific, U.K.)

4.1.4 Bacterial Cell Reagents

Luria-Bertani (LB) Medium Plus Ampicillin

Tryptone	10 g
Yeast Extract	5 g
Sodium Chloride	10 g
Agar	20 g
Deionized water to a final volume of 1 litre	
pH to 7.0 with 5 N Sodium Hydroxide	
Ampicillin	100 mg

SOC Media

Tryptone	10 g
Yeast Extract	5 g
Sodium Chloride	10 g
Deionized water to a final volume of 1 litre	
Potassium Chloride	2.5 mM
Magnesium Chloride	10 mM
Glucose	20 mM

4.1.5 Transfection Reagents

Thermo Fisher Scientific, U.K.

Gibco® Opti-MEM®

Lipofectamine RNAiMAX™ Reagent

Lipofectamine 3000® Reagent

P3000™ Reagent

4.2 Mammalian Cell Cultures

4.2.1 Mammalian Cell lines

All cell lines were grown in recommended media ***(Table 4.1)*** at 37°C in 5% CO_2. All media was pre-warmed to 21°C before use, and the culture medium was renewed every 48 – 72 hours. Short tandem repeat profiling was performed using the Cell Authentication Service by Eurofins Medigenomix to ensure the quality and integrity of the cell lines used.

Cell line	Supplier	Catalogue number	Media	Serum
22Rv1	ATCC	CRL-2505	RMPI	FBS
VCaP	ATCC	CRL-2876	DMEM	FBS
LNCaP	ATCC	CRL-1740	$RMPI^R$	FBS
LNCaP95	Dr Meeker/Dr Luo*	NA	$RMPI^W$	CSS
PNT2	Sigma-Aldrich	95012613	RPMI	FBS

Table 4.1: Cell lines and culture conditions. ATCC – American type culture collection; FBS – fetal bovine serum; CSS – charcoal stripped serum; * - LNCaP95 cells were kindly provided by Drs. Alan K Meeker and Jun Luo (Johns Hopkins University, Baltimore, Maryland, USA); R – with phenol red;

Cell passaging was performed by removing the culture medium and washing the cells with PBS. Following this, the cells were treated with TrypLE™ Express Enzyme (1X) with phenol red and incubated at 37°C for 5 minutes, or until all cells had detached. Cells were then collected in fresh growth medium and centrifuged at 4200 rpm for 5 minutes. For experimental use, cell pellets were then resuspended in fresh media and cells plated at the required density.

4.2.2 Cryopreservation and thawing of cells

Monolayers were disassociated by trypsinisation and pelleted as described above. Subsequently, cell pellets were resuspended in freezing media (50 % (v/v) culture medium, 40 % (v/v) FBS and 10% Dimethyl Sulfoxide (DMSO)) and transferred to cryovials. Cryovials were then stored in liquid nitrogen. Frozen cells were subsequently thawed at 37°C, following which thawed cells were carefully added to 10 mL of pre-warmed culture medium. Cells were then collected by centrifugation at 4200 rpm for 5 minutes and re-suspended in the desired volume of culture medium.

4.2.3 Transfection Methods

4.2.3.1 Small interfering RNA (siRNA)

All siRNA were ONTARGETplus pools (Dharmacon; GE healthcare, Chicago, IL), as listed in ***Table 4.2***, and used in combination with 0.4% RNAiMax™ transfection reagent (Invitrogen, Carlsbad, CA) as per manufacturer's instructions. All siRNA experiments were conducted at a concentration of 50 nM unless otherwise specified. Following siRNA transfection, for growth experiments cells were incubated at 37°C and grown for 6 days or until 80-90% confluence (see **section 4.2.4**), while for western blot and qPCR experiments cells were incubated at 37°C for 72 hours, after which cells were harvested for analysis as described previously. Following transfection, the culture media was not changed for the duration of the experiment.

Gene target	Supplier	Catalogue ID
Control	Dharmacon (GE healthcare, Chicago, IL)	D-001810-10
JMJD6		L-010363
U2AF2 (U2AF65)		L-012380

Table 4.2: ON-TARGETplus siRNA pools.

4.2.3.2 JMJD6 plasmid overexpression

Wild-type (pcDNA3-JMJD6-WT) and catalytically inactive mutant (pcDNA3-JMJD6-ASM2 and pcDNA3-JMJD6-BM1) JMJD6 expression constructs were kindly donated by Dr A. Böttger [281, 282].

JMJD6 plasmid extraction

Plasmid DNA was re-transformed into XL1-Blue Competent Cells (E. Coli; Agilent, California, U.S.A) according to the manufacturer's instruction. Single cell derived colonies were selected on LB agar plates containing ampicillin (described in **section 4.1.4**) incubated overnight at 37°C. One colony was then picked and used to inoculate 200 mL of LB medium with ampicillin and incubated overnight, rotating at 37°C. The medium was then centrifuged at 3500 rpm for 15 minutes, after which plasmid DNA was extracted using a Qiagen midi prep kit (Qiagen, Manchester, U.K.) as per the manufacturer's instructions. Final DNA concentration was determined using a UV-Vis spectrophotometer (Nanodrop; Thermo Fisher Scientific, U.K.).

Plasmid transfection

pcDNA3-JMJD6-WT ($JMJD6^{WT}$), pcDNA3-JMJD6-ASM2 ($JMJD6^{MUT1}$), and pcDNA3-JMJD6-BM1 ($JMJD6^{MUT2}$) plasmid DNA was transfected into prostate cancer cell lines using Lipofectamine 3000 (Invitrogen, Carlsbad, CA) as per manufacturer's instructions. Mammalian cell transfection reactions were performed in 6 well plates. Per reaction, 250 μL of Gibco® Opti-MEM® medium and 7.5 μL of Lipofectamine 3000® were mixed with a combination of plasmid DNA and P3000™ reagent (2 μL/μg of plasmid DNA used; Invitrogen, Carlsbad, CA). The transfection mixture was then incubated at 21°C for 5 minutes, after which 250 μL was added to 1750 μL of appropriate cell culture medium to produce a total volume of 2000 μL per well. All treatments were performed using 1 μg of total plasmid. For experiments requiring lower concentrations, the empty vector control plasmid (pcDNA3) was added to $JMJD6^{WT}$, $JMJD6^{MUT1}$ or $JMJD6^{MUT2}$, respectively, to make up the difference (e.g. 0.5 μg $JMJD6^{WT}$ + 0.5 μg empty vector control plasmid = 1 μg total plasmid input). Following plasmid transfection, cells were incubated at 37°C for 72 hours, after which cells were harvested for analysis as described previously.

4.2.3.3 Drugs

Enzalutamide was from Selleckchem (Houston, TX; S1250). DMSO was from Fisher Scientific U.K. (BP231-1). 2,4-Pyridinedicarboxylic acid (2,4-PDCA) was purchased from Sigma-Aldrich (Dorset, U.K.; 04473).

4.2.4 Cell growth assays

Cells were plated in 48-well tissue culture plates, treated as indicated the following day, and grown for 6 days, or until 80-90% confluence, as per previously published methods [189, 215]. To quantify growth of LNCaP95, 22Rv1 and PNT2 cell lines, cells were fixed with 10% (w/v) aqueous trichloroacetic acid and incubated at 4^{o}C for 30 minutes prior to washing and air drying. Subsequently these cells were stained with sulforhodamine B (SRB) for 30 minutes prior to removal of excess dye with 1% (v/v) aqueous acetic acid and further air drying. Following this, protein bound dye was dissolved in 10 mM Tris base solution, transferred to a 96-well plate and optical density determined at 510 nm using the Synergy HT microplate reader (BioTek, Swindon, U.K.). VCaP cell growth assays were analysed using CellTiter-Glo® Luminescent Cell Viability Assay (Promega, Southampton, U.K.) as per manufacturer's instructions and luminescence quantified using the Synergy HT microplate reader (BioTek, Swindon, U.K.).

4.2.5 Hypoxia studies

Hypoxic treatments at 1% O_2 were carried out in a Don Whitley H35 Hypoxystation©. Cells were seeded in 6-well tissue culture plates with appropriate media and incubated for 24 hours. Hypoxic cells were compared to matched cells incubated for 24 hours at 21% O_2 (normoxia).

4.2.6 Cell Harvest and Lysis

Unless otherwise stated, experimental cells used for protein and mRNA quantification were lysed directly from cell culture plates. Following removal of the culture medium, cells were washed in 1 mL of PBS. Subsequently cells were lysed for analysis by application of either 80 μL of RIPA lysis buffer supplemented with protease inhibitor cocktail (Roche, Hertfordshire, U.K.) for protein quantification, or 350 μL of RLT lysis buffer (Qiagen, Manchester, U.K.) for RNA quantification. Cell lysates for protein quantification were then transferred to a 1.5 mL Eppendorf tube and placed on ice for further analysis as described below, while cells requiring RNA quantification were processed using the RNeasy Mini Kit (Qiagen, Manchester, U.K.) as per manufacturer's instructions.

4.2.7 Protein Manipulation

4.2.7.1 Protein Quantification

Following cell lysis with RIPA buffer supplemented with cOmplete™ EDTA-free Protease Inhibitor Cocktail (Roche, Hertfordshire, U.K.) as described previously, samples were cooled on ice for 5 minutes, then centrifuged at 13,000 rpm for 15 minutes. Subsequently, the resultant pellets of cell debris were removed prior to protein quantification.

Protein quantification was performed using Pierce™ BCA Protein Assay Kit (Thermo Fisher Scientific, U.K). Samples were analysed as duplicates using 96 well plate. 5 µl of each sample was placed in each well, after which 200 µl of BCA Working Reagent was added to each sample. Working Reagent was prepared by mixing 50 parts of BCA Reagent A with 1 part of BCA Reagent B (50:1, Reagent A:B). Samples were then incubated for 20 minutes at 37°C following which absorbance at 562 nm was determined using a spectrophotometer; Synergy HT microplate reader (BioTek, Swindon, U.K.). Calculations of protein concentrations were done by comparing samples to a standard curve of samples containing known concentrations of BSA.

4.2.7.2 Western blot

Proteins were fractionated by SDS-PAGE using 4-12% NuPAGE® Bis-Tris gel plates (Invitrogen, Carlsbad, CA) prior to transfer onto Immobilon-P™ PVDF membranes of 0.45µm pore size (Millipore, Watford, U.K.) using a Mini Trans-Blot® Cell (Bio-Rad, Watford, U.K.) at 150 ampules for 120 minutes. Blocking of non-specific binding to the membrane was performed at 21°C for 60 minutes on a tube roller (Roller Shaker, Stuart) in 5 % (w/v) non-fat marvel milk in TBST. Primary antibody was then added at the recommended dilution ***(Table 4.3)***, and the membrane incubated at 4°C overnight on a tube roller. Subsequently, the membrane was washed three times in TBST, followed by further incubation with the appropriate horseradish peroxidase conjugated secondary antibody at 21°C for one hour. The membrane was then washed a further three times for five minutes prior to incubation with Clarity™ western enhanced chemiluminescence (ECL) substrate (Bio-Rad, Watford, U.K.) at 21°C for 5 minutes. Chemiluminescence was detected on the Chemidoc Touch imaging system

(Bio-Rad, Watford, U.K.). Electronic protein quantification by densitometry was performed using Bio-Rad Image Lab™ software version 6.

Protein target	Supplier	Catalogue ID
AR-FL	DAKO	M3562
AR-V7	RevMAb Biosciences	31-1109-00
JMJD6	Santa Cruz	sc-28348
GAPDH	Santa Cruz	sc-32233
Tubulin	Santa Cruz	sc-32293
PSA	DAKO	A0562
U2AF65	Santa Cruz	sc-53942

Table 4.3: Primary antibodies used for Western blot analysis.

4.2.8 RNA Manipulation

4.2.8.1 RNA extraction

As described previously, RNA was extracted from cells cultured in 6 well plates and lysed directly with 350 µL of RLT buffer (Qiagen, Manchester, U.K.) in each well. Cell lysates were then transferred into individual gDNA Eliminator spin columns (Qiagen, Manchester, U.K.) placed in a 2 mL collection tubes, and centrifuged for 30 seconds at 13,000 rpm. 350 µL of 70% ethanol was then added to the flow-through and mixed well by pipetting, after which 700 µL of each sample was transferred to a RNeasy spin column (Qiagen, Manchester, U.K.) placed in a 2 mL collection tube and centrifuged for 15 seconds at 13,000 rpm. 700 µL of Buffer RW1 (Qiagen, Manchester, U.K.) was then added to each RNeasy Mini spin column and samples were again centrifuged for 15 seconds at 13,000 rpm. Next, each RNeasy Mini spin column was washed twice with 500 µL of Buffer RPE (Qiagen, Manchester, U.K.) and centrifuged for 15 seconds at 13,000 rpm after the first wash, and for 2 minutes after the second wash. Following the second wash, each RNeasy spin column was placed in a new 2 mL collection tube and centrifuged at 13,300 rpm for 1 minute to further dry the membrane, after which each RNeasy spin column was placed in a new 1.5 mL collection tube and 30–50

µL of RNase-free water was added directly to the spin column membrane prior to further centrifugation for 1 minute at 13,000 rpm to elute the RNA. Samples were subsequently kept on ice at all times.

4.2.8.2 Production of copy DNA (cDNA)

Extracted RNA was converted into cDNA using the First Strand cDNA Synthesis Kit (Roche, Basel, Switzerland). 15 µL of master-mix, as described in ***Table 4.4A***, was added to 5 µL of extracted RNA. The mixtures were then vortexed and briefly centrifuged prior to PCR amplification using the protocol outlined in ***Table 4.4B***.

A

Reagent	**Quantity (µL)**
5X Reaction Buffer *250 mM Tris-HCl (pH 8.3), 250 mM KCl, 20 mM MgCl2, 50 mM DTT*	4
10 mM dNTP Mix	2
Random Hexamer Primer (100 µM)	1
Oligo(dT)18 Primer (100 µM)	1
RiboLock RNase Inhibitor (20 U/µL)	1
RevertAid RT (200 U/µL)	1
Nuclease-free Water	5*

B

Temperature (°C)	Duration (minutes)
25	5
42	60
70	5
4	Hold

Table 4.4: RNA to cDNA conversion protocols. (A) Master-mix for cDNA synthesis. *Substituted with 5 µL RNA if concentration of extracted RNA low. **(B)** PCR Protocol for cDNA synthesis.

4.2.8.3 Quantitative reverse transcription polymerase chain reaction (qRT-PCR)

Synthesised cDNA was diluted with nuclease-free water. Subsequently, 4.5 µL of cDNA was mixed with 5 µL of TaqMan™ Fast Advanced MasterMix (Thermo Fisher Scientific, U.K.) and 0.5 µL of appropriate probe ***(Table 4.5)*** in a 384 well plate. Each sample was prepared in duplicate. Quantitative analysis was then performed using the ViiA™ 7 Real-Time PCR System (Thermo Fisher Scientific, U.K.), after which fold change in mRNA expression levels was calculated by the comparative Ct method, using the formula 2-(-(ΔΔCt) [283].

Gene target	Supplier	Assay ID
JMJD6	ThermoFisher Scientific, U.K.	Hs00397095_m1
AR-FL		Hs00171172_m1
AR-V7		Hs04260217_m1
AR (Exon 2- Intron 2)		Hs00001102_cn
AR (Intron 3)		Hs04117242_cn_F
GAPDH		Hs02786624_g1
B2M		Hs00187842_m1
CDC73		Hs00363810_m1

Table 4.5: TaqMan probes used for qRT-PCR analysis.

4.2.8.4 RNA immunoprecipitation (RIP) Assay

The RIP assay described herein was kindly performed by Soojin Kim, Research Scientist II, in collaboration with Prof. Stephen Plymate's research group (Department of Medicine, University of Washington School of Medicine and VAPSHCS-GRECC, Seattle, Washington, U.S.A.), using previously established methods [97]. Subsequently, analysis of the raw data acquired from this experiment was performed by me, as described in **section 4.2.8.3**

Cells were transfected with either 25 nM non-targeting control siRNA (Dharmacon; GE Healthcare, Chicago, IL) or 25 nM JMJD6 siRNA (Dharmacon; GE Healthcare, Chicago, IL) using Lipofectamine RNAiMax (Invitrogen, Carlsbad, CA) and OPTI-MEM media (Thermo Fisher Scientific, Waltham, MA) as per manufacturer's instructions. After 72 hours, cells were cross-linked with final concentration of 0.3% formaldehyde (Thermo Fisher Scientific, Waltham, MA). The RIP assay was performed using an EZ-Magna RIP (Cross-linked) Nuclear RNA-binding Protein Immunoprecipitation Kit (Millipore, Burlington, MA; 17-10521) according to the manufacturer's protocol, and immunoprecipitated with 4 µg of U2AF65 antibody (Sigma Aldrich, St. Louis, MO). RNA purification and DNAse I treatment was performed using RNeasy Plus Universal Mini Kit (Qiagen, Germantown, Maryland). The resultant RNAs were subjected to cDNA synthesis and RT-qPCR analysis. RIP data were derived from two independent experiments.

P1F:	5'-AGGGATGACTCTGGGAGGTAA-3'
P1R:	5'-CTATGAAAGGGTCAGCCTGTC-3'
P2F:	5'-ACCTCCCCAACTTTACATGCT-3'
P2R:	5'-CAGGGTCTGGTCATTTTGAGA-3'
P3F:	5'-GGTTTAGCAGGTATTTGGGATG-3'
P3R:	5'-TTCTGGGTTGTCTCCTCAGTG-3'

Table 4.6: RNA immunoprecipitation assay primers (AR-V7 specific splice sites). F = forward primer, R = reverse primer. P1: 5' splice site for both AR-FL and AR-V7. P2: 3' splice site for AR-V7. P3: 3' splice site for AR-FL.

4.2.8.5 RNA-sequencing (RNA-seq)

RNA-sequencing was kindly performed by Dr Jonathan Welti, Senior Scientific Officer, ICR. RNA-seq analyses comparing (1) LNCaP and LNCaP95 prostate cancer cells, and (2) LNCaP95 prostate cancer treated with either I-BET151 or vehicle (DMSO 0.1%), were performed as per previously described protocols [215]. Analyses performed comparing treatment (I-BET151 at concentrations of 500 nM and 2 μM for 8 and 48 hours each; both of which we have shown to downregulate AR-V7 [215]) with equivalent vehicle (DMSO 0.1% for 8 and 48 hours; for quality control (QC) data see ***Appendix A*** and ***B***). For RNA-seq analyses of LNCaP95 prostate cancer cells treated with JMJD6 siRNA compared to non-targeting control siRNA, following RNA extraction as described previously, RNA quality was analysed using the Agilent RNA ScreenTape assay (Didcot, U.K.). Prior to sequencing, transfection efficiency was also determined by qPCR to ensure adequate knockdown of JMJD6 (for QC data see ***Appendix C*** and ***D***). Next-generation library preparation was then performed using 100 ng of total RNA from each sample with the Agilent SureSelect (Didcot, U.K.) library prep kit as per manufacturer's instructions. Library quality was confirmed using the Agilent Bioanalyzer High Sensitivity DNA ScreenTape Assay (Didcot, U.K.). The libraries were then quantified and normalised by qPCR using Qiagen GeneRead Quantification Kit (Manchester, U.K.). Library clustering was performed on a cBot with Illumina HiSeq PE Cluster kit v3. The libraries were sequenced as paired-end 101 base pair reads on an Illumina HiSeq 2500 with an Illumina HiSeq SBS kit v3. Base calling and quality scoring were performed using Real-Time Analysis (version 1.18.64) and FASTQ file generation. De-multiplexing was performed using BCL2FASTQ. Bioinformatic analysis was performed by Dr. Wei Yuan, senior bioinformatician within the de Bono research group, ICR.

4.3 Patient Clinical Data and Tissue Samples

4.3.1 Patients and tissue samples

All patients had metastatic CRPC treated at the Royal Marsden Hospital (RMH) and provided written informed consent, being enrolled into protocols approved by the RMH ethics review committee (reference no. 04/Q0801/60). Patient clinical data were retrospectively collected from the Royal Marsden Hospital electronic patient record system.

ICR/RMH cohort. 74 patients were identified as having sufficient formalin-fixed, paraffin embedded (FFPE) metastatic CRPC biopsies available for assessment, of whom 64 also had matched, same-patient, diagnostic, castration-sensitive prostate cancer (CSPC) tissue samples. All tissue blocks were freshly sectioned and only considered for IHC analyses if adequate material was present (≥50 tumour cells). All CSPC biopsies demonstrated adenocarcinoma.

4.3.2 Access to data repositories

International Stand Up To Cancer/Prostate Cancer Foundation (SU2C/PCF) cohort. Whole exome (n=231) and transcriptome (n=108) sequencing data from metastatic CRPC patients generated by the SU2C/PCF Prostate Cancer Dream Team were downloaded and reanalysed [103].

4.3.3 Antibody validation

Antibody specificity was determined by Western blot and immunohistochemistry (IHC) comparing detection of JMJD6 protein expression in LNCaP95 cells cultured with either non-targeting control siRNA or ON-TARGETplus pooled JMJD6 siRNA (Dharmacon; GE healthcare, Chicago, IL). Immunohistochemical staining of cell pellets for antibody validation was performed with the help of Ines Figueiredo. AR-V7 antibody validation was performed by Western blot and IHC of both prostate cancer cells, and patient prostate cancer tissue samples, as previously described [284]. As part of these validation studies, Western blot analyses were performed of LNCaP95 whole cell lysates treated with a non-targeting control siRNA, or siRNAs targeting either AR exon 1, cryptic exon 3B, or exon 7. These analyses

identified a single protein band, which was downregulated following treatment with siRNAs directed at components of AR-V7 (cryptic exon 3B and exon 1), but not with siRNA directed at exon 7 (which is present in AR-FL), or non-targeting control siRNA [189, 284].

4.3.4 Tissue analysis

Immunohistochemical staining of patient tissue biopsies was kindly performed by Ines Figueiredo (Higher Scientific Officer, ICR), Ana Ferreira (Higher Scientific Officer, ICR), and Ruth Riisnaes (Senior Scientific Officer, ICR). JMJD6 IHC was performed using a mouse anti-JMJD6 antibody (Santa Cruz Biotechnology; sc-28348; 200 μg/mL stock). Antigen retrieval was achieved by microwaving slides in pH 6 Antigen Retrieval Buffer (TCS Biosciences, Buckingham, U.K.; HDS05-100) for 18 minutes at 800 W prior to incubation with anti-JMJD6 antibody (1:50 dilution) for 1 hour at 21°C [284]. The reaction was visualised using the EnVision system (DAKO; K4061). JMJD6 antibody specificity for IHC was confirmed from LNCaP95 cell pellets following treatment with JMJD6 siRNA compared to non-targeting control siRNA with the help of Ines Figueiredo. AR-V7 IHC was performed as per a previously described protocol [284]. JMJD6 and AR-V7 quantification for each sample was determined by a pathologist blinded to relevant clinical data using the modified histochemical-score (H-score) method to determine the overall percentage of JMJD6 positivity across the entire stained tumour sample. The modified H-Score is a semi-quantitative method of assessing the extent of target immunoreactivity by immunohistochemistry [285, 286]; The percentage of cells at each staining intensity level is calculated, and an H-score is assigned using the formula below, yielding a range from 0 to 300.

H-Score = [(% of weak staining) × 1] + [(% of moderate staining) × 2] + [(% of strong staining) × 3]

4.4 Liquid Chromatography Mass Spectrometry (LC-MS) assays for *JMJD6* inhibition by 2,4-PDCA

LC-MS assay for inhibition of JMJD6 by 2,4-PDCA was kindly performed and analysed by Dr Anthony Tumber, senior postdoctoral researcher in Prof. Christopher Schofield's

research group (Chemistry Research Laboratory, Department of Chemistry, University of Oxford, Oxford, U.K.), using previously established methods [287].

Hydroxylation of a 12-mer peptide substrate (NPKRSRSREHRR, prepared with a C-terminal amide) of the pre-mRNA splicing factor LUC7L2 by Jmjd6 (1-362, prepared as reported) [288, 289] was monitored by LC-MS using an Agilent 1290 infinity II LC system equipped with an Agilent 1290 infinity binary pump and coupled to an Agilent 6550 Accurate Mass Quadrupole Time of Flight (Q-TOF) mass spectrometer. Note this construct has hydroxylation but not demethylation activity [289].

All $JMJD6_{1-362}$ enzyme reactions were performed in 50 mM Tris.Cl pH 7.5 (prepared fresh each day) at 37°C. L (+)-Ascorbic acid sodium salt (code 11140), ferrous ammonium sulphate (FAS) as ammonium iron (II) sulphate hexahydrate (215406), and 2-oxoglutarate (2OG) were from Sigma Aldrich (Dorset, U.K.). The LUC7L2 peptide substrate was synthesized to >95% purity (LC-MS) by GL-Biochem (Shanghai, China). L-ascorbic Acid (50 mM in deionized water), 2-OG (10 mM in deionized water) and iron (II) sulphate (400 mM in 10 mM HCl) solutions were prepared freshly each day.

$JMJD6_{1-362}$ (10 μM) was pre-incubated with an 8-point and 3-fold serial dilution of 2, 4-PDCA (100 – 0.046 μM) for 15 minutes and the enzyme reaction initiated by addition of LUC7L2 substrate (100 μM LUC7L2, 400 μM L-ascorbate, 100 μM FAS, 500 μM 2-OG final concentrations). The enzyme reaction was progressed for 2 hours at 37°C, then stopped by the addition of formic acid to a final concentration of 1.0 % (v/v). The quenched enzyme reaction was injected (6 μl injections) onto a Proswift RP-4H 1X50 mm LC column (Thermo Fisher Scientific, U.K.) and the LUC7L2 and LUC7L2-hydroxylated peptides were fractionated using a linear gradient of Solvent A (0.1% (v/v) formic acid in LCMS water) and Solvent B (0.1% (v/v) formic acid in 100% LCMS grade acetonitrile). Details of the gradient conditions, flow rates and maximum pressure limits are summarized in ***Table 4.7***. Peptide ionization was monitored in the positive ion electrospray ionisation (ESI) mode with a drying gas temperature of 280°C, a drying gas flow rate of 13 L/minute, nebulizer gas pressure of 40 PSI, sheath gas temperature of 350°C, sheath gas flow rate of 12 L/min and a nozzle voltage of

1000V. Ion chromatogram data for the +2 charge state of both the non-hydroxylated and hydroxylated peptides were extracted and integrated using MassHunter qualitative software (Agilent, Didcot, U.K.). The % conversion of the peptide substrate to the +16 hydroxylated peptide was calculated using the equation: % conversion = 100 x hydroxylated / (hydroxylated + non-hydroxylated peptide). The IC_{50} for 2, 4-PDCA was determined from non-linear regression curve fitting using GraphPad prism 6.0.

Time (min)	% Solvent A	% Solvent B	Flow (ml/min)	Max Pressure Limit (Bar)
0	95	5	0.2	600
1.0	80	20	0.2	600
9.0	45	55	0.2	600
10.0	0	100	0.2	600
11.0	0	100	0.2	600
12.0	95	5	0.2	600

Table 4.7: Gradient conditions for fractionation of LUC7L2 peptides.

4.5 Bioinformatic Analyses and Statistics

All bioinformatic analyses presented in this thesis were performed with the help of Dr. Wei Yuan, senior bioinformatician within the de Bono research group, ICR.

4.5.1 AR activity, AR-V7 activity and gene expression evaluation

Paired-end transcriptome sequencing reads were aligned to the human reference genome (GRCh37/hg19) using TopHat2 (v2.0.7). Gene expression, Fragments Per Kilobase of transcript per Million mapped reads (FPKM), was calculated using Cufflinks [290]. AR signalling activity was determined through the measurement of AR pathway signalling based on either (1) the expression levels of 43 genes regulated by AR in prostate cancer cell line and metastatic prostate cancer RNA-seq datasets (AR signature; determined using two previously described gene expression signatures [215, 291, 292]; ***Table 4.8***), or (2) the HALLMARK_ANDROGEN_RESPONSE gene set from the MSidDB (M5908 [293]; Androgen

response (H)). AR-V7 signalling activity was determined using the previously published AR-V7-associated signature based on the expression levels of 59 genes associated with AR-V7 expression in metastatic CRPC (AR-V7 signature; ***Table 4.9***) [284].

ABCC4	ACSL3	ADAM7	APPBP2
ATXN3	BMPR1B	C1orf116	CAMKK2
CENPN	CRLS1	DYNLL2	EAF2
ELK4	ELL2	EVI5	FADS1
FKBP5	GNAI3	GNMT	HERC3
HMGCR	INSIG1	KLK2	KLK3
MAF	MAP7	MED28	MPHOSPH9
MTERFD2	NGLY1	NKX3-1	NNMT
PIAS1	PMEPA1	PTGER4	RRP12
SLC30A7	SPCS3	TARP	TMEM50A
TMPRSS2	UBE2J1	ZBTB10	

Table 4.8: AR regulated genes included in AR activity score (AR Signature).

AKAP12	CS	HOXB13	SMPDL3A	WWC1	ZNF726
ANKRD30B	CTPS2	IFT57	SNX1	ZFX	ZNF761
AR	CYP4F8	LRRC41	SPATS2	ZNF138	ZNF813
ATF7	DCAF6	MALT1	SRC	ZNF174	ZNF85
BAZ2A	DOPEY2	NUDT4	STEAP1	ZNF285	
C4orf36	ELL2	PITPNA	STEAP2	ZNF43	
CAPN7	FASN	PPP2R3A	TMBIM6	ZNF525	
CBR4	GALNT7	PPP3CA	TMSB4Y	ZNF528	
CCDC115	GRIN3A	PTER	TTTY15	ZNF583	
CDYL2	GSPT1	RAB40B	UBE2E3	ZNF680	
CROT	HOMER2	RAB5B	USP54	ZNF682	

Table 4.9: 59 genes associated with AR-V7 expression in metastatic CRPC (AR-V7 signature).

4.5.2 Pathway analysis and determination of alternative splicing events

Following RNA-seq as described previously, paired end raw reads in FASTQ format were aligned to the reference human genome (hg19) using RNA-seq spliced read mapper TopHat (v2.0.7), with default settings [294]. The library and mapping quality were estimated using Picard tools (http://broadinstitute.github.io/picard). QC assessments made to ensure accuracy of sequencing presented in ***Appendix A***, ***B*** and ***D***. The median number of 100 base pair reads for each sample was 14 million. Alternative splicing events (skipped exons, alternative 5' splice sites, alternative 3' splice sites, mutually exclusive exons and retained introns) based on Ensembl v61 annotation were accessed using MATS v3.0.8 [295]. Pathway analyses were performed by Gene Set Enrichment Analyses (GSEA) using gene sets downloaded from the HALLMARK collection in the Molecular Signatures Database; MYC_TARGETS_V1 (M5926), MYC_TARGETS_V2 (M5928), G2M_CHECKPOINT (M5901), E2F_TARGETS (M5925) and MTORC1_SIGNALING (M5924) [296].

4.5.3 Statistical analysis

All statistical analyses were performed using Stata v13.1 or GraphPad Prism v7 and are indicated within all figures and tables. H-Scores are reported as median values and interquartile ranges. Comparison of JMJD6 expression levels between CSPC and metastatic CRPC tissue samples, and correlations with next generation sequencing data, were determined using the Wilcoxon matched-pair signed rank test. Comparisons between JMJD6 and AR-V7 expression levels in metastatic CRPC tissue samples made using Mann-Whitney test. Median survival from CRPC biopsy was defined as time from CRPC biopsy to date of death. Median survival was estimated using the Kaplan-Meier method.

5

Identifying transcriptional regulators of AR-V7

5.1 Research in context

The progression of prostate cancer to lethal castration-resistant disease is predominately driven by persistent unregulated AR signalling [103, 297]. As such, therapies including abiraterone and enzalutamide, which target the AR signalling axis, have become the standard of care for treating metastatic CRPC, improving both progression-free survival, and overall survival [19, 20]. However, despite the success of these second-generation AR-targeted therapies, some patients never respond to these agents, while nearly all eventually acquire resistance leading to disease progression, which is invariably fatal [18]. This resistance is in part due to the development of alternatively spliced variants of the AR (AR-SVs) that are truncated and lack the regulatory AR LBD; the target of current AR-directed therapies [5, 27, 92]. Consequently, these AR-SVs remain constitutively active in the absence of androgen and promote prostate cancer cell survival and proliferation [5, 27, 92]. Of the many AR-SVs that have been reported, AR-V7 is the most prevalent and the best studied, and has been associated with resistance to AR targeting therapies and poorer overall survival [91, 92]. Efforts to pharmacologically inhibit AR-SVs directly have however proved challenging due to their lack of a ligand binding domain, and the inherently disordered nature of the AR NTD [298]. As such, there remains an urgent unmet clinical need for novel therapeutic strategies to overcome AR-SVs and improve patient outcomes from lethal prostate cancer.

As outlined in **chapter two**, one such strategy to abrogate AR-V7-mediated resistance in metastatic CRPC is to target epigenetic processes that regulate proteins involved in AR-V7 generation. In this regard, BET inhibitors have recently attracted particular interest as they have been shown to downregulate AR-V7 protein expression and reduce the growth of enzalutamide-resistant patient-derived prostate cancer models, in part by blocking alternative splicing by the spliceosome [215]. However, BET proteins have pleiotropic roles and regulate many signalling pathways and consequently dose-limiting toxicities have so far restricted their clinical utility [277]. Therefore, while targeting mRNA splicing represents a promising therapeutic strategy for overcoming oncogenic AR-V7 signalling in metastatic CRPC, a better understanding of the mechanisms underlying this process is now needed to support the development of alternative, more tolerable, agents capable of preventing the generation of AR-V7.

In this chapter I describe results arising from the hypothesis that key spliceosome-related proteins that drive AR-V7 generation can be identified by a triangulation approach, analysing: 1) adaptations in prostate cancer cells as they become resistant to androgen deprivation by RNA-seq studies; 2) RNA-seq changes induced by BET inhibition, which downregulates AR-V7; 3) the top hits from a targeted siRNA screen of spliceosome-related genes. In doing so, I identify key regulators of AR-V7 which if targeted directly, I hypothesise could potentially replicate the encouraging preclinical effects seen with BET inhibition, while mitigating the adverse effects reported with these agents.

5.2 Specific Aims

- To identify genes with reported roles relating to the spliceosome, that are significantly more highly expressed in androgen-deprivation-resistant LNCaP95 cells that produce AR-V7 protein, when compared to the parental androgen-deprivation-sensitive cell lineage LNCaP, which does not produce AR-V7 protein.

- To ascertain which genes with reported roles relating to the spliceosome are most significantly downregulated following BET inhibition, at concentrations and time-points that result in AR-V7 downregulation.
- To determine which genes with reported roles relating to the spliceosome most markedly downregulate AR-V7 protein, relative to AR-FL, following siRNA knockdown in a targeted siRNA screen.

5.3 Regulation of AR-V7 expression in *in vitro* models of metastatic CRPC

5.3.1 Overview of experimental strategy

BET inhibition has been reported to reduce the expression of AR-V7 by downregulating the expression of the splicing factors SRSF1 and U2AF65. However, BET inhibition has been shown to impact global splicing, modulating a wide range of alternative splicing events, not just AR splicing [215]. To determine which of the proteins downregulated by BET inhibition are the most specific for the regulation of AR-V7 splicing, and therefore the most appropriate for further validation as novel therapeutic targets in metastatic CRPC, I adopted an orthogonal three-stage investigative approach ***(figure 5.1)***.

Stage One: **RNA-seq analysis of prostate cancer cell lines.** To determine which genes relating to the spliceosome are significantly more highly expressed in LNCaP95 cells (that produce AR-V7 protein and are AR deprivation resistant) compared to parental LNCaP cells (that do not produce AR-V7 protein and are AR deprivation sensitive), *since identified genes may be key to driving the expression of AR-V7*.

Stage Two: **RNA-seq analysis of prostate cancer cells following BET inhibition.** To determine which genes relating to the spliceosome are significantly downregulated by BET inhibition, which has been shown to downregulate AR-V7 expression [215], *since the identified genes may be necessary for AR-V7 splicing.*

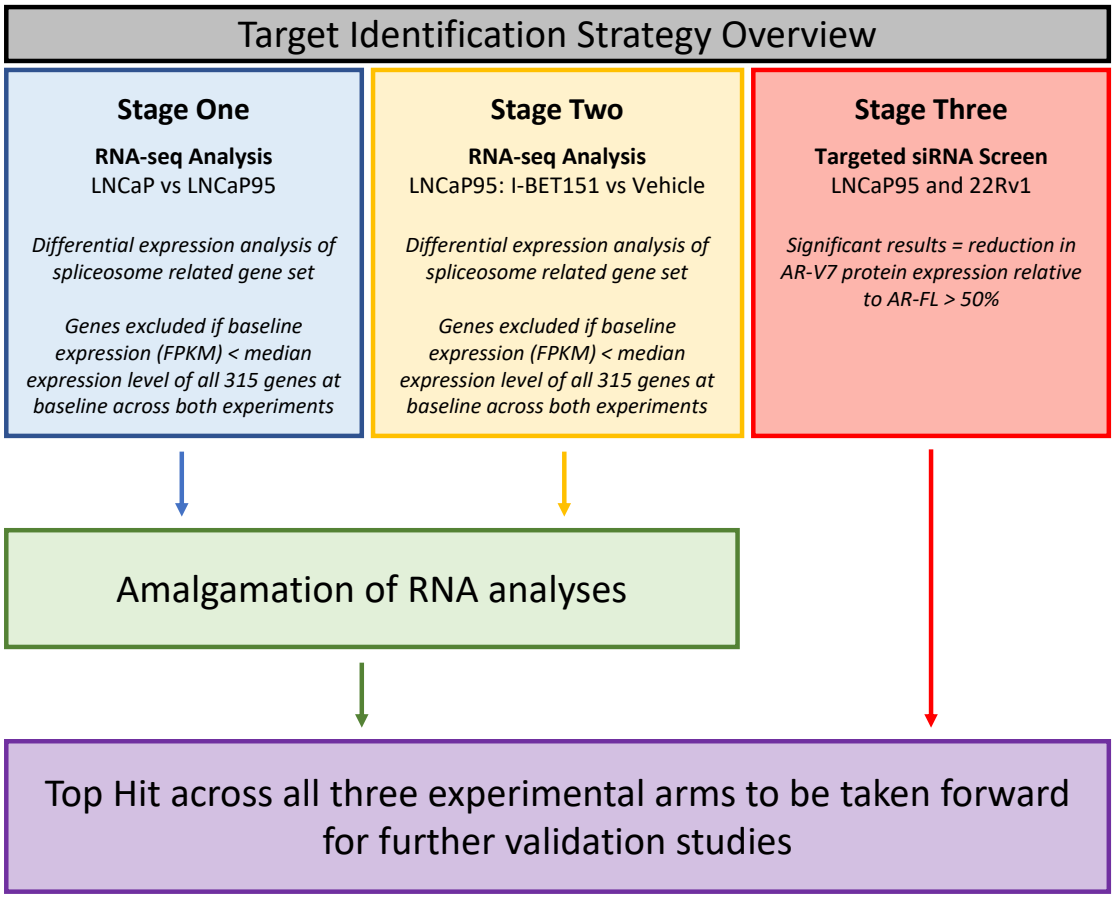

Figure 5.1: Overview of the strategy for identifying key regulators of AR-V7 generation.

Stage Three: High-throughput in vitro targeted siRNA screen of genes relating to the spliceosome. To determine which genes relating to the spliceosome preferentially regulate the production of AR-V7 protein rather than AR-FL, *in an attempt to validate a target that could abrogate AR-V7 expression which can cause endocrine resistance.*

5.3.2 RNA-seq analyses of prostate cancer cell lines

To begin to dissect the biological mechanisms regulating AR-V7 splicing in lethal prostate cancer, in collaboration with Dr Jonathan Welti and Dr Wei Yuan, RNA-seq analyses of castration-sensitive LNCaP prostate cancer cells (do not produce AR-V7 protein), and androgen-deprivation-resistant LNCaP95 prostate cancer cells (do produce AR-V7 protein), were performed as described in **section 4.2.8.5**. Differential mRNA expression levels of 315 genes with roles relating to the spliceosome, as defined by gene ontology (GO) annotations

in the molecular signatures database [296] *(spliceosome related gene set; **Table 5.1**)*, were then determined.

JMJD6	HNRNPU	CELF6	FIP1L1	POLR2G
CPSF1	ZMAT5	RBMX2	PDCD7	PPIL3
SF3B1	ISY1	THOC2	SNRNP200	ZCRB1
POLR2A	SF3B3	DBR1	HNRNPA2B1	SNRNP25
HSPA6	FMR1	SRSF6	NSRP1	WBP4
CPSF3	SNRNP35	HNRNPH3	ELAVL2	NUDT21
DDX39B	HTATSF1	PCBP2	RBM25	SNU13
SRRM1	SF3A3	DDX39A	RBMXL1	SRSF1
THRAP3	C1QBP	POLR2D	PPIG	RBFOX1
ACIN1	AAR2	SF3B2	SRSF11	SART3
PCF11	THOC3	KHSRP	SF1	PRPF40B
POLR2B	SNRNP48	SF3B6	HELB	DHX35
NFX1	DHX16	SPEN	HNRNPK	RBFOX3
CHERP	USP39	LOC100996657	XAB2	SRRM2
CPSF2	SNW1	PSPC1	RBM4	PRPF8
POLR2F	RALY	RNF113A	CSTF3	YBX1
NOL3	CCDC12	HNRNPC	GTF2F1	GTF2F2
PRMT5	POLR2E	GEMIN4	SF3B4	RNPC3
PHF5A	HSPA8	PRPF40A	PSIP1	ZRANB2
HNRNPH2	LSM6	SRSF3	LMNTD2	TRA2B
USP4	EIF4A3	ZRSR2	GEMIN8	IVNS1ABP
PUF60	POLR2L	LSM8	CELF4	TRA2A
CLP1	NCBP2	RBM17	WBP11	ALYREF
RBM15B	HNRNPA3	CLNS1A	RNPS1	SCAF11
NCBP1	SRRT	AQR	HNRNPF	RAVER2
POLR2C	DHX15	EFTUD2	CSTF1	SNRNP70
RBM8A	THOC1	PLRG1	DDX42	SNRPC
PPARGC1A	RBM10	PTBP1	DHX38	SNRPN
PRPF19	SRSF7	UPF3B	POLR2J	WDR83
SKIV2L2	FRG1	NONO	SNRPA1	SNUPN
LSM2	RBM22	ZCCHC8	PRPF18	TFIP11
SRSF4	SMC1A	NAA38	U2AF2	TIA1
DDX41	GPATCH1	POLR2I	SNRNP27	SYF2
PRMT7	DQX1	LUC7L	SNRPF	SF3A1
SETX	SMN1	U2AF1	HNRNPM	BUD31
SF3A2	LUC7L3	CELF2	SNRPG	HNRNPL
SLU7	MAGOH	SFSWAP	POLR2H	SF3B5
UHMK1	DNAJC8	HSPA1A	SART1	CWC22
RBMY1A1	SMNDC1	MAGOHB	LSM5	PABPN1
RBMX	DDX23	POLR2K	CDK13	HNRNPD
CPSF7	SRSF9	PPIE	SRSF12	LSM4
RBFOX2	BCAS2	RBM11	PAPOLA	USP49
SNRPB2	RBM41	RSRC1	SFPQ	PRPF31
DHX32	PABPC1	SNRPA	PRPF4B	SUGP1
DDX46	DCPS	CSTF2	HNRNPA0	CASC3
HMX2	LSM1	TXNL4A	PPAN	GEMIN7
HNRNPA1L2	LUC7L2	HNRNPUL1	ZMAT2	DHX9
RBM5	PNN	CWC15	METTL3	FUS
WDR77	CELF1	SNRPD2	CELF3	PRPF6
LSM3	CACTIN	SRSF2	SYNCRIP	RP9
CDC40	SNRPD3	PPIL1	BUD13	UBL5
HSPA2	SRPK1	SNRPB	CD2BP2	METTL14
WTAP	NOVA2	PRPF4	PRPF3	PRPF39
API5	PCBP1	GEMIN6	HNRNPH1	GCFC2
PRPF38B	SNRPD1	TXNL4B	SRRM4	LSM7
GEMIN5	CTNNBL1	HNRNPR	GEMIN2	YTHDC1
PQBP1	SRSF8	DHX8	CWC27	DDX1
CRNKL1	DDX5	SAP18	STRAP	ELAVL1
LUC7L2	CDC5L	CCAR1	GPKOW	PPIH
RBM15	TCERG1	SNRPE	ZNF638	RAVER1
SRSF5	U2SURP	SNRNP40	DGCR14	NOVA1
HSPA1L	U2AF1L4	PPWD1	SRPK2	HNRNPA1
HSPA1B	DDX20	TGS1	RNF113B	PRPF38A

Table 5.1: Spliceosome related gene set

Genes of interest were considered those significantly more highly expressed in LNCaP95 prostate cancer cells, which produce AR-V7 protein, relative to LNCaP prostate cancer cells, which do not express AR-V7 protein ***(figure 5.2)***.

A

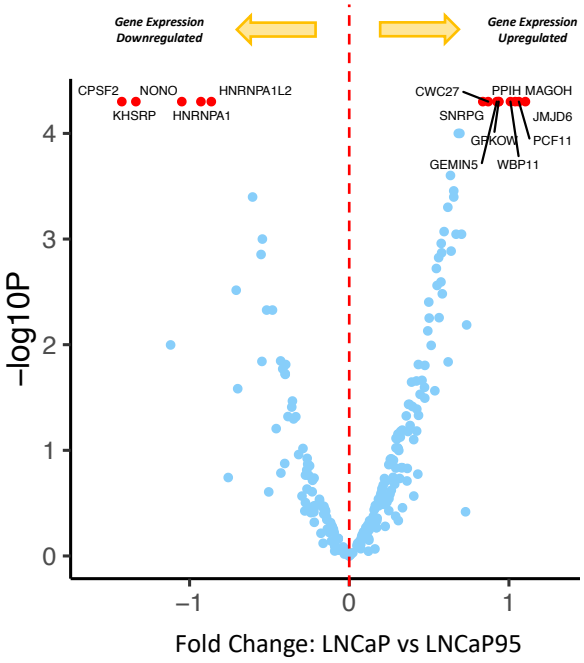

B

Identified Genes of Interest
JMJD6
CWC27
PPIH
MAGOH
SNRPG
GRKOW
GEMIN5
WBP11
PCF11

Figure 5.2: Differential mRNA expression of genes related to the spliceosome between LNCaP and LNCaP95 prostate cancer cell lines. (A) Volcano plot illustrating differential mRNA expression of 315 genes with GO annotations relating to the spliceosome *(spliceosome related gene set)*, as determined by RNA-seq analyses comparing castration-sensitive LNCaP (no AR-V7 protein) and androgen-deprivation-resistant LNCaP95 (detectable AR-V7 protein) prostate cancer cell lines. Blue dots represent genes with baseline expression (FPKM) greater than the median expression level of all 315 genes at baseline across both RNA-seq experiments (**section 5.3.2** and **5.3.3**). Top 15 genes most differentially expressed (up- or down-regulated; FPKM) indicated by red dots. **(B)** Identified genes of interest; list of evaluated genes significantly more highly expressed in LNCaP95 cells relative to LNCaP cells. RNA-seq raw data from LNCaP and LNCaP95 cells acquired by Dr Jonathan Welti. Bioinformatic analysis of RNA-seq raw data performed with the help of Dr Wei Yuan.

5.3.3 RNA-seq analyses of prostate cancer cell lines following BET inhibition

Next, to determine the impact of BET inhibition on the *spliceosome related gene set* ***(Table 5.1)***, in collaboration with Dr Jonathan Welti and Dr Wei Yuan, RNA-seq analyses were also performed comparing LNCaP95 prostate cancer cells treated with either a BET inhibitor (I-BET151) or vehicle (DMSO 0.1%). Subsequently, changes in the mRNA expression levels of these genes following BET inhibition were determined, with genes of interest being considered to be those that were significantly downregulated following BET inhibitor treatment, which has been previously shown to downregulate AR-V7 expression [215] ***(figure 5.3)***.

A

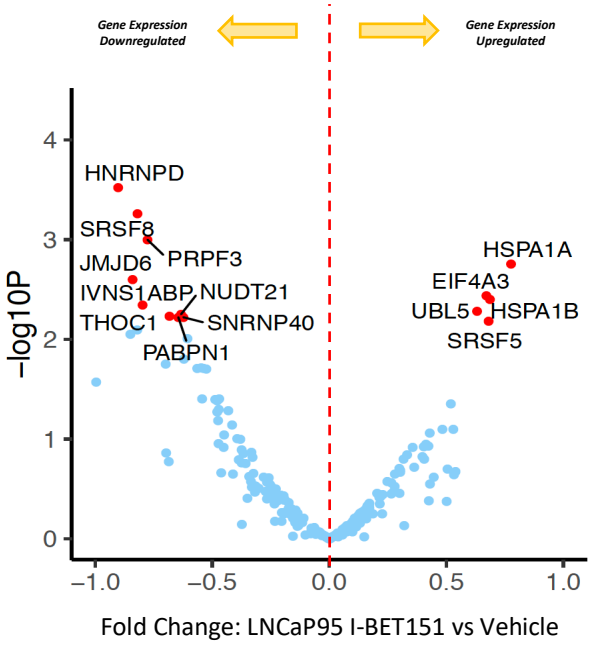

B

Identified Genes of Interest
HNRNPD
SRSF8
PRPF3
JMJD6
IVNS1ABP
NUDT21
THOC1
SNRNP40
PABPN1

Figure 5.3: Differential mRNA expression of genes related to the spliceosome between LNCaP95 prostate cancer cells treated with either I-BET151 or vehicle. (A) Volcano plot illustrating differential mRNA expression of 315 genes with GO annotations relating to the spliceosome *(spliceosome related gene set)*, as determined by RNA-seq analyses comparing LNCaP95 prostate cancer cells treated with either a BET inhibitor (I-BET151) or vehicle (DMSO 0.1%). Blue dots represent genes with baseline expression (FPKM) greater than the median expression level of all 315 genes at baseline across both RNA-seq experiments (**section 5.3.2** and **5.3.3**). Top 15 genes most differentially expressed (up- or down-regulated; FPKM) indicated by red dots. **(B)** Identified genes of interest; list of evaluated genes significantly downregulated in LNCaP95 cells by BET inhibitor treatment. RNA-seq raw data acquisition from treated LNCaP95 cells was performed by Dr Jonathan Welti. Bioinformatic analysis of RNA-seq raw data was performed with the help of Dr Wei Yuan.

5.3.4 High-throughput in vitro siRNA screen of genes relating to the spliceosome

Alongside these RNA-seq analyses, with the help of Dr Jonathan Welti, a separate protein-based siRNA screen was also performed specifically aimed at identifying proteins that are key to the production of AR-V7 protein, but that inhibition of which did not impact the levels of normal AR-FL. We hypothesised that any identified proteins would be critical for the survival of castration-resistant prostate cancer cells, but not benign prostatic epithelial cells.

5.3.4.1 Optimisation of siRNA knockdown conditions for high-throughput screen

To enable high-throughput screening, culture conditions were first optimised to ensure sufficient knockdown of target genes could be achieved in 48 well plates. For this, LNCaP95 prostate cancer cells seeded in increasing cell densities were treated with a range of AR siRNA concentrations. Subsequently, Western blot analyses were performed to quantify

AR, AR-V7 and GAPDH (housekeeping protein) protein levels to determine at which concentration of siRNA, and at which seeding density, AR knockdown was most efficient ***(figure 5.4)***.

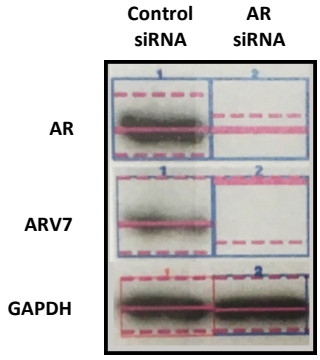

Figure 5.4: Western blot illustrating optimisation of siRNA conditions for high-throughput screen. LNCaP95 prostate cancer cells seeded in increasing cell densities were treated with a range of AR siRNA concentrations. Subsequently, Western blot analyses were performed to quantify levels of AR, AR-V7 and GAPDH and determine at which concentration of siRNA, and at which seeding density, knockdown was most efficient.

5.3.4.2 High-throughput siRNA screen

Following optimisation of culture conditions, all 315 genes in the *spliceosome related gene set* were individually silenced to determine their impact on AR-V7 protein levels relative to AR-FL in the AR-V7 producing prostate cancer cell lines 22Rv1 and LNCaP95. Genes were then ranked in an order determined by the degree of AR-V7 downregulation relative to AR-FL across both cell lines, with proteins causing the greatest reduction in AR-V7:AR-FL ratio being ranked highest ***(Table 5.2; Supplementary Table 12.1)***. Only genes that when knocked down by siRNA resulted in a reduction of AR-V7 protein levels relative to AR-FL of more than 50%, as determined by Western blot densitometry, were considered as genes of interest.

22Rv1	
Gene	**AR-V7:AR-FL Ratio**
JMJD6	0.31
SF3B1	0.33
HSPA6	0.39
HNRNPH2	0.42
KHSRP	0.45
ACIN1	0.46
SF3B6	0.47
SNW1	0.48
HNRNPK	0.48
RBM8A	0.49

LNCaP95	
Gene	**AR-V7:AR-FL Ratio**
HTATSF1	0.21
JMJD6	0.27
NFX1	0.29
PHF5A	0.34
NOL3	0.37
CPSF1	0.37
THRAP3	0.39
PDCD7	0.42
POLR2A	0.43
USP4	0.46

Average	
Gene	**AR-V7:AR-FL Ratio**
JMJD6	0.29
CPSF1	0.43
SF3B1	0.47
POLR2A	0.47
HSPA6	0.50
CPSF3	0.57
DDX39B	0.59
SRRM1	0.62
THRAP3	0.62
ACIN1	0.63

Table 5.2: siRNA screen of spliceosome related gene set; Summary of Top 10 genes. Score provided is a ratio of AR-V7 downregulation relative to AR-FL, as determined by Western blot densitometry. Results shown for 22Rv1 and LNCaP95 prostate cancer cell lines, alongside average score across both cell lines. The siRNA screen was performed together with Dr Jonathan Welti. Notably, the raw data acquisition for the portion of the siRNA screen pertaining to LNCaP95 cells was performed entirely by Dr Welti.

5.3.5 Amalgamation of RNA-seq analyses and siRNA screen

Overall, nine genes relating to the spliceosome were found to be significantly more highly expressed in the AR-V7 expressing prostate cancer cell line LNCaP95 than in its castration-sensitive parental lineage LNCaP; these were JMJD6, CWC27, PPIH, MAGOH, SNRPG, GRKOW, GEMIN5, PCF11 and WBP11. Furthermore, the genes HNRNPD, SRSF8, PRPF3, JMJD6, IVNS1ABP, NUDT21, THOC1, SNRNP40 and PABPN1 were found to be significantly downregulated following BET inhibition. Therefore, only one gene, JMJD6, was identified as a gene of interest across both RNA-seq experiments. Strikingly, JMJD6 was also the only gene identified in these RNA-seq analyses that downregulated AR-V7 protein levels relative to AR-FL by >50% in the targeted siRNA screen. Moreover, JMJD6 was in fact the top hit across both 22Rv1 and LNCaP95 cell lines. Taken together, these results suggested that JMJD6 may be a potentially important regulator of AR-V7 expression in CRPC ***(figure 5.5)***.

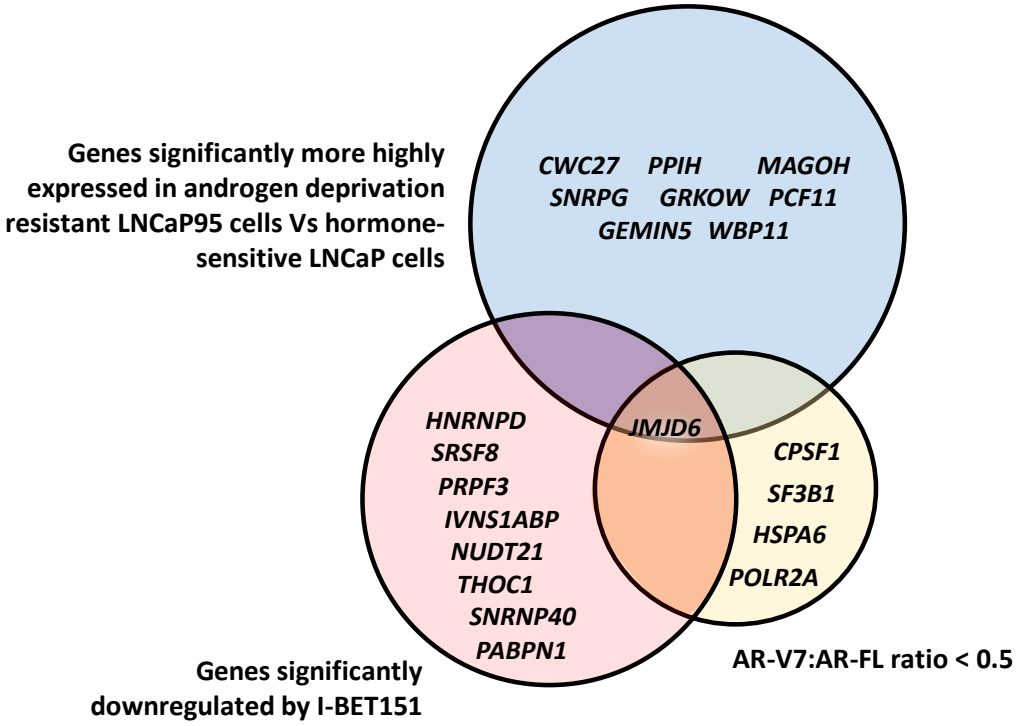

Figure 5.5: Venn diagram amalgamating RNA-seq analyses with siRNA screen results. Genes of interest were pre-defined as: (1) being upregulated in AR-V7 producing LNCaP95 prostate cancer cells relative to LNCaP prostate cancer cells (no AR-V7 protein expression); (2) being downregulated following BET inhibition (downregulates AR-V7 expression); and (3) resulting in a > 50% reduction in AR-V7 protein levels (Western blot) relative to AR-FL following gene silencing (siRNA). These analyses identified JMJD6 as the only gene to meet all three criteria, suggesting it to be a potentially important regulator of AR-V7 expression in *in vitro* models of CRPC.

5.4 BET inhibition and JMJD6

To validate, and investigate the nature of, the relationship between BET inhibition, JMJD6 and AR-V7, Western blot analyses were performed of LNCaP95 prostate cancer cells treated with I-BET151 for 48 hours. As shown in ***figure 5.6***, BET inhibition led to a concurrent dose-dependent reduction in both JMJD6 and AR-V7 protein levels, with these both occurring to a similar extent, and at the same concentrations of I-BET151.

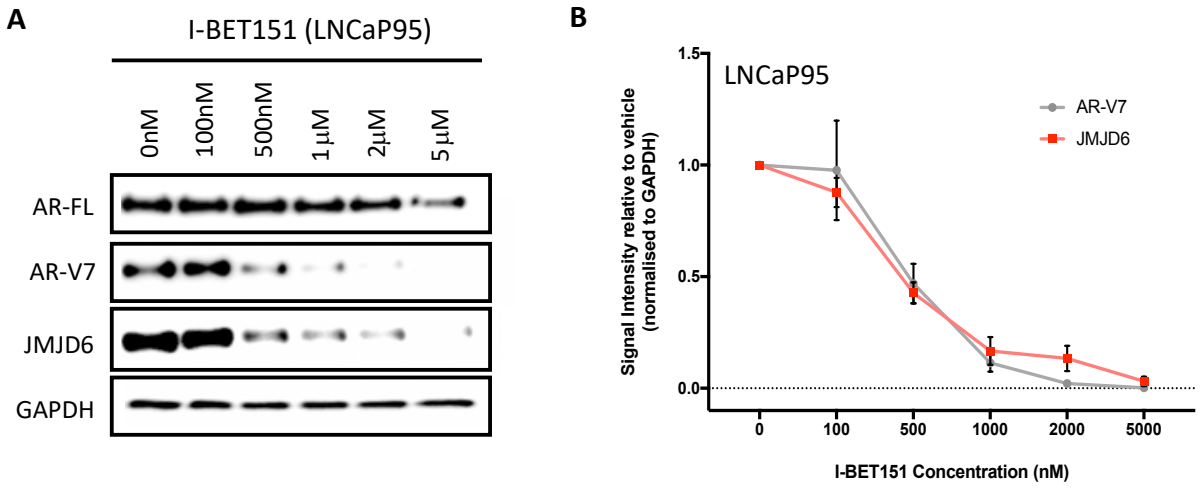

Figure 5.6: BET inhibition downregulates JMJD6 and AR-V7 protein levels. (A) Single Western blot demonstrating that I-BET151 downregulates both AR-V7 and JMJD6 protein levels in LNCaP95 prostate cancer cells in a dose-dependent manner. **(B)** Densiometric quantification of JMJD6 (red line) and AR-V7 (grey line) protein levels (n=4; densitometry for each biological replicate normalized to GAPDH and vehicle). Demonstrates that protein levels of both JMJD6 and AR-V7 decrease in a dose-dependent manner following BET inhibition with I-BET151.

5.5 Discussion

In this chapter, I adopted a three-stage triangulation approach to identify the 2-oxoglutarate (2OG) dependent dioxygenase JMJD6 as being a potentially important regulator of AR-V7 in preclinical models of lethal prostate cancer.

RNA-seq data evaluating the expression levels of 315 genes relating to the spliceosome, as defined by GO annotations from the Molecular Signatures Database, demonstrated that the expression of JMJD6 mRNA was significantly higher in androgen-deprivation-resistant LNCaP95 prostate cancer cells that produce AR-V7, than in their castration-sensitive parental lineage LNCaP, which does not produce AR-V7 protein. In

addition, treatment of LNCaP95 cells with I-BET151, which downregulates AR-V7 levels [215], reduced JMJD6 mRNA expression. Taken together, these results suggested that JMJD6 may be associated with AR-V7 levels since its expression is increased contemporaneously with increased expression of AR-V7, and is also reduced when AR-V7 is downregulated. In addition to these analyses, in an independent protein-based siRNA screen, JMJD6 knockdown caused a marked reduction in AR-V7 protein expression relative to AR-FL, which when considered alongside the aforementioned RNA-seq data, added further credence to the hypothesis that JMJD6 may be an important regulator of AR-V7 in these *in vitro* models of CRPC.

JMJD6 is a member of the ferrous iron and 2OG-dependent Jumonji C (JmjC) domain containing family of oxygenases, and has been implicated in the development of numerous cancers including breast, lung, colorectal and oral squamous carcinoma. However, JMJD6 has never been previously thought to contribute to the progression of prostate cancer. Therefore, the data presented herein suggest a novel role for JMJD6 in prostate cancer biology as a regulator of AR-V7 generation, meriting further evaluation in patient samples, and other *in vitro* models of lethal prostate cancer.

5.5.1 Limitations

While this chapter identified JMJD6 as a potential regulator of AR-V7 expression, the data presented here are limited by the *in vitro* nature of the studies used. There is an increasing appreciation that prostate cancer comprises different disease subtypes, each with their own characteristics and behaviour. Therefore, while cancer cell lines provide an invaluable tool in the study of basic functional biology, they do not sufficiently capture the complexities of prostate cancer in patients. Furthermore, each cell line is genomically different. For example, the LNCaP cells utilised in the work presented in this chapter possess an AR mutation (T878A) that makes the AR more promiscuous [299, 300], and a PTEN frame-shift mutation (exon 1, codon 6 AAA to A) [301]. Therefore, while comparative analyses between these cells and LNCaP95 prostate cancer cells may be considered a reasonable representation of the progression of prostate cancer to castration-resistant disease in patients, given that LNCaP95 cells are the androgen-deprivation-resistant progeny of LNCaP cells established through long-term androgen deprivation. Concerns remain regarding the

applicability of these *in vitro* findings to other prostate cancer models, and patients, which will often harbour very different aberrations. Moreover, cell lines are homogeneous, whereas prostate cancer in patients appears more heterogeneous, particularly at the point of metastatic castration-resistant disease, raising further concerns as to the translatability of *in vitro* discoveries to patients. Currently however, until better models of prostate cancer biology are validated, there remains a limited pool of prostate cancer models from which to choose. Therefore, I believe the investigative approach taken in this chapter represents the most cost-effective way of undertaking such *in vitro* discovery work, and lays a good foundation on which subsequent more representative, and focused, validation studies can be based.

Another limitation of the results presented here concerns the siRNA screen. While mRNA-based data analyses offer a global view of changes in biological pathways and gene expression, there is no guarantee that changes in mRNA expression are reflected at a protein level. Nor is it straightforward to differentiate between cause and effect. The protein-based siRNA screen presented in this chapter therefore provides an invaluable supplement to these analyses by informing on the biological relevance of genes identified by RNA-seq (in this case the effect of siRNA knockdown of each evaluated gene on AR-V7 and AR-FL protein levels). However, the targeted siRNA screen performed in this chapter involved individual silencing of 315 different genes, necessitating the use of a high-throughput method. While culture conditions for this were optimised, as outlined in **section 5.3.4.1**, the degree of knockdown for each individual protein targeted by siRNA in the screen could not be determined. As a consequence, the siRNA screen is vulnerable to false negative results. In other words, it is possible that some genes considered not to impact AR-V7 levels within the screen may indeed have a role in regulating AR-V7, but this was not identified because silencing of the target gene was inadequate. While suboptimal, this was necessary to enable cost-effective completion of the siRNA screen, which overall provides vital information needed to validate, and correctly interpret, the findings of the accompanying RNA-seq analyses.

5.6 Conclusion

In conclusion, the results presented in this chapter identify for the first time that the 2OG-dependent oxygenase JMJD6 may be a potentially important regulator of AR-V7 expression, meriting further evaluation in patient samples, and more focused *in vitro* studies, to validate its suitability as a novel therapeutic target for overcoming oncogenic AR-V7 signalling in lethal prostate cancer.

6

Establishing the clinical relevance of JMJD6

6.1 Research in context

The success of translational research is highly dependent on the ability of *in vitro* models to replicate human disease. As discussed in **section 5.5.1**, this represents a significant obstacle in the study of prostate cancer given that available *in vitro* models are limited in number, and are often poorly representative of the disease in patients. However, this issue is not limited to prostate cancer biology, representing a considerable challenge across nearly all solid cancer types. As such, encouraging preclinical data rarely translate into meaningful clinical benefit, illustrated best by the high rates of attrition of drug development programmes [256].

Consequently, the interrogation of patient clinical samples has become an invaluable tool in establishing the clinical relevance, and importance, of genes/proteins identified *in vitro* as potential therapeutic targets. For example, while the inhibition of a transmembrane receptor in cell culture models may result in the inhibition of cancer cell growth, if evaluation of patient tissue samples reveals that the expression of the said receptor is negligible or rare, efforts to develop chemical inhibitors of that receptor are liable to be in vain, and this is unlikely to be a clinically useful therapeutic target. Moreover, in the case of prostate cancer, if the expression of a gene/protein is low at diagnosis, but increases significantly as patients progress to metastatic CRPC, this may indicate its importance for disease progression, and

suggests that pharmacological inhibition may indeed be of clinical benefit; but perhaps only once patients develop castration-resistance. Elucidating the degree of expression of a potential therapeutic target in patients, and how these levels change over time, is therefore critical in maximising the cost-effectiveness of a drug development programme. This is not only to identify the most appropriate clinical setting in which to employ a newly developed agent, but also to ensure that resources are not wasted by pursuing flawed targets.

Therefore, having identified JMJD6 as protein of interest *in vitro*, to establish its potential clinical relevance, I explored the expression of JMJD6 in patient samples across two clinical cohorts. First, I interrogated whole exome and transcriptome data (SU2C/PCF cohort**; section 4.3.2**) to determine the frequency of JMJD6 gene alterations, and the level of JMJD6 mRNA expression, in metastatic CRPC patient biopsies. Alongside these analyses, I also immunohistochemically evaluated JMJD6 protein levels in matched, same-patient, diagnostic castration-sensitive, and metastatic castration-resistant, tissue biopsies (ICR/RMH cohort; **section 4.3.1**) to determine both the degree of JMJD6 expression in these samples, and how JMJD6 protein levels change over time. Subsequently, I correlated these findings with patient clinical outcome data, to evaluate the potential clinical relevance of JMJD6 in lethal prostate cancer.

6.2 Specific aims

- To establish the incidence of JMJD6 genomic alterations in metastatic CRPC patient samples, and determine how these correlate with JMJD6 mRNA expression levels.
- To study how JMJD6 mRNA expression levels in metastatic CRPC patient samples correlate with AR and AR-V7 signalling activity.
- To quantify the levels of JMJD6 protein in both diagnostic castration-sensitive, and metastatic castration-resistant prostate cancer tissue samples.
- To identify associations between JMJD6 protein levels in metastatic CRPC patient tissue samples and clinical outcomes.

6.3 Evaluation of JMJD6 gene alterations and mRNA expression in metastatic CRPC patient whole exome and transcriptome data

With the assistance of Dr. Wei Yuan, senior bioinformatician within the de Bono research group, whole exome next generation sequencing data for 231 metastatic CRPC patients, generated by the International Stand Up To Cancer/Prostate Cancer Foundation (SU2C/PCF) Prostate Cancer Dream Team, were downloaded and reanalysed [103]. JMJD6 genomic alterations were detected in 47% (n=108) of metastatic CRPC biopsies within this cohort, with these being predominately gains (37%; n=86) or amplifications (8%; n=18) ***(figure 6.1A)***. Importantly, these genomic alterations correlated with an increase in JMJD6 mRNA expression (analysis of n=108 transcriptomes; ***figure 6.1B***).

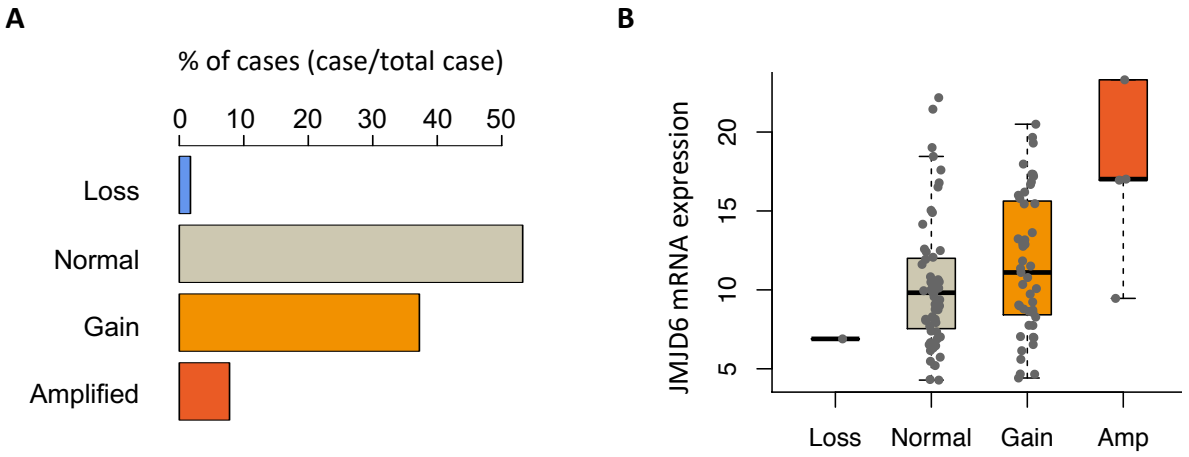

Figure 6.1: JMJD6 genomic alterations are common in metastatic CRPC patient samples and associate with increased JMJD6 mRNA expression. (A) Interrogation of 231 metastatic CRPC whole exomes revealed alterations of the JMJD6 gene locus in 47% (n=108) of metastatic CRPC patient biopsies, with these being predominately gains (37%; n=86) or amplifications (8%; n=18). **(B)** JMJD6 gain and amplification both associated with an increase in JMJD6 mRNA expression (FPKM; n=108 metastatic CRPC patient transcriptomes). Amp = amplified. Bioinformatic analyses were performed with the help of Dr Wei Yuan.

In addition, JMJD6 mRNA expression levels correlated significantly with androgen response (H) ***(figure 6.2A)***, AR signature ***(figure 6.2B)***, and a previously reported AR-V7 signature ***(figure 6.2C)***, in these metastatic CRPC biopsies (*p<0.001, p<0.001* and *p=0.011* respectively), with the correlation between JMJD6 mRNA expression and both AR and AR-V7 signatures being independent of AR copy number (*p=0.24* and *p=0.65*, respectively; ***figure 6.2D and E***). Next, to investigate how the observed correlation between JMJD6 mRNA expression and AR-V7 signature compared with other transcripts, I ranked the correlation of

all expressed transcripts with the AR-V7 signature. Interestingly, as shown in ***figure 6.2F***, the correlation observed between JMJD6 mRNA expression and AR-V7 signature was not as strong as for some other genes, suggesting that variability in JMJD6 mRNA expression alone does not fully explain AR-V7 protein expression. This may be in keeping with the regulation of JMJD6 function by post-translational events as well as 2OG levels, or the need for key downstream spliceosome components. Moreover, such analyses carry a false discovery rate as a consequence of multiple testing.

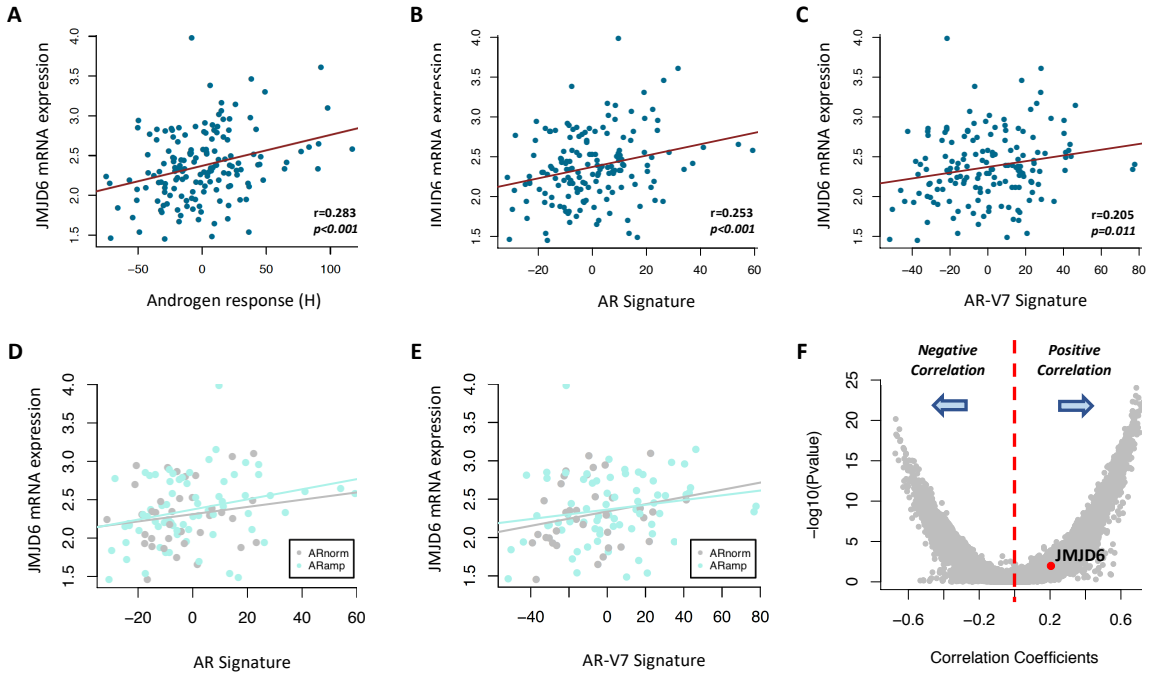

Figure 6.2: JMJD6 mRNA expression correlates with AR and AR-V7 activity in metastatic CRPC patient transcriptomes. (A-C) Scatter plots showing positive correlations between JMJD6 mRNA expression and **(A)** androgen response (H), **(B)** AR signature (derived from 43 AR regulated transcripts) and **(C)** AR-V7 signature (derived from 59 genes associated with ARV7 expression in CRPC) in metastatic CRPC biopsies from SU2C/PCF cohort. **(D - E)** Scatter plots illustrating the correlation between JMJD6 mRNA expression and both **(D)** AR signature, and **(E)** AR-V7 signature in the SU2C/PCF cohort, with patients subdivided by AR copy number; normal AR copy number represented by light blue dots and regression line, and AR amplification represented by grey dots and regression line. Shows that correlation between JMJD6 mRNA expression and both AR and AR-V7 signatures is independent of AR copy number, with no significant difference between AR normal and AR amplified regression lines with either signature (AR signature *p = 0.24;* AR-V7 signature *p = 0.65*; *p values* calculated by multi-regression analysis). **(F)** Volcano plot summarising the results of a genome-wide screen investigating the correlation between AR-V7 signature and other genes in the genome (SU2C/PCF cohort). Grey dots represent the correlation coefficients for each individual gene other than JMJD6, which is highlighted by the red dot. JMJD6 mRNA expression shown as log FPKM. *p values* were calculated by linear regression analysis. Bioinformatic analyses were performed with the help of Dr Wei Yuan.

Taken together, these results indicated that the JMJD6 gene is expressed in metastatic CRPC, and that its expression is associated with both AR and AR-V7 signalling activity, supporting the further evaluation of JMJD6 as a gene of interest in metastatic CRPC.

6.4 Evaluation of JMJD6 protein expression in patient tissue biopsies

6.4.1 Anti-Jmjd6 antibody validation

As described in **section 4.3.3**, anti-JMJD6 antibody specificity was validated by Western blot, confirming the detection of only a single band in LNCaP95 whole cell lysates, and IHC, demonstrating a reduction in nuclear JMJD6 protein staining following treatment with a JMJD6-specific siRNA compared to non-targeting control siRNA ***(figure 6.3)***.

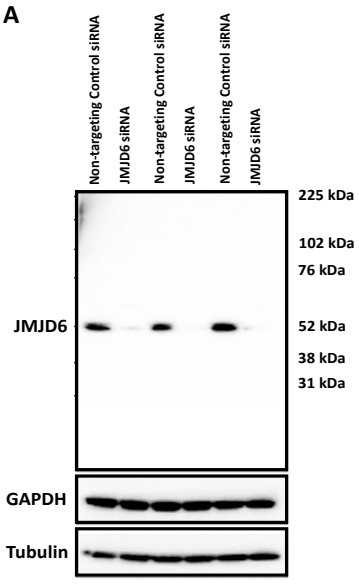

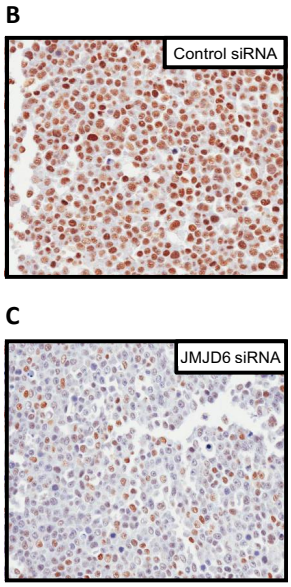

Figure 6.3: anti-Jmjd6 antibody validation. (A) Antibody specificity was confirmed by the detection of a single band in LNCaP95 whole cell lysates by Western blot, with downregulation following treatment with JMJD6 siRNA compared to non-targeting control siRNA (shown in triplicate). **(B)** Micrograph of LNCaP95 prostate cancer cells treated with non-targeting control siRNA demonstrating positive brown nuclear staining for JMJD6. **(C)** Micrograph of LNCaP95 prostate cancer cells treated with JMJD6 siRNA demonstrates a marked reduction in nuclear JMJD6 protein expression, with predominately blue, negative staining for JMJD6. IHC staining of treated LNCaP95 cell pellets performed by Ines Figueiredo.

6.4.2 IHC quantification of JMJD6 protein levels in CSPC and metastatic CRPC patient tissue biopsies

Following thorough antibody validation, JMJD6 protein expression was evaluated in 74 metastatic CRPC clinical biopsies, of which 64 patients also had sufficient matched, same patient, diagnostic, castration-sensitive tissue for analysis ***(figure 6.4A-C)***. A breakdown of patient characteristics for this cohort is shown in ***Table 6.1***. Interestingly, these data revealed a significant and substantial increase in nuclear JMJD6 protein levels in metastatic CRPC biopsies (median H-score [interquartile range]; CSPC 12.5 [0.0-67.5] vs CRPC 80 [20.0-130.0]; $p < 0.001$) ***(figure 6.4D)***. In addition, immunohistochemical analyses of these metastatic CRPC biopsies revealed a significantly higher expression of AR-V7 in patients with higher JMJD6

Clinical characteristics	
Diagnostic castration-sensitive tissue samples (CSPC) [64 patients had matched CSPC tissue availible for analysis (n=64)]	
Histology (N, %)	
Adenocarcinoma	64, 100%
Metastatic castration-resistant tissue samples (CRPC; n=74)	
Gleason score (N, %)	
<7	7, 9%
7	17, 23%
>7	50, 68%
NR	0, 0%
Metastatic at diagnosis (N, %)	
M0	35, 47%
M1	30, 41%
NR	9, 12%
Treatment intent (N, %)	
Radical	32, 43%
Palliative	42, 57%
Biopsy site (N, %)	
Bone	41, 55%
Lymph node	21, 28%
Other	12, 16%
Systemic therapies prior to biopsy^	
0	1, 1%
1	20, 27%
2	20, 27%
3	20, 27%
4	12, 16%
5	1, 1%
AR targeting therapy prior to biopsy	
Post abiraterone or enzalutamide	62, 84%

Table 6.1: ICR/RMH patient cohort characteristics. 74 metastatic CRPC patient tissue biopsies were identified as being suitable for evaluation of JMJD6 and AR-V7 protein levels, of which 64 also had matched, same-patient diagnostic castration sensitive prostate cancer tissue samples available for analysis. N – number, NR – not recorded, AR – androgen receptor, ^ - systemic therapies include docetaxel, cabazitaxel, abiraterone and enzalutamide.

protein levels, when dichotomized by median metastatic CRPC JMJD6 H-Score (median AR-V7 H-score in patients with low metastatic CRPC JMJD6 expression = 50 [0.0-105.0; n = 33] vs median AR-V7 H-score in patients with high metastatic CRPC JMJD6 expression 100 [22.5-147.5; n = 41]; *p = 0.036*) ***(figure 6.4E)***. In keeping with this association, further subdivision of nuclear JMJD6 protein levels into quartiles revealed a positive trend, with patients that exhibited the highest levels of nuclear JMJD6 protein in their evaluated CRPC tissue sample (top quartile) also having higher levels of nuclear AR-V7 protein, although this trend did not reach significance (median AR-V7 H-score in bottom quartile = 25 [0.3-107.5] vs median AR-V7 H-score in top quartile = 120 [25.0-170.0]; *p = 0.07*) ***(figure 6.4F)***. To better evaluate concordance between JMJD6 and AR-V7 protein levels in these CRPC patient biopsies therefore, given that both JMJD6 and AR-V7 H-Scores represent continuous variables,

Spearman's rank analyses were also performed, revealing a positive correlation between JMJD6 and AR-V7 protein levels in these CRPC tissue samples (r = 0.24, p = 0.04) ***(figure 6.4G)***.

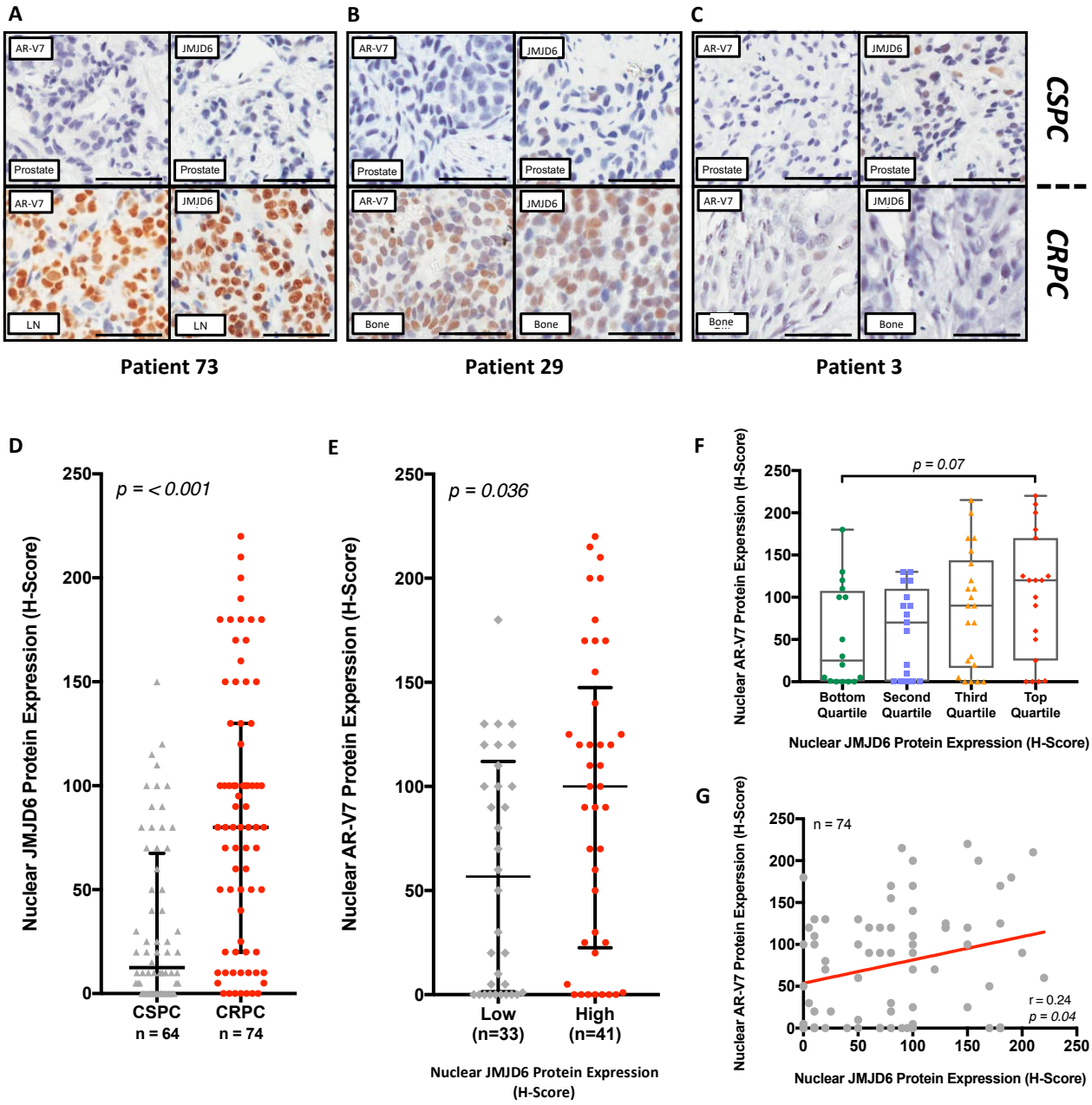

Figure 6.4: JMJD6 protein levels increase in metastatic CRPC and associate with AR-V7 levels. (A-C) Micrographs of AR-V7 and JMJD6 IHC in matched, same-patient, diagnostic castration-sensitive (top of panel) and metastatic CRPC (bottom of panel) biopsies from three different patients *(RMH/ICR patient cohort)*. All scale bars set to 100 μm. JMJD6 protein levels in metastatic CRPC tissue samples were similar to AR-V7 protein levels in metastatic CRPC. **(D)** JMJD6 protein levels were significantly higher (*p<0.001*) in metastatic CRPC biopsies (n=74) than in CSPC biopsies (n=64) (median H-score [IQR]; CSPC 12.5 [0.0-67.5] vs CRPC 80 [20.0-130.0]; Wilcoxon rank-sum analysis). **(E)** AR-V7 protein levels were significantly higher (*p=0.036*) in metastatic CRPC tissue samples from patients with high (H-Score ≥ median) metastatic CRPC JMJD6 protein levels (Low 50 [0.0-105.0; n = 33] vs High 100 [22.5-147.5; n = 41]; Mann-Whitney test). **(F)** Nuclear JMJD6 protein levels (as quantified by H-Score) subdivided into quartiles with median AR-V7 protein levels (as quantified by H-Score) determined for each quartile. Demonstrates positive trend, suggesting that patient CRPC tissue samples with higher levels of JMJD6 protein also have higher levels of AR-V7 protein (Bottom Quartile = 25 [0.3-107.5] vs Top Quartile = 120 [25.0-170.0]; p = 0.07). **(F)** Scatter plot showing nuclear JMJD6 and AR-V7 protein levels for all patients. Grey dots represent each individual patient's JMJD6 and AR-V7 H-Score. Demonstrates a positive correlation between JMJD6 and AR-V7 protein expression in these evaluated CRPC patient biopsies (n=74; r = 0.24; *p = 0.04*). IHC staining of patient tissue biopsies were kindly performed by Ines Figueiredo, Ana Ferreira, and Ruth Riisnaes

6.5 Correlation of JMJD6 protein levels in metastatic CRPC patient tissue biopsies with patient clinical outcome data

To determine the clinical significance of the upregulation in JMJD6 protein levels seen in the metastatic CRPC patient biopsies evaluated in **section 6.4.2** (ICR/RMH cohort), I subsequently retrospectively evaluated these patients' medical records, correlating JMJD6 metastatic CRPC protein levels with survival from the time of each patient's metastatic CRPC tissue biopsy. This revealed that JMJD6 protein levels in metastatic CRPC associated with a worse prognosis, with patients with the highest levels of JMJD6 in their metastatic CRPC biopsy (H-Score ≥ 75th percentile) having a significantly shorter median survival than those with the lowest levels (H-Score < 25th percentile) (14 months [n=16] vs 8 months [n=19]; hazard ratio 2.15; 95% confidence interval 1.19 - 5.92; *p=0.017*) ***(figure 6.5)***.

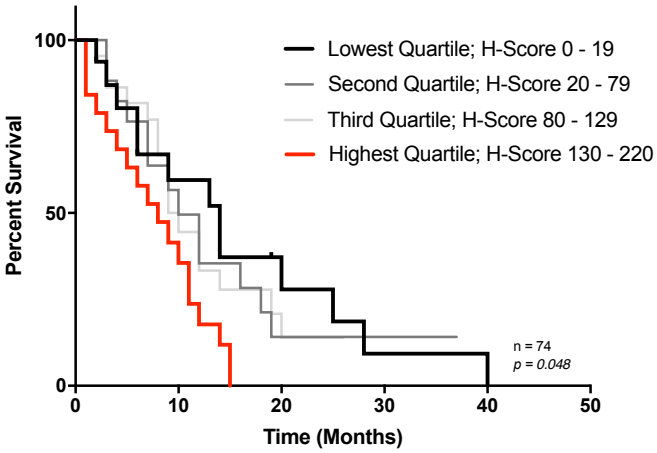

Figure 6.5: JMJD6 protein levels in metastatic CRPC tissue biopsies associated with a worse prognosis. Median survival from the time of metastatic CRPC tissue biopsy was significantly shorter in patients with the highest levels of JMJD6 (H-Score ≥ 75th percentile) in their metastatic CRPC tissue sample (n=74, *p=0.048*; Log-rank test).

Overall, these results suggest that JMJD6 is a clinically relevant protein in metastatic CRPC; increasing significantly with the emergence of castration-resistant disease, and associating with both higher levels of AR-V7 and a worse prognosis.

6.6 Discussion

Through interrogation of two independent patient data sets, in this chapter I have shown that JMJD6 is expressed in prostate cancer, and that its levels increase significantly

with the emergence of castration-resistance. This may, in part, be driven by gains and amplifications of the JMJD6 gene, which my results indicate are relatively common in metastatic CRPC and are associated with increased JMJD6 mRNA expression. In addition to these potential genomic drivers of JMJD6 upregulation however, tumour microenvironmental factors may also play a role in the observed increase of JMJD6 expression in metastatic CRPC. JMJD6 has been reported to be upregulated by hypoxia [302], which is considered to be an early event in prostate carcinogenesis [303]. In addition, as a 2OG-dependent oxygenase, changes in 2OG availability (a key tricarboxylic acid (TCA) cycle intermediate which is also generated by glutaminolysis) may also impact on JMJD6 expression and/or activity. This is particularly relevant given that 2OG levels can vary depending on cell replication rate, oxygen availability, androgen deprivation, and the presence of genomic aberrations (e.g. PTEN loss), all of which are common in prostate cancer [103, 303]. Understanding the mechanisms underlying the upregulation of JMJD6 seen in metastatic CRPC is therefore an important avenue for future work that may have wider implications for prostate cancer biology. The results presented in this chapter also add further credence to the potential role of JMJD6 as a regulator of AR-V7. JMJD6 protein levels were found to associate with AR-V7 expression in metastatic CRPC patient biopsies, while JMJD6 mRNA levels corelated significantly with AR-V7 activity. In keeping with this relationship with AR-V7, which has been reported to confer a shorter overall survival, JMJD6 protein levels also appeared to associate with a worse prognosis in metastatic CRPC.

Taken together, these data indicate that JMJD6 protein is produced in prostate cancer cells, that the level of JMJD6 increases significantly with the emergence of castration-resistant disease, and that this upregulation of JMJD6 correlates with a higher level of AR-V7. Furthermore, my results also suggest that higher JMJD6 levels in metastatic CRPC cells likely correlate with a worse prognosis. Overall therefore, these data indicated that JMJD6 is a clinically relevant protein in metastatic CRPC that merits further evaluation as a therapeutic target for abrogating oncogenic AR-V7 signalling.

6.6.1 Limitations

While the results presented in this chapter are encouraging, in that they suggest JMJD6 may be a clinically relevant protein in metastatic CRPC that is associated with AR-V7

expression and signalling activity, mRNA and protein expression data do not on their own inform on protein function. Therefore, the conclusions drawn from these results are limited by the assumption that detectable protein is functional protein. While this would be true if JMJD6-mediated regulation of AR-V7 occurred through a protein scaffold function of JMJD6, it has been convincingly demonstrated that JMJD6 possesses catalytic activity, and this cannot be inferred from mRNA or protein expression levels alone; and it is this which may explain why some patients with low JMJD6 protein levels have high levels of AR-V7, and *vice versa*.

In addition, while the data presented in this chapter reveal that JMJD6 protein levels are clinically relevant in lethal prostate cancer, associating with a worse prognosis, this finding must be tempered by the relatively limited sample size and heterogeneity of the patient cohort evaluated (ICR/RMH cohort). Sampling of castration-resistant tissue is also typically performed at different times in the trajectory of a patient's disease; as such it does not represent a standardised timepoint. Consequently, making definitive inferences on the impact of JMJD6 expression on survival from this is challenging. Instead, more definitive evaluation of the association between JMJD6 protein levels and patient outcomes is now needed in larger, prospective datasets.

6.7 Conclusion

In conclusion, the results presented in this chapter demonstrate that JMJD6 is a clinically relevant protein in lethal prostate cancer. They indicate that JMJD6 protein is produced in prostate cancer cells, that the level of JMJD6 increases significantly with the emergence of castration-resistant disease, and that this upregulation of JMJD6 correlates with a higher level of AR-V7. Furthermore, they suggest that JMJD6 protein levels are associated with a worse prognosis in metastatic CRPC.

7

JMJD6, AR-V7, and prostate cancer cell growth

7.1 Research in context

Discovery of an association and/or correlation between a variable, such as a gene or environmental factor, and a disease is often an important first stepping-stone to understanding the pathophysiology of a disease. For example, the association between smoking and lung cancer [304, 305]. However, *correlation does not imply causation*. In the previous chapter, **chapter six**, I have demonstrated that JMJD6 protein levels increase with the emergence of castration-resistance, and that this upregulation correlates with AR-V7 protein levels. However, this alone does not prove that JMJD6 has a role in the expression of AR-V7.

In this chapter therefore, I utilise established *in vitro* models of lethal prostate cancer to investigate the relationship between JMJD6 and AR-V7, and ascertain the importance of JMJD6 for prostate cancer cell growth. Through siRNA-mediated gene silencing experiments, I determine the effect of JMJD6 knockdown on AR-V7 mRNA and protein levels in hormone-sensitive and castration-resistant prostate cancer cell lines. In addition, I investigate how JMJD6 knockdown impacts the growth of not only prostate cancer cells, but also normal benign prostatic epithelial cells.

Together, these studies seek to test the hypothesis that JMJD6 knockdown can overcome AR-V7-mediated resistance to AR directed therapies, and establish whether there is indeed a regulatory link between JMJD6 and AR-V7 protein production, as is suggested by their correlation in metastatic CRPC tissue samples.

7.2 Specific Aims

- To determine the impact of JMJD6 gene silencing on AR-V7 mRNA and protein levels.
- To ascertain the importance of JMJD6 for prostate cancer cell growth.
- To investigate whether JMJD6 knockdown can prevent the induction of AR-V7, and overcome AR-V7 driven resistance to AR directed therapies.

7.3 JMJD6 and AR-V7 expression

To elucidate the role of JMJD6 in the expression of AR-V7, I treated the AR-V7 producing prostate cancer cell lines 22Rv1 and LNCaP95 with either JMJD6 siRNA (25 nM), or a non-targeting control siRNA (25 nM), for 72 hours. As shown in ***figure 7.1***, JMJD6 siRNA knockdown led to a reduction of both AR-V7 mRNA and protein levels in both cell lines.

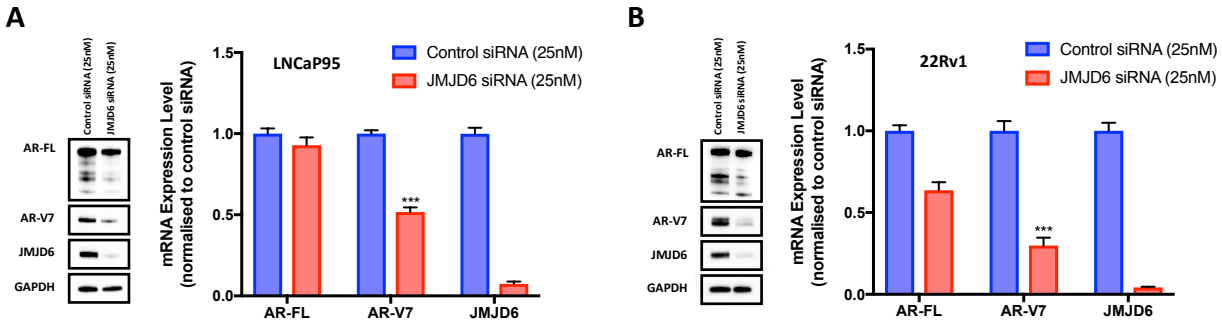

Figure 7.1: JMJD6 siRNA knockdown downregulates AR-V7 expression. JMJD6 siRNA knockdown reduced both AR-V7 protein (Western blot) and mRNA (qPCR; Bar chart) levels in **(A)** LNCaP95, and **(B)** 22Rv1 cell lines. Control siRNA (blue bars) and JMJD6 siRNA (red bars) both used at 25 nM concentration. Single representative Western blot shown from three separate biological replicates. Mean RNA expression (normalised to housekeeping genes (B2M and GAPDH) and control siRNA at equivalent concentration; defined as 1.0) with standard error of the mean from three separate biological replicates is shown. qPCR analysis of each biological replicate was performed in technical duplicate. *p values (*, $p \leq 0.05$; **, $p \leq 0.01$; ***, $p \leq 0.001$)* were calculated compared to control (at equivalent concentration) using mean value of technical replicates for each of the three biological replicates (n=3) with unpaired Student's t tests.

7.4 JMJD6 knockdown and prostate cancer cell growth

To ascertain the importance of JMJD6 for prostate cancer cell survival and proliferation, I performed growth assays following JMJD6 gene silencing in both prostate cancer cells, and normal prostatic epithelial cells. Cells were treated with either a JMJD6 siRNA (25 nM) or a non-targeting control siRNA (25 nM), and the effect on growth was determined after six days. Treatment with JMJD6 siRNA resulted in a significant reduction in the growth of the castration-resistant, AR-V7 producing, prostate cancer cell lines LNCaP95 and 22Rv1 compared to treatment with a non-targeting control siRNA ***(figure 7.2)***. PNT2 cells however, which are an immortalised model of normal prostatic epithelium, were relatively unaffected.

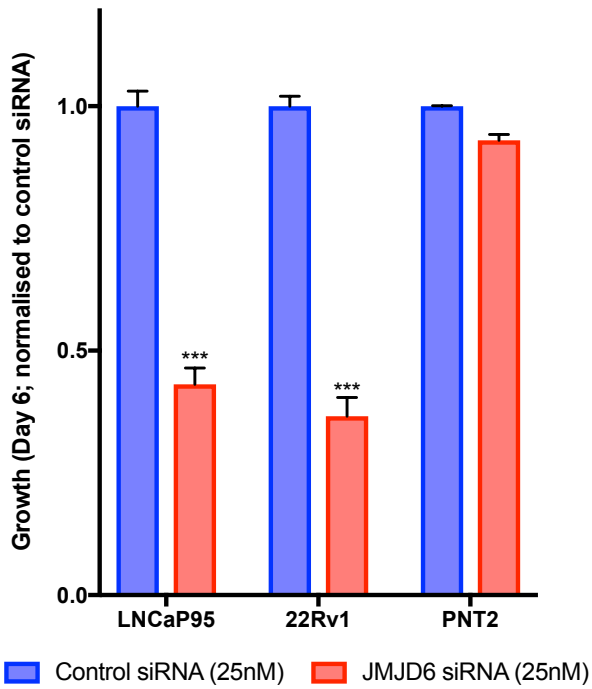

Figure 7.2: JMJD6 siRNA knockdown reduces prostate cancer cell growth *in vitro*. Bar graph demonstrating that JMJD6 siRNA knockdown (25nM; red bars) significantly reduced the growth of the castration-resistant, AR-V7 producing, prostate cancer cell lines LNCaP95 and 22Rv1 compared to non-targeting control siRNA (25nM; blue bars) after six days growth, while PNT2 cells (immortalised normal prostatic epithelial cells) were relatively unaffected. Mean cell growth (normalised to control siRNA at same concentration +/- vehicle) shown with standard error of the mean; n ≥ 4 data points (at least 2 biological replicates with 2 technical replicates). *p values (*, p ≤ 0.05; **, p ≤ 0.01; ***, p ≤ 0.001)* were calculated compared to control (at equivalent concentration) using mean value of technical replicates with unpaired Student's t tests.

The effect of JMJD6 knockdown was also evaluated in the hormone-sensitive VCaP prostate cancer cell line, which contains the TMPRSS2/ERG rearrangement that is found in 30-40% of advanced prostate cancers, and which possesses a high copy gene amplification of AR. Furthermore, VCaP cells upregulate the expression of AR-V7 in response to androgen-deprivation *in vitro* [306, 307]. VCaP Cells were treated with either a JMJD6 siRNA (25 nM) or a non-targeting control siRNA (25 nM), both with (enzalutamide 10 μM) and without (DMSO

0.1%) AR blockade, and the effect on growth was determined after five days. As seen in 22Rv1 and LNCaP95 prostate cancer cells ***(figure 7.2)***, JMJD6 siRNA knockdown reduced VCaP prostate cancer cell growth compared to a non-targeting control siRNA. As expected, this was similarly the case with enzalutamide (10 μM) treatment alone. Importantly, however, combination treatment with JMJD6 siRNA *and* enzalutamide had a significantly more profound effect on cell growth, and inhibited VCaP cell viability and proliferation more than either JMJD6 siRNA alone or enzalutamide treatment alone.

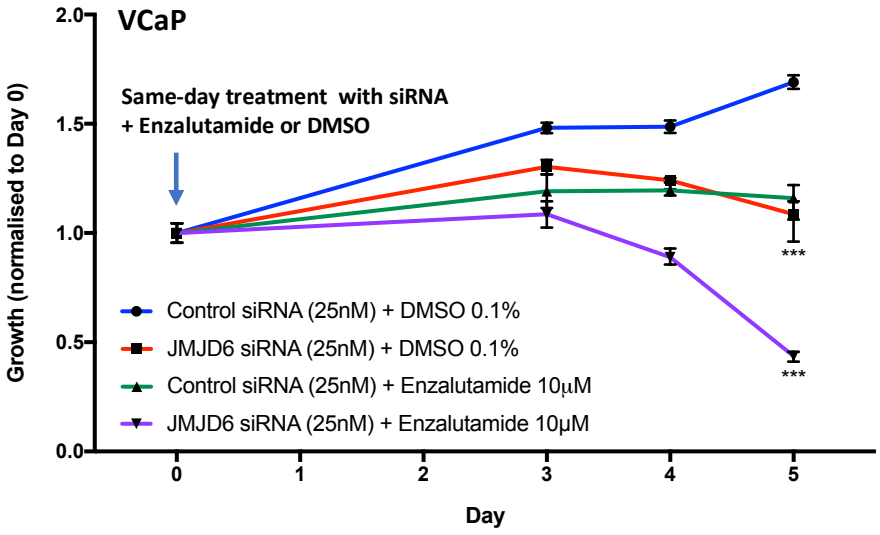

Figure 7.3: JMJD6 siRNA knockdown reduces VCaP prostate cancer cell growth both alone, and in combination with enzalutamide. Line graph illustrating the impact of treatment with JMJD6 siRNA (25 nM) +/- enzalutamide (10 μM) on the growth of hormone-sensitive, AR amplified and AR-V7 producing VCaP PC cells compared to controls after five days. As seen in 22Rv1 and LNCaP95 prostate cancer cell lines, JMJD6 siRNA knockdown (red line) significantly reduced VCaP prostate cancer cell growth compared to control siRNA (blue line). In addition, combination treatment with enzalutamide (purple line) resulted in a significantly more profound reduction of VCaP cell growth than either JMJD6 siRNA alone (red) or enzalutamide alone (green). n=3; Mean cell growth (normalised to control siRNA at same concentration + DMSO 0.1%) shown with standard error of the mean. *p values (*, $p \leq 0.05$; **, $p \leq 0.01$; ***, $p \leq 0.001$)* were calculated for each condition compared to control (at equivalent concentration) using mean value of technical replicates with unpaired Student's t tests.

7.5 JMJD6 inhibits the induction of AR-V7 in response to AR blockade *in vitro*

To better understand the increased reduction in VCaP prostate cancer cell growth observed following combination treatment with JMJD6 siRNA and enzalutamide, Western blot and mRNA analyses were performed of VCaP cells following 72 hours of treatment with either non-targeting control siRNA or JMJD6 siRNA (25 nM), both with (enzalutamide 10 μM)

and without (DMSO 0.1%) AR blockade ***(figure 7.4)***. JMJD6 knockdown downregulated AR-V7 protein and mRNA levels, as previously observed in LNCaP95 and 22Rv1 cell lines ***(figure 7.1)***; moreover, and critically, the induction of AR-V7 seen in response to AR blockade was also significantly attenuated by JMJD6 knockdown.

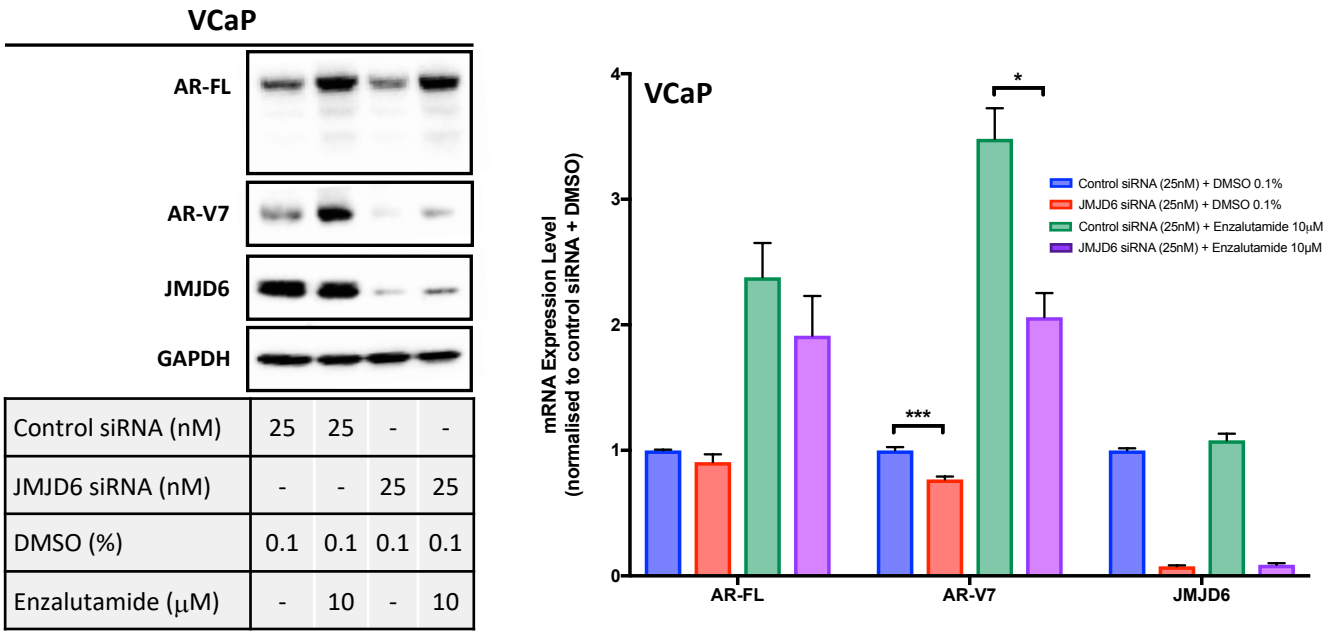

Figure 7.4: JMJD6 siRNA knockdown reduces the induction of AR-V7 in VCaP prostate cancer cells following AR blockade. JMJD6 gene silencing downregulates AR-V7 protein (Western blot) and mRNA (qPCR; Bar chart) levels at baseline in VCaP prostate cancer cells. JMJD6 knockdown also inhibits the induction of AR-V7 (protein and mRNA) in response to AR blockade (enzalutamide 10 μM). Single representative Western blot shown from three separate biological replicates. Mean mRNA expression (normalised to housekeeping genes (B2M, GAPDH and CDC73), and control siRNA at equivalent concentration + DMSO 0.1%; defined as 1.0) with standard error of the mean from three separate biological replicates is shown. qPCR analysis of each biological replicate was performed in technical duplicate. *p values (*, $p \leq 0.05$; **, $p \leq 0.01$; ***, $p \leq 0.001$)* were calculated for each condition compared to control (at equivalent concentration) using mean value of technical replicates for each of the three biological replicates (n=3) with unpaired Student's t tests.

7.6 Deconvolution of the siRNA pool

The results presented in **sections 7.3** to **7.5** demonstrate that JMJD6 siRNA knockdown downregulates AR-V7 protein levels. However, these studies were performed using a pooled JMJD6 siRNA comprising of four different individual siRNAs. To deconvolve the effect of the individual siRNAs within the siRNA pool therefore, I performed Western blot analyses using 22Rv1 prostate cancer cells following 72 hours of treatment with either a non-targeting control siRNA (25nM), or one of the individual JMJD6-specific siRNAs (25nM) which constitute the siRNA pool (JMJD6 siRNA$^{1-4}$). Overall, as shown in ***figure 7.5***, good concordance

was seen between the individual siRNAs and the pooled siRNA, with AR-V7 protein levels being consistently downregulated following JMJD6 knockdown.

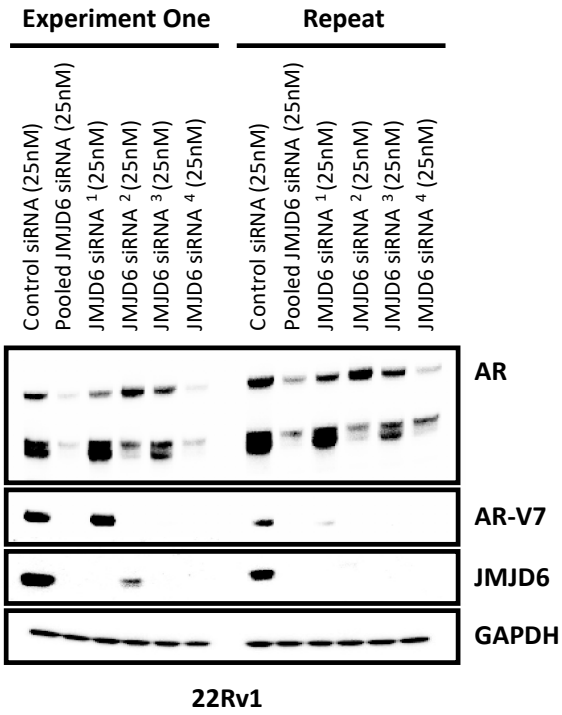

Figure 7.5: The effect of the individual JMJD6 siRNAs which constitute the JMJD6 pooled siRNA on AR-V7. Western blot of 22Rv1 prostate cancer cells following 72 hours of treatment with either a non-targeting control siRNA (25nM), pooled JMJD6 siRNA (25nM), or one of the individual JMJD6-specific siRNAs (25nM) which constitute the siRNA pool (JMJD6 siRNA$^{1-4}$). Good concordance seen between the individual siRNAs and the pooled siRNA, with AR-V7 protein levels being downregulated following JMJD6 knockdown. Single western blot demonstrating two biological replicates.

Notably, however, unlike JMJD6 siRNA^{2}, siRNA^{3} and siRNA^{4}, AR-V7 downregulation with JMJD6 siRNA^{1} was inconsistent. Therefore, to further validate these findings, I also performed Western blot analyses using 22Rv1 prostate cancer cells following 72 hours of treatment with either a non-targeting control siRNA (25nM), or an alternative JMJD6-specific individual siRNA (JMJD6 siRNA^{5}) purchased from a different manufacturer (Sigma); Importantly, JMJD6 siRNA^{5} targets a different region of the JMJD6 sequence to any of the other individual siRNAs ***(Table 7.1; figure 7.6)***.

Individual siRNA	Target Sequence
JMJD6 individual siRNA 1 (JMJD6 siRNA^{1})	GGAGAGCACUCGAGAUGAU
JMJD6 individual siRNA 2 (JMJD6 siRNA^{2})	GGACCCGGCACAACUACUA
JMJD6 individual siRNA 3 (JMJD6 siRNA^{3})	GGUAUAGGAUUUUGAAGCA
JMJD6 individual siRNA 4 (JMJD6 siRNA^{4})	GGAUAACGAUGGCUACUCA
JMJD6 individual siRNA 5 (JMJD6 siRNA^{5})	GGUGAACACCCUAAAAGAA

Table 7.1: Target sequences of individual siRNAs.

```
   1 aaaggcgccg ggactgagcg aagggcgttt gggtactgcc gtcgccgccg cccaggccgg
  61 ggaggggtgc gttagtgtca ggaagcgggc tgcgccgagg tcgtagcgga accagctggc
 121 gaccccgcag aatgaaccac aagagcaaga agcgcatccg cgaggccaag cggagtgcgc
 181 ggccggagct caaggactcg ctggattgga cccggcacaa ctactacgag agcttctcgc
 241 tgagcccggc ggccgtggcg gataacgtgg aaagggcaga tgctttacag ctgtctgtgg
 301 aagaatttgt ggagcggtat gaaagacctt acaagcccgt ggttttgttg aatgcgcaag
 361 agggctggtc tgcgcaggag aaatggactc tggagcgcct aaaaaggaaa tatcggaacc
 421 agaagttcaa gtgtggtgag gataacgatg gctactcagt gaagatgaag atgaaatact
 481 acatcgagta catggagagc actcgagatg atagtcccct ttacatcttt gacagcagct
 541 atggtgaaca ccctaaaaga aggaaacttt tggaagacta caaggtgcca aagtttttca
 601 ctgatgacct tttccagtat gctggggaga agcgcaggcc cccttacagg tggtttgtga
 661 tggggccacc acgctccgga actgggattc acatcgaccc tctgggaacc agtgcctgga
 721 atgccttagt tcagggccac aagcgctggt gcctgtttcc taccagcact cccagggaac
 781 tcatcaaagt gacccgagac gaaggaggga accagcaaga cgaagctatt acctggttta
 841 atgttattta tccccggaca cagcttccaa cctggccacc tgaattcaaa cccctggaaa
 901 tcttacaaaa accaggagag actgtctttg taccaggagg ctggtggcat gttgtcctca
 961 atctcgacac tactatcgcc atcacccaaa attttgccag cagcaccaac ttccctgtgg
1021 tatggcacaa gacggtaaga gggagaccaa agttatcaag gaaatggtat aggattttga
1081 agcaagagca ccccgagttg gcagtcctcg cagactcggt tgaccttcag gagtccacag
1141 ggatagcttc cgacagctcc agcgactctt ccagctcctc cagctccagt tcgtcagact
1201 ccgactcaga gtgcgagtct ggatccgagg gcgatgggac agtgcaccgc aggaagaaga
1261 ggaggacgtg cagcatggtg ggaaacgggg acaccacctc ccaggacgac tgtgtcagca
1321 aagagcgcag ctcctccagg attagggaca cttgtggagg ccgggctcac ccctgagcag
1381 ataaagagac tctccctgag gtgctttcag cgtaagcttt tggcagccac ccaactcagt
1441 tctcgcatct tctgctccta ccttctcctc tgtcttcttt gaatttggat attccttccc
```

Figure 7.6: Target regions of individual siRNAs used. The individual siRNAs studied target different regions of the JMJD6 sequence. Each individual siRNA's target sequence is highlighted in a different colour: JMJD6 siRNA[1] = green; JMJD6 siRNA[2] = blue; JMJD6 siRNA[3] = red; JMJD6 siRNA[4] = orange; JMJD6 siRNA[5] = purple. Note: Full JMJD6 sequence not shown.

As shown in ***figure 7.7***, JMJD6 knockdown with JMJD6 siRNA[5] again downregulated AR-V7 protein levels. Taken together therefore, these results support the findings presented in **sections 7.3** to **7.5** using the pooled siRNA, and suggest that the changes in AR-V7 protein levels seen in these experiments are likely a consequence of JMJD6 gene silencing, rather than an off-target effect.

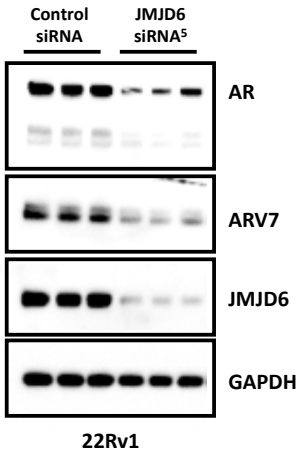

Figure 7.7: An alternative individual JMJD6 siRNA, JMJD6 siRNA[5], also downregulates AR-V7 protein levels. Western blot of 22Rv1 prostate cancer cells following 72 hours of treatment with either a non-targeting control siRNA (25nM) or individual JMJD6-specific siRNA 5 (JMJD6 siRNA[5]; 25nM), which is not part of the JMJD6 siRNA pool. Treatment with JMJD6 siRNA[5] also downregulated AR-V7 protein levels, replicating the effect of both the pooled JMJD6 siRNA, and the individual siRNAs that constitute the siRNA pool (JMJD6 siRNA[1-4]). Single western blot performed in technical triplicate.

7.7 Discussion

The results presented in this chapter demonstrate that JMJD6 is an important regulator of AR-V7 transcription, with JMJD6 knockdown reducing both AR-V7 mRNA and protein levels across a range of *in vitro* prostate cancer models with differing genomic backgrounds. Importantly, my results indicate that JMJD6 knockdown also inhibits the induction of AR-V7 protein expression in response to AR blockade in hormone-sensitive VCaP prostate cancer cells, suggesting limited functional redundancy in these tested models.

My results also indicate that JMJD6 is important for prostate cancer cell survival and proliferation. JMJD6 knockdown reduced the growth of the castration-resistant, AR-V7 producing, prostate cancer cell lines 22Rv1 and LNCaP95. Similarly, JMJD6 gene silencing also inhibited the growth of the hormone-sensitive, AR-V7 producing, VCaP prostate cancer cell line. Strikingly, however, JMJD6 siRNA knockdown in combination with AR blockade (enzalutamide) had a significantly more profound effect on VCaP cell growth compared to either JMJD6 siRNA alone, or enzalutamide alone; supporting, *in vitro*, my original hypothesis that targeting JMJD6 may overcome AR-V7-mediated resistance to AR directed therapies.

Taken together, these results demonstrate that JMJD6 is important for prostate cancer cell viability and proliferation, and that JMJD6 is required for the expression of AR-V7 in these *in vitro* models of lethal prostate cancer. Moreover, the studies presented in this chapter suggest that within the context of metastatic CRPC cells, targeting JMJD6 significantly impacts on the induction of AR-V7 at primary AR blockade. This may be critically important given that for AR-V7 therapies to be successful, novel therapeutics will be needed that can block AR-V7 generation, rather than just counteract its oncogenic effects once endocrine resistance is established [284].

7.7.1 Limitations

While the preclinical results presented in this chapter are encouraging, the conclusions drawn from these are likely, in part, to be dependent on the molecular characteristics of the various models used. This is particularly relevant given that the roles of JMJD6 appear to be pleiotropic [308, 309]; though it should be noted that this in itself does

not preclude therapeutically useful targeting of 2OG oxygenases, as shown by the clinical approvals of HIF prolyl-hydroxylase inhibitors [310]. Aside from the likelihood of its multiple context dependent substrates and partners [281, 289], the activity of JMJD6, like other 2OG oxygenases could be limited by oxygen and/or 2OG availability, which as discussed in **section 6.6**, may vary between different prostate cancer cell lines depending on replication rate, androgen deprivation, and the cell's molecular background. Nonetheless, the results reported here were replicated in a number of different cell lines with differing genomic backgrounds, supporting future *in vivo* studies on the role of JMJD6 in prostate cancer.

JMJD6 has been reported to function as both a lysyl hydroxylase and an arginine demethylase [308]. In addition, JMJD6 has also been reported to be involved in stoichiometric protein scaffold type interactions, which may or may not be linked to its catalytic activity. Indeed, a stoichiometric mechanism has been proposed for the AT hook domain of JMJD6 with respect to its role in adipogenesis in a manner independent of catalysis [311]. Therefore, while the siRNA-mediated knockdown of JMJD6 employed in this chapter has been successful in demonstrating the importance of JMJD6 for prostate cancer cell growth and AR-V7 generation, it does not inform on the mechanisms through which JMJD6 exerts its effects, as both enzymatic and protein scaffold functions are lost through downregulation of JMJD6 protein levels; which is a limitation of this work.

Another limitation of the siRNA-mediated gene silencing techniques adopted in this chapter is their potential to cause sequence-specific off-target effects. While siRNAs are widely used for gene inactivation in basic research, and therapeutically for that matter, such undesired effects are often unpredictable, as siRNAs can equally affect partially complementary sequences [312]. To minimise this issue, I elected to use a pooled JMJD6 siRNA consisting of 4 individual siRNAs. Having multiple siRNAs, each targeting a different region of the JMJD6 mRNA sequence, enables a lower concentration of each individual siRNA to be used, diluting the potential sequence-specific off-target effects of each individual siRNA to below detectable limits [312]. Furthermore, the pooled siRNAs I have used for these experiments have a 2'-O-methyl ribosyl substitution at position 2 in the guide strand. This has been shown to reduce silencing of most off-target transcripts that may be partially complementary to the seed region of the siRNA guide strand [313]. Therefore, while off-target

effects are an undesired consequence of siRNA-based experiments, I have considered this limitation when planning my experiments and taken steps to mitigate the likelihood of, and extent to which, these may confound my results.

7.8 Conclusion

In conclusion, the results presented in this chapter demonstrate that JMJD6 is important for prostate cancer cell viability and proliferation, and is required for the expression of AR-V7 in *in vitro* models of lethal prostate cancer. Furthermore, JMJD6 knockdown attenuated the induction of AR-V7 in response to AR blockade with enzalutamide, suggesting limited functional redundancy in these models. JMJD6 is thus a promising target for abrogating AR-V7 oncogenic signalling in preclinical models of CRPC, however further work in understanding the mechanisms through which JMJD6 regulates AR-V7 expression is required before the suitability of JMJD6 as a target for drug development efforts can be fully established.

8

Elucidating the mechanism through which JMJD6 Regulates AR-V7

8.1 Research in context

In **chapter seven** I demonstrated that JMJD6 gene silencing downregulates AR-V7 mRNA and protein levels in preclinical models of metastatic CRPC, indicating that JMJD6 is important in the regulation of AR-V7 transcription. In this chapter I investigate the mechanism through which this occurs.

While not itself a core spliceosome component, JMJD6 has been reported to interact with a number of proteins, many of which are involved in mRNA splicing [281, 288, 314]. As such, JMJD6 has previously been implicated in the regulation of alternative splicing events [315-318]. Perhaps the best described example of this is its interaction with the splicing regulatory factor U2AF65. As outlined in **section 1.2**, U2AF65 maintains splicing fidelity by assisting the core spliceosome component U2 in binding to the correct 3' splice site. JMJD6 has been demonstrated to post-translationally modify U2AF65, hydroxylating lysine residues in the U2A65 arginine-serine rich region, including K15, K38 and K276 [288]. In doing so, JMJD6 has been reported to modulate U2AF65-mediated alternative splicing events [318].

Importantly, U2AF65 has previously been reported to play a critical role in the expression of AR-V7, having been shown *in vitro* to be recruited to AR-V7 specific splice sites in response to ADT [97]. In keeping with this, U2AF65 siRNA knockdown has been shown to downregulate AR-V7, but not AR-FL, in preclinical models of metastatic CRPC [97]; highlighting the importance of U2AF65 for the generation of AR-V7.

In this chapter, I address the hypothesis that JMJD6-mediated regulation of AR-V7 production occurs through either the regulation of U2AF65 levels and/or of its recruitment to AR-V7 specific splice sites. Utilising metastatic CRPC patient transcriptome data (SU2C/PCF cohort) I correlate U2AF65 mRNA expression with androgen response (H), AR signature, and AR-V7 signature. In addition, I present results from *in vitro* studies investigating the relationship between JMJD6, U2AF65, and AR-V7, as well as the broader role of JMJD6 on alternative splicing in prostate cancer cells.

8.2 Specific aims

- To evaluate the change in JMJD6, U2AF65 and AR-V7 protein levels following both JMJD6 and U2AF65 siRNA knockdown.
- To determine the effect of JMJD6 gene silencing on the recruitment of U2AF65 to AR-V7 specific splice sites.
- To study the broader impact of JMJD6 knockdown on the frequency of alternative splicing events in prostate cancer cells.

8.3 Investigating the relationship between U2AF65 and AR-V7 in metastatic CRPC patient samples

To investigate the relationship between the SR factor U2AF65 and AR-V7, and better appreciate its potential clinical relevance, with the help of Dr Wei Yuan, I interrogated transcriptome data from 108 metastatic CRPC patient biopsies (SU2C/PCF cohort) to

determine associations between U2AF65 mRNA expression and both AR and AR-V7 signalling activity. As I observed with JMJD6 mRNA expression **(section 6.3; *figure 6.2*)**, U2AF65 mRNA expression levels correlated significantly with androgen response (H; ***figure 8.1A***), AR signature ***(figure 8.1B)***, and AR-V7 signature ***(figure 8.1C)*** in this patient cohort *(p<0.001, p<0.001 and p<0.001 respectively)*.

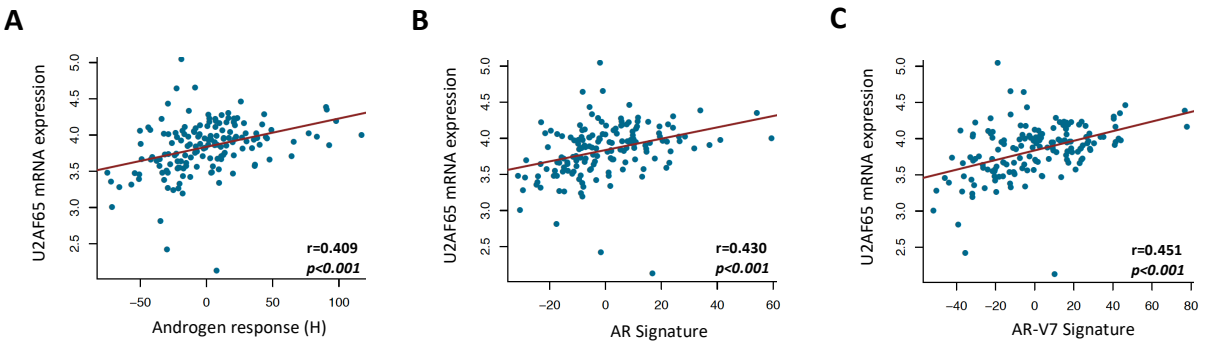

Figure 8.1: mRNA expression of the SR factor U2AF65 correlates with AR and AR-V7 activity. (A-C) Scatter plots showing correlations between U2AF65 mRNA expression and (A) Androgen response (H), (B) AR signature (derived from 43 AR regulated transcripts) and (C) AR-V7 signature (derived from 59 ARV7 regulated transcripts) in metastatic CRPC biopsies (SU2C/PCF cohort). U2AF65 mRNA expression shown as log FPKM. *p values* were calculated by linear regression analysis. Bioinformatic analyses performed with the help of Dr Wei Yuan.

8.4 Determining the relationship between JMJD6, U2AF65 and AR-V7 *in vitro*

To determine the relationship between JMJD6, U2AF65 and AR-V7, I studied the impact of JMJD6 and U2AF65 protein depletion (both individually and concurrently) on the level of AR-V7, as well as on the levels of both JMJD6 and U2AF65 themselves. As shown in ***figure 8.2***, in castration-resistant, AR-V7 producing 22Rv1 prostate cancer cells, JMJD6 siRNA (25nM) and U2AF65 siRNA (25nM) both significantly decreased AR-V7 protein expression; replicating my results presented in **chapter three**, and previous reports on U2AF65 [97]. Importantly however, JMJD6 siRNA did not impact U2AF65 protein levels, nor did U2AF65 knockdown impact JMJD6 expression, in keeping with reported data [318].

Taken together, these results indicated that JMJD6-mediated regulation of AR-V7 does not occur through regulation of U2AF65 protein levels.

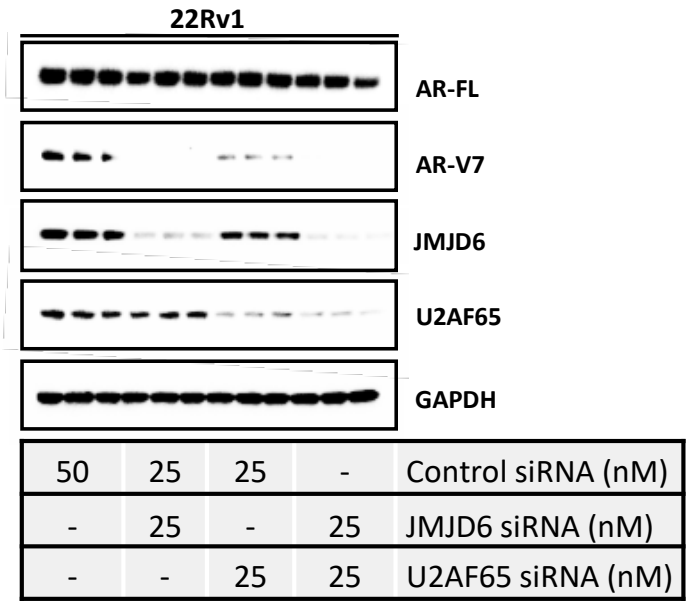

Figure 8.2: JMJD6 and U2AF65 gene silencing reduced AR-V7 protein levels, but not levels of U2AF65 or JMJD6 respectively. Single Western blot in triplicate demonstrating reduction in AR-V7 protein levels with both JMJD6 and U2AF65 siRNA. However, JMJD6 siRNA did not impact U2AF65 protein levels, nor did U2AF65 siRNA impact JMJD6 protein levels.

8.5 Elucidating the role of JMJD6 in the regulation of U2AF65 recruitment to AR-V7 specific splice sites in prostate cancer cells

Having seen no change in U2AF65 protein levels following JMJD6 siRNA knockdown ***(figure 8.2)***, I next investigated the possibility that JMJD6-mediated regulation of AR-V7 instead occurred through regulation of U2AF65 recruitment to AR-V7 specific splice sites.

In collaboration with Soojin Kim, Research Scientist II at the University of Washington, RIP analyses were performed to quantify the amount of U2AF65 bound to AR-V7 specific splice sites following JMJD6 siRNA knockdown (25 nM) compared to a non-targeting control siRNA (25 nM), as per previously published protocols [97]. The primers used to identify these splice sites **(section 4.2.8.4; *Table 4.6*)** have been previously described [97] and overlap the junctions between the introns and exons indicated in ***figure 8.3A***. Crucially therefore, detection of these pre-mRNA sequences which contain the AR-V7 splice sites by qPCR does not rely on the expression of spliced AR-V7 which I have shown to be downregulated by JMJD6 siRNA in this model. Antibodies against U2AF65, but not control IgG, precipitated AR pre-mRNA at the P1 (containing the 5' splice site for both AR and AR-V7) and P2 (containing the 3' splice site for AR-V7) regions in 22Rv1 cells treated with control siRNA; this effect being

significantly reduced with JMJD6 siRNA ***(figure 8.3B)***. Taken together, these results indicated that *in vitro*, JMJD6 regulates the recruitment of the SR factor U2AF65 to AR-V7 splice sites.

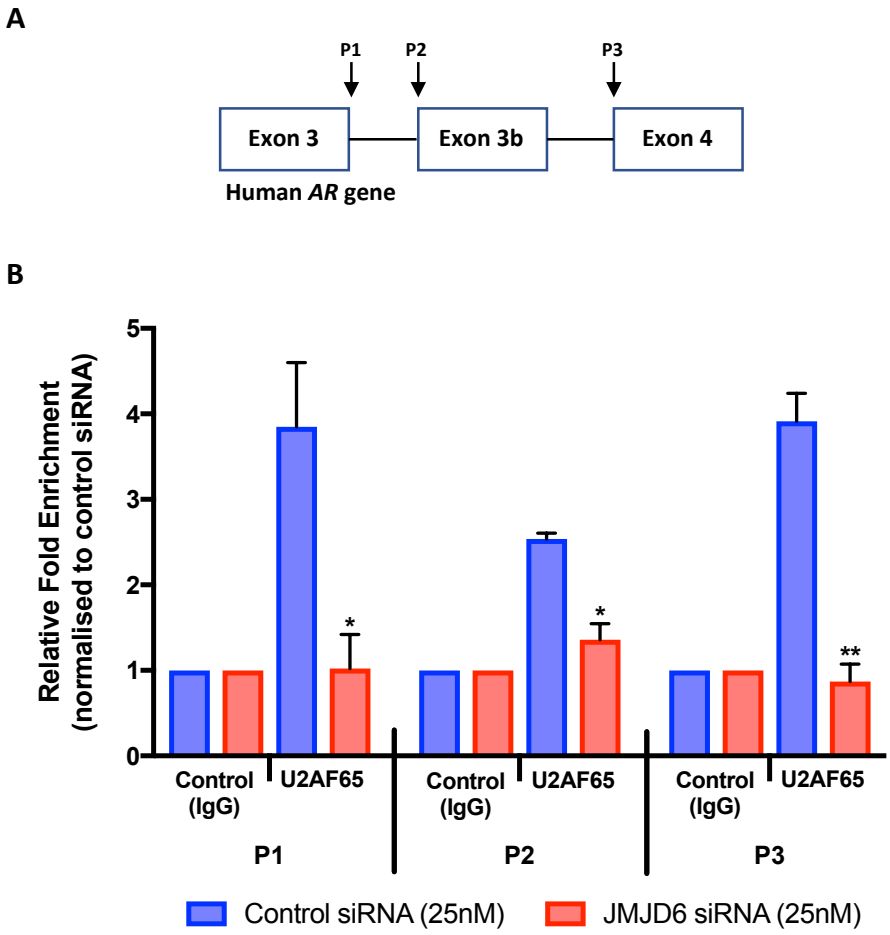

Figure 8.3: JMJD6 regulates recruitment of the SR factor U2AF65 to AR-V7 specific splice sites. (A) Schematic diagram of the human AR gene illustrating the regions (P1-P3) targeted in RNA immunoprecipitation (RIP) assay. P1 contains the 5' splice site for both AR and AR-V7. P2 contains the 3' splice site for AR-V7. P3 contains the 3' splice site for FL-AR. **(B)** Summary bar chart showing a reduction in detectable U2AF65 at the AR-V7 specific splice sites P1 (containing the 5' splice site for both AR and AR-V7) and P2 (containing the 3' splice site for AR-V7), as well as the 3' splice site for AR (P3) in 22Rv1 PC cells treated with JMJD6 siRNA (red bars) compared to non-targeting control siRNA (blue bars). These results Indicated that JMJD6 regulates the recruitment of the SR factor U2AF65 to AR-V7 splice sites. RIP data derived from two independent experiments conducted in triplicate. *p values (*, p ≤ 0.05; **, p ≤ 0.01; ***, p ≤ 0.001)* were calculated for each condition compared to control (at equivalent concentration) using mean value of technical replicates with unpaired Student's t tests. RIP assay raw data acquisition was performed by Soojin Kim.

8.6 Investigating the broader role of JMJD6 in the regulation of alternative splicing in prostate cancer cells

To explore how JMJD6 regulates alternative splicing events in CRPC cells more broadly, together with Dr Jonathan Welti (Senior Scientific Officer, ICR) and Dr Wei Yuan (Bioinformatician, ICR), RNA-seq analyses were performed of LNCaP95 prostate cancer cells

prior to, and after, treatment with either JMJD6 siRNA or non-targeting control siRNA *(See **Appendix A** and **B** for QC data)*. JMJD6 knockdown led to substantial changes (determined by normalised-read count fold change >2.0 or <1/2 and false discovery rate <0.05) in 753 alternative splicing events involving 698 genes ***(figure 8.4A; Supplementary Table 12.2)***, with the majority of these occurring less frequently. Consistent with its assigned role in SR protein modification [289], these results indicated that JMJD6 knockdown reduces the overall incidence of alternative splicing events. Importantly, these finding were independent of changes in gene expression levels following JMJD6 siRNA knockdown, with only 5 of the 698 genes that were found to be differentially alternatively spliced following JMJD6 knockdown being significantly downregulated ***(Supplementary Table 12.3)***. Furthermore, in keeping with my previous results showing that JMJD6 knockdown downregulated AR-V7 expression **(section 7.3*; figure 7.1*)**, JMJD6 knockdown reduced AR-V7 cryptic exon expression ***(figure 8.4B)***.

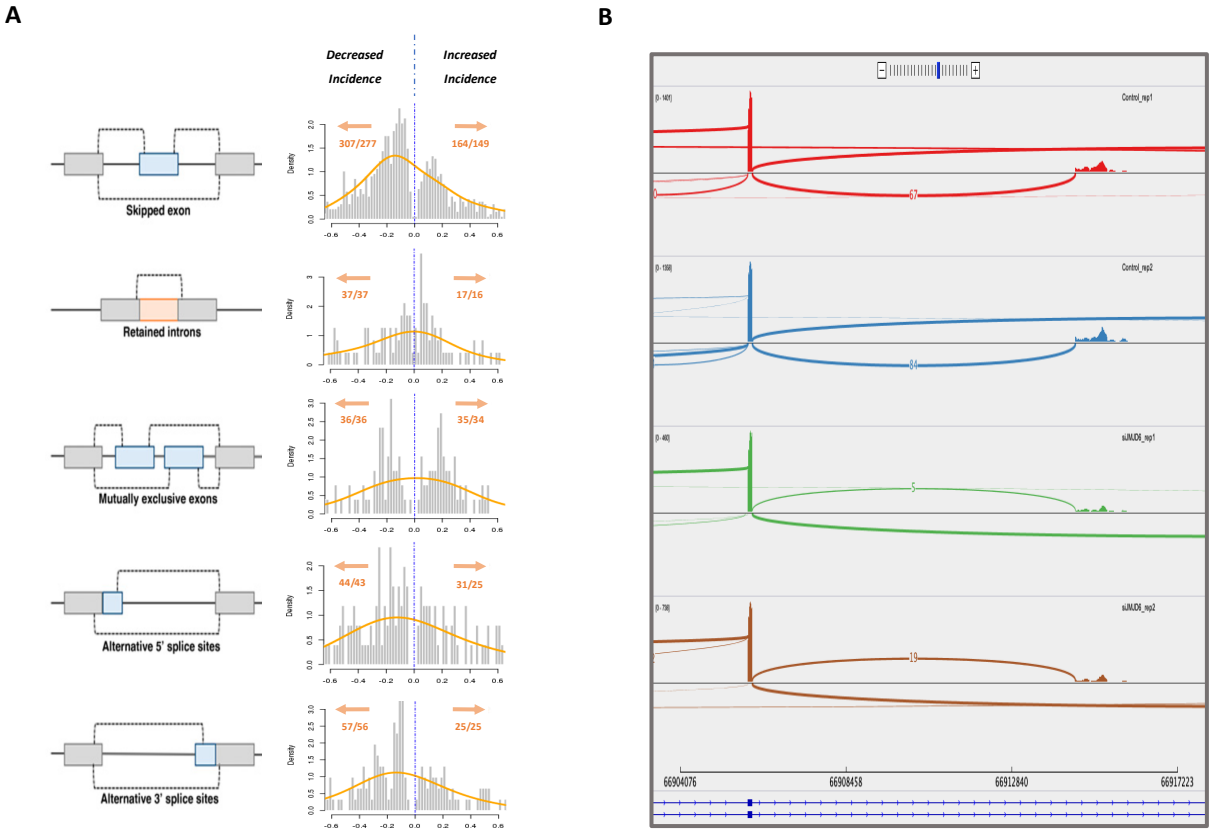

Figure 8.4: JMJD6 knockdown impacts numerous alternative splicing events in LNCaP95 prostate cancer cells. (A) Schematic representation of alternative splicing events alongside corresponding histogram of alternative splicing mean differences between non-targeting control siRNA (blue dotted line; defined as 0.0) and JMJD6 siRNA in LNCaP95 PC cells. Left shift denotes decrease in splicing events. Total number of alternative splicing events (x) occurring in total number of genes (y) shown in orange (x/y). JMJD6 knockdown led to substantial changes in 753 alternative splicing events, with the majority of these occurring less frequently. **(B)** Sashimi plot represents reduced AR-V7 cryptic exon expression after JMJD6 siRNA knockdown. Arcs representing splice junctions that connect exons. The bridge number between exon 3 and cryptic exon in intron 3 is the AR-V7 expression level. JMJD6 siRNA knockdown reduced AR cryptic exon 3 expression. RNA-seq raw data acquisition from treated LNCaP95 cells performed by Dr Jonathan Welti. Bioinformatic analyses were performed with the help of Dr Wei Yuan.

Mean AR-V7 signature score [284] was also reduced by JMJD6 siRNA knockdown ***(figure 8.5A)***, corroborating my previous results showing that JMJD6 knockdown downregulated AR-V7 expression **(section 7.3*; figure 7.1*)**. In addition, unsupervised Gene Set Enrichment Analyses, broadly evaluating which pathways associated with JMJD6 expression, identified that JMJD6 knockdown also significantly downregulated the expression of genes involved in key signalling pathways for prostate cancer cell survival and proliferation, with MYC signalling activity being most significantly downregulated in LNCaP95 prostate cancer cells treated with JMJD6 siRNA compared to those treated with a non-targeting control siRNA ***(figure 8.5B-F)*** [296].

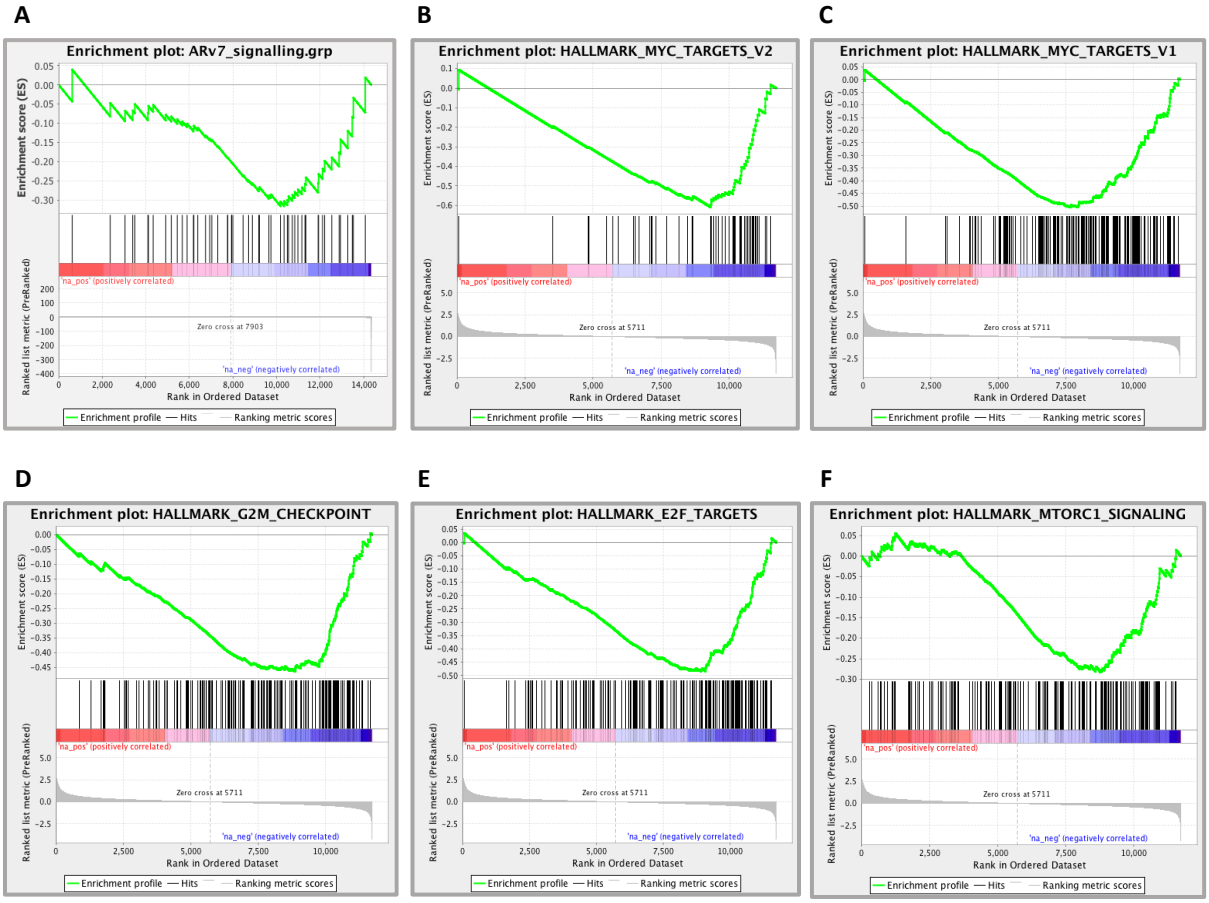

Figure 8.5: JMJD6 gene silencing downregulates the expression of genes in key cell signalling pathways implicated in prostate cancer cell survival and proliferation. (A) JMJD6 knockdown in LNCaP95 prostate cancer cells associated with a reduction in AR-V7 signature activity (derived from 59 genes transcripts associated with AR-V7 expression in CRPC); Enrichment Score (ES) = -0.32. **(B - F)** Gene Set Enrichment Analyses (GSEA) demonstrating that in LNCaP95 prostate cancer cells, 72 hours treatment with JMJD6 siRNA led to a reduction in the expression of genes involved in key prostate cancer cell survival pathways compared to non-targeting control siRNA. **(B)** MYC pathway signature V1; ES = -0.5, FDR < 0.0001. **(C)** MYC pathway signature V2; ES = -0.6, FDR < 0.0001. **(D)** G2M pathway signature; ES = -0.46, FDR < 0.0001. **(E)** E2F pathway signature; ES = -0.48, FDR < 0.0001. **(F)** MTORC1 pathway signature; ES = -0.28, FDR = 0.04 [296]. Bioinformatic analyses were performed with the help of Dr Wei Yuan.

8.7 Discussion

The *in vitro* results presented in this chapter indicate that JMJD6 regulates the expression of AR-V7, at least in part, by modulating the recruitment of the SR factor U2AF65 to AR-V7 specific pre-mRNA splice sites, which has previously been shown to be critical for the expression of AR-V7 [97]. These findings thus point towards a previously unknown JMJD6/U2AF65/AR-V7 regulatory triad, wherein JMJD6 regulates U2AF65 recruitment to AR-V7 specific splice sites, which then facilitates the generation of AR-V7 through its interactions with the spliceosome. However, these studies do not inform on the function of JMJD6 through which this regulation is achieved; as discussed in **section 7.6.1**, in addition to JMJD6 having been reported to possess both arginine demethylase and lysyl hydroxylase catalytic activity, it has also been reported to be involved in stoichiometric protein scaffold type interactions. Therefore, while these results are important, further work is required to ascertain through which of its reported roles does JMJD6 regulate the recruitment of U2AF65, and whether this is amenable to pharmacological targeting.

The RNA-seq analyses presented in this chapter highlight the potential importance of JMJD6, not only for AR-V7 splicing, but also alternative splicing more globally. This is perhaps unsurprising considering its assigned role in SR protein modification [289], and suggests that like BET inhibition, inhibition of JMJD6 may be associated with adverse effects. Before this can be ascertained however, the functional significance of the changes in alternative splicing detected in these studies require further evaluation. Furthermore, it must be borne in mind that whereas the downregulation of JMJD6 protein levels by siRNA impacts both the enzymatic and protein scaffold functions of JMJD6, small-molecule inhibition may maintain potentially important scaffold functions. Therefore, pharmacological inhibition of JMJD6 may produce a different pattern of events, possibly resulting in a more limited change in global splicing. In addition to these considerations, given the critical role of U2AF65 in maintaining splicing fidelity, it is possible that a number of these changes in alternative splicing events are linked to the loss of U2AF65 regulation by JMJD6 following JMJD6 knockdown. If so, given that JMJD6 has been reported to bind the arginine–serine-rich domains of proteins such as U2AF65 in a selective, context-dependent manner [281]. This raises the intriguing possibility that the regulation of U2AF65-mediated alternative splicing events by JMJD6 may vary

between cell types, and with different cellular stresses (e.g. androgen deprivation and hypoxia). In other words, the regulation of U2AF65-mediated alternatively spliced events by JMJD6 may be potentially more important for some cells (e.g. hormone-deprived prostate cancer cells) than others (e.g. benign cells of either prostatic or non-prostatic origin). Therefore, whilst targeting U2AF65 directly can be predicted to be associated with a number of adverse effects; due to its pivotal role in the splicing machinery. It is conceivable that modulating U2AF65-mediated AR-V7 splicing by instead targeting JMJD6, may reduce AR-V7 production in castration-resistant prostate cancer cells, while not significantly impacting other physiologically important U2AF65-mediated alternative splicing events in benign cells, thereby limiting potential toxicities. Further work is thus required to evaluate the impact of both JMJD6 siRNA knockdown *and* small-molecule inhibition, on the frequency of alternative splicing events in other prostate cancer cell lines, models of normal prostatic epithelium, benign cells of non-prostatic origin, and *in vivo*, before the true implications of JMJD6 inhibition can be fully appreciated.

8.7.1 Limitations

The RIP assays presented in this chapter reveal important results regarding the mechanism through which JMJD6 regulates the production of AR-V7. These results indicate that JMJD6 siRNA knockdown reduces the recruitment of the SR factor U2AF65 to AR-V7 specific pre-mRNA splice sites. One potential pitfall regarding these analyses is that if JMJD6 knockdown were to interrupt global transcriptional processes, this would reduce the amount of pre-mRNA in the JMJD6 siRNA experimental arm, which the primers used for these RIP assays are targeting. Therefore, the perceived reduction in U2AF65 recruitment could in fact be due to there being less pre-mRNA to bind. This scenario may be plausible given that JMJD6 has been implicated in transcriptional-pause release [314]. However, this role of JMJD6 requires further evaluation given that it has been proposed to be dependent on the demethylase activity of JMJD6 [314], which has not been convincingly validated [289, 319]. Furthermore, my results indicate that JMJD6 preferentially regulates the production of AR-V7, with JMJD6 knockdown not clearly impacting AR-FL protein levels ***(figure 8.2)***. Taken together therefore, the results presented in this chapter would suggest that JMJD6 does indeed regulate the recruitment of U2AF65 to AR-V7 splice sites, rather than this result being

a consequence of an inhibition of global transcription; although this cannot be completely ruled out. In addition to this issue, these analyses do not ascertain whether the observed reduction in U2AF65 recruitment to AR-V7 splice sites is due to a direct interaction with JMJD6. While the lysyl-5-hydroxylation of lysine residues in the U2AF65 arginine-serine rich region by JMJD6 has been well described [288], these reports are principally based on cell-free mass spectrometry analyses. As such, while U2AF65 may indeed be a substrate for JMJD6 lysyl hydroxylation, this does not infer that the two proteins directly interact *in vitro* or *in vivo*. Given that JMJD6 has the potential to hydroxylate/interact with SR proteins other than U2AF65 [281, 288, 308, 320], it cannot be ruled out that the observed reduction in U2AF65 recruitment following JMJD6 knockdown instead occurs through loss of interaction between JMJD6 and some other intermediary factor(s) which subsequently modulates U2AF65 recruitment. Consequently, this is a limitation of this work. Nevertheless, a direct interaction between JMJD6 and U2AF65 *in vitro* has been previously reported; JMJD6 has been reported to interact with U2AF65 in an RNA dependent manner in HEK293T human embryonic kidney cells [318]. Supporting a direct effect of JMJD6 on U2AF65. Overall, the results presented in this chapter identify a novel mechanism underlying AR-V7 production, whereby JMJD6, either directly, or through modulation of other SR proteins, regulates U2AF65 recruitment to AR-V7 specific splice sites, facilitating the generation of AR-V7. However, further work is required to determine whether JMJD6 interacts directly with U2AF65 in these prostate cancer models, or if additional factors are implicated in this regulatory mechanism.

The principle limitation of the RNA-seq analyses described in this chapter is that of coverage. If an alternatively spliced transcript is expressed at a low level, it can be missed due to insufficient depth of sequencing. Consequently, in a control (non-targeting control siRNA) vs treatment (JMJD6 siRNA) study such as the one presented in this chapter, if the expression of a transcript in one condition is significantly lower than in the other, the splicing event will be missed. This is particularly problematic given that biases in sample preparation, sequencing, and/or analysis can result in regions of the genome that either lack coverage, or conversely have much higher coverage than expected [321]. Taken together, these issues can limit the confidence with which conclusions on changes in alternative splicing events can be made. Therefore, as discussed above, further work is required, using multiple models, to

more definitively evaluate the impact of JMJD6 inhibition on the frequency of alternative splicing events.

8.8 Conclusion

In conclusion, the results presented in this chapter identify a novel mechanism underlying the generation of AR-V7, wherein JMJD6 regulates the recruitment of the SR factor U2AF65 to AR-V7 specific pre-mRNA splice sites, which then facilitates the production of AR-V7 through its interaction with the spliceosome.

9

Establishing the Impact of Inhibiting JMJD6 Catalytic Activity on AR-V7 Expression

9.1 Research in context

When considering whether a protein that has been found to contribute to the pathophysiology of a disease should be taken forward into an anticancer drug development programme as a novel therapeutic target, it is important to understand which function of that protein promotes its oncogenic effects. This is important because while some functions may be amenable to small-molecule inhibition, such as protein enzymatic reactions, inhibition of other functions may be more challenging, for example protein-protein interactions. It is therefore vital to ascertain which function of a prospective drug target must be interrupted in order to achieve a therapeutic effect, so as to enable selection of appropriate candidate compounds that are capable of abrogating that function.

JMJD6 has been reported to have pleotropic roles, with publications suggesting that it possesses both lysyl hydroxylase and arginine demethylase catalytic activity [320]. While the function of isolated JMJD6 as a lysyl hydroxylase has been corroborated by several groups [288, 322, 323], evidence supporting its ability to catalyse N-methyl arginine demethylation is, however, less robust [324, 325]. JMJD6 has also been reported to be involved in

stoichiometric protein scaffold type interactions in a manner independent of enzymatic function [311]. In **chapter seven**, I have demonstrated that JMJD6 knockdown downregulates AR-V7 mRNA and protein levels. However, as discussed in **section 7.6.1,** consequent to the reduction in JMJD6 protein by the siRNA-mediated gene silencing techniques used in these experiments, these studies were unable to determine which of the reported roles of JMJD6 facilitate the generation of AR-V7, since both enzymatic *and* protein scaffold functions are lost through downregulation of JMJD6 protein. In this chapter therefore, I investigate which function of JMJD6 is most important for its regulation of AR-V7 production.

In **chapter eight**, I show that JMJD6 regulates the recruitment of the SR factor U2AF65 to AR-V7 specific pre-mRNA splice sites. JMJD6 has been previously demonstrated to hydroxylate U2AF65 [288], thereby regulating U2AF65-mediated alternative splicing events [318]. Building on these reports, I investigate the importance of JMJD6 catalytic activity for AR-V7 production. As a 2OG-dependent dioxygenase, the catalytic activity of JMJD6 may be limited by oxygen availability, as is the case for other 2OG oxygenases such as the hypoxia-inducible factor prolyl-hydroxylases [326]. Leveraging this characteristic, I explore the impact of hypoxia on the expression of AR-V7 in *in vitro* models of CRPC. In addition, I use overexpression and mutagenesis studies to investigate the importance of a functional JMJD6 active site on AR-V7 levels. Subsequently, I interrogate the 'druggability' of JMJD6 using the canSAR Drug Discovery Platform [327, 328], and identify compounds capable of inhibiting JMJD6 activity. Together, these studies consider whether JMJD6 is a pharmacologically tractable target for overcoming oncogenic AR-V7 signalling in lethal prostate cancer.

9.2 Specific Aims

- To evaluate the effect of hypoxia on AR-V7 levels *in vitro*.
- To determine how mutagenesis of key residues in the JMJD6 active site impacts AR-V7 production in prostate cancer cells.
- To interrogate the potential druggability of JMJD6 using the canSAR drug discovery platform [327, 328].

- To identify small-molecule inhibitors of JMJD6, and ascertain their effect on AR-V7 protein levels *in vitro*.

9.3 Investigating the impact of hypoxia on AR-V7 generation

As a 2OG-dependent dioxygenase, JMJD6 catalytic activity may be limited by oxygen availability [326]. Indeed, JMJD6 regulation of alternative splicing events has been previously reported to be regulated in an oxygen-dependent manner [316]. To investigate the importance of JMJD6 catalytic activity for AR-V7 generation therefore, I first evaluated changes in AR, AR-V7 and JMJD6 protein (Western blot) and mRNA (qPCR) levels in castration-resistant 22Rv1 prostate cancer cells following 24 hours of incubation under hypoxic conditions (1% O_2) compared to normoxic (21% O_2) controls ***(figure 9.1)***. Hypoxia was associated with a reduction in both AR-V7 mRNA and protein levels. Unexpectedly, hypoxia also resulted in a reduction in JMJD6 protein levels, although this was not reflected at the mRNA level, with qPCR analyses in fact demonstrating a small increase in JMJD6 mRNA expression with hypoxia; this is in keeping with JMJD6 transcription being induced by hypoxia but JMJD6 protein levels being regulated post-transcriptionally by this [302]. Interestingly, hypoxia also resulted in an accumulation of detectable unspliced pre-mRNA intermediates of AR transcription (AR exon 2-intron 2 and AR intron 3). Taken together, these results suggest that in this *in vitro* model of CRPC, oxygen is an important co-factor for AR-V7 splicing, and that in the absence of oxygen the cellular splicing machinery can stall; as indicated by the accumulation of unspliced AR pre-mRNA intermediates. These findings are intriguing and may support the hypothesis that JMJD6 catalytic activity is important for JMJD6-mediated AR-V7 production. However, given the wide-ranging effects of hypoxia on cellular transcriptional processes, these results alone cannot be taken as evidence that JMJD6 catalysis directly impacts AR-V7 production.

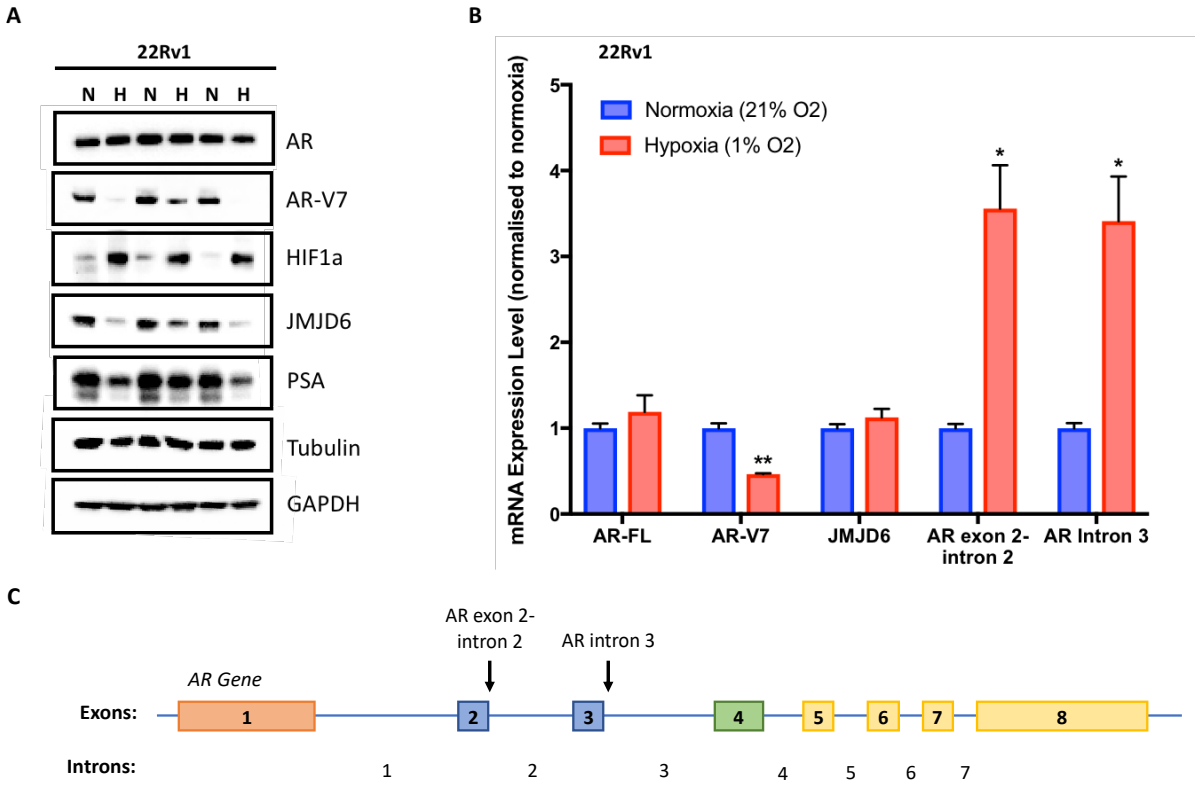

Figure 9.1: Hypoxia reduced AR-V7 and JMJD6 protein levels and is associated with an accumulation of unspliced AR pre-mRNA intermediates. (A) Western blot of 22Rv1 whole cell lysates following culture under hypoxic conditions (1% O_2) for 24 hours compared to normoxic controls (21% O_2). This demonstrates a reduction in AR-V7 and JMJD6 protein levels in response to hypoxia, associated with an increase in HIF1α protein levels. N = Normoxia; H = Hypoxia. **(B)** Summary bar charts showing corresponding mRNA levels. AR-V7 mRNA levels significantly decrease following exposure to hypoxia (red bars) compared to normoxic controls (blue bars), however JMJD6 mRNA levels do not. In addition, an accumulation of unspliced pre-mRNA intermediates of AR transcription was observed. (A) and (B) derived from single experiment performed in triplicate. Mean RNA expression (normalised to housekeeping genes (B2M, GAPDH and CDC73) and normoxic controls; defined as 1.0) with standard error of the mean shown. *p values (*, $p \leq 0.05$; **, $p \leq 0.01$; ***, $p \leq 0.001$)* were calculated for each condition compared to control (normoxia) using unpaired Student's t tests. **(C)** Schematic diagram demonstrating the target loci for the qPCR probes directed against the unspliced AR pre-mRNA intermediates AR exon 2-intron 2 and AR intron 3.

9.4 Ascertaining the importance of a functional JMJD6 catalytic site for AR-V7 production

To more specifically study the importance of a functional JMJD6 catalytic site for AR-V7 production, I next performed JMJD6 overexpression and mutagenesis studies. 22Rv1 prostate cancer cells were transfected with a JMJD6 wild-type (WT) plasmid ($JMJD6^{WT}$) for 72 hours; Western blot and mRNA analyses demonstrated increased expression of both AR-V7

protein and mRNA with JMJD6 overexpression ***(figure 9.2A)***. Conversely, transfection with inactivating mutations of active site residues in the JMJD6 catalytic domain by pcDNA3-JMJD6-ASM2 (*MUT1*; D189A and H187A) [282] and pcDNA3-JMJD6-BM1 (*MUT2*; N287A and T285A) resulted in markedly decreased AR-V7 protein levels ***(figure 9.2B)***. To validate these findings, both JMJD6^{WT}, and the catalytically inactive mutant JMJD6^{MUT1}, were next transfected into the VCaP prostate cancer cell line; AR-V7 expression was induced by JMJD6^{WT} but not by JMJD6^{MUT1} ***(figure 9.2C)***. Taken together, these results further support the hypothesis that JMJD6-mediated expression of AR-V7 requires JMJD6 catalytic activity.

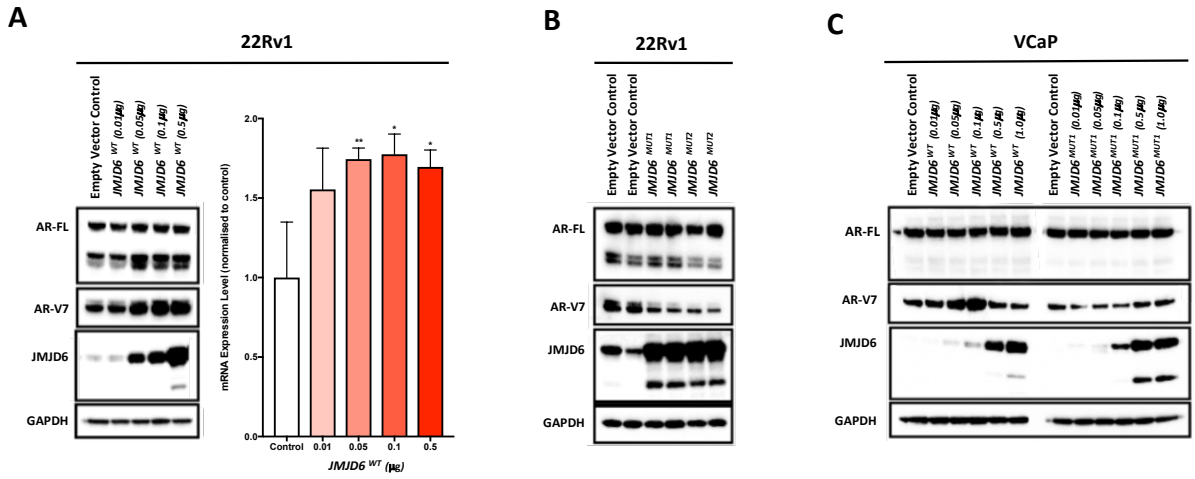

Figure 9.2: Evidence JMJD6-mediated AR-V7 generation requires a functional JMJD6 active site. (A) Transfection of JMJD6 wild-type (JMJD6^{WT}) plasmid into 22Rv1 prostate cancer cells increased AR-V7 protein (Western blot) and mRNA (Bar chart; qPCR) levels. Mean mRNA levels (normalised to housekeeping genes (B2M and GAPDH), and an empty vector control plasmid at equivalent concentration (defined as 1.0), with standard error of the mean from three experiments is shown. p values (*, $p \leq 0.05$; **, $p \leq 0.01$; ***, $p \leq 0.001$) were calculated for each condition compared to control (at equivalent concentration) using the mean value of technical replicates with unpaired Student's t tests. **(B)** Conversely, transfection with inactivating mutations of active site residues in the JMJD6 catalytic domain by JMJD6^{MUT1} (D189A and H187A) and JMJD6^{MUT2} (N287A and T285A) decreased AR-V7 protein levels (empty vector control, JMJD6^{MUT1} and JMJD6^{MUT2} = 1µg of total plasmid). **(C)** To validate these findings, both JMJD6^{WT}, and the catalytically inactive mutant JMJD6^{MUT1}, were also transfected into the VCaP prostate cancer cell line; AR-V7 expression was induced by JMJD6^{WT} but not by JMJD6^{MUT1}, suggesting that JMJD6-mediated AR-V7 expression requires enzymatically active JMJD6. Western blot presented in (C) is a singleton Western blot replicating findings presented in (B) in an alternative cell line model.

9.5 Interrogating the potential druggability of JMJD6

Having determined that JMJD6 catalytic activity may be important for the expression of AR-V7, in collaboration with Prof. Bissan Al-Lazikani (professor of computational biology

and chemogenomics, ICR), I next interrogated the potential druggability of JMJD6 using the canSAR drug discovery platform [327-329] to ascertain whether JMJD6 catalysis may be amenable to pharmacological inhibition. Importantly, studies comparing the physicochemical and geometric properties of JMJD6 with known drug targets such as protein kinases, indicated that JMJD6 contains a 'druggable' pocket within its tertiary structure (defined as sites that harbour physiochemical and geometric properties consistent with binding orally-bioavailable small molecules [328]; ***figure 9.3***). Furthermore, consistent with crystallographic studies [330, 331], these analyses demonstrated that the amino acids (D189, H187A, N287 and T285), important for JMJD6 catalytic activity, lie within this druggable cavity.

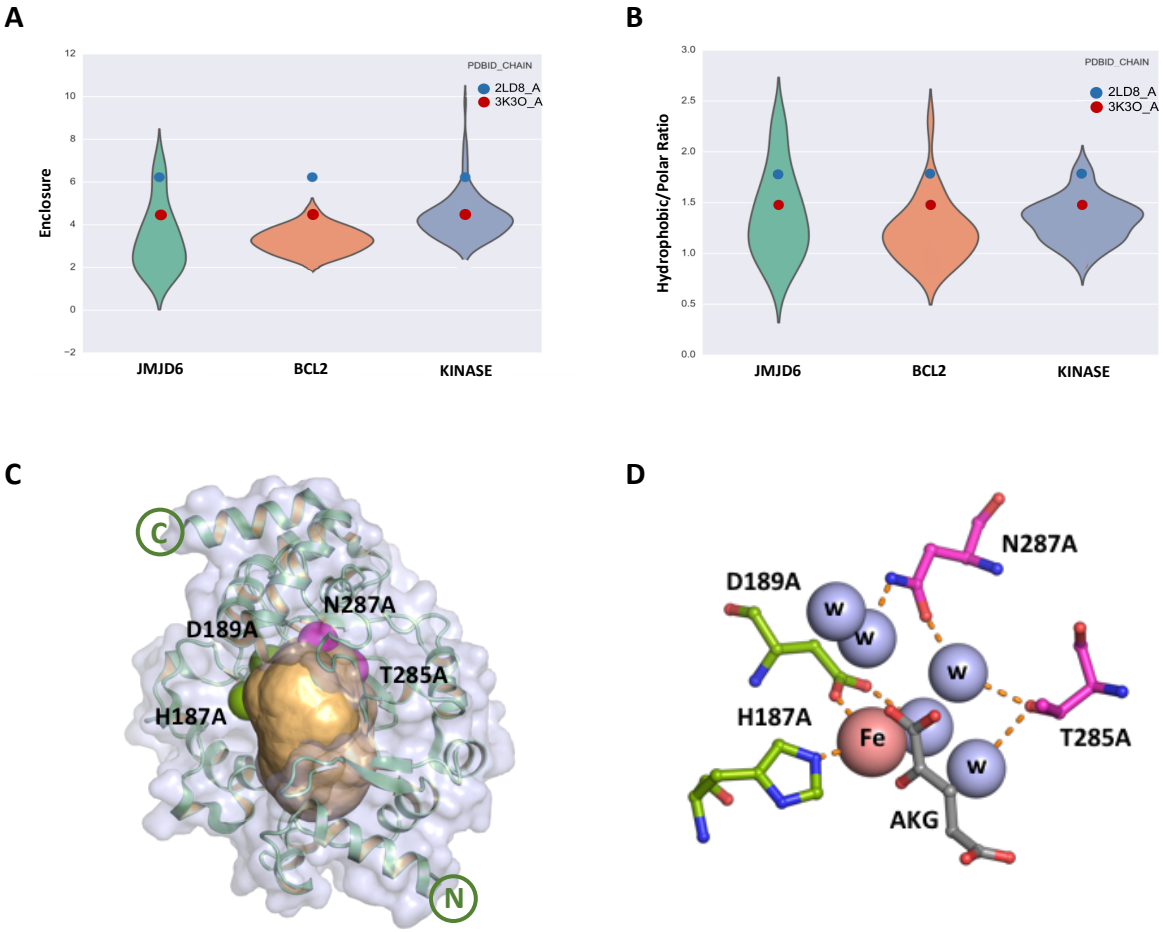

Figure 9.3: JMJD6 is a pharmacologically tractable protein. Comparing 25 physicochemical and geometric properties of JMJD6 with known drug targets indicated that parameters of the JMJD6 druggable cavity fall within the same ranges as those of protein kinases, suggesting it to be druggable. This was calculated using the canSAR Drug Discovery Platform [223, 224]. The cavity enclosure **(A)** and the ratio of hydrophobic to polar chemical groups **(B)** within the cavity are shown as evidence. **(C-D)** Graphic representation of the JMJD6 tertiary structure [225]. The inactivating substitutions of active site residues in the JMJD6 catalytic domain by JMJD6^{MUT1} (D189A and H187A; green spheres) and JMJD6^{MUT2} (N287A and T285A; magenta spheres) reside within a predicted druggable pocket (shown in orange), identified by the canSAR knowledgebase. All druggability assessments and associated figures were done by Patrizio di Micco.

9.6 Determining the impact of JMJD6 small-molecule inhibition on AR-V7 production

Having predicted JMJD6 to be a potentially pharmacologically tractable enzymatic target through computational analyses, in collaboration with Prof. Christopher Schofield (professor of organic chemistry, University of Oxford), I next utilised LC-MS assays to evaluate the effect of the 2OG mimic pyridine-2,4-dicarboxylic acid (2,4-PDCA) on JMJD6 catalytic activity. This compound is a relatively broad-spectrum, active site binding, 2OG-dependent oxygenase inhibitor [332-334]. 2,4-PDCA resulted in a dose-dependent reduction in isolated JMJD6-mediated lysyl-5-hydroxylation of the known downstream target LUC7-Like (LUC7L) [281, 289], identifying 2,4-PDCA as an inhibitor of JMJD6 lysyl hydroxylase catalytic activity ***(figure 9.4)***.

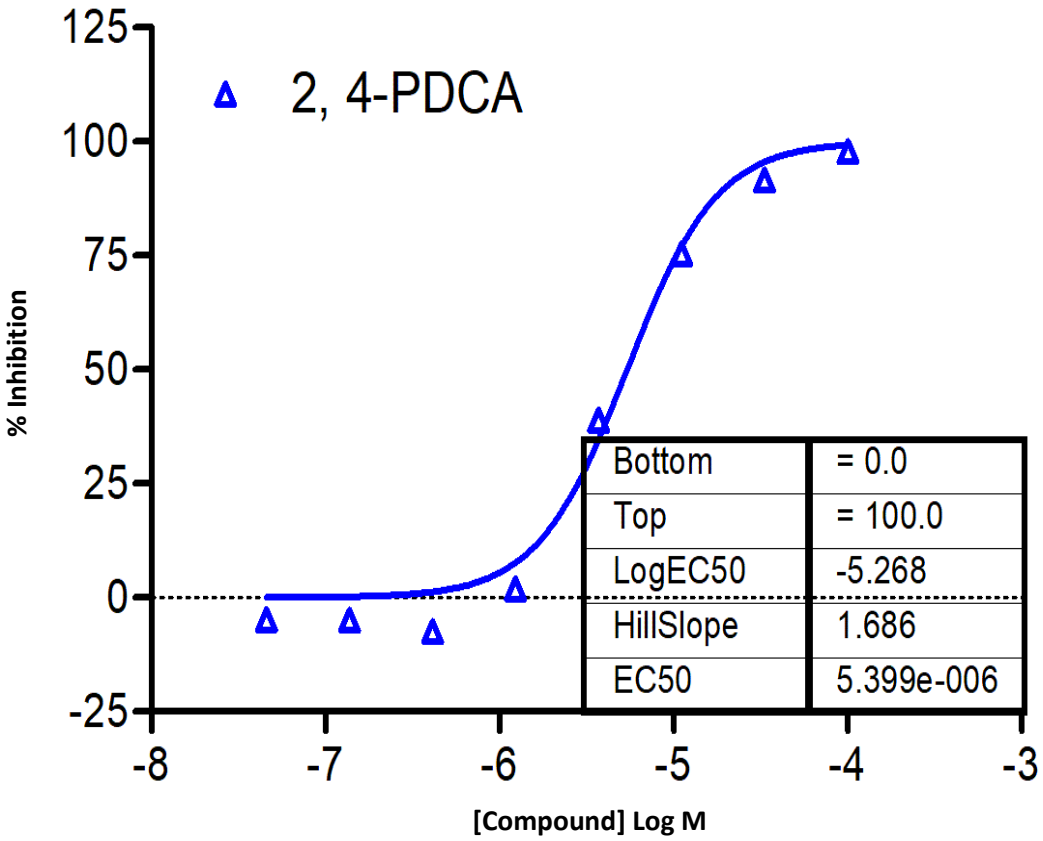

Figure 9.4: The 2OG mimic 2,4-PDCA is a JMJD6 inhibitor. Liquid chromatography-mass spectrometry (LC-MS) analysis demonstrating that the 2OG mimic pyridine-2,4-dicarboxylic acid (2,4-PDCA) resulted in a dose-dependent reduction in isolated JMJD6-mediated lysyl-5-hydroxylation of the known downstream target LUC7L; indicating that 2,4-PDCA is an inhibitor of JMJD6 lysyl hydroxylase catalytic activity. LC-MS raw data acquisition, analysis of results, and provision of figure 9.4 by Dr Anthony Tumber (collaborator, University of Oxford).

To determine the impact of 2,4-PDCA *in vitro*, I subsequently treated 22Rv1 prostate cancer cells with 2,4-PDCA for 48 hours. As shown in ***figure 9.5***, 2,4-PDCA resulted in a dose-dependent reduction in AR-V7 protein levels, supporting my previous siRNA and mutagenesis experiments. Taken together, these data reveal 2,4-PDCA to be an inhibitor of JMJD6 lysyl hydroxylation that is capable of reducing AR-V7 protein levels *in vitro*.

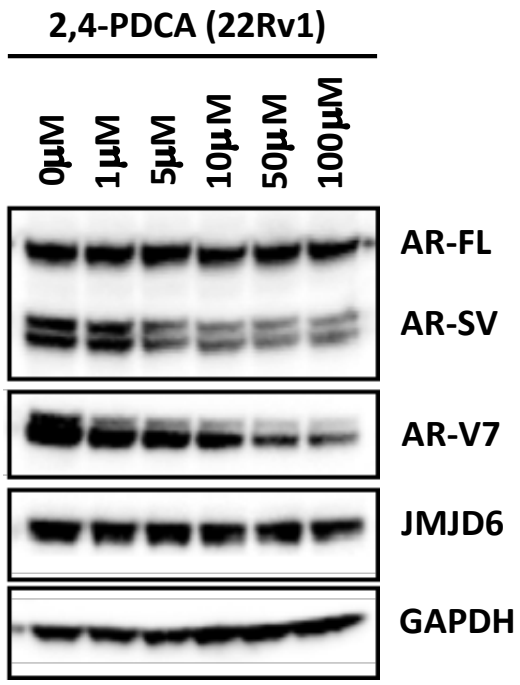

Figure 9.5: 2,4-PDCA reduced AR-V7 protein levels *in vitro*. Western blot showing that 2,4-PDCA caused a dose-dependent reduction of AR-V7 protein levels in 22Rv1 prostate cancer cells. Single representative Western blot shown from two separate experiments.

9.7 Discussion

The *in vitro* results presented in this chapter reveal that in 22Rv1 prostate cancer cells, oxygen is an important requirement for AR-V7 splicing, with AR-V7 mRNA and protein levels being significantly reduced by hypoxia. Given that oxygen may be an important co-factor for the catalytic activity of the 2OG-dependent dioxygenase JMJD6 [316], this result supports a role for JMJD6 catalysis in AR-V7 splicing. However, as described in **section 9.3**, in view of the broad range of cellular transcriptional changes that occur in response to hypoxia, driven by the transcription factor hypoxia inducible factor 1-alpha (HIF1a) [335], these results alone cannot be taken as evidence that JMJD6 catalysis directly impacts AR-V7 production.

These hypoxia experiments also showed that oxygen deprivation slightly increases JMJD6 mRNA levels. Although this was not statistically significant, this is in keeping with reports that JMJD6 mRNA expression is inducible by hypoxia [302]. Conversely, despite this, JMJD6 protein levels were reduced by hypoxia. This reduction in JMJD6 protein, but not mRNA, suggests post-transcriptional regulation of JMJD6 and a loss of JMJD6 protein stability by hypoxia. Interestingly, JMJD6 has been reported to lysyl hydroxylate itself [322], although the functional significance of this remains undefined. This therefore raises the intriguing possibility that JMJD6 catalytic activity is required to maintain its own protein stability. If so, this could be of clinical utility as a pharmacodynamic biomarker of therapeutic agents targeting JMJD6 activity. However, given that 2,4 PDCA did not seem to replicate this reduction in JMJD6 protein, it may be the case that hypoxia impacts the protein stability of JMJD6 through some other mechanism. Further work is therefore required to determine (1) whether the observed loss of JMJD6 protein stability in response to hypoxia is limited to this particular model, and (2) if this occurs as a consequence of inhibition of JMJD6 catalytic activity, or due to some other factor which is promoted/inhibited by hypoxia.

To more specifically study the importance of JMJD6 catalysis in the production of AR-V7 therefore, I also performed JMJD6 overexpression and mutagenesis studies. These enabled the inhibition of JMJD6 catalytic activity in the presence of oxygen, and without downregulation of JMJD6 protein levels. Although stable JMJD6 knockout clones have been reported to have been generated from glioblastoma cells using CRISPR-Cas9 gene editing technology [336], viable homogeneous JMJD6$^{-/-}$ knockout clones could not be generated for use in these experiments from either of the prostate cancer cell lines 22Rv1 or LNCaP95. While this highlights the importance of JMJD6 for prostate cancer cell survival, my inability to perform reliable knockout and rescue experiments due to cell kill, and the reliance of these mutagenesis experiments on a dominant negative effect to elicit their inhibitory properties, are limitations of this work. Nonetheless, the results presented in this chapter indicate that JMJD6-mediated regulation of AR-V7 expression is dependent on an intact JMJD6 catalytic site, and importantly, that the JMJD6 catalytic site resides within a druggable pocket. Notably, analogous pockets have been targeted in other 2OG oxygenases, in some cases leading to clinically approved drugs [330, 333]. In keeping with these findings, 2,4-PDCA, which is shown

herein to inhibit JMJD6 lysyl-5-hydroxylation, downregulates AR-V7 protein levels in castration-resistant prostate cancer cells.

Taken together therefore, the results presented in this chapter, demonstrate the importance of a functional JMJD6 active site for AR-V7 protein production. In addition, these results determine that the JMJD6 active site is druggable, supporting the proposal that JMJD6 is a viable therapeutic target for drug discovery efforts to abrogate oncogenic AR-V7 signalling.

9.7.1 Limitations

The main limitation regarding the work described in this chapter is the lack of a validated downstream *in vitro* 'read-out' of physiologically relevant effects of JMJD6 catalysis. Whilst the plasmids and methods I have used have been previously characterized [282, 288], without an established quantifiable marker of JMJD6 catalysis in these models other than AR-V7, it is not possible to definitively state that the changes in AR-V7 levels observed are dependent solely on JMJD6 catalytic activity. This is of particular relevance when considering my overexpression and mutagenesis experiments; I am unable to be completely certain that overexpressed JMJD6^{WT} is fully functional, although it did increase AR-V7 levels, nor that the mutants are completely inactive. Thus, I cannot rule out that JMJD6-mediated regulation of AR-V7 involves a stoichiometric protein scaffold type interaction, which may or may not be linked to lysine-hydroxylation (or other JMJD6 catalysed reaction). To investigate the role of JMJD6 catalysis in regulating AR-V7 levels therefore, I also inhibited JMJD6 with the small molecule 2,4-PDCA, which inhibits JMJD6 lysyl-5-hydroxylation. Importantly, 2,4-PDCA also downregulated AR-V7 levels, supporting my hypothesis that catalysis by JMJD6 regulates AR-V7. However, in these studies 2,4-PDCA was employed as a tool to provide 'proof-of-principle' evidence that prostate cancer cell inhibition of JMJD6 is possible, and can impact on AR-V7 protein levels. Moreover, the permeability of 2,4-PDCA is low, with high concentrations being required to elicit its effects *in vitro* [337, 338]. 2,4-PDCA itself is therefore unlikely to be useful for *in vivo* studies, which I have been unable to pursue with this agent. Furthermore, 2,4-PDCA is a broad-spectrum 2OG oxygenase inhibitor and may have off-target effects such as inhibiting other JmjC-domain containing proteins, some of which are reported to impact AR-

V7 expression; recently JMJD1A/KDM3A [212] and KDM4B [213] have been reported the regulate AR-V7 splicing.

Overall therefore, although JMJD6 represents a 'druggable' target of considerable interest in prostate cancer, further *in vivo* work employing potent, selective, JMJD6 inhibitors is required to confirm that JMJD6 inhibition is a viable strategy for abrogating oncogenic AR-V7 signalling in lethal prostate cancer. Encouragingly, a very recent study describes a more drug-like JMJD6 inhibitor with *in vivo* activity and minimal toxicity [339], which now merits study in prostate cancer models.

9.8 Conclusion

In conclusion, the results presented in this chapter highlight the importance of a functional JMJD6-active site for AR-V7 protein production, and show that the JMJD6 active site is druggable. These results therefore support the proposal that JMJD6 is a viable therapeutic target for drug discovery efforts to abrogate oncogenic AR-V7 signalling.

10

Thesis Discussion

The results presented in this thesis reveal for the first time that the 2OG dependent dioxygenase JMJD6 plays an important role in prostate cancer biology. My results show that JMJD6 is important for prostate cancer cell survival, and is a key regulator of AR-V7 production *in vitro*.

10.1 JMJD6 background

JMJD6 is an intriguing yet still poorly understood protein. Having only been discovered twenty years ago, JMJD6 was initially named phosphatidylserine receptor (PSR) to reflect its attributed role as a cell surface phosphatidylserine receptor that was required for the recognition and clearance of apoptotic cells [340]. More recently, this role has been rejected, with subsequent reports demonstrating that PSR was in fact principally located within the cell nucleus, and possessed a central JmjC fold [341, 342]. These reports led to the renaming of PSR as JMJD6, and its reclassification as a member of the large family of JmjC domain-containing oxygenases; these proteins are ferrous iron- and 2OG-dependent, and are able to catalyse hydroxylation and demethylation reactions on both protein and nucleic acid substrates [343].

10.1.1 Basic structure

The JMJD6 gene is located on chromosome 17q25 [344]. The full-length JMJD6 protein consists of 403 amino acids positioned around a central JmjC domain (UniProt ID Q6NYC1 [344]), which forms a double-stranded β-helix (DSBH) fold common to all 2OG-dependent dioxygenases [343, 344]. The JMJD6 DSBH consists of eight anti-parallel β-strands that form a barrel-like structure within which lies an iron-binding site, formed by the residues His187, Asp189 and His273 [288]. Importantly, this iron-binding site is reported to be key to the catalytic activity of JMJD6 [288, 314, 325].

Adjacent to the JmjC domain, in the carboxy-terminus of JMJD6, resides a poly-serine (polyS) domain [320], which has been proposed to be important for the nuclear/nucleolar shuttling of JMJD6; alternatively spliced variants of JMJD6 which lack this domain reside predominantly within the nucleolus and nuclear speckles, rather than the nucleoplasm [345]. The remaining structure of JMJD6 is however based predominately on sequence motif predictions and are as yet unconfirmed. JMJD6 has been predicted to exhibit five nuclear localisation sites (NLS), of which three have been validated [309, 342], a nuclear export signal (NES), and a putative sumoylation site [346]. In addition to these, JMJD6 has also been predicted to contain a hybrid AT-hook domain [342]. While this domain demonstrates similarities to both a canonical AT-hook, which preferentially binds DNA, and an extended AT-hook, which has a higher affinity for RNA, the sequence of the JMJD6 AT-hook remains distinct [320]. Consequently, while JMJD6 has been demonstrated to interact with RNA [318, 346, 347], evidence to date argues against a role for JMJD6 in DNA binding [347].

10.1.2 Catalytic activity

While the function of isolated JMJD6 as a lysyl hydroxylase has been corroborated by several groups [288, 322, 323], evidence supporting its ability to catalyse N-methyl arginine demethylation is less robust [324, 325]. For example, JMJD6 has been demonstrated to lysyl-5-hydroxylate residues K15 and K276 in the arginine-serine rich region of endogenous U2AF65 cultured from HeLa cells [288], and endogenous p53 on position K382 in HCT116 colon cancer cells [323]. In addition, JMJD6 has also been reported to hydroxylate itself at position K167

[322], which has been proposed to enable JMJD6 to form multimers [319], however the physiological functions of these remain to be ascertained.

In contrast, JMJD6 arginine demethylase activity has to date only been demonstrated either indirectly [324], or via assays with *Escherichia coli* purified recombinant JMJD6 protein [325]. Moreover, while the lysyl hydroxylase activity of JMJD6 appears to be a direct effect, the demethylase activity of JMJD6 is reported to occur as a multi-step process; the arginine demethylase activity of JMJD6 is proposed to involve an initial hydroxylation reaction catalysed by JMJD6, which then yields an unstable hemiaminal intermediate that fragments to produce a demethylated arginine residue [308, 343]. Taken together therefore, the role of JMJD6 as a canonical demethylase is controversial, however this remains to be unequivocally refuted [289].

10.1.3 The Biological functions of JMJD6

10.1.3.1 The role of JMJD6 in embryogenesis and organogenesis

JMJD6 knockout mice typically do not survive past the neonatal stage and demonstrate delays in pulmonary, renal, gastrointestinal, thymic and ophthalmic tissue differentiation [348, 349]. Homozygous knockout mice also develop major cerebral and craniofacial defects as well as severe cardiopulmonary malformations [350], while erythropoiesis in the foetal liver is impeded at an early erythroblast stage [309, 349, 351]. In addition, abnormal thymic differentiation has been reported to result in multi-organ autoimmunity [352]. In contrast to these reports, genetic ablation of dJMJD6 expression in *Drosophila* produces no discernible phenotype, with homozygous knockout flies being viable and fertile [353]. Interestingly however, overexpression of dJMJD6 has been reported to result in a phenotypic change that may be of some relevance to prostate cancer biology, with this resulting in rotated male genitalia [353].

10.1.3.2 JMJD6 as an epigenetic regulator of chromatin structure

In 2007, Chang et al. reported for the first time that JMJD6 functioned as a histone arginine demethylase, suggesting that JMJD6 may be an epigenetic regulator of gene expression. In this study, the authors demonstrated that JMJD6 catalysed the demethylation of *N*-dimethylated arginine residues at histone H3 (H3Arg2Me^2) and H4 (H4Arg3Me^2), producing the monomethyl arginine histone marks H3Arg2Me^1 and H4Arg3Me^1 respectively [325]; these histone marks have been associated with transcriptional activation [354, 355]. The role of JMJD6 as a histone demethylase has been arguably corroborated in part by a subsequent report that JMJD6 regulates RNA pol II promotor-proximal pause release [314]; as described in **section 10.1.3.3** below, Brd4-dependent recruitment of JMJD6 to enhancer regions (termed anti-pause enhancers) has been reported to result in H4Arg3Me^2 demethylation and transcriptional elongation [314]. More recently, however, this view has been challenged as other groups have been unable to replicate these findings when using matrix-assisted laser desorption/ionization (MALDI) MS to analyse histone H3 and H4 fragment peptides [288, 319, 356]. JMJD6 has on the other hand been more consistently demonstrated to lysyl hydroxylate histones. For example, using amino acid composition analyses, Unoki et al. reported significant differences in levels of monohydroxylation of lysine residues in the tails of histone H3 and H4 between wild-type and JMJD6 knockout mice [356]. Interestingly, the authors of this study suggested that JMJD6 mediated histone hydroxylation may inhibit acetylation and methylation at the same site, which could be an important epigenetic regulatory mechanism [356], although this now needs to be validated *in vivo*.

10.1.3.3 JMJD6 as a regulator of RNA polymerase II promotor-proximal pause release

Promoter-proximal pause release of RNA Poll II has been proposed to be a major regulator of the transcription response to cellular stress such as heat shock, hypoxia and inflammation [357]. Shortly after the initiation of transcription, RNA Pol II has been reported to pause [358]. The release of paused RNA Pol II, enabling the progression of transcription and production of nascent pre-mRNA, is reported to occur principally through the action of the positive transcription elongation factor-b (P-TEFb) complex [359]. It has recently been reported that JMJD6 also contributes to this mechanism of transcriptional control. In a study

by Lui et al., the authors report that in a subset of BRD4 transcriptional targets, BRD4 recruits JMJD6 at distal enhancer regions of genes referred to as anti-pause enhancers. Subsequently, JMJD6 demethylates both the repressive histone mark H4Arg3Me^2, and the 5'-methyl cap of the snRNA 7SK [314]. In doing so JMJD6 assists in the dissociation of P-TEFb from the inhibitory 7SK snRNA/HEXIM complex, and promotes transcription elongation [314]. However, as discussed in **section 10.1.2**, given the uncertainties regarding the arginine demethylase activity of JMJD6, this role of JMJD6 has been questioned, and requires further validation.

10.1.3.4 JMJD6 as a regulator of splicing

JMJD6 has been previously reported in the literature to interact with a number of proteins involved in RNA processing [281, 288, 289, 318]. In addition, and in keeping with the results presented in this thesis, JMJD6 knockdown has been demonstrated to cause changes in the frequency of a range of alternative splicing events [315, 318]. Unsurprisingly therefore, JMJD6 has previously been implicated in the regulation of alternative splicing. For example, siRNA knockdown of JMJD6 has been reported to increase the production of an alternatively spliced variant of vascular endothelial cell growth factor receptor 1 (VEGFR1), which is encoded by the FLT1 gene [316]. This alternatively spliced variant possesses an extension of exon 13, which leads to the incorporation of a premature stop codon that truncates the VEGFR1 protein, and deletes its transmembrane domain. Subsequently, rather than remaining bound to the cell membrane, the alternatively spliced protein is secreted into the extracellular space where it sequesters vascular endothelial growth factor (VEGF) and inhibits endothelial cell angiogenesis [316]. The regulation of VEGFR1 alternative splicing by JMJD6 described in this study was attributed to the interaction of JMJD6 with the SR factor U2AF65 [316]. The interaction between JMJD6 and U2AF65 is perhaps the best described example of an interaction between JMJD6 and a regulator of spliceosome assembly. As described in **section 1.2.1**, U2AF65 is an accessory factor to the snRNP U2, one of the core components of the spliceosome, and is important in the process of 3' splice site definition. JMJD6 has been previously reported to lysyl-5-hydroxylate U2AF65 [288], and by doing so has been shown to regulate U2AF65-mediated alternative splicing events [318]. Further evidence in support of a JMJD6-U2AF65 pathway in the regulation of alternative splicing stems from work in

erythropoietic protoporphyria (EPP), an autosomal recessive disease caused by a partial deficiency of the enzyme ferrochelatase (FECH). In a study by Barman-Aksözen et al., iron deficiency in erythroleukemic K562 and lymphoblastoid cell lines, increased the proportion of aberrantly spliced ferrochelatase, with similar splicing patterns seen when either JMJD6 or U2AF65 were knocked down by siRNA [317]. Taken together, the authors concluded that the JMJD6-mediated modification of U2AF65 regulated the splicing of FECH [317].

Although modulation of U2AF65 is the most commonly reported way in which JMJD6 regulates alternative splicing events, JMJD6 also has the potential to hydroxylate/interact with SR proteins other than U2AF65 [281, 288, 308, 320]. While these proteins may not be directly involved with spliceosome assembly, as is the case with U2AF65, these *trans*-acting splicing factors play similarly important roles in the regulation of spliceosome activity and splice site selection.

Interestingly, across all these examples, reported functionally relevant JMJD6-mediated alternative splicing events appear to predominately result in intron retention (see **chapter one**, ***figure 1.3***). This alternative splicing event commonly results in the inclusion of a premature stop codon and produces a truncated protein variant that either functions aberrantly, or is subject to nonsense-mediated decay. Interestingly, the inclusion of a cryptic exon into mature mRNA, as occurs with the alternative splicing of the AR to produce AR-V7 [29], is thought to occur as a consequence of an intron retention alternative splicing event [360, 361].

10.1.3.5 JMJD6 and the response to hypoxia

As a 2OG dependent dioxygenase, the catalytic activity of JMJD6 may be limited by oxygen availability, as is the case for other 2OG oxygenases such as the hypoxia-inducible factor prolyl hydroxylases [326]. In keeping with this paradigm, recent reports suggest a relationship between JMJD6 and hypoxia. For example, the transcription of JMJD6 has been reported to be inducible by hypoxia [302], while hypoxia has been reported to mimic the effect of JMJD6 knockdown [316]. Further evidence in support of a role for JMJD6 in the response to hypoxia was provided by Alahari et al. who reported that JMJD6 impacts HIF1a

protein stability by regulating the expression of the von Hippel-Lindau (VHL) tumour suppressor protein in JEG3 cells [362]; thereby proposing a novel role for JMJD6 as an oxygen sensor in the human placenta [362].

10.1.4 The role of JMJD6 in cancer

JMJD6 upregulation has been associated with a poor prognosis and increased tumour aggressiveness in a number of tumour types including melanoma, lung, breast and colon cancer [323, 363-365]. However, which of its enzymatic functions is predominantly responsible for this remains to be elucidated, with a number of possible mechanisms having been postulated in the literature.

10.1.4.1 JMJD6 interacts with p53 and influences cell survival and apoptosis

JMJD6-mediated hydroxylation of p53 has been reported to inhibit its tumour suppressor function. For example, Wang et al. have demonstrated, using both *in vitro* and *in vivo* models of colon carcinoma, that p53 is hydroxylated by JMJD6 at position K382 in its carboxy-terminal domain with this antagonising CBP/p300-mediated acetylation at the same residue [323]. While the significance of this post-translational modification has yet to be fully appreciated, p53 acetylation by CBP/p300 has been reported to 'fine-tune' the function of p53 and induce the expression of its target genes p21 (promotes cell cycle arrest) and BCL2 Binding Component 3 (BBC3) (promotes apoptosis) [366]. Consequently, this may explain why following knockdown of JMJD6 with siRNA, colon carcinoma HCT116 cells were more prone to apoptosis following treatment with the DNA damaging agent VP16 [323].

A role for JMJD6 in the regulation of apoptosis has also been reported in the context of breast carcinoma. JMJD6 knockdown in breast cancer cell lines has been demonstrated to reduce tumour cell invasiveness and suppress proliferation, while JMJD6 overexpression has been correlated with the reverse [363]. One possible explanation for this may be that JMJD6 co-operates with c-MYC to enhance tumorigenesis. Utilising the MMTV-Myc transgenic mouse model of mammary carcinogenesis, Aprelikova et al. demonstrated that JMJD6 binds to the promoter of p19ARF (cyclin-dependent kinase inhibitor 2A in humans) and causes

demethylation of H4Arg3Me[2a], exerting an inhibitory effect that leads to reduced levels of p53 [363]. In doing so, the authors propose that JMJD6 suppresses MYC-induced apoptosis [363]. Furthermore, they add that JMJD6 overexpression in MMTV-Myc cell lines, which most likely occurs due to a copy number gain, increases tumour burden, induces epithelial to mesenchymal transition, and enhances tumour metastasis [363].

10.1.4.2 JMJD6 and alternative splicing in cancer

The concept of JMJD6 as a regulator of alternative splicing has also been alluded to in the development and progression of cancer. For example, elevated expression of JMJD6 has been correlated with advanced clinicopathological stage and aggressiveness in melanoma and is associated with poor prognosis [315]. One possible explanation for this finding is that JMJD6, which is upregulated in melanoma, forms part of a positive feedback loop that promotes carcinogenesis. In a study by Liu et al., the authors reported that in BRAF mutant melanoma cells, inherent hyperactive MAPK signalling led to downstream aberrant activation of c-Jun. Subsequently, this upregulated JMJD6 transactivation, which led to the preferential expression of the full-length enzyme serine/threonine-protein kinase (PAK1), instead of the alternatively spliced isoform PAK1Δ15. Consequently, PAK1, which phosphorylates both RAF and MEK1, then further increased MAPK signalling [315]. In this way, the authors concluded that JMJD6 enhanced MAPK signalling and promoted tumour cell proliferation, invasion, and angiogenesis [315].

10.1.4.3 JMJD6 and microRNA

JMJD6 has been reported to interact with microRNAs (miRNAs) leading to the development of both breast and non-small cell lung cancer (NSCLC). miRNAs are small non-coding RNAs that have been reported to regulate a wide range of biological processes. In cancer cells, miRNAs can become markedly dysregulated and as a consequence have been proposed to function as either oncogenes or tumour suppressors under certain conditions in a variety of cancer types [367].

In breast cancer, JMJD6 has been positively correlated with the expression of the miRNA HOX transcript antisense intergenic RNA (HOTAIR), a non-coding RNA that can

downregulate the expression of genes such as the novel tumour suppressor Protocadherin 10 (PCHD10) [368, 369]. In a study by Biswas et al., chromatin immunoprecipitation analyses determined that JMJD6 bound directly to the promotor region of HOTAIR [369]. Furthermore, in this study, JMJD6 catalysis was reported to induce the expression of HOTAIR, resulting in increased breast cancer cell invasiveness [369]. In keeping with these results, the authors also found that concurrent high expression of both JMJD6 and HOTAIR in breast cancer tumour samples was associated with reduced survival [369].

Similarly, JMJD6 has also been reported to contribute to tumorigenesis in NSCLC through an interaction with the miRNA miR-770. miR-770 has been found to be downregulated in NSCLC where it is associated with reduced overall survival [370]. Under non-malignant conditions, miR-770 has been reported to act as tumour suppressor by binding to the 3' untranslated region (UTR) of JMJD6 and downregulating its expression [370]. However, in NSCLC cells, where miR-770 is downregulated, JMJD6 expression is allowed to increase. Consequently, this has been reported to enable JMJD6-mediated activation of the WNT/β-catenin pathway and promote tumour cell growth [370].

10.1.5 Summary of JMJD6 background

JMJD6 is a 2OG-dependent dioxygenase that has been reported to have pleiotropic roles and a variety of interacting partners. Consequently, JMJD6 has been implicated in the regulation of numerous cellular processes that can impact cancer progression and treatment resistance. However, many of the studies on which these conclusions are based have principally employed biochemical assays to investigate the function of JMJD6. Further work is therefore required to confirm the precise role of JMJD6, and to improve understanding of how JMJD6 contributes to the biology of cancer, particularly in *in vitro* and *in vivo* cancer models.

10.2 Final discussion of results

Resistance to AR-directed therapies including abiraterone and enzalutamide is inevitable in advanced prostate cancer, and is invariably fatal. Resistance to these therapeutic agents is at least in part driven by constitutively active AR-SVs that remain undrugged in the clinic. The results presented in this thesis demonstrate that the 2OG-dependent dioxygenase JMJD6, which has been previously associated with a poor prognosis and increased tumour aggressiveness in other tumour types [323, 363-365], is a pharmacologically tractable protein that is critical for prostate cancer cell growth and the production of AR-V7 protein in multiple models of prostate cancer. Importantly, in addition to these *in vitro* results, the immunohistochemical and RNA-seq analyses performed on patient tissue samples reported in this study reveal that JMJD6 is expressed in prostate cancer, with its levels increasing significantly with the emergence of castration-resistance. Furthermore, upregulation of JMJD6 associates with both increased levels of AR-V7 protein in metastatic CRPC biopsies, and with poorer survival. Taken together, my results indicate that that JMJD6 is an actionable therapeutic target for overcoming oncogenic AR-V7 signalling in CRPC that merits further evaluation in drug discovery efforts.

Importantly, I have found that in addition to reducing levels of AR-V7 protein, JMJD6 knockdown also inhibits the *induction* of AR-V7 protein in response to AR blockade in hormone-sensitive VCaP cells, indicating that the targeting of JMJD6 impacts on the production of AR-V7 at primary AR blockade. This is of particular therapeutic relevance because for AR-V7 targeting to be successful, novel treatment strategies are needed that can block AR-V7 generation rather than just counteract its oncogenic effects once resistance to AR-directed therapy is established [284]. Moreover, the reduction in AR-V7 levels and prostate cancer cell growth seen following JMJD6 siRNA knockdown suggests limited functional redundancy in these tested models, which is particularly striking given that recently two other 2OG dependent JmjC-domain containing oxygenases, JMJD1A/KDM3A [212] and KDM4B [213], have also been reported to be important in the regulation of AR-V7 (as discussed in **section 1.5.2**). However, while JMJD1A/KDM3A and KDM4B are assigned as N-methyl lysine demethylases (KDMs) [371, 372], like other JmjC KDMs, other roles for them including N-methyl arginine demethylation are possible [373]. Given their roles in histone

modification, it is thus not clear to what extent KDM4B/JMJD1A directly regulate AR splicing. Therefore, although it is likely that other 2OG-dependent JmjC-domain containing proteins such as JMJD1A/KDM3A and KDM4B play a role in the overall activity of the spliceosome machinery and AR splicing, albeit probably through alternative mechanisms, my results demonstrate that targeting the 2OG-dependent catalytic activity of JMJD6 is a promising prostate cancer drug discovery strategy. A better understanding of the interplay between these different JmjC-domain containing proteins in the complex spliceosome machinery is however now required.

My *in vitro* results indicate that JMJD6 regulates the expression of AR-V7, at least in part, by modulating the recruitment of the SR factor U2AF65 to AR-V7 specific pre-mRNA splice sites, which has been previously shown to be critical for the expression of AR-V7 [97]. My evidence implies that the JMJD6-mediated regulation of AR-V7 expression is dependent on an intact JMJD6 catalytic site, and importantly, that the catalytic site resides within a druggable pocket. JMJD6 has been previously reported in the literature to lysyl-5-hydroxylate U2AF65 [288], and by doing so has been shown to regulate U2AF65-mediated alternative splicing events [318]. In keeping with these reports, my results demonstrate that 2,4-PDCA, which I show in **chapter nine** inhibits JMJD6 lysyl-5-hydroxylation, downregulates AR-V7 protein levels in castration-resistant prostate cancer cells. Taken together these findings point towards a JMJD6/U2AF65/AR-V7 regulatory pathway, wherein JMJD6 enzymatic activity, most likely through hydroxylation of U2AF65, and/or other SR proteins, regulates U2AF65 recruitment to AR-V7 specific splice sites, thereby facilitating the generation of AR-V7 through interaction with the spliceosome.

While the preclinical results presented in this thesis are encouraging, I acknowledge that my conclusions are likely dependent on the molecular backgrounds of the various models used. This is particularly relevant given the apparent pleiotropic roles of JMJD6, at least in some contexts [308, 309]. However, as discussed in **section 7.6.1**, this fact alone does not preclude the therapeutically useful targeting of 2OG oxygenases, as shown by the clinical approvals of HIF prolyl hydroxylase inhibitors [310]. Overall, given that the results reported here have been replicated in a number of different cell lines with differing genomic

backgrounds, I believe they support the pursuit of subsequent *in vivo* studies on the role of JMJD6 in prostate cancer.

As detailed in **section 9.7.1**, the lack of a validated downstream *in vitro* 'read-out' of physiologically relevant effects of JMJD6 catalysis has represented another significant obstacle in research on JMJD6. Unexpectedly therefore, the effect of JMJD6 knockdown/inhibition on AR-V7 levels is also of wider general interest. I believe that the results of this thesis will support further research into JMJD6 functional biology, and improve understanding of this fascinating yet still poorly understood regulatory protein.

10.3 Clinical implications and considerations resulting from this thesis

10.3.1 Targeting JMJD6 and on-target toxicity

A key finding from the results presented in this thesis is that JMJD6 is important for prostate cancer cell growth. In **chapter seven**, I have shown that JMJD6 knockdown by siRNA reduces the growth of multiple prostate cancer cell lines. Interestingly, this finding is in keeping with results from the publicly accessible pan-cancer Cancer Dependency Map (depmap) data repository indicating that JMJD6 is commonly essential to a range of different cancer types [374]; suggesting that the results of this thesis may also be of relevance to other cancers.

While these results indicate that JMJD6 may be a therapeutic target in metastatic CRPC, questions remain as to the effect of JMJD6 knockdown on non-malignant cells. As discussed in **section 10.1**, through its proposed roles in the regulation of transcription, splicing, and chromatin remodelling, JMJD6 has been implicated in a number of important normal physiological processes including embryogenesis and the response to hypoxia. Unsurprisingly therefore, loss of JMJD6 has been found to be embryonically lethal, with JMJD6 knockout mice developing a number of severe embryonic defects [308, 320]. However, as shown in ***figure 7.2***, JMJD6 knockout in PNT2 prostate cancer cells, which are immortalised normal prostatic epithelial cells, had relatively little effect on cell growth. Similarly, other groups have successful developed homogeneous JMJD6 knockout CRISPR clones [336]. These data likely reflects the context-dependent nature of JMJD6 [308], and suggests that while

JMJD6 may be critically important to some cells at specific times, it may be less so in other cells in different circumstances. This is important when considering potential future anti-JMJD6 therapies, because if inhibition of JMJD6 is as lethal to non-malignant cells as it is to malignant cells, the clinical utility of such treatments may be constrained by dose limiting toxicities.

Due to the lack of validated, specific, small-molecule inhibitors of JMJD6, much of the literature pertaining to JMJD6 centres on reports from studies using CRISPR, siRNA or shRNA techniques to knockout/downregulate JMJD6 expression. However, as discussed in **section 7.6.1**, all these methods are limited by their inability to differentiate between effects which are due to loss of JMJD6 enzymatic activity, and those that are due to loss of JMJD6 as a protein scaffold, as downregulation of JMJD6 protein levels interrupts both these functions. This gap in our understanding of JMJD6 biology is, however, of considerable significance. For example, in this thesis I have shown that it is most likely the catalytic activity of JMJD6, as opposed to its protein scaffold function, that is important for the production of AR-V7. It may, however, be the case that in prostate cancer cells (or indeed other benign and malignant cells) it is the interruption of cellular processes caused by the loss of JMJD6 as a protein scaffold that is principally responsible for the inhibition of cell growth observed following JMJD6 siRNA knockdown. Consequently, treatment with a small-molecule that inhibits JMJD6 catalytic activity but maintains JMJD6 protein scaffold function may not adversely impact cell survival, making on-target toxicity less of a concern. In this scenario, JMJD6 would, however, still represent a novel therapeutic target in CRPC because although it may not kill prostate cancer cells directly, it could still elicit an anti-cancer effect by inhibiting AR-V7 oncogenic signalling and re-sensitising resistant cancer cells to AR-directed therapies. In addition, I have shown in **section 6.4.2,** that JMJD6 protein levels increase significantly as patients progress to lethal CRPC. Coupled with my results indicating the importance of JMJD6 for prostate cancer cell survival, these data suggest that JMJD6 may have a more important role in castration-resistant prostate cancer cells than it does in other cells. Consequently, a therapeutic window may exist in which JMJD6 inhibition could achieve an anti-cancer effect by killing prostate cancer cells, while enabling non-malignant cells to survive, limiting associated toxicities.

Further *in vivo* work is now required, with selective inhibitors of JMJD6, to resolve these outstanding issues and determine which functions of JMJD6 are most important for the different roles attributed to JMJD6, and the toxicities associated with their selective inhibition; this will be key to validating the suitability of JMJD6 as a therapeutic target in CRPC long-term.

10.3.2 The importance of AR-V7 for the progression of CRPC

The emergence of AR-V7 in CRPC has been convincingly demonstrated to be a biologically credible mechanism of resistance to AR-directed therapies *in vitro* [179-181]. These reports are, in addition, corroborated by clinical studies indicating that AR-V7 expression is associated with both a shorter progression-free survival on AR-directed therapies, and a shorter overall survival [89, 184-186]. As discussed in **section 1.5.2**, however, evidence linking these data mechanistically, and confirming a causative relationship between AR-V7 expression and resistance to AR-directed therapies *in vivo*, is still lacking. Although AR-V7 expression clearly increases in CRPC, the speed with which changes in AR-V7 levels occur following AR signalling inhibition, and conflicting reports as to the ability of AR-V7 to confer resistance to enzalutamide in pre-clinical studies [183] and a worse prognosis in patients [187, 188], raises questions regarding the true biological and clinical significance of AR-V7 in lethal prostate cancer. Consequently, there remains an urgent need to better understand the importance of AR-V7 for CRPC progression, so as to improve treatment for patients with lethal prostate cancer.

In this thesis, I show that JMJD6 is an important regulator of AR-V7 production in pre-clinical models of CRPC. Therefore, the results of this thesis provide new opportunities for investigating the importance of AR-V7 for prostate cancer progression through further study of the interaction between AR-V7 and JMJD6. In **chapter seven**, I show that JMJD6 knockdown downregulates AR-V7 expression and inhibits prostate cancer cell growth. These data do not, however, inform on the extent to which the downregulation of AR-V7 and JMJD6 individually contribute to this reduction in growth. To further investigate this, subsequent studies are needed to disentangle this relationship, and better appreciate the individual importance of JMJD6 and AR-V7 to prostate cancer progression. For example, having found JMJD6 siRNA

knockdown to 1) inhibit prostate cancer cell growth, and 2) downregulate AR-V7 expression, siRNA studies targeting AR-V7, rather than JMJD6, could now be performed to ascertain whether or not AR-V7 knockdown reproduces the inhibition of growth seen following JMJD6 knockdown. If AR-V7 siRNA knockdown replicates the inhibition of prostate cancer cell growth seen following JMJD6 knockdown, this would support the role of AR-V7 in maintaining prostate cancer cell survival and proliferation. However, if AR-V7 knockdown alone does not impact prostate cancer cell growth, this would instead suggest that JMJD6 knockdown inhibits prostate cancer cell growth through some other mechanism, such as by downregulating MYC signalling activity ***(figure 8.5)***, or interrupting the alternative splicing of other genes that are important for prostate cancer cell survival. In addition, subsequent experiments could also be performed to determine whether or not restoration of AR-V7 levels by AR-V7 plasmid overexpression can rescue prostate cancer cell growth following JMJD6 knockdown. If this were the case, this would again support the hypothesis that AR-V7 is important for prostate cancer cell survival, and suggest that the inhibition of growth seen following JMJD6 knockdown occurs principally as a consequence of the associated downregulation of AR-V7. These studies could then be expanded to study the role of AR-V7 following AR blockade; AR-V7 could be overexpressed in castration-sensitive prostate cancer cells, such as LNCaP cells, to determine whether or not this confers resistance to treatment with enzalutamide. Similarly, AR-V7 overexpressing stable CRISPR clones could also be developed to determine if overexpression of AR-V7 confers resistance to combination therapy with JMJD6 siRNA and enzalutamide. Subsequently, if successful, equivalent studies could then be pursued in *in vivo* mouse models. Ultimately, however, until novel therapies are developed capable of abrogating AR-V7 signalling in patients, the biological and clinical significance of AR-V7 will remain challenging to ascertain.

10.3.3 Treatment initiation and patient stratification for future anti-JMJD6 directed therapies

Knowledge of when in the course of a patient's disease is the best time to initiate treatment with a novel therapeutic is a key consideration for optimising that patient's response to treatment. The results of this thesis demonstrate that JMJD6 siRNA knockdown and small-molecule inhibition downregulate AR-V7 levels. Moreover, as shown in **section 7.5**, JMJD6 knockdown also reduces the upregulation of AR-V7 at the time of primary AR blockade.

Given that AR-V7 expression has been proposed as a mechanism of resistance to AR directed therapies, these data therefore point towards two possible strategies with regards to initiation of a future anti-JMJD6 directed therapy. The first, is to begin treatment upon progression on a first-line anti-androgen agent for the treatment of CRPC such as abiraterone or enzalutamide. The second, is to instead commence treatment at the same time as initiating first-line AR directed therapy in CRPC. Of these two options, combination therapy with a JMJD6 inhibitor alongside first-line AR directed therapy in CRPC is likely to be the most efficacious approach, because, as described in **section 7.6**, for such anti-AR-V7 strategies to be successful, novel therapeutics will need to block AR-V7 generation, rather than just counteract its oncogenic effects once endocrine resistance is established [284]. In this scenario, inhibition of JMJD6 could minimize, or possibly prevent, the production of AR-V7 following AR blockage, thereby mitigating against this mechanism of resistance to AR directed therapy, and improving the efficacy and progression-free survival achieved with agents such as abiraterone and enzalutamide.

Determining which patients are most likely to benefit from a new therapy is equally important for maximising its clinical utility. As discussed in **section 1.8.3.1**, predictive biomarkers, such as DNA repair aberrations and PSMA expression levels, have become important tools for identifying patients in whom therapies such as PARP inhibitors and PSMA-based theranostics, respectively, are likely to be most beneficial. Likewise, identification of predictive biomarkers for future anti-JMJD6 directed therapies will also be key in maximising the clinical utility of such agents. In **section 8.6**, I demonstrate that the MYC signalling pathway is the most significant molecular pathway downregulated by JMJD6 siRNA knockdown *in vitro*. MYC is a recognised driver of prostate cancer progression, as discussed in **section 1.4.2**. Importantly, the MYC gene is amplified in approximately 25% of patients with metastatic CRPC [375]. This cohort of patient could therefore represent a patient population in which anti-JMJD6 therapy could be particularly efficacious, not only in combination with AR directed therapies as described above, but possibly also as a monotherapy. In **section 8.6**, I also report that JMJD6 knockdown downregulates a number of alternative splicing events other than AR splicing. Alternative splicing events have been shown to be common in NEPC, and have been suggested to contribute to the development of the neuroendocrine phenotype [118, 119]. NEPC may therefore represent another prostate cancer sub-type which may

derive clinical benefit from treatment with anti-JMJD6 directed therapy, which now merits further investigation. A third population of patient that may prove sensitive to anti-JMJD6 directed therapy are those with PTEN loss. PTEN is a tumour suppressor gene that is lost in approximately 40% of patients with metastatic CRPC [103]. Importantly, PTEN loss has been reported to upregulate glutaminolysis in prostate cancer cells, resulting in an increase in levels of 2OG. As a 2OG-dependent dioxygenase, JMJD6 catalytic activity is dependent on the availability of 2OG, therefore it is conceivable that JMJD6 activity may be enhanced in cells lacking PTEN. If so, this may mean that patients with metastatic CRPC and detectable PTEN loss by immunohistochemistry may benefit from treatment with a JMJD6 inhibitor. Perhaps more intriguingly however, given that glutamine metabolism can serve as a surrogate marker of 2OG levels, as 2OG is the end product of glutaminolysis, and that glutamine uptake can be visualised through positron emission tomography (PET), patients may be able to be selected for anti-JMJD6 directed therapy non-invasively based on high glutamine uptake in their cancers. The relationship between JMJD6 and cancer cell metabolism therefore also warrants further investigation in subsequent studies.

10.3.4 Cancer cell metabolic dysregulation and JMJD6 activity

As a 2OG-dependent dioxygenase, JMJD6 catalytic activity is dependent on the availability of 2OG. 2OG, or a-ketoglutarate, is a TCA cycle intermediate and is derived through numerous metabolic pathways. The activity of JMJD6 is therefore potentially intimately linked to changes in cellular metabolism. While aerobic respiration is the archetypal energy source for benign cells, the increased bioenergetic requirements of malignant cells necessitates greater reliance on alternative energy sources. Consequently, glutaminolysis has been reported to be an important metabolic pathway in prostate cancer cells, generating 2OG from glutamine, so as to maintain anaplerosis [376, 377]. In keeping with this concept, AR-V7 signalling has been reported to directly upregulate glutaminolysis, resulting in increased levels of glutamine and 2OG in AR-V7 expressing cells [378]. Taken together, these reports support the hypothesis that JMJD6 may be more active in prostate cancer cells than in normal prostatic cells, particularly those that are castration-resistant and express AR-V7, owing to an increased availability of 2OG.

In addition to 2OG, other TCA cycle intermediates have also been reported to impact JMJD6 activity. However, unlike 2OG, which enhances JMJD6 catalytic activity, the TCA cycle intermediates succinate and fumarate have been demonstrated to inhibit JMJD6 catalytic activity [332]. The balance between these different TCA cycle intermediates therefore represents a mechanism through which JMJD6 activity may be regulated by changes in cellular metabolism. This is particularly important, as metabolic reprogramming commonly occurs as a consequence of the genomic alterations and environmental stresses that drive prostate cancer progression. For example, MYC amplification, which has been reported in approximately 25% of patients with metastatic CRPC, and PTEN loss, which has been reported to occur in approximately 40% of patients with metastatic CRPC, have both been demonstrated to upregulate glycolysis and glutaminolysis [379-381]. Similarly, RB1 loss, which has a reported incidence of 21% in metastatic CRPC [103], also upregulates glutamine metabolism [382], while mutations of TP53, detectable in approximately half of patients with metastatic CRPC [103], have been associated with increased glycolytic flux [383, 384]. By increasing the activity of these metabolic pathways, common genomic alterations such as these directly impact on the levels of TCA cycle intermediates and, potentially, modify the activity of JMJD6. However, the extent to which genomic alternations impact the levels of TCA cycle intermediates such as 2OG, succinate, and fumarate, and how subsequent differences between the levels of these substrates affect JMJD6 activity, requires further elucidation. Once known, these genomic alterations could serve as predictive biomarkers for future anti-JMJD6 directed therapies by informing on the activity of JMJD6 in patients' cancers.

Common microenvironmental stresses can also impact prostate cancer cell metabolism. For example, tumour hypoxia, which is a common and early occurrence in prostate cancer, increases rates of glycolysis and glutaminolysis [303, 385, 386]. Like many of the genomic alterations discussed above therefore, hypoxia can also alter levels of TCA cycle intermediates. Interestingly, hypoxia has also been reported to increase isocitrate dehydrogenase-dependent carboxylation of 2OG, converting 2OG to citrate rather than succinate [387]; elucidation of how this reversal of flux through the TCA cycle in hypoxia impacts JMJD6 activity now warrants further evaluation. However, while tumour hypoxia may

alter the levels of TCA cycle intermediates, the requirement for oxygen to maintain JMJD6 catalytic activity may mean that the impact of these changes are not functionally significant.

On the contrary, HIF1a, the master regulator of the hypoxic response, can be upregulated in cancer cells in the absence of hypoxia, termed pseudohypoxia, enabling the molecular sequalae of hypoxia to be instigated in the presence of oxygen [388]. In this scenario, changes in TCA cycle intermediates may indeed have an impact on JMJD6 activity. The stabilisation of HIF1a in the absence of hypoxia has been most commonly associated with inactivating mutations of VHL [389], however, unlike in renal cell carcinoma, genomic alterations of VHL have not been commonly identified in prostate cancer [103, 375]. PTEN loss on the other hand, is common in prostate cancer, and has similarly been reported to result in stabilisation of HIF1a [388, 390], contributing to the upregulation of glycolytic flux seen with this genomic alteration. Therefore, PTEN loss prostate cancer may represent a key prostate cancer subtype in which JMJD6 is particularly important. Interestingly, pseudohypoxia can also result from genomic alterations of TCA cycle enzymes. Both deletion and mutation of succinate dehydrogenase (SDH), the enzyme responsible for converting succinate to fumarate, have been reported to cause an accumulation of succinate in affected cells, resulting in the inhibition of HIF prolyl hydroxylases [391]. HIF prolyl hydroxylases hydroxylate HIF1a, marking it for degradation by the proteasome. Thus, genomic alterations of SDH can upregulate HIF1a levels in the absence of hypoxia, and have consequently been implicated in tumorigenesis [392]. However, given that HIF prolyl hydroxylases and JMJD6 share a common JmjC domain, it is likely such genomic alterations would suppress, rather than promote, JMJD6 catalytic activity.

Considered alongside the potential role of JMJD6 as a key regulator of alternative splicing, the relationship between metabolism and JMJD6 activity raises the intriguing possibility that JMJD6 may serve as a metabolic sensor, activating different transcriptional programs in response to changing cellular metabolic states and environmental stressors to promote cell survival. JMJD6, and other 2OG-dependent dioxygenases, may therefore represent a critical missing-link between the metabolic reprogramming that occurs as a consequence of the genomic and environmental drivers of prostate cancer progression, and

downstream transcriptional programs. Further work is needed to better understand this complex interplay.

11

Conclusions and future work

11.1 Conclusions

The main conclusions derived from the data presented in this thesis are that:

- The 2OG-dependent dioxygenase JMJD6 is critical to prostate cancer cell growth, and is an important regulator of AR-V7 protein levels in preclinical models of CRPC.

- JMJD6 knockdown inhibits the induction of AR-V7 protein in response to primary AR blockade.

- JMJD6 protein levels are upregulated with the emergence of castration-resistance in clinical metastatic CRPC patient tissue biopsies, and associate with both AR-V7 expression and worse survival.

- There exists a novel JMJD6/U2AF65/AR-V7 regulatory pathway, whereby JMJD6 enzymatic activity regulates U2AF65 recruitment to AR-V7 specific splice sites, facilitating the generation of AR-V7.

- The JMJD6 active site is required to facilitate the lysyl-5-hydroxylation of splicing regulatory proteins and is amenable to small-molecule inhibition in a manner exploited clinically for other 2OG oxygenases.

11.2 Future work

The results presented in this thesis reveal that JMJD6 is upregulated in CRPC and is associated with a worse survival. In addition, my results identify a novel regulatory mechanism whereby JMJD6 recruits the SR factor U2AF65 to AR-V7 specific splice sites to promote the production of AR-V7. Nonetheless, questions remain as to what factors drive the observed upregulation of JMJD6 in CRPC, and whether the observed JMJD6-mediated recruitment of U2AF65 to AR-V7 splice sites is a direct effect of JMJD6 on U2AF65, or if JMJD6 regulates U2AF65 recruitment through modulation of one or more intermediate factors. Further work is therefore required to better understand both the factors that regulate JMJD6 expression, and the downstream proteins with which JMJD6 interacts. Furthermore, given that the data presented in this thesis predominantly results from *in vitro* analyses, *in vivo* validation of these findings is also required.

11.2.1 Determining the upstream regulators of JMJD6

Having demonstrated the importance of JMJD6 for prostate cancer biology, a better understanding of the mechanisms influencing its activity and upregulation is now needed to identify novel strategies for overcoming JMJD6-mediated disease progression and treatment resistance in CRPC. Previously, this task has been complicated by the lack of a measurable readout of JMJD6 activity. However, as shown in this thesis, AR-V7 may serve as one such biomarker. This knowledge could subsequently be leveraged to identify regulators of JMJD6 *in vitro*. Given that AR-V7 levels are downregulated by JMJD6 knockdown/inhibition, and upregulated with JMJD6 overexpression, unbiased genome-wide CRISPR based screens can identifying genes that regulate JMJD6 activity through detection of changes in AR-V7 levels. Subsequently, chromatin immunoprecipitation (ChIP) assay can be used to determine which identified genes bind the JMJD6 promoter. In addition, targeted evaluation of predicted

potential regulators of JMJD6 (such as oxygen, iron, and 2OG availability) can also be performed using AR-V7 as a marker of JMJD6 activity.

11.2.2 Elucidate the downstream effectors underlying JMJD6 mediated regulation of AR-V7

In this thesis I demonstrate that JMJD6 is a key transcriptional regulator of AR-V7. However, whether JMJD6 regulates U2AF65 recruitment to AR-V7 splice sites directly or through the modulation of other intermediate factors remains to be determined. My results also indicate that JMJD6 is important for prostate cancer cell survival. This finding is likely a consequence of more than just the role of JMJD6 in regulating the production of AR-V7, suggesting that JMJD6 may play a wider role in prostate cancer biology. However, the extent of this role remains uncertain. Immunoprecipitation-MS analyses and fluorescence proximity ligation assays in prostate cancer cell lines could help resolve some of these outstanding issues by identifying proteins that interact with JMJD6 *in vitro*, and determining how these interactions are impacted by important microenvironment stresses (e.g. AR signalling blockade and hypoxia) and 2OG levels. In addition, potential mechanisms of resistance to JMJD6 inhibition could also be explored by interrogating RNA-seq data from prostate cancer cell lines prior to, and after, both short- and long-term JMJD6 inhibition, to uncover genes and signalling pathways significantly upregulated following downregulation of JMJD6 activity. The functional significance of upregulated genes and pathways for AR-V7 expression and prostate cancer cell growth could then be studied through *in vitro* down- (siRNA knockdown/chemical inhibition) and up- (gene overexpression/pathway ligands) regulation assays. Together, these studies would improve understanding of the downstream mechanisms through which JMJD6 modulates transcriptional programs, including but not limited to AR-V7 splicing. In doing so they would provide invaluable insights into prostate cancer biology, inform on potential mechanisms of resistance to anti-JMJD6 therapies, and identify novel therapeutic targets downstream of JMJD6 that could also be taken forward to aid future drug development efforts. These studies would also shed light on the relationship between JMJD6 and other JmjC domain containing oxygenases, such as JMJD1A/KDM3A and KDM4B, which may have important implications for prostate cancer biology with regards to transcriptional regulation and the response to cell stress.

11.2.3 In vivo validation of thesis results

JMJD6 knockout is embryonically lethal [348, 349]. Consequently, *in vivo* studies of JMJD6 loss of function are challenging. However, *in vivo* validation of the results presented in this thesis is a necessary step in establishing the suitability of JMJD6 as a therapeutic target in CRPC. One possible strategy for overcoming this is to generate prostate-specific conditional JMJD6 knockout mice. While this would only enable knockout of JMJD6 in the prostate, it would provide invaluable information on the importance of JMJD6 for the development of prostate cancer, castration-resistance and disease progression. Alongside this, heterozygous JMJD6 'knockout-first' mice could be crossbred with a tamoxifen-inducible Cre under a ubiquitously expressed promotor (e.g. R26-CreERT2). Subsequently, JMJD6 could then be deleted across all tissues at different time points in the life-cycle of the generated mice to evaluate the tolerability of JMJD6 loss-of-function.

In addition to these mouse studies, evaluation of the potential therapeutic utility of targeting JMJD6 could also be evaluated in patient-derived xenograft (PDX) models of lethal prostate cancer. This would be particularly helpful in studying the effect of pharmacological inhibition of JMJD6 on prostate cancer growth, for example with 2,4-PDCA. However, as discussed in **section 9.7.1**, other more permeable and selective JMJD6 inhibitors may need to be identified through high-throughput drug screens to maximise the yield of these experiments.

11.3 Summary of thesis

In summary, this thesis demonstrates that JMJD6 inhibition has the potential to overcome oncogenic AR-V7 signalling, and is an eminently tractable new therapeutic target for metastatic CRPC that merits further evaluation in *in vivo* studies.

I believe this thesis is an example of how a better understanding of the cellular mechanisms that contribute to disease progression and treatment resistance can lead to the development of novel therapeutic strategies that have the potential to transform the care provided to patients with advanced prostate cancer.

12

Supplementary Tables

Supplementary Table 12.1: Targeted siRNA screen results.

22Rv1		LNCaP95		Average	
Gene	**AR-V7:AR-FL Ratio**	**Gene**	**AR-V7:AR-FL Ratio**	**Gene**	**AR-V7:AR-FL Ratio**
JMJD6	0.31	HTATSF1	0.21	JMJD6	0.29
SF3B1	0.33	JMJD6	0.27	CPSF1	0.43
HSPA6	0.39	NFX1	0.29	SF3B1	0.47
HNRNPH2	0.42	PHF5A	0.34	POLR2A	0.47
KHSRP	0.45	NOL3	0.37	HSPA6	0.50
ACIN1	0.46	CPSF1	0.37	CPSF3	0.57
SF3B6	0.47	THRAP3	0.39	DDX39B	0.59
SNW1	0.48	PDCD7	0.42	SRRM1	0.62
HNRNPK	0.48	POLR2A	0.43	THRAP3	0.62
RBM8A	0.49	USP4	0.46	ACIN1	0.63
CPSF1	0.50	HSPA8	0.48	PCF11	0.66
POLR2A	0.52	CPSF2	0.53	POLR2B	0.68
DDX39B	0.57	CPSF3	0.54	NFX1	0.68
AAR2	0.58	CLP1	0.56	CHERP	0.69
CHERP	0.59	SRRM1	0.56	CPSF2	0.70
RBMX2	0.59	PPIG	0.57	POLR2F	0.70
CPSF3	0.60	PSIP1	0.59	NOL3	0.70
PUF60	0.62	DHX15	0.59	PRMT5	0.71
PCF11	0.62	LSM8	0.60	PHF5A	0.71
CSTF3	0.63	SF3B1	0.61	HNRNPH2	0.72
POLR2B	0.63	HSPA6	0.61	USP4	0.72

LSM2	0.64	SRSF2	0.61	PUF60	0.72
SNRNP35	0.64	LSM6	0.61	CLP1	0.72
EIF4A3	0.64	TIA1	0.61	RBM15B	0.73
SRRT	0.65	PCBP2	0.61	NCBP1	0.74
HNRNPH3	0.66	DDX39B	0.62	POLR2C	0.74
RBMXL1	0.68	CCDC12	0.62	RBM8A	0.74
POLR2F	0.68	CLNS1A	0.63	PPARGC1A	0.75
SRRM1	0.68	ISY1	0.63	PRPF19	0.75
SRSF7	0.69	NCBP1	0.64	SKIV2L2	0.75
SRSF11	0.69	ZMAT5	0.64	LSM2	0.76
THOC1	0.70	RBM15B	0.65	HNRNPU	0.76
LOC100996657	0.70	DHX16	0.66	ZMAT5	0.76
RBM10	0.71	CWC27	0.66	ISY1	0.76
TFIP11	0.72	FMR1	0.66	SF3B3	0.77
LSM5	0.72	PRPF8	0.66	FMR1	0.77
PPARGC1A	0.73	SKIV2L2	0.67	SNRNP35	0.77
SF3B3	0.73	THOC3	0.68	HTATSF1	0.78
FRG1	0.73	PRMT5	0.68	SF3A3	0.78
PRMT5	0.73	GTF2F2	0.69	C1QBP	0.78
THOC2	0.73	CELF6	0.69	AAR2	0.79
POLR2C	0.74	ALYREF	0.69	THOC3	0.79
RBM17	0.74	PCF11	0.71	SNRNP48	0.81
SNRNP200	0.75	SRSF8	0.71	DHX16	0.81
SF3B2	0.75	POLR2F	0.72	USP39	0.81
C1QBP	0.75	POLR2B	0.72	SNW1	0.81
HNRNPU	0.75	SART3	0.72	RALY	0.81
SF3A3	0.75	POLR2D	0.72	CCDC12	0.81
RNF113A	0.76	POLR2E	0.73	POLR2E	0.82
ZRSR2	0.77	PLRG1	0.73	HSPA8	0.82
PABPN1	0.77	USP39	0.73	LSM6	0.82
PRPF19	0.77	PRPF19	0.73	EIF4A3	0.82
CSTF1	0.77	POLR2C	0.74	POLR2L	0.82
HNRNPA3	0.79	FIP1L1	0.74	NCBP2	0.82
SNRNP48	0.79	RBM25	0.74	HNRNPA3	0.82
U2AF2	0.79	PPIH	0.74	SRRT	0.83
PRPF40A	0.81	SMC1A	0.75	DHX15	0.83
RNPS1	0.81	UPF3B	0.75	THOC1	0.83
RBM15B	0.82	RBM4	0.75	RBM10	0.83
TGS1	0.82	NCBP2	0.75	SRSF7	0.83
IVNS1ABP	0.82	POLR2L	0.76	FRG1	0.84
AQR	0.82	HNRNPU	0.77	RBM22	0.84
SRSF6	0.83	RBM22	0.77	SMC1A	0.84

NSRP1	0.83	DDX39A	0.77	CELF6	0.84
SRRM4	0.83	ZNF638	0.77	RBMX2	0.85
SKIV2L2	0.83	PPARGC1A	0.77	THOC2	0.85
NCBP1	0.84	RALY	0.78	DBR1	0.85
HNRNPC	0.84	ACIN1	0.79	SRSF6	0.85
SNRNP25	0.84	SCAF11	0.79	HNRNPH3	0.85
DDX42	0.84	PSPC1	0.80	PCBP2	0.85
SPEN	0.84	CHERP	0.80	DDX39A	0.86
RALY	0.85	SRSF3	0.80	POLR2D	0.86
GEMIN4	0.85	SF3B3	0.80	SF3B2	0.86
THRAP3	0.86	SF3A3	0.80	KHSRP	0.86
ZCCHC8	0.86	DBR1	0.81	SF3B6	0.86
PRPF39	0.86	C1QBP	0.81	SPEN	0.86
CPSF2	0.86	HSPA1L	0.81	LOC100996657	0.87
HNRNPA2B1	0.87	SMN1	0.82	PSPC1	0.88
NOVA2	0.87	SNRNP48	0.82	RNF113A	0.88
FMR1	0.87	PUF60	0.82	HNRNPC	0.88
CTNNBL1	0.87	WBP11	0.83	GEMIN4	0.88
SNRPA	0.88	RAVER2	0.84	PRPF40A	0.88
WBP4	0.88	PTBP1	0.84	SRSF3	0.88
ZMAT5	0.88	TRA2B	0.84	ZRSR2	0.88
USP39	0.88	NAA38	0.85	LSM8	0.88
CLP1	0.89	LSM7	0.85	RBM17	0.89
POLR2L	0.89	SNRPD2	0.86	CLNS1A	0.89
DBR1	0.89	SNRPC	0.86	AQR	0.89
NCBP2	0.89	EFTUD2	0.86	EFTUD2	0.89
RBMX	0.89	METTL14	0.86	PLRG1	0.90
ZMAT2	0.89	HNRNPA3	0.86	PTBP1	0.90
ISY1	0.90	POLR2G	0.87	UPF3B	0.90
RBMY1A1	0.90	NONO	0.87	NONO	0.90
DHX38	0.90	SRSF6	0.88	ZCCHC8	0.90
POLR2E	0.90	HNRNPF	0.88	NAA38	0.91
ELAVL2	0.90	SRSF4	0.88	TIA1	0.91
GEMIN8	0.91	LSM2	0.88	SRSF4	0.91
RBM22	0.91	SPEN	0.88	FIP1L1	0.91
GEMIN2	0.91	PRPF4B	0.88	PDCD7	0.91
THOC3	0.91	SNRPA1	0.89	SNRNP200	0.91
TRA2A	0.91	SRSF9	0.89	HNRNPA2B1	0.91
PRPF38A	0.92	SNRNP35	0.90	NSRP1	0.92
PQBP1	0.92	SF1	0.90	ELAVL2	0.92
HELB	0.92	XAB2	0.91	RBM25	0.92
EFTUD2	0.92	GEMIN4	0.91	RBMXL1	0.92

NONO	0.93	SF3B4	0.91	PPIG	0.92
RBFOX3	0.93	POLR2J	0.92	SRSF11	0.93
HNRNPH1	0.93	RNPC3	0.92	SF1	0.93
SMC1A	0.93	LMNTD2	0.92	HELB	0.93
SNRNP70	0.93	HNRNPC	0.92	HNRNPK	0.93
GTF2F1	0.94	STRAP	0.92	XAB2	0.93
LSM3	0.94	SRPK1	0.92	RBM4	0.93
SRSF4	0.94	CELF4	0.92	CSTF3	0.93
DDX39A	**0.94**	DHX35	0.93	GTF2F1	0.93
GCFC2	0.95	NOVA1	0.93	SF3B4	0.94
PTBP1	0.95	GTF2F1	0.93	PSIP1	0.94
SF1	0.95	HSPA2	0.93	LMNTD2	0.94
PSPC1	0.95	API5	0.93	GEMIN8	0.94
PRPF18	0.95	HNRNPD	0.93	CELF4	0.94
U2SURP	0.95	ELAVL2	0.94	WBP11	0.95
PRPF4	0.95	HELB	0.94	RNPS1	0.95
ZCRB1	0.96	FRG1	0.94	HNRNPF	0.95
DHX16	0.96	RBM10	0.94	CSTF1	0.95
SNU13	0.96	SRPK2	0.95	DDX42	0.95
SNRPN	0.96	ZCCHC8	0.95	DHX38	0.96
XAB2	0.96	PRPF40A	0.95	POLR2J	0.96
LMNTD2	0.96	SNUPN	0.95	SNRPA1	0.96
SF3B4	0.96	THOC1	0.96	PRPF18	0.96
CELF4	0.96	THOC2	0.96	U2AF2	0.96
NAA38	0.96	SRRM2	0.96	SRSF8	0.96
SRSF3	0.97	HNRNPA2B1	0.96	ZMAT2	0.97
RBFOX1	0.97	PRPF40B	0.96	POLR2G	0.97
PPIL3	0.97	PRPF18	0.96	PPIL3	0.97
YTHDC1	0.97	AQR	0.96	ZCRB1	0.97
DHX8	0.97	PPIL3	0.97	SNRNP25	0.97
NUDT21	0.98	SRSF1	0.97	WBP4	0.97
USP4	0.98	ZRANB2	0.97	NUDT21	0.97
YBX1	0.98	SF3B2	0.97	SNU13	0.98
DDX1	0.98	NUDT21	0.97	SRSF1	0.98
GPATCH1	0.99	HSPA1B	0.97	RBFOX1	0.98
PRPF3	0.99	ELAVL1	0.98	SART3	0.98
POLR2D	0.99	TXNL4A	0.98	PRPF40B	0.98
SRSF1	0.99	GEMIN6	0.98	DHX35	0.99
CASC3	0.99	GEMIN8	0.98	RBFOX3	0.99
CELF6	1.00	ZCRB1	0.98	SRRM2	0.99
PABPC1	1.00	PCBP1	0.98	PRPF8	0.99
POLR2J	1.00	GEMIN7	0.98	YBX1	0.99

FUS	**1.00**	SF3A1	0.98	GTF2F2	0.99
PRPF38B	1.00	SRSF7	0.98	RNPC3	0.99
RAVER1	1.01	WDR83	0.99	ZRANB2	0.99
PRPF40B	1.01	RNF113A	0.99	TRA2B	1.00
PNN	1.01	AAR2	1.00	IVNS1ABP	1.00
SNRPB	1.01	RBFOX1	1.00	TRA2A	1.00
CCDC12	1.01	RBM8A	1.00	ALYREF	1.00
RNF113B	1.01	SNU13	1.00	SCAF11	1.00
DDX41	1.01	ZRSR2	1.00	RAVER2	1.00
DGCR14	1.02	HNRNPR	1.00	SNRNP70	1.01
U2AF1L4	1.02	SRRT	1.00	SNRPC	1.01
PPWD1	1.02	LUC7L2	1.00	SNRPN	1.01
CDC40	1.02	EIF4A3	1.00	WDR83	1.01
SNRNP40	1.02	RBM15	1.01	SNUPN	1.01
SRRM2	1.02	SRSF5	1.01	TFIP11	1.01
GPKOW	1.02	YBX1	1.01	GCFC2	1.02
UBL5	1.02	TXNL4B	1.01	LSM7	1.02
PPIE	1.02	SUGP1	1.01	YTHDC1	1.02
ZRANB2	1.02	NSRP1	1.01	DDX1	1.02
SNRPA1	1.02	HNRNPH2	1.01	ELAVL1	1.02
LSM6	1.03	DHX38	1.01	PPIH	1.02
HNRNPF	1.03	PPIL1	1.02	HNRNPH1	1.02
WDR83	1.03	BUD13	1.02	SRRM4	1.02
SNRPE	1.03	SNRPD3	1.03	GEMIN2	1.02
SNRPD1	1.04	LOC100996657	1.03	CWC27	1.03
SAP18	1.04	LUC7L3	1.03	STRAP	1.03
LSM1	1.04	GEMIN5	1.03	GPKOW	1.03
UPF3B	1.04	RBM17	1.03	ZNF638	1.03
NOL3	1.04	GPKOW	1.03	DGCR14	1.03
CCAR1	1.04	ZMAT2	1.04	SRPK2	1.03
DHX35	1.04	CCAR1	1.04	RNF113B	1.03
CDK13	1.05	SAP18	1.04	RAVER1	1.03
DHX9	1.05	HNRNPH3	1.04	GEMIN6	1.04
DDX23	1.05	PRPF6	1.05	TXNL4B	1.04
DDX20	1.05	DGCR14	1.05	HNRNPR	1.04
RP9	1.06	RBFOX3	1.05	DHX8	1.04
POLR2I	1.06	CD2BP2	1.05	SAP18	1.04
WBP11	1.06	SNRPE	1.05	CCAR1	1.04
PLRG1	1.06	RNF113B	1.05	SNRPE	1.04
DHX15	1.06	DDX1	1.05	SNRNP40	1.04
CD2BP2	1.06	SNRPN	1.06	PPWD1	1.05
ELAVL1	1.06	RBM5	1.06	TGS1	1.05

TXNL4B	1.06	SNRPD1	1.06	NOVA1	1.05
PHF5A	1.07	RAVER1	1.06	PCBP1	1.05
RBFOX2	1.07	YTHDC1	1.06	SNRPD1	1.05
POLR2G	1.07	SNRPG	1.06	CTNNBL1	1.05
SNUPN	1.07	SF3A2	1.06	BUD13	1.06
RNPC3	1.07	DDX42	1.07	CD2BP2	1.06
HNRNPR	1.08	WBP4	1.07	PRPF3	1.06
NFX1	1.08	SNRNP40	1.07	UBL5	1.06
FIP1L1	1.08	PRPF31	1.07	METTL14	1.06
WTAP	1.09	WTAP	1.07	PRPF39	1.06
PCBP2	1.09	PPWD1	1.08	PPIL1	1.07
BUD13	1.09	SNRNP70	1.08	SNRPB	1.07
GEMIN6	1.09	SNRNP200	1.08	PRPF4	1.07
CRNKL1	1.10	RNPS1	1.08	SNRPD3	1.07
RBM25	1.10	GCFC2	1.09	SRPK1	1.07
HNRNPA0	1.11	TRA2A	1.09	NOVA2	1.08
PPAN	1.11	LSM4	1.09	CDC40	1.08
PPIL1	1.11	USP49	1.09	HSPA2	1.08
RBM4	1.12	SNRNP25	1.10	WTAP	1.08
PCBP1	1.12	CWC15	1.10	LUC7L2	1.08
SRPK2	1.12	SNRPB2	1.10	RBM15	1.09
SNRPD3	1.12	DHX32	1.10	SRSF5	1.09
STRAP	1.13	UBL5	1.10	HSPA1L	1.10
TRA2B	1.15	DHX8	1.10	HSPA1B	1.10
HSPA8	1.15	CSTF2	1.10	PRPF38A	1.10
SNRPC	1.16	RBMX2	1.11	SUGP1	1.10
CLNS1A	1.16	WDR77	1.11	CASC3	1.11
LUC7L2	1.16	HNRNPA1	1.11	GEMIN7	1.11
USP49	1.16	HNRNPH1	1.11	DHX9	1.11
LSM8	1.16	SFSWAP	1.12	FUS	1.11
LSM4	1.16	HNRNPUL1	1.12	PRPF6	1.11
POLR2H	1.17	PPAN	1.12	RP9	1.11
RBM15	1.17	HMX2	1.12	HNRNPA0	1.12
NOVA1	1.17	HNRNPA1L2	1.12	PPAN	1.12
RAVER2	1.17	SMNDC1	1.12	PABPN1	1.12
CPSF7	1.17	HNRNPA0	1.13	HNRNPD	1.13
HNRNPA1	1.17	SNRPB	1.13	LSM4	1.13
SRSF5	1.17	U2AF2	1.13	USP49	1.13
PRPF6	1.18	PRPF3	1.13	PRPF31	1.13
TCERG1	1.18	RBM41	1.13	U2SURP	1.13
CACTIN	1.18	CELF3	1.13	U2AF1L4	1.14
DDX46	1.18	CSTF1	1.14	DDX20	1.14

DCPS	1.18	GEMIN2	1.14	HNRNPA1	1.14
LSM7	1.18	CDC40	1.14	API5	1.14
PRPF31	1.19	UHMK1	1.14	PRPF38B	1.14
HNRNPUL1	1.19	SNW1	1.14	GEMIN5	1.15
POLR2K	1.19	DDX46	1.15	PQBP1	1.15
DQX1	1.19	BCAS2	1.16	SNRPA	1.15
CSTF2	1.20	SLU7	1.16	CSTF2	1.15
SUGP1	1.20	DNAJC8	1.17	TXNL4A	1.15
MAGOH	1.20	SNRNP27	1.17	HNRNPUL1	1.15
SLU7	1.20	HSPA1A	1.17	CWC15	1.15
TIA1	1.21	SRSF11	1.17	SNRPD2	1.16
CWC15	1.21	DHX9	1.17	SRSF2	1.16
HMX2	1.21	RBMXL1	1.17	PRPF4B	1.16
HNRNPA1L2	1.21	DCPS	1.17	DHX32	1.16
SRSF8	1.22	RP9	1.17	DDX46	1.16
SCAF11	1.22	IVNS1ABP	1.17	HMX2	1.17
UHMK1	1.22	CELF2	1.18	HNRNPA1L2	1.17
HSPA2	1.23	PRPF4	1.19	RBM5	1.17
SRPK1	1.23	SETX	1.19	WDR77	1.17
HSPA1B	1.23	SYF2	1.19	LSM3	1.17
DHX32	1.23	SRSF12	1.20	PABPC1	1.18
SART1	1.23	MAGOH	1.21	DCPS	1.18
WDR77	1.23	BUD31	1.21	LSM1	1.18
HNRNPM	1.24	CPSF7	1.21	SF3A2	1.18
GEMIN7	1.24	RBM11	1.21	SLU7	1.18
MAGOHB	1.24	RSRC1	1.22	UHMK1	1.18
SART3	1.24	SRRM4	1.22	RBMY1A1	1.18
PRMT7	1.25	SF3B5	1.22	RBMX	1.19
DNAJC8	1.25	FUS	1.22	CPSF7	1.19
GEMIN5	1.26	CASC3	1.22	RBFOX2	1.19
METTL14	1.26	CTNNBL1	1.22	SNRPB2	1.20
CELF1	1.27	DDX20	1.23	LUC7L3	1.20
RSRC1	1.27	MAGOHB	1.24	MAGOH	1.20
RBM11	1.27	CSTF3	1.24	DNAJC8	1.21
RBM5	1.28	SF3B6	1.26	SMNDC1	1.21
PPIG	1.28	U2AF1L4	1.26	DDX23	1.22
CELF2	1.29	SART1	1.27	SRSF9	1.22
BCAS2	1.29	PRPF39	1.27	BCAS2	1.22
ZNF638	1.29	TGS1	1.27	RBM41	1.23
PSIP1	1.29	KHSRP	1.28	CELF2	1.23
LUC7L	1.29	U2AF1	1.28	SFSWAP	1.23
SNRPB2	1.29	NOVA2	1.28	HSPA1A	1.23

SF3A2	1.29	SNRPF	1.28	MAGOHB	1.24
SMNDC1	1.30	PRPF38B	1.29	POLR2K	1.24
PPIH	1.30	PRPF38A	1.29	PPIE	1.24
DDX5	1.30	PRMT7	1.29	RBM11	1.24
HSPA1A	1.30	POLR2K	1.29	RSRC1	1.24
GTF2F2	1.30	TFIP11	1.31	SNRPG	1.24
ALYREF	1.31	U2SURP	1.31	POLR2H	1.24
HNRNPD	1.32	LUC7L	1.31	SART1	1.25
PRPF8	1.32	LSM1	1.32	LSM5	1.25
RBM41	1.33	RBFOX2	1.32	CDK13	1.25
U2AF1	1.33	POLR2H	1.32	DDX41	1.26
TXNL4A	1.33	SYNCRIP	1.33	PRMT7	1.27
CDC5L	1.33	METTL3	1.34	SETX	1.27
HTATSF1	1.34	PABPC1	1.35	GPATCH1	1.27
SFSWAP	1.35	DQX1	1.36	DQX1	1.28
SNRPF	1.35	CDC5L	1.37	SMN1	1.28
SETX	1.35	PQBP1	1.38	POLR2I	1.29
API5	1.35	DDX23	1.38	LUC7L	1.30
LUC7L3	1.36	HNRNPK	1.38	U2AF1	1.30
HNRNPL	1.38	DDX5	1.39	SNRNP27	1.31
HSPA1L	1.38	HNRNPM	1.41	SNRPF	1.32
CWC27	1.39	LSM3	1.41	HNRNPM	1.32
SYNCRIP	1.40	PAPOLA	1.42	SYF2	1.32
PDCD7	1.41	SNRPA	1.42	SF3A1	1.33
SNRPG	1.42	CDK13	1.46	BUD31	1.33
CWC22	1.43	PPIE	1.46	DDX5	1.34
SFPQ	1.44	RBMY1A1	1.47	CDC5L	1.35
PRPF4B	1.44	PABPN1	1.48	TCERG1	1.36
BUD31	1.45	HNRNPL	1.48	CELF3	1.36
SNRNP27	1.45	CWC22	1.48	SYNCRIP	1.36
SYF2	1.45	RBMX	1.49	CRNKL1	1.37
LUC7L2	1.45	DDX41	1.50	PNN	1.38
SNRPD2	1.46	CELF1	1.51	CELF1	1.39
PAPOLA	1.52	POLR2I	1.52	CACTIN	1.41
SRSF9	1.54	SFPQ	1.53	HNRNPL	1.43
CELF3	1.59	TCERG1	1.54	SF3B5	1.43
SF3B5	1.64	GPATCH1	1.56	CWC22	1.45
SF3A1	1.67	CACTIN	1.63	PAPOLA	1.47
SRSF2	1.71	CRNKL1	1.65	SFPQ	1.49
SMN1	1.75	LUC7L2	1.70	SRSF12	1.51
SRSF12	1.82	PNN	1.74	LUC7L2	1.58
METTL3	1.91	LSM5	1.79	METTL3	1.63

Supplementary Table 12.2: Alternatively spliced events list.

Gene	Event Type	Event_ID	Difference	Direction	*p value*	FDR
HNRNPDL	SE	ENSG00000152795_HNRNPDL_4_-_ 83346715_ 83346820_ 83345781_ 83346036_ 83347189_ 83347282_0.357,0.33	-0.215	Down	8.09E-14	2.46E-09
CDKL3	SE	ENSG00000006837_CDKL3_5_-_133695587_133695782_133685939_133686118_133706688_133706732_0.0,0.143	0.928	Up	2.19E-11	3.33E-07
AFMID	SE	ENSG00000183077_AFMID_17_+_ 76201173_ 76201271_ 76200908_ 76200981_ 76201520_ 76201599_1.0,1.0	-0.948	Down	1.26E-10	1.28E-06
ENDOV	SE	ENSG00000173818_ENDOV_17_+_ 78395627_ 78395762_ 78389449_ 78389621_ 78396005_ 78396045_1.0,1.0	-0.915	Down	5.78E-10	4.40E-06
ASAH2B	SE	ENSG00000204147_ASAH2B_10_+_ 52504961_ 52505034_ 52502674_ 52502770_ 52509102_ 52509162_1.0,1.0	-0.304	Down	1.21E-09	6.32E-06
SEPT9	SE	ENSG00000184640_SEPT9_17_+_ 75447448_ 75447610_ 75446657_ 75446868_ 75478225_ 75478417_1.0,1.0	-0.863	Down	1.25E-09	6.32E-06
KCNG1	SE	ENSG00000026559_KCNG1_20_-_ 49630265_ 49630381_ 49628895_ 49628953_ 49639406_ 49639631_0.0,0.0	1	Up	1.51E-09	6.57E-06
FAM86EP	SE	ENSG00000251669_FAM86EP_4_-_ 3948870_ 3949947_ 3943486_ 3945099_ 3954837_ 3954900_1.0,1.0	-0.742	Down	2.24E-09	8.51E-06
LSM14B	SE	ENSG00000149657_LSM14B_20_+_ 60701281_ 60701495_ 60699672_ 60699836_ 60705274_ 60705352_0.283,0.164	0.776	Up	3.94E-09	1.20E-05
LIN9	SE	ENSG00000183814_LIN9_1_-_226488873_226488906_226475364_226475498_226496809_226496955_0.0,0.0	1	Up	4.36E-09	1.21E-05
TUG1	SE	ENSG00000253352_TUG1_22_+_ 31368033_ 31368158_ 31367424_ 31367765_ 31368840_ 31369342_1.0,1.0	-0.848	Down	7.47E-09	1.89E-05
KLK4	SE	ENSG00000167749_KLK4_19_-_ 51411614_ 51411751_ 51410189_ 51410342_ 51411834_ 51412085_0.784,0.737	-0.224	Down	1.58E-08	3.70E-05
SENP6	SE	ENSG00000112701_SENP6_6_+_ 76332466_ 76332574_ 76331247_ 76331341_ 76333615_ 76333676_1.0,0.931	-0.514	Down	2.12E-08	4.60E-05
C9orf3	SE	ENSG00000148120_C9orf3_9_+_ 97844856_ 97845001_ 97842975_ 97843062_ 97848963_ 97849441_1.0,1.0	-0.682	Down	2.37E-08	4.81E-05
ASAH2B	SE	ENSG00000204147_ASAH2B_10_+_ 52504887_ 52505034_ 52502674_ 52502770_ 52509102_ 52509162_1.0,1.0	-0.505	Down	2.54E-08	4.82E-05
ASAP1	SE	ENSG00000153317_ASAP1_8_-_131373915_131374017_131370262_131370389_131414130_131414216_0.148,0.178	0.512	Up	2.74E-08	4.82E-05
SENP1	SE	ENSG00000079387_SENP1_12_-_ 48460709_ 48460748_ 48459378_ 48459463_ 48465449_ 48465504_1.0,1.0	-0.209	Down	2.85E-08	4.82E-05
ATP11A	SE	ENSG00000068650_ATP11A_13_+_113532530_113532617_113530089_ 113530255_113536189_113540427_1.0,1.0	-0.692	Down	3.42E-08	5.48E-05
MTRF1	SE	ENSG00000120662_MTRF1_13_-_ 41835826_ 41835961_ 41834628_ 41835051_ 41836350_ 41836467_0.0,0.145	0.758	Up	3.97E-08	6.05E-05
WNK2	SE	ENSG00000165238_WNK2_9_+_ 96069058_ 96069103_ 96060134_ 96060349_ 96070609_ 96070866_1.0,1.0	-0.648	Down	5.96E-08	8.64E-05
TBC1D1	SE	ENSG00000065882_TBC1D1_4_+_ 38054726_ 38054846_ 38053519_ 38053681_ 38055819_ 38055959_0.0,0.0	0.818	Up	6.54E-08	9.05E-05
LEF1	SE	ENSG00000138795_LEF1_4_-_108984778_108984813_108969752_108969907_108985491_108985540_1.0,1.0	-0.635	Down	7.51E-08	9.94E-05
AP1G1	SE	ENSG00000166747_AP1G1_16_-_ 71840588_ 71840631_ 71823225_ 71823385_ 71841703_ 71842053_1.0,1.0	-0.682	Down	1.09E-07	0.000138421
SLC30A6	SE	ENSG00000152683_SLC30A6_2_+_ 32431954_ 32432002_ 32422775_ 32422895_ 32445281_ 32446809_1.0,1.0	-0.681	Down	1.28E-07	0.000155893
ZNF195	SE	ENSG00000005801_ZNF195_11_-_ 3382972_ 3383119_ 3381949_ 3382018_ 3392204_ 3392377_1.0,1.0	-0.559	Down	1.54E-07	0.000173074

IRF3	SE	ENSG00000126456_IRF3_19_-_ 50167699_ 50167930_ 50166599_ 50166771_ 50168887_ 50168962_0.0,0.0	0.715	Up	1.59E-07	0.00017 3074
OBSCN	SE	ENSG00000154358_OBSCN_1_+_228480223_228480487_228479598_22 8479862_228481053_228481317_1.0,1.0	-0.683	Down	1.97E-07	0.00020 7021
RP11-33B1.1	SE	ENSG00000245958_RP11-33B1.1_4_+_120418965_120419058_120415640_120415678_12043350 5_120433619_1.0,1.0	-0.614	Down	2.35E-07	0.00023 8111
TM2D1	SE	ENSG00000162604_TM2D1_1_-_ 62189959_ 62190097_ 62175000_ 62175109_ 62190573_ 62190785_0.601,1.0	-0.8	Down	2.66E-07	0.00023 8234
EGF	SE	ENSG00000138798_EGF_4_+_110914402_110914525_110909739_1109 09865_110915888_110916036_1.0,1.0	-0.434	Down	2.63E-07	0.00023 8234
STRADA	SE	ENSG00000266173_STRADA_17_-_ 61784606_ 61784778_ 61783994_ 61784099_ 61787850_ 61787974_1.0,1.0	-0.61	Down	2.48E-07	0.00023 8234
IQCH	SE	ENSG00000103599_IQCH_15_+_ 67687628_ 67687901_ 67681168_ 67681344_ 67692451_ 67692643_1.0,1.0	-0.832	Down	2.94E-07	0.00025 5863
ARHGEF39	SE	ENSG00000137135_ARHGEF39_9_-_ 35662942_ 35663071_ 35662508_ 35662738_ 35663318_ 35663389_0.509,0.206	0.643	Up	3.14E-07	0.00025 8403
LRRC23	SE	ENSG00000010626_LRRC23_12_+_ 7015008_ 7015118_ 7014748_ 7014923_ 7015572_ 7015826_1.0,0.936	-0.432	Down	3.12E-07	0.00025 8403
BTN2A1	SE	ENSG00000112763_BTN2A1_6_+_ 26463024_ 26463125_ 26459708_ 26460056_ 26463471_ 26463753_0.0,0.0	0.436	Up	3.42E-07	0.00027 4263
ZNF606	SE	ENSG00000166704_ZNF606_19_-_ 58511175_ 58511264_ 58499962_ 58500089_ 58512050_ 58512107_1.0,1.0	-0.536	Down	3.77E-07	0.00029 4516
LRRC23	SE	ENSG00000010626_LRRC23_12_+_ 7019053_ 7019190_ 7016478_ 7016609_ 7023054_ 7023392_1.0,1.0	-0.597	Down	4.31E-07	0.00032 8118
OSBPL5	SE	ENSG00000021762_OSBPL5_11_-_ 3141650_ 3141854_ 3140776_ 3140861_ 3143226_ 3143328_0.948,1.0	-0.235	Down	4.52E-07	0.00033 5596
EXO5	SE	ENSG00000164002_EXO5_1_+_ 40975122_ 40975297_ 40974461_ 40974580_ 40975404_ 40975462_0.228,0.181	0.713	Up	4.70E-07	0.00034 0442
SLC9A8	SE	ENSG00000197818_SLC9A8_20_+_ 48467346_ 48467381_ 48466115_ 48466217_ 48471974_ 48472118_0.545,0.4	0.477	Up	4.81E-07	0.00034 0442
RERE	SE	ENSG00000142599_RERE_1_-_ 8483226_ 8483307_ 8482786_ 8482867_ 8483620_ 8483726_1.0,1.0	-0.638	Down	5.83E-07	0.00036 9842
KANSL2	SE	ENSG00000139620_KANSL2_12_-_ 49072818_ 49073021_ 49065581_ 49065745_ 49073437_ 49073616_1.0,0.946	-0.272	Down	5.81E-07	0.00036 9842
RSRC2	SE	ENSG00000111011_RSRC2_12_-_123005050_123005128_123003386_123003598_123005931_1230059 75_1.0,1.0	-0.323	Down	5.73E-07	0.00036 9842
NEK7	SE	ENSG00000151414_NEK7_1_+_198233254_198233365_198222169_198 222310_198288541_198291550_0.0,0.357	0.822	Up	5.66E-07	0.00036 9842
EGF	SE	ENSG00000138798_EGF_4_+_110929307_110929386_110925660_1109 25778_110932357_110932657_1.0,1.0	-0.581	Down	7.03E-07	0.00043 6897
L3MBTL3	SE	ENSG00000198945_L3MBTL3_6_+_130370900_130370975_130370426_ 130370538_130372393_130372553_1.0,1.0	-0.621	Down	7.18E-07	0.00043 7363
RP11-345J4.5	SE	ENSG00000261740_RP11-345J4.5_16_-_ 29461432_ 29461597_ 29458122_ 29458347_ 29463429_ 29465434_1.0,1.0	-0.907	Down	7.77E-07	0.00046 3441
SGSM2	SE	ENSG00000141258_SGSM2_17_+_ 2270564_ 2270699_ 2268508_ 2268635_ 2274555_ 2274709_0.0,0.0	0.498	Up	8.36E-07	0.00048 9407
ARHGAP44	SE	ENSG00000006740_ARHGAP44_17_+_ 12832245_ 12832363_ 12823071_ 12823148_ 12844372_ 12844441_1.0,1.0	-0.299	Down	8.61E-07	0.00049 4221
PPM1M	SE	ENSG00000164088_PPM1M_3_+_ 52280989_ 52281244_ 52280710_ 52280828_ 52281697_ 52281810_1.0,1.0	-0.55	Down	9.21E-07	0.00051 8866
TM9SF4	SE	ENSG00000101337_TM9SF4_20_+_ 30724679_ 30724800_ 30723876_ 30723976_ 30729343_ 30729468_0.0,0.0	0.674	Up	9.69E-07	0.00053 6238
PRKD2	SE	ENSG00000105287_PRKD2_19_-_ 47217119_ 47217258_ 47214163_ 47214295_ 47219387_ 47219853_1.0,1.0	-0.23	Down	1.01E-06	0.00055 0578
SPRED2	SE	ENSG00000198369_SPRED2_2_-_ 65561248_ 65561399_ 65559337_ 65559434_ 65561738_ 65561907_1.0,1.0	-0.838	Down	1.03E-06	0.00055 1286

GAB1	SE	ENSG00000109458_GAB1_4_+_144355240_144355321_144354643_144354869_144359151_144359194_1.0,1.0	-0.504	Down	1.09E-06	0.000573637
SLC4A7	SE	ENSG00000033867_SLC4A7_3_-_ 27472788_ 27473160_ 27465527_ 27465643_ 27475445_ 27475595_1.0,1.0	-0.666	Down	1.15E-06	0.000593085
ELL3	SE	ENSG00000128886_ELL3_15_-_ 44068236_ 44068349_ 44067919_ 44068121_ 44068706_ 44068770_1.0,1.0	-0.231	Down	1.22E-06	0.00059879
LEF1	SE	ENSG00000138795_LEF1_4_-_108984778_108984819_108968747_108969907_108985491_108985540_1.0,1.0	-0.367	Down	1.19E-06	0.00059879
DNASE1L1	SE	ENSG00000013563_DNASE1L1_X_-_153637447_153637532_153633774_153633996_153640227_153640449_1.0,1.0	-0.408	Down	1.21E-06	0.00059879
PRR3	SE	ENSG00000204576_PRR3_6_+_ 30529104_ 30529285_ 30525090_ 30525227_ 30529610_ 30529901_1.0,1.0	-0.553	Down	1.30E-06	0.000626831
HMGN1	SE	ENSG00000205581_HMGN1_21_-_ 40719304_ 40719409_ 40717755_ 40717884_ 40720217_ 40720265_1.0,1.0	-0.453	Down	1.69E-06	0.000802598
NPHP3	SE	ENSG00000113971_NPHP3_3_-_132415574_132415657_132413670_132413809_132416103_132416206_1.0,1.0	-0.393	Down	1.73E-06	0.000810121
CEP57L1	SE	ENSG00000183137_CEP57L1_6_+_109450506_109450695_109416764_109416778_109466421_109466584_0.0,0.0	0.687	Up	1.92E-06	0.000886673
TXN	SE	ENSG00000136810_TXN_9_-_113013099_113013159_113007057_113007123_113018691_113018920_1.0,1.0	-0.292	Down	1.98E-06	0.000899626
PHYKPL	SE	ENSG00000175309_PHYKPL_5_-_177639973_177640104_177638890_177638971_177641796_177641886_1.0,1.0	-0.494	Down	2.07E-06	0.00092518
PCNT	SE	ENSG00000160299_PCNT_21_+_ 47864606_ 47864734_ 47862409_ 47862486_ 47865196_ 47865682_1.0,1.0	-0.436	Down	2.26E-06	0.000935172
ANKMY1	SE	ENSG00000144504_ANKMY1_2_-_241468453_241468926_241465220_241465266_241492330_241492474_1.0,1.0	-0.419	Down	2.15E-06	0.000935172
DET1	SE	ENSG00000140543_DET1_15_-_ 89079542_ 89079612_ 89073853_ 89074946_ 89089770_ 89089884_0.399,0.857	-0.59	Down	2.20E-06	0.000935172
NAPB	SE	ENSG00000125814_NAPB_20_-_ 23377708_ 23377825_ 23375775_ 23375822_ 23383629_ 23383709_1.0,1.0	-0.526	Down	2.27E-06	0.000935172
C11orf65	SE	ENSG00000166323_C11orf65_11_-_108302472_108302565_108277822_108277876_108332205_108332296_1.0,1.0	-0.884	Down	2.38E-06	0.000966526
FAM47E-STBD1	SE	ENSG00000272414_FAM47E-STBD1_4_+_ 77177330_ 77177676_ 77172873_ 77172973_ 77184856_ 77184996_1.0,1.0	-0.536	Down	2.56E-06	0.001025585
CLHC1	SE	ENSG00000162994_CLHC1_2_-_ 55436539_ 55436652_ 55433405_ 55433512_ 55436765_ 55436967_1.0,1.0	-0.488	Down	2.63E-06	0.001036438
WDR31	SE	ENSG00000148225_WDR31_9_-_116093263_116093396_116091160_116091235_116094186_116094330_1.0,1.0	-0.448	Down	2.66E-06	0.001036438
ZNF562	SE	ENSG00000171466_ZNF562_19_-_ 9771395_ 9771550_ 9762954_ 9764557_ 9785690_ 9785720_1.0,1.0	-0.29	Down	2.70E-06	0.001039174
XIAP	SE	ENSG00000101966_XIAP_X_+_122994016_122994143_122993676_122993755_123019480_123019561_1.0,1.0	-0.475	Down	2.88E-06	0.001080496
PACRGL	SE	ENSG00000163138_PACRGL_4_+_ 20711305_ 20711396_ 20709425_ 20709493_ 20714410_ 20714545_1.0,1.0	-0.254	Down	2.87E-06	0.001080496
ZNF749	SE	ENSG00000186230_ZNF749_19_+_ 57953252_ 57953379_ 57946696_ 57946961_ 57954658_ 57956853_1.0,1.0	-0.506	Down	2.93E-06	0.001086609
CCDC15	SE	ENSG00000149548_CCDC15_11_+_124863064_124863139_124857022_124858030_124873762_124873855_1.0,1.0	-0.407	Down	3.45E-06	0.001246777
MLPH	SE	ENSG00000115648_MLPH_2_+_238449444_238449600_238448990_238449176_238451209_238451302_1.0,1.0	-0.45	Down	3.42E-06	0.001246777
FAM173A	SE	ENSG00000103254_FAM173A_16_+_ 772083_ 772134_ 771800_ 771941_ 772308_ 772601_1.0,1.0	-0.27	Down	3.55E-06	0.001255201

TM2D3	SE	ENSG00000184277_TM2D3_15_-_102191898_102191976_102190206_102190364_102192473_102192587_0.505,0.425	0.215	Up	3.62E-06	0.001261919
NLE1	SE	ENSG00000073536_NLE1_17_-_33461961_33462078_33460357_33460517_33462267_33462470_0.318,0.194	-0.245	Down	3.91E-06	0.001314512
IRAK4	SE	ENSG00000198001_IRAK4_12_+_44154727_44154775_44152752_44152819_44161905_44162075_1.0,1.0	-0.469	Down	3.90E-06	0.001314512
CDK20	SE	ENSG00000156345_CDK20_9_-_90585482_90585545_90584710_90584834_90585690_90585812_1.0,1.0	-0.429	Down	3.93E-06	0.001314512
PGC	SE	ENSG00000096088_PGC_6_-_41712134_41712252_41710027_41710227_41712395_41712546_1.0,1.0	-0.359	Down	4.11E-06	0.001342644
POLK	SE	ENSG00000122008_POLK_5_+_74889790_74889874_74886168_74886265_74892046_74893003_1.0,1.0	-0.344	Down	4.13E-06	0.001342644
FBXL6	SE	ENSG00000182325_FBXL6_8_-_145581116_145581162_145580649_145580781_145581287_145581446_1.0,1.0	-0.397	Down	4.15E-06	0.001342644
IKBKG	SE	ENSG00000073009_IKBKG_X_+_153770496_153770667_153769469_153769606_153780202_153780404_1.0,1.0	-0.545	Down	4.22E-06	0.001351502
LIMCH1	SE	ENSG00000064042_LIMCH1_4_+_41628724_41629027_41621204_41621457_41631508_41631751_1.0,1.0	-0.482	Down	4.40E-06	0.001380771
CMC2	SE	ENSG00000103121_CMC2_16_-_81034852_81034939_81009899_81010076_81040338_81040463_0.381,0.381	0.619	Up	4.47E-06	0.001388397
PHF3	SE	ENSG00000118482_PHF3_6_+_64389900_64390062_64356431_64356700_64401626_64401933_0.447,0.852	0.351	Up	4.62E-06	0.001404799
SNAP47	SE	ENSG00000143740_SNAP47_1_+_227919285_227919448_227916239_227916487_227946695_227947186_1.0,1.0	-0.383	Down	4.58E-06	0.001404799
SLC2A8	SE	ENSG00000136856_SLC2A8_9_+_130164835_130165032_130162185_130162285_130166016_130166070_1.0,0.897	-0.572	Down	4.80E-06	0.001415309
MAPK7	SE	ENSG00000166484_MAPK7_17_+_19283796_19283814_19283094_19283260_19283920_19283936_0.0,0.0	0.206	Up	4.84E-06	0.001415309
CHCHD4	SE	ENSG00000163528_CHCHD4_3_-_14163416_14163586_14160644_14160813_14166154_14166370_1.0,1.0	-0.443	Down	4.81E-06	0.001415309
PHF3	SE	ENSG00000118482_PHF3_6_+_64394029_64395812_64356523_64356700_64401626_64401933_0.591,0.931	0.239	Up	5.32E-06	0.001543276
RBCK1	SE	ENSG00000125826_RBCK1_20_+_401514_401650_400201_400375_402770_402882_1.0,1.0	-0.642	Down	5.50E-06	0.001570813
TAPBP	SE	ENSG00000231925_TAPBP_6_-_33271904_33271994_33267470_33269548_33272073_33272415_0.684,0.655	0.284	Up	5.52E-06	0.001570813
MYO6	SE	ENSG00000196586_MYO6_6_+_76604947_76604977_76602246_76602407_76608089_76608128_1.0,1.0	-0.341	Down	5.60E-06	0.001579339
EXTL2	SE	ENSG00000162694_EXTL2_1_-_101343949_101344003_101343074_101343459_101354308_101354420_0.0,0.0	0.365	Up	5.87E-06	0.001592701
PEX11A	SE	ENSG00000166821_PEX11A_15_-_90229661_90229777_90224761_90227179_90233807_90233893_1.0,1.0	-0.373	Down	5.77E-06	0.001592701
LIMCH1	SE	ENSG00000064042_LIMCH1_4_+_41553141_41553208_41526425_41526495_41553337_41553412_1.0,0.825	-0.51	Down	5.91E-06	0.001592701
HERC2P3	SE	ENSG00000180229_HERC2P3_15_-_20657620_20657812_20651111_20651299_20658603_20658755_1.0,1.0	-0.397	Down	5.89E-06	0.001592701
IRF3	SE	ENSG00000126456_IRF3_19_-_50163969_50164085_50162831_50163090_50165204_50165585_1.0,1.0	-0.306	Down	5.87E-06	0.001592701
DZANK1	SE	ENSG00000089091_DZANK1_20_-_18440796_18440950_18435890_18436005_18445893_18446096_0.856,0.655	0.244	Up	6.09E-06	0.001612226
PPP2R3C	SE	ENSG00000092020_PPP2R3C_14_-_35560275_35560413_35557156_35557216_35565763_35565839_0.778,0.656	0.283	Up	6.28E-06	0.001634799
FHOD3	SE	ENSG00000134775_FHOD3_18_+_34238037_34238151_34205473_34205712_34261398_34261533_0.0,0.452	0.774	Up	6.28E-06	0.001634799
TMEM53	SE	ENSG00000126106_TMEM53_1_-_45120611_45120881_45111031_45111136_45125845_45125967_0.826,0.421	0.377	Up	6.63E-06	0.001709246
IRF3	SE	ENSG00000126456_IRF3_19_-_50163969_50164101_50162825_50163090_50165204_50165585_1.0,1.0	-0.387	Down	6.69E-06	0.0017119

TYSND1	SE	ENSG00000156521_TYSND1_10_-_ 71903597_ 71903728_ 71897736_ 71899897_ 71906288_ 71906432_1.0,1.0	-0.401	Down	7.13E-06	0.00180 9331
SCRN3	SE	ENSG00000144306_SCRN3_2_+_175262063_175262132_175260522_17 5261021_175263002_175263170_0.0,0.0	0.549	Up	7.32E-06	0.00182 5079
FOXM1	SE	ENSG00000111206_FOXM1_12_-_ 2974520_ 2974565_ 2973848_ 2973918_ 2975558_ 2975687_0.734,0.883	-0.235	Down	7.55E-06	0.00186 9343
BRCA2	SE	ENSG00000139618_BRCA2_13_+_ 32918694_ 32918790_ 32910401_ 32915333_ 32920963_ 32921033_1.0,1.0	-0.278	Down	8.68E-06	0.00196 1193
DIP2A	SE	ENSG00000160305_DIP2A_21_+_ 47924273_ 47924402_ 47918494_ 47918746_ 47929169_ 47929289_0.757,0.509	0.334	Up	8.05E-06	0.00196 1193
ZNF562	SE	ENSG00000171466_ZNF562_19_-_ 9768684_ 9768811_ 9764383_ 9764557_ 9785690_ 9785776_1.0,1.0	-0.343	Down	8.61E-06	0.00196 1193
DOPEY1	SE	ENSG00000083097_DOPEY1_6_+_ 83863612_ 83863762_ 83863229_ 83863339_ 83863898_ 83863960_1.0,1.0	-0.315	Down	8.22E-06	0.00196 1193
ZHX3	SE	ENSG00000174306_ZHX3_20_-_ 39842373_ 39842539_ 39830696_ 39833706_ 39867327_ 39867436_1.0,1.0	-0.331	Down	8.68E-06	0.00196 1193
NCOA1	SE	ENSG00000084676_NCOA1_2_+_ 24778883_ 24778924_ 24777257_ 24777442_ 24787163_ 24787299_1.0,1.0	-0.385	Down	8.58E-06	0.00196 1193
ZBTB8OS	SE	ENSG00000176261_ZBTB8OS_1_-_ 33100368_ 33100393_ 33093108_ 33093145_ 33116033_ 33116161_1.0,1.0	-0.59	Down	8.79E-06	0.00196 7431
MRRF	SE	ENSG00000148187_MRRF_9_+_125048058_125048225_125047447_12 5047566_125048317_125048445_1.0,1.0	-0.492	Down	9.00E-06	0.00199 8662
IGFLR1	SE	ENSG00000126246_IGFLR1_19_-_ 36230610_ 36230670_ 36230115_ 36230527_ 36231924_ 36232124_1.0,1.0	-0.561	Down	9.10E-06	0.00200 6716
GBA	SE	ENSG00000177628_GBA_1_-_155210876_155210971_155209676_155209868_155213885_155214021_0.675,0.165	0.58	Up	9.61E-06	0.00210 3876
HIST1H2BJ	SE	ENSG00000124635_HIST1H2BJ_6_-_ 27095042_ 27095180_ 27094057_ 27094241_ 27100145_ 27100541_0.601,1.0	-0.729	Down	1.01E-05	0.00218 4489
TTN-AS1	SE	ENSG00000237298_TTN-AS1_2_+_179396040_179396305_179388178_179388363_179400458_ 179400555_1.0,1.0	-0.483	Down	1.02E-05	0.00218 8894
DIP2A	SE	ENSG00000160305_DIP2A_21_+_ 47924270_ 47924402_ 47918494_ 47918746_ 47929169_ 47929289_0.642,0.278	0.47	Up	1.07E-05	0.00226 127
CCDC43	SE	ENSG00000180329_CCDC43_17_-_ 42757952_ 42758020_ 42754850_ 42756411_ 42759370_ 42759506_1.0,1.0	-0.256	Down	1.10E-05	0.00230 2079
DPY19L2P1	SE	ENSG00000189212_DPY19L2P1_7_-_ 35187402_ 35187494_ 35184602_ 35184702_ 35189699_ 35189886_1.0,1.0	-0.432	Down	1.10E-05	0.00230 2079
WASF1	SE	ENSG00000112290_WASF1_6_-_110481837_110481935_110448671_110448832_110499800_110499945_0.328,0.207	0.51	Up	1.12E-05	0.00232 8363
MKS1	SE	ENSG00000011143_MKS1_17_-_ 56292101_ 56292259_ 56291619_ 56291748_ 56293448_ 56293604_1.0,1.0	-0.44	Down	1.17E-05	0.00240 8956
PXDN	SE	ENSG00000130508_PXDN_2_-_ 1691403_ 1691475_ 1687851_ 1687923_ 1695699_ 1695771_1.0,1.0	-0.535	Down	1.19E-05	0.00243 9756
PKIG	SE	ENSG00000168734_PKIG_20_+_ 43211225_ 43211372_ 43160425_ 43160619_ 43218437_ 43218507_0.139,0.042	0.369	Up	1.21E-05	0.00245 9117
HDX	SE	ENSG00000165259_HDX_X_-_ 83695539_ 83695593_ 83616473_ 83616620_ 83723479_ 83724583_1.0,1.0	-0.353	Down	1.27E-05	0.00255 6433
PMF1	SE	ENSG00000160783_PMF1_1_+_156195347_156195459_156182816_156182967_156203418_156203519_1.0,1.0	-0.514	Down	1.35E-05	0.00270 6326
ARHGAP12	SE	ENSG00000165322_ARHGAP12_10_-_ 32128232_ 32128247_ 32120666_ 32120728_ 32128564_ 32128639_1.0,1.0	-0.37	Down	1.40E-05	0.00274 0311
C8orf44	SE	ENSG00000213865_C8orf44_8_+_ 67588979_ 67589137_ 67579886_ 67579936_ 67589876_ 67590189_1.0,1.0	-0.532	Down	1.39E-05	0.00274 0311
MAPKBP1	SE	ENSG00000137802_MAPKBP1_15_+_ 42107456_ 42107603_ 42106747_ 42106937_ 42107821_ 42107997_1.0,1.0	-0.317	Down	1.43E-05	0.00279 1375

ANKMY2	SE	ENSG00000106524_ANKMY2_7_-_ 16664607_ 16664706_ 16655368_ 16655529_ 16666664_ 16666803_1.0,1.0	-0.284	Down	1.46E-05	0.00281 9764
PRPF39	SE	ENSG00000185246_PRPF39_14_+_ 45565626_ 45565695_ 45565305_ 45565431_ 45565798_ 45565961_0.401,0.0	0.728	Up	1.46E-05	0.00281 9764
HERC2P3	SE	ENSG00000180229_HERC2P3_15_-_ 20657620_ 20657841_ 20651111_ 20651299_ 20658603_ 20658755_1.0,1.0	-0.355	Down	1.52E-05	0.00284 181
TOP1MT	SE	ENSG00000184428_TOP1MT_8_-_144414656_144414771_144413393_144413509_144416909_144417024_0.523,0.354	-0.421	Down	1.51E-05	0.00284 181
METTL23	SE	ENSG00000181038_METTL23_17_+_ 74723051_ 74723295_ 74722924_ 74722961_ 74725771_ 74725876_1.0,1.0	-0.469	Down	1.51E-05	0.00284 181
FAM195A	SE	ENSG00000172366_FAM195A_16_+_ 692119_ 692249_ 691928_ 692043_ 696471_ 696608_0.0,0.0	0.397	Up	1.49E-05	0.00284 181
BDP1	SE	ENSG00000145734_BDP1_5_+_ 70858601_ 70858722_ 70858100_ 70858347_ 70860580_ 70863647_1.0,0.874	-0.475	Down	1.59E-05	0.00289 5937
GGA3	SE	ENSG00000125447_GGA3_17_-_ 73244920_ 73245089_ 73242792_ 73242877_ 73257628_ 73257681_0.474,1.0	-0.737	Down	1.67E-05	0.00297 9525
PRIMPOL	SE	ENSG00000164306_PRIMPOL_4_+_185606565_185606652_185603401_185603490_185606729_185606838_1.0,1.0	-0.262	Down	1.67E-05	0.00297 9525
TTLL11	SE	ENSG00000175764_TTLL11_9_-_124622615_124622722_124584249_124585158_124632775_124633027_0.531,0.0	0.734	Up	1.71E-05	0.00297 9525
MAP2K5	SE	ENSG00000137764_MAP2K5_15_+_ 68020253_ 68020283_ 67995674_ 67995746_ 68040568_ 68040595_1.0,1.0	-0.408	Down	1.70E-05	0.00297 9525
C5orf45	SE	ENSG00000161010_C5orf45_5_-_179267871_179267959_179264275_179264885_179268906_179269064_1.0,1.0	-0.292	Down	1.75E-05	0.00297 9829
KLHDC10	SE	ENSG00000128607_KLHDC10_7_+_129736760_129736847_129710349_129710649_129756284_129756506_0.822,0.661	-0.46	Down	1.75E-05	0.00297 9829
FER	SE	ENSG00000151422_FER_5_+_108103793_108103939_108083522_108083701_108133824_108134090_0.328,0.573	0.489	Up	1.74E-05	0.00297 9829
C3orf18	SE	ENSG00000088543_C3orf18_3_-_ 50602896_ 50603292_ 50599152_ 50599178_ 50604893_ 50605111_0.409,0.7	0.446	Up	1.78E-05	0.00298 82
GPR98	SE	ENSG00000164199_GPR98_5_+_ 89975365_ 89975446_ 89971896_ 89972026_ 89977131_ 89977271_0.0,0.387	0.806	Up	1.85E-05	0.00303 7486
ZNF827	SE	ENSG00000151612_ZNF827_4_-_146684241_146684274_146678778_146682750_146686130_146686317_1.0,1.0	-0.44	Down	1.88E-05	0.00305 5257
LPCAT4	SE	ENSG00000176454_LPCAT4_15_-_ 34653600_ 34653733_ 34651789_ 34652410_ 34654396_ 34654522_1.0,1.0	-0.379	Down	1.92E-05	0.00311 0787
DCLRE1C	SE	ENSG00000152457_DCLRE1C_10_-_ 14978536_ 14978592_ 14977461_ 14977563_ 14981808_ 14981868_1.0,1.0	-0.368	Down	1.96E-05	0.00316 014
GAA	SE	ENSG00000171298_GAA_17_+_ 78075609_ 78075689_ 78075392_ 78075424_ 78078353_ 78078931_0.323,0.805	0.436	Up	2.01E-05	0.00321 2655
WASF3	SE	ENSG00000132970_WASF3_13_+_ 27254171_ 27254338_ 27246008_ 27246126_ 27255190_ 27255457_1.0,1.0	-0.399	Down	2.03E-05	0.00322 606
SDR39U1	SE	ENSG00000100445_SDR39U1_14_-_ 24910879_ 24911001_ 24910059_ 24910132_ 24911383_ 24911472_1.0,0.914	-0.341	Down	2.18E-05	0.00342 3667
ST7-OT4	SE	ENSG00000214188_ST7-OT4_7_+_116595027_116595207_116594673_116594733_116738666_116738860_1.0,1.0	-0.385	Down	2.21E-05	0.00344 2977
WDR62	SE	ENSG00000075702_WDR62_19_+_ 36592565_ 36592676_ 36592115_ 36592219_ 36592915_ 36593053_1.0,1.0	-0.265	Down	2.22E-05	0.00344 6302
SAC3D1	SE	ENSG00000168061_SAC3D1_11_+_ 64808757_ 64809338_ 64808372_ 64808578_ 64811696_ 64812271_1.0,1.0	-0.385	Down	2.23E-05	0.00344 6302
SNX10	SE	ENSG00000086300_SNX10_7_+_ 26396626_ 26396747_ 26393676_ 26393804_ 26400594_ 26400651_1.0,1.0	-0.464	Down	2.31E-05	0.00353 2612
ALDOA	SE	ENSG00000149925_ALDOA_16_+_ 30066104_ 30066248_ 30064784_ 30064820_ 30075049_ 30075359_0.0,0.329	0.739	Up	2.35E-05	0.00357 1281

PAQR3	SE	ENSG00000163291_PAQR3_4_-_ 79843982_ 79844137_ 79843294_ 79843575_ 79845010_ 79845101_0.486,0.24	-0.363	Down	2.45E-05	0.00367 0417
EXO5	SE	ENSG00000164002_EXO5_1_+_ 40975122_ 40975297_ 40974461_ 40974580_ 40980186_ 40980518_0.069,0.0	0.514	Up	2.50E-05	0.00373 343
MAP2	SE	ENSG00000078018_MAP2_2_+_210561265_210561472_210561037_21 0561074_210565000_210565062_1.0,0.0	0.5	Up	2.57E-05	0.00377 7263
CAMTA1	SE	ENSG00000171735_CAMTA1_1_+_ 6867042_ 6867148_ 6845577_ 6845635_ 6931816_ 6932079_0.221,0.63	-0.425	Down	2.56E-05	0.00377 7263
GOLGA2	SE	ENSG00000167110_GOLGA2_9_-_131035063_131035144_131030698_131030803_131036128_131036132_0.136,0.0	0.283	Up	2.61E-05	0.00381 2847
PIGO	SE	ENSG00000165282_PIGO_9_-_ 35096151_ 35096477_ 35095140_ 35095563_ 35096557_ 35096591_0.0,0.0	0.439	Up	2.65E-05	0.00385 4043
MKS1	SE	ENSG00000011143_MKS1_17_-_ 56292101_ 56292199_ 56291619_ 56291748_ 56293448_ 56293604_1.0,1.0	-0.223	Down	2.77E-05	0.00401 1108
KIAA1191	SE	ENSG00000122203_KIAA1191_5_-_175786483_175786570_175775252_175775359_175788604_175788764_1.0,1.0	-0.448	Down	3.00E-05	0.00430 5117
OGG1	SE	ENSG00000114026_OGG1_3_+_ 9796387_ 9796569_ 9793453_ 9793633_ 9807492_ 9808352_1.0,1.0	-0.346	Down	3.02E-05	0.00431 1637
SLC37A3	SE	ENSG00000157800_SLC37A3_7_-_140043211_140043363_140037083_140037149_140045668_140045770_0.866,0.679	0.213	Up	3.04E-05	0.00432 1165
B4GALNT4	SE	ENSG00000182272_B4GALNT4_11_+_ 380670_ 380951_ 380291_ 380445_ 381668_ 382109_1.0,1.0	-0.339	Down	3.34E-05	0.00468 654
PRKRIP1	SE	ENSG00000128563_PRKRIP1_7_+_102036423_102036984_102016658_102016769_102039994_102040095_1.0,1.0	-0.365	Down	3.34E-05	0.00468 654
ECHDC2	SE	ENSG00000121310_ECHDC2_1_-_ 53363108_ 53363156_ 53362074_ 53362269_ 53364845_ 53364896_1.0,0.748	-0.622	Down	3.36E-05	0.00468 7121
ZNF445	SE	ENSG00000185219_ZNF445_3_-_ 44492805_ 44492974_ 44492359_ 44492454_ 44496612_ 44497188_1.0,1.0	-0.324	Down	3.43E-05	0.00477 092
SDR39U1	SE	ENSG00000100445_SDR39U1_14_-_ 24910883_ 24911001_ 24909988_ 24910132_ 24911383_ 24911466_1.0,0.856	-0.604	Down	3.49E-05	0.00480 252
DLGAP4	SE	ENSG00000080845_DLGAP4_20_+_ 35093667_ 35093770_ 35089870_ 35089913_ 35125107_ 35125469_1.0,0.277	-0.639	Down	3.53E-05	0.00482 0402
SLC43A1	SE	ENSG00000149150_SLC43A1_11_-_ 57259063_ 57259099_ 57256723_ 57256865_ 57259188_ 57259335_1.0,1.0	-0.309	Down	3.59E-05	0.00486 0079
AFMID	SE	ENSG00000183077_AFMID_17_+_ 76198783_ 76198832_ 76187050_ 76187141_ 76202026_ 76202131_1.0,1.0	-0.263	Down	3.63E-05	0.00486 6172
P4HTM	SE	ENSG00000178467_P4HTM_3_+_ 49041530_ 49041693_ 49039932_ 49040029_ 49044119_ 49044548_1.0,1.0	-0.317	Down	3.63E-05	0.00486 6172
CCDC171	SE	ENSG00000164989_CCDC171_9_+_ 15594038_ 15594170_ 15591363_ 15591554_ 15623264_ 15623411_1.0,1.0	-0.352	Down	3.65E-05	0.00486 6172
CEP57L1	SE	ENSG00000183137_CEP57L1_6_+_109476993_109477080_109476432_109476510_109480227_109480305_1.0,1.0	-0.313	Down	3.74E-05	0.00492 2974
AKAP13	SE	ENSG00000170776_AKAP13_15_+_ 86205618_ 86205684_ 86201767_ 86201821_ 86207793_ 86207986_0.576,0.629	-0.511	Down	3.72E-05	0.00492 2974
MPDZ	SE	ENSG00000107186_MPDZ_9_-_ 13143464_ 13143563_ 13139985_ 13140148_ 13147546_ 13147657_0.0,0.0	0.433	Up	3.79E-05	0.00493 1231
PXN	SE	ENSG00000089159_PXN_12_-_120653362_120653464_120652905_120653220_120659425_120659561_0.026,0.1	0.203	Up	3.83E-05	0.00495 7991
C4orf36	SE	ENSG00000163633_C4orf36_4_-_ 87853373_ 87853471_ 87847018_ 87847478_ 87854546_ 87854694_0.128,0.24	0.652	Up	3.95E-05	0.00503 7121
MYO5A	SE	ENSG00000197535_MYO5A_15_-_ 52641014_ 52641023_ 52638557_ 52638658_ 52643450_ 52643678_0.0,0.0	0.511	Up	3.92E-05	0.00503 7121
TPCN1	SE	ENSG00000186815_TPCN1_12_+_113663048_113663141_113659264_113659431_113664532_113664769_1.0,0.857	-0.519	Down	3.94E-05	0.00503 7121
SCYL3	SE	ENSG00000000457_SCYL3_1_-_169828181_169828353_169824936_169825098_169831753_169831938_0.668,0.691	0.321	Up	3.96E-05	0.00503 7121

IFT122	SE	ENSG00000163913_IFT122_3_+_129183477_129183624_129182402_129182469_129188184_129188260_1.0,1.0	-0.246	Down	4.16E-05	0.005215034
COBL	SE	ENSG00000106078_COBL_7_-_ 51240152_ 51240227_ 51203854_ 51204028_ 51251798_ 51251896_0.0,0.115	0.323	Up	4.15E-05	0.005215034
SFMBT1	SE	ENSG00000163935_SFMBT1_3_-_ 53077151_ 53077270_ 53003116_ 53003274_ 53080475_ 53080766_0.0,0.212	0.789	Up	4.34E-05	0.005416535
GORAB	SE	ENSG00000120370_GORAB_1_+_170505450_170505562_170502604_170502792_170508350_170508708_0.0,0.0	0.609	Up	4.74E-05	0.005782946
TACC2	SE	ENSG00000138162_TACC2_10_+_123892123_123892249_123872553_123872748_123954554_123954691_1.0,1.0	-0.299	Down	4.75E-05	0.005782946
IL15RA	SE	ENSG00000134470_IL15RA_10_-_ 6005705_ 6005804_ 6002329_ 6002530_ 6008107_ 6008302_0.0,0.0	0.347	Up	4.81E-05	0.005831693
KIF9	SE	ENSG00000088727_KIF9_3_-_ 47284540_ 47284735_ 47282290_ 47282505_ 47286280_ 47286414_1.0,1.0	-0.432	Down	4.86E-05	0.005852162
GGCT	SE	ENSG00000006625_GGCT_7_-_ 30537356_ 30537512_ 30536592_ 30536851_ 30540151_ 30540297_0.0,0.0	0.216	Up	5.18E-05	0.006156068
PNISR	SE	ENSG00000132424_PNISR_6_-_ 99851704_ 99851758_ 99850415_ 99850586_ 99852478_ 99852578_1.0,1.0	-0.248	Down	5.23E-05	0.006196658
DDX55	SE	ENSG00000111364_DDX55_12_+_124090477_124090706_124086645_124086803_124092146_124092209_0.274,0.159	0.61	Up	5.46E-05	0.006411152
ZNF786	SE	ENSG00000197362_ZNF786_7_-_148777682_148777809_148771477_148771630_148787714_148787797_1.0,1.0	-0.27	Down	5.62E-05	0.006578308
SLC37A3	SE	ENSG00000157800_SLC37A3_7_-_140045015_140045063_140037083_140037149_140045668_140045770_0.69,0.489	0.351	Up	5.69E-05	0.006593748
BANP	SE	ENSG00000172530_BANP_16_+_ 88008653_ 88008809_ 87985039_ 87985121_ 88014641_ 88014733_1.0,1.0	-0.244	Down	5.70E-05	0.006593748
TEAD2	SE	ENSG00000074219_TEAD2_19_-_ 49859215_ 49859227_ 49858568_ 49858676_ 49860508_ 49860571_0.0,0.093	0.517	Up	5.73E-05	0.006608745
OCIAD1	SE	ENSG00000109180_OCIAD1_4_+_ 48833243_ 48833266_ 48833079_ 48833158_ 48834636_ 48834699_0.0,0.3	0.737	Up	5.80E-05	0.006640329
AHI1	SE	ENSG00000135541_AHI1_6_-_135818325_135818387_135813365_135813429_135818720_135818903_0.257,0.862	0.441	Up	5.80E-05	0.006640329
ZNF845	SE	ENSG00000213799_ZNF845_19_+_ 53844076_ 53844178_ 53837001_ 53837045_ 53844487_ 53844575_0.224,0.0	0.384	Up	5.92E-05	0.006749472
WNK2	SE	ENSG00000165238_WNK2_9_+_ 96061351_ 96061543_ 96060134_ 96060349_ 96070609_ 96070866_1.0,1.0	-0.279	Down	6.00E-05	0.006818770
TGFBR2	SE	ENSG00000163513_TGFBR2_3_+_ 30664690_ 30664765_ 30648092_ 30648469_ 30686238_ 30686407_0.661,1.0	-0.49	Down	6.07E-05	0.006869797
DYX1C1	SE	ENSG00000256061_DYX1C1_15_-_ 55724694_ 55724800_ 55722505_ 55722977_ 55727102_ 55727256_0.0,0.63	0.585	Up	6.21E-05	0.006996571
CENPK	SE	ENSG00000123219_CENPK_5_-_ 64850623_ 64850725_ 64848319_ 64848376_ 64857289_ 64857391_0.555,0.852	0.265	Up	6.27E-05	0.007046394
PIGO	SE	ENSG00000165282_PIGO_9_-_ 35095875_ 35095973_ 35095051_ 35095563_ 35096151_ 35096217_1.0,1.0	-0.394	Down	6.46E-05	0.007174123
ZC3HC1	SE	ENSG00000091732_ZC3HC1_7_-_129688813_129688984_129679303_129679387_129691060_129691209_0.711,0.593	0.327	Up	6.67E-05	0.007278945
TMEM25	SE	ENSG00000149582_TMEM25_11_+_118404134_118404266_118402864_118403176_118404571_118404602_0.878,0.902	-0.283	Down	6.67E-05	0.007278945
AP1G1	SE	ENSG00000166747_AP1G1_16_-_ 71841703_ 71841741_ 71823222_ 71823385_ 71841917_ 71842053_0.0,0.0	0.243	Up	6.80E-05	0.007382702
SLC26A1	SE	ENSG00000145217_SLC26A1_4_-_ 986508_ 986723_ 984915_ 985518_ 987088_ 987224_1.0,0.44	-0.638	Down	6.82E-05	0.007382702
EEF1D	SE	ENSG00000104529_EEF1D_8_-_144672777_144672908_144672157_144672251_144679048_144679275_0.0,0.34	0.83	Up	7.09E-05	0.007628796

BANP	SE	ENSG00000172530_BANP_16_+_ 88008653_ 88008813_ 87985086_ 87985121_ 88014641_ 88014733_1.0,1.0	-0.245	Down	7.46E-05	0.00793 6532
CXorf38	SE	ENSG00000185753_CXorf38_X_-_ 40498260_ 40499572_ 40496258_ 40496408_ 40506258_ 40506393_1.0,1.0	-0.353	Down	7.55E-05	0.00794 1998
RBBP8NL	SE	ENSG00000130701_RBBP8NL_20_-_ 60990176_ 60990343_ 60988876_ 60989612_ 60990633_ 60990716_1.0,1.0	-0.291	Down	7.55E-05	0.00794 1998
DBF4B	SE	ENSG00000161692_DBF4B_17_+_ 42809545_ 42809633_ 42808332_ 42808383_ 42811457_ 42811531_0.0,0.149	0.594	Up	7.59E-05	0.00794 1998
TBCD	SE	ENSG00000141556_TBCD_17_+_ 80867160_ 80867183_ 80863811_ 80863929_ 80869633_ 80869665_1.0,1.0	-0.21	Down	7.72E-05	0.00799 2942
RALGAPB	SE	ENSG00000170471_RALGAPB_20_+_ 37198530_ 37198639_ 37195738_ 37195875_ 37202792_ 37202941_1.0,1.0	-0.307	Down	7.93E-05	0.00818 7167
C6orf52	SE	ENSG00000137434_C6orf52_6_-_ 10685081_ 10685156_ 10683419_ 10683465_ 10687198_ 10687397_0.0,0.0	0.22	Up	8.21E-05	0.00843 726
FAM86C2P	SE	ENSG00000160172_FAM86C2P_11_-_ 67564154_ 67564304_ 67559237_ 67560764_ 67570472_ 67570535_0.138,0.0	0.35	Up	8.23E-05	0.00843 726
WNK1	SE	ENSG00000060237_WNK1_12_+_ 988738_ 989197_ 987377_ 987527_ 990857_ 990955_0.482,0.532	-0.223	Down	8.52E-05	0.00864 8722
SGK1	SE	ENSG00000118515_SGK1_6_-_134491963_134492053_134490383_134491573_134492160_134492316_1.0,1.0	-0.677	Down	8.83E-05	0.00889 1839
ACIN1	SE	ENSG00000100813_ACIN1_14_-_ 23559190_ 23559310_ 23550956_ 23551045_ 23559730_ 23559842_0.349,0.239	-0.206	Down	9.00E-05	0.00900 2419
IGFLR1	SE	ENSG00000126246_IGFLR1_19_-_ 36231280_ 36231465_ 36230157_ 36230527_ 36231924_ 36232124_1.0,1.0	-0.31	Down	9.11E-05	0.00902 7383
CHMP4C	SE	ENSG00000164695_CHMP4C_8_+_ 82665298_ 82665476_ 82644668_ 82645051_ 82667604_ 82667719_1.0,1.0	-0.246	Down	9.15E-05	0.00904 6516
MB	SE	ENSG00000198125_MB_22_-_ 36013209_ 36013312_ 36006930_ 36007153_ 36019237_ 36019448_0.564,0.775	0.302	Up	9.32E-05	0.00912 3313
C4orf29	SE	ENSG00000164074_C4orf29_4_+_128922870_128922915_128905493_128905578_128930074_128930153_0.0,0.0	0.681	Up	9.36E-05	0.00913 3248
PDDC1	SE	ENSG00000177225_PDDC1_11_-_ 770313_ 770398_ 767219_ 767373_ 771332_ 771426_0.0,0.0	0.327	Up	9.42E-05	0.00913 3262
OSBPL5	SE	ENSG00000021762_OSBPL5_11_-_ 3141773_ 3141854_ 3140776_ 3140861_ 3143226_ 3143328_0.655,1.0	-0.459	Down	9.48E-05	0.00916 1568
FAM160A1	SE	ENSG00000164142_FAM160A1_4_+_152403675_152403800_152330503_152330617_152487289_152487516_0.0,0.26	0.662	Up	9.71E-05	0.00926 2856
HDLBP	SE	ENSG00000115677_HDLBP_2_-_242208368_242208520_242207891_242207956_242208620_242208710_0.489,0.544	0.484	Up	9.69E-05	0.00926 2856
LETMD1	SE	ENSG00000050426_LETMD1_12_+_ 51449932_ 51450028_ 51447560_ 51447643_ 51450132_ 51450285_1.0,1.0	-0.222	Down	9.85E-05	0.00934 3877
ZNF562	SE	ENSG00000171466_ZNF562_19_-_ 9770054_ 9770143_ 9767222_ 9767329_ 9771395_ 9771550_1.0,1.0	-0.254	Down	0.000101 04	0.00952 1371
SLC45A4	SE	ENSG00000022567_SLC45A4_8_-_142231675_142231864_142229748_142229928_142264087_142264328_1.0,1.0	-0.233	Down	0.000100 92	0.00952 1371
HERC3	SE	ENSG00000138641_HERC3_4_+_ 89597368_ 89597392_ 89591289_ 89591403_ 89597484_ 89597574_0.793,1.0	-0.432	Down	0.000102 67	0.00964 4921
LIMCH1	SE	ENSG00000064042_LIMCH1_4_+_ 41631508_ 41631751_ 41621204_ 41621457_ 41633164_ 41633494_1.0,1.0	-0.524	Down	0.000105 43	0.00984 3741
TTC6	SE	ENSG00000139865_TTC6_14_+_ 38222303_ 38222440_ 38218918_ 38219048_ 38259921_ 38260042_1.0,1.0	-0.297	Down	0.000106 5	0.00988 3163
SLC41A2	SE	ENSG00000136052_SLC41A2_12_-_105325409_105325569_105322077_105322472_105351865_105352066_0.189,0.65	-0.419	Down	0.000107 46	0.00991 1605
PARP11	SE	ENSG00000111224_PARP11_12_-_ 3973001_ 3973123_ 3939055_ 3939184_ 3982377_ 3982521_1.0,1.0	-0.258	Down	0.000107 36	0.00991 1605

KIAA1958	SE	ENSG00000165185_KIAA1958_9_+_115380150_115380234_115336336_115337531_115407929_115408102_0.0,0.0	0.3	Up	0.00010944	0.010063718
ATP2C1	SE	ENSG00000017260_ATP2C1_3_+_130613551_130613619_130612834_130613181_130649259_130649370_0.881,1.0	-0.221	Down	0.00011138	0.010150405
UFM1	SE	ENSG00000120686_UFM1_13_+_ 38932229_ 38932269_ 38928375_ 38928433_ 38933437_ 38933470_0.538,0.437	0.415	Up	0.00011263	0.010233247
ZNF639	SE	ENSG00000121864_ZNF639_3_+_179042829_179043110_179040863_179041079_179045348_179045419_1.0,1.0	-0.302	Down	0.00011632	0.010443899
DPM1	SE	ENSG00000000419_DPM1_20_-_ 49557641_ 49557746_ 49557401_ 49557492_ 49558567_ 49558663_1.0,1.0	-0.228	Down	0.00011679	0.010455347
GMIP	SE	ENSG00000089639_GMIP_19_-_ 19746452_ 19746530_ 19746223_ 19746378_ 19747515_ 19747596_1.0,1.0	-0.245	Down	0.00011935	0.010565521
TMEM129	SE	ENSG00000168936_TMEM129_4_-_ 1719242_ 1719430_ 1718327_ 1719155_ 1719878_ 1719962_0.68,0.872	0.224	Up	0.00011998	0.010565521
B4GALNT1	SE	ENSG00000135454_B4GALNT1_12_-_ 58024982_ 58025147_ 58024762_ 58024869_ 58025697_ 58025916_1.0,1.0	-0.253	Down	0.00011931	0.010565521
ZNF92	SE	ENSG00000146757_ZNF92_7_+_ 64852814_ 64852941_ 64838711_ 64838913_ 64863253_ 64865997_1.0,1.0	-0.211	Down	0.00011984	0.010565521
RAB17	SE	ENSG00000124839_RAB17_2_-_238486646_238486798_238485899_238486025_238494640_238494800_1.0,1.0	-0.215	Down	0.00012135	0.010616834
PICALM	SE	ENSG00000073921_PICALM_11_-_ 85701292_ 85701421_ 85692914_ 85693046_ 85707868_ 85707972_0.464,0.539	0.434	Up	0.0001235	0.010740554
C2	SE	ENSG00000166278_C2_6_+_ 31901942_ 31902076_ 31901643_ 31901742_ 31903699_ 31903767_0.203,0.604	0.597	Up	0.00012463	0.010807513
NEK1	SE	ENSG00000137601_NEK1_4_-_170476870_170477002_170458959_170459062_170477082_170477246_0.339,0.596	0.424	Up	0.0001259	0.010863336
ZNF75A	SE	ENSG00000162086_ZNF75A_16_+_ 3358312_ 3358836_ 3355405_ 3355643_ 3361752_ 3361948_1.0,1.0	-0.331	Down	0.00013137	0.01126418
GOSR2	SE	ENSG00000108433_GOSR2_17_+_ 45008464_ 45008573_ 45006885_ 45006950_ 45009432_ 45009565_0.789,0.619	0.238	Up	0.00013316	0.011353676
TCTN1	SE	ENSG00000204852_TCTN1_12_+_111082771_111082934_111078250_111078322_111085000_111085141_0.315,0.535	0.468	Up	0.00013315	0.011353676
ABHD2	SE	ENSG00000140526_ABHD2_15_+_ 89647133_ 89647275_ 89645671_ 89645807_ 89656955_ 89657055_1.0,1.0	-0.298	Down	0.00013607	0.011472943
ACAD10	SE	ENSG00000111271_ACAD10_12_+_112167609_112167760_112165765_112165947_112174634_112174808_1.0,1.0	-0.492	Down	0.00013707	0.011525492
ZNF573	SE	ENSG00000189144_ZNF573_19_-_ 38263577_ 38263622_ 38262203_ 38262336_ 38264300_ 38264391_0.312,0.131	-0.202	Down	0.00013856	0.011618611
AC104667.3	SE	ENSG00000234949_AC104667.3_2_+_238500514_238500674_238499811_238499910_238503582_238504624_1.0,0.538	0.231	Up	0.00013991	0.011699502
BCAS3	SE	ENSG00000141376_BCAS3_17_+_ 59457866_ 59457932_ 59445687_ 59445855_ 59469337_ 59469543_0.253,0.0	0.414	Up	0.00014528	0.01202122
WRN	SE	ENSG00000165392_WRN_8_+_ 30947980_ 30948048_ 30946405_ 30946481_ 30948349_ 30948458_1.0,1.0	-0.309	Down	0.00014804	0.012178606
TMEM25	SE	ENSG00000149582_TMEM25_11_+_118403631_118403922_118403124_118403176_118404571_118404602_0.88,0.917	-0.244	Down	0.00014896	0.012212459
FAM86A	SE	ENSG00000118894_FAM86A_16_-_ 5141794_ 5141896_ 5140084_ 5140566_ 5143484_ 5143565_1.0,0.912	-0.368	Down	0.00015187	0.012293937
MTMR14	SE	ENSG00000163719_MTMR14_3_+_ 9731647_ 9731827_ 9730627_ 9730766_ 9739394_ 9739550_1.0,1.0	-0.222	Down	0.00015362	0.012378174
ZNF44	SE	ENSG00000197857_ZNF44_19_-_ 12404046_ 12404190_ 12386770_ 12386897_ 12405506_ 12405666_0.496,0.7	-0.413	Down	0.00015518	0.012397189
GTDC1	SE	ENSG00000121964_GTDC1_2_-_144728219_144728329_144710339_144710410_144764748_144765102_1.0,1.0	-0.371	Down	0.00015678	0.012427156

PEX10	SE	ENSG00000157911_PEX10_1_-_ 2342068_ 2342307_ 2341809_ 2341890_ 2343829_ 2343953_0.227,0.109	0.265	Up	0.000156 36	0.01242 7156
TMEM241	SE	ENSG00000134490_TMEM241_18_-_ 20950179_ 20950225_ 20936557_ 20936627_ 20951385_ 20951434_0.238,0.231	0.441	Up	0.000168 64	0.01319 1699
SPG11	SE	ENSG00000104133_SPG11_15_-_ 44881449_ 44881612_ 44878035_ 44878048_ 44884528_ 44884636_0.775,0.769	0.228	Up	0.000169 46	0.01319 1699
DMTF1	SE	ENSG00000135164_DMTF1_7_+_ 86783705_ 86783844_ 86781755_ 86781871_ 86792810_ 86792933_1.0,0.6	-0.601	Down	0.000171 69	0.01329 7198
SLC1A3	SE	ENSG00000079215_SLC1A3_5_+_ 36683965_ 36684100_ 36680496_ 36680691_ 36686166_ 36688436_1.0,1.0	-0.24	Down	0.000174 23	0.01342 611
SYNE4	SE	ENSG00000181392_SYNE4_19_-_ 36497324_ 36497573_ 36496234_ 36496339_ 36499118_ 36499269_0.323,0.301	0.569	Up	0.000178 44	0.01371 5856
LPHN1	SE	ENSG00000072071_LPHN1_19_-_ 14275432_ 14275517_ 14273759_ 14274218_ 14277827_ 14277842_1.0,0.756	-0.482	Down	0.000181 09	0.01388 3955
NEDD1	SE	ENSG00000139350_NEDD1_12_+_ 97311398_ 97311515_ 97301381_ 97301634_ 97313762_ 97313896_1.0,1.0	-0.243	Down	0.000187 02	0.01412 0113
UBA1	SE	ENSG00000130985_UBA1_X_+_ 47057565_ 47057754_ 47053235_ 47053423_ 47058201_ 47058318_0.0,0.05	0.278	Up	0.000186 65	0.01412 0113
GNB1	SE	ENSG00000078369_GNB1_1_-_ 1771067_ 1771121_ 1770628_ 1770677_ 1821802_ 1821840_0.0,0.194	0.534	Up	0.000189 06	0.01420 1166
FAM222B	SE	ENSG00000173065_FAM222B_17_-_ 27161310_ 27161344_ 27117395_ 27117443_ 27169699_ 27169808_0.707,0.211	0.474	Up	0.000190 21	0.01422 5002
DNAH14	SE	ENSG00000185842_DNAH14_1_+_225465111_225465204_225463615_ 225463783_225477586_225477784_1.0,0.545	-0.772	Down	0.000193 9	0.01446 5433
MKL1	SE	ENSG00000196588_MKL1_22_-_ 40990677_ 40990739_ 40948109_ 40948371_ 41032481_ 41032695_1.0,1.0	-0.27	Down	0.000201 53	0.01485 9954
AASS	SE	ENSG00000008311_AASS_7_-_121722841_121722945_121721553_121721649_121726065_121726233_0.0,0.0	0.262	Up	0.000203 72	0.01494 1607
SPOP	SE	ENSG00000121067_SPOP_17_-_ 47714120_ 47714171_ 47700094_ 47700238_ 47745388_ 47745440_1.0,0.814	-0.426	Down	0.000203 67	0.01494 1607
SLC9A8	SE	ENSG00000197818_SLC9A8_20_+_ 48467298_ 48467381_ 48466115_ 48466217_ 48471974_ 48472118_0.238,0.294	0.512	Up	0.000209 59	0.01526 1616
IL15RA	SE	ENSG00000134470_IL15RA_10_-_ 6005705_ 6005801_ 6002357_ 6002530_ 6008107_ 6008302_0.0,0.0	0.268	Up	0.000210 61	0.01529 9457
PPP6R3	SE	ENSG00000110075_PPP6R3_11_+_ 68326033_ 68326147_ 68315534_ 68315672_ 68334481_ 68334634_1.0,0.687	-0.564	Down	0.000215 05	0.01539 2454
ATXN3	SE	ENSG00000066427_ATXN3_14_-_ 92560089_ 92560194_ 92559595_ 92559662_ 92562436_ 92562481_1.0,0.872	-0.265	Down	0.000214 67	0.01539 2454
MLPH	SE	ENSG00000115648_MLPH_2_+_238428552_238428672_238427181_238427291_238434243_238434448_1.0,1.0	-0.226	Down	0.000215	0.01539 2454
MKNK1	SE	ENSG00000079277_MKNK1_1_-_ 47025905_ 47025949_ 47023090_ 47024472_ 47027149_ 47027314_0.0,0.202	0.423	Up	0.000213 04	0.01539 2454
CMC2	SE	ENSG00000103121_CMC2_16_-_ 81014374_ 81014484_ 81009698_ 81010076_ 81040338_ 81040500_0.295,0.87	0.417	Up	0.000219 12	0.01541 3511
BOK	SE	ENSG00000176720_BOK_2_+_242498869_242499118_242498135_242498408_242501762_242501891_0.798,1.0	-0.254	Down	0.000221 08	0.01541 3511
FAAH2	SE	ENSG00000165591_FAAH2_X_+_ 57458350_ 57458470_ 57407344_ 57407462_ 57473360_ 57473472_1.0,1.0	-0.299	Down	0.000220 26	0.01541 3511
ATG2A	SE	ENSG00000110046_ATG2A_11_-_ 64669987_ 64670152_ 64669731_ 64669858_ 64670759_ 64670836_1.0,1.0	-0.336	Down	0.000220 41	0.01541 3511
PAM	SE	ENSG00000145730_PAM_5_+_102360837_102361038_102355493_102355547_102363885_102363942_0.45,0.235	0.55	Up	0.000217 91	0.01541 3511
RTFDC1	SE	ENSG00000022277_RTFDC1_20_+_ 55045655_ 55045997_ 55043713_ 55043822_ 55046669_ 55046725_1.0,1.0	-0.456	Down	0.000224 72	0.01542 1316
UBXN8	SE	ENSG00000104691_UBXN8_8_+_ 30609023_ 30609035_ 30601706_ 30601794_ 30610551_ 30610622_1.0,1.0	-0.298	Down	0.000224 95	0.01542 1316
ACSL1	SE	ENSG00000151726_ACSL1_4_-_185691408_185691486_185689469_185689604_185694234_185694308_1.0,1.0	-0.208	Down	0.000226 92	0.01548 6536

TRAPPC6A	SE	ENSG00000007255_TRAPPC6A_19_-_ 45668384_ 45668452_ 45668110_ 45668228_ 45681392_ 45681495_0.555,0.383	0.332	Up	0.000230 17	0.01563 822
MPDU1	SE	ENSG00000129255_MPDU1_17_+_ 7489268_ 7489396_ 7487166_ 7487283_ 7489973_ 7490095_1.0,1.0	-0.22	Down	0.000230 91	0.01565 3376
MPDU1	SE	ENSG00000129255_MPDU1_17_+_ 7489263_ 7489396_ 7487169_ 7487283_ 7489973_ 7490095_1.0,1.0	-0.206	Down	0.000232 61	0.01572 5278
LA16c-431H6.6	SE	ENSG00000261732_LA16c-431H6.6_16_+_ 1716073_ 1716178_ 1715057_ 1715139_ 1716422_ 1716601_0.758,0.752	-0.436	Down	0.000235 34	0.01577 7944
UBE2F	SE	ENSG00000184182_UBE2F_2_+_238903385_238903451_238881736_23 8881867_238933982_238934053_0.0,0.576	0.712	Up	0.000235 14	0.01577 7944
ZIK1	SE	ENSG00000171649_ZIK1_19_+_ 58096319_ 58096358_ 58095512_ 58095980_ 58099906_ 58100033_0.0,0.0	0.326	Up	0.000236 05	0.01579 1047
MIB2	SE	ENSG00000197530_MIB2_1_+_ 1560937_ 1561033_ 1560665_ 1560808_ 1562029_ 1562134_1.0,0.939	-0.207	Down	0.000237 57	0.01579 8046
ARHGAP44	SE	ENSG00000006740_ARHGAP44_17_+_ 12877405_ 12877627_ 12862033_ 12862214_ 12883374_ 12883550_1.0,1.0	-0.48	Down	0.000239 35	0.01586 8014
COL4A5	SE	ENSG00000188153_COL4A5_X_+_107816803_107816884_107815040_1 07815067_107819139_107819202_1.0,1.0	-0.211	Down	0.000246 58	0.01628 0436
ATG2A	SE	ENSG00000110046_ATG2A_11_-_ 64669981_ 64670152_ 64669731_ 64669858_ 64670759_ 64670836_1.0,1.0	-0.333	Down	0.000249 5	0.01643 767
AFMID	SE	ENSG00000183077_AFMID_17_+_ 76201683_ 76201819_ 76201520_ 76201599_ 76202026_ 76202131_1.0,0.858	-0.491	Down	0.000250 93	0.01649 6325
ZNF586	SE	ENSG00000083828_ZNF586_19_+_ 58287910_ 58288037_ 58281037_ 58281246_ 58290118_ 58291945_0.526,0.676	0.314	Up	0.000261 67	0.01694 6201
RHBDD1	SE	ENSG00000144468_RHBDD1_2_+_227702788_227702870_227700670_ 227700803_227729319_227729781_0.677,1.0	-0.665	Down	0.000272 79	0.01748 0226
BCL2L12	SE	ENSG00000126453_BCL2L12_19_+_ 50172107_ 50172194_ 50169941_ 50170056_ 50176954_ 50177173_1.0,1.0	-0.506	Down	0.000274 63	0.01748 1878
LIMK2	SE	ENSG00000182541_LIMK2_22_+_ 31621705_ 31621805_ 31608280_ 31608410_ 31654276_ 31654412_0.777,0.425	0.315	Up	0.000275 1	0.01748 1878
DSN1	SE	ENSG00000149636_DSN1_20_-_ 35399275_ 35399380_ 35396371_ 35396445_ 35399827_ 35399876_0.881,1.0	-0.201	Down	0.000285 46	0.01802 6422
TRAF3	SE	ENSG00000131323_TRAF3_14_+_103357661_103357754_103342694_1 03342862_103363597_103363738_1.0,1.0	-0.208	Down	0.000294 57	0.01848 6887
STAU1	SE	ENSG00000124214_STAU1_20_-_ 47774973_ 47775034_ 47770469_ 47770608_ 47775475_ 47775683_0.41,0.0	0.795	Up	0.000296 93	0.01855 8129
ASPM	SE	ENSG00000066279_ASPM_1_-_197069560_197074315_197065127_197065294_197086918_197087113_0.691,0.605	0.238	Up	0.000300 34	0.01869 497
CTC1	SE	ENSG00000178971_CTC1_17_-_ 8139148_ 8139277_ 8138370_ 8138603_ 8139375_ 8139660_0.862,0.548	0.258	Up	0.000302 47	0.01878 8729
PVR	SE	ENSG00000073008_PVR_19_+_ 45162009_ 45162168_ 45161029_ 45161178_ 45164558_ 45164590_0.766,1.0	-0.208	Down	0.000303 21	0.01879 6783
PLA2G7	SE	ENSG00000146070_PLA2G7_6_-_ 46677063_ 46677155_ 46675727_ 46675898_ 46678281_ 46678395_1.0,1.0	-0.22	Down	0.000304 15	0.01881 6374
PTPN4	SE	ENSG00000088179_PTPN4_2_+_120677644_120677817_120672754_12 0672818_120689999_120690125_1.0,1.0	-0.223	Down	0.000306 61	0.01893 0284
DPH7	SE	ENSG00000148399_DPH7_9_-_140470760_140470854_140470531_140470619_140471921_140472055_1.0,1.0	-0.347	Down	0.000317 41	0.01941 2536
PORCN	SE	ENSG00000102312_PORCN_X_+_ 48367811_ 48367965_ 48367417_ 48367491_ 48368171_ 48368344_1.0,1.0	-0.511	Down	0.000317 61	0.01941 2536
ILF3	SE	ENSG00000129351_ILF3_19_+_ 10795091_ 10795152_ 10794592_ 10794646_ 10798021_ 10798384_0.958,0.842	-0.227	Down	0.000322 59	0.01967 734
UNC119	SE	ENSG00000109103_UNC119_17_-_ 26875609_ 26875723_ 26873725_ 26874867_ 26879355_ 26879686_1.0,1.0	-0.248	Down	0.000323 67	0.01970 3701
STAP2	SE	ENSG00000178078_STAP2_19_-_ 4328671_ 4328806_ 4327312_ 4327382_ 4329957_ 4330058_0.893,0.794	-0.228	Down	0.000329 93	0.01996 5194

ANKS6	SE	ENSG00000165138_ANKS6_9_-_101552385_101552888_101547113_101547158_101558414_101558821_0.752,1.0	-0.342	Down	0.00033248	0.019980278
SAC3D1	SE	ENSG00000168061_SAC3D1_11_+_64810496_64810636_64808412_64808578_64811696_64812300_1.0,1.0	-0.21	Down	0.00033217	0.019980278
PAQR3	SE	ENSG00000163291_PAQR3_4_-_79843294_79843575_79839093_79841835_79843982_79844137_0.249,0.398	0.676	Up	0.00033666	0.020092867
BAZ2B	SE	ENSG00000123636_BAZ2B_2_-_160287373_160287667_160285710_160285771_160289267_160292064_1.0,1.0	-0.253	Down	0.00034329	0.020448112
ZNF83	SE	ENSG00000167766_ZNF83_19_-_53177434_53177506_53164014_53164096_53193695_53193749_0.725,0.116	-0.42	Down	0.00035528	0.020998114
BAD	SE	ENSG00000002330_BAD_11_-_64044375_64044515_64039084_64039275_64051653_64051848_0.262,0.374	-0.285	Down	0.00035887	0.021169057
MYO9A	SE	ENSG00000066933_MYO9A_15_-_72244117_72244237_72231192_72231268_72252241_72252296_0.3,0.392	0.478	Up	0.00036226	0.021204971
ZHX3	SE	ENSG00000174306_ZHX3_20_-_39896102_39896252_39868237_39868344_39897629_39897723_1.0,1.0	-0.245	Down	0.00036036	0.021204971
WIBG	SE	ENSG00000170473_WIBG_12_-_56308059_56308150_56297170_56297264_56320859_56320895_1.0,0.547	-0.5	Down	0.00037007	0.021537541
YAF2	SE	ENSG00000015153_YAF2_12_-_42604156_42604256_42555429_42555567_42604349_42604482_0.84,1.0	-0.511	Down	0.00037493	0.02173745
PARD3	SE	ENSG00000148498_PARD3_10_-_34625126_34625171_34620044_34620272_34626202_34626354_1.0,1.0	-0.5	Down	0.000380 4	0.021894974
ARNTL2	SE	ENSG00000029153_ARNTL2_12_+_27529278_27529320_27523061_27523163_27533179_27533337_0.204,0.0	0.464	Up	0.00038504	0.022030056
GOSR2	SE	ENSG00000108433_GOSR2_17_+_45008467_45008573_45006885_45006950_45009432_45009565_0.694,0.586	0.265	Up	0.000387 4	0.022040598
LIN7A	SE	ENSG00000111052_LIN7A_12_-_81283029_81283148_81242029_81242101_81331419_81331483_1.0,0.59	0.205	Up	0.00038859	0.022066721
SERTAD3	SE	ENSG00000167565_SERTAD3_19_-_40948229_40948422_40947712_40947993_40950121_40950182_0.065,0.0	0.211	Up	0.000397 1	0.022466554
SRFBP1	SE	ENSG00000151304_SRFBP1_5_+_121358064_121358102_121330293_121330365_121362636_121364314_1.0,0.519	0.24	Up	0.00039875	0.022471114
TRIM16	SE	ENSG00000221926_TRIM16_17_-_15586167_15586278_15584178_15584267_15586349_15586471_1.0,1.0	-0.424	Down	0.00040389	0.022532961
ERBB2IP	SE	ENSG00000112851_ERBB2IP_5_+_65364704_65364848_65349233_65350779_65367996_65368122_1.0,0.663	-0.569	Down	0.00040285	0.022532961
LPXN	SE	ENSG00000110031_LPXN_11_-_58331627_58331674_58322313_58322413_58338028_58338186_0.9,1.0	-0.276	Down	0.00040868	0.022699599
PDCD2L	SE	ENSG00000126249_PDCD2L_19_+_34895553_34895895_34895329_34895443_34900065_34900415_0.514,1.0	0.243	Up	0.00041114	0.022719953
ESPL1	SE	ENSG00000135476_ESPL1_12_+_53682321_53682483_53681755_53682125_53682873_53683087_1.0,1.0	-0.204	Down	0.00041129	0.022719953
SOS2	SE	ENSG00000100485_SOS2_14_-_50682091_50682150_50671001_50671127_50697914_50698080_0.0,0.0	0.352	Up	0.00041721	0.023005634
BCL6	SE	ENSG00000113916_BCL6_3_-_187444518_187444686_187443286_187443417_187446147_187446332_1.0,1.0	-0.209	Down	0.00044263	0.023912544
FUK	SE	ENSG00000157353_FUK_16_+_70500784_70501374_70500034_70500160_70502751_70502871_0.433,0.276	0.645	Up	0.00044547	0.023957921
C1orf86	SE	ENSG00000162585_C1orf86_1_-_2118276_2118645_2115916_2116952_2125077_2125349_1.0,0.732	-0.509	Down	0.00046911	0.024744426
MAPT	SE	ENSG00000186868_MAPT_17_+_44049224_44049311_44039686_44039836_44055740_44055806_1.0,1.0	-0.3	Down	0.00047356	0.024809393
SYNE4	SE	ENSG00000181392_SYNE4_19_-_36498026_36498170_36496234_36496339_36499118_36499269_0.396,0.228	0.567	Up	0.00047352	0.024809393
BIN1	SE	ENSG00000136717_BIN1_2_-_127808729_127808819_127808377_127808488_127815048_127815177_0.845,1.0	-0.251	Down	0.00047978	0.025092201
TSGA10	SE	ENSG00000135951_TSGA10_2_-_99735013_99735149_99734029_99734222_99743510_99743639_0.0,0.164	0.214	Up	0.00048601	0.025244438

PGAP2	SE	ENSG00000148985_PGAP2_11_+_ 3844842_ 3844970_ 3829523_ 3829545_ 3845112_ 3845587_1.0,1.0	-0.324	Down	0.000485 44	0.02524 4438
RAB8B	SE	ENSG00000166128_RAB8B_15_+_ 63516046_ 63516178_ 63515240_ 63515272_ 63536954_ 63537015_0.435,0.461	0.411	Up	0.000484 99	0.02524 4438
BLOC1S6	SE	ENSG00000104164_BLOC1S6_15_+_ 45893431_ 45893605_ 45884332_ 45884474_ 45897625_ 45897712_1.0,1.0	-0.238	Down	0.000494 71	0.02538 4594
LRP5	SE	ENSG00000162337_LRP5_11_+_ 68213040_ 68213154_ 68207340_ 68207384_ 68213903_ 68214001_0.048,0.0	0.251	Up	0.000494 03	0.02538 4594
ENOX2	SE	ENSG00000165675_ENOX2_X_-_129917520_129917664_129843216_129843305_130035657_130035705_0.663,0.88	0.228	Up	0.000512 09	0.02606 5336
ZNF397	SE	ENSG00000186812_ZNF397_18_+_ 32825225_ 32825315_ 32823115_ 32823257_ 32834195_ 32834366_0.378,0.378	0.396	Up	0.000513 6	0.02609 8404
SLC35B3	SE	ENSG00000124786_SLC35B3_6_-_ 8417634_ 8417727_ 8417116_ 8417228_ 8420953_ 8421061_1.0,1.0	-0.219	Down	0.000518 59	0.02611 9786
PCCA	SE	ENSG00000175198_PCCA_13_+_101167680_101167821_101101505_101101559_101179928_101180006_1.0,1.0	-0.22	Down	0.000526 6	0.02627 6246
TMEM206	SE	ENSG00000065600_TMEM206_1_-_212550903_212551048_212537823_212538718_212553236_212553379_1.0,1.0	-0.218	Down	0.000533 02	0.02650 9961
MTL5	SE	ENSG00000132749_MTL5_11_-_ 68512458_ 68512579_ 68509785_ 68509862_ 68514675_ 68514834_1.0,0.933	-0.209	Down	0.000546 49	0.02692 269
CMC2	SE	ENSG00000103121_CMC2_16_-_ 81015410_ 81015482_ 81009697_ 81010076_ 81040338_ 81040502_0.644,0.888	0.234	Up	0.000549 99	0.02700 0961
SNX10	SE	ENSG00000086300_SNX10_7_+_ 26393676_ 26393804_ 26386039_ 26386086_ 26396626_ 26396747_0.342,0.0	0.679	Up	0.000552 64	0.02701 4163
PLCB4	SE	ENSG00000101333_PLCB4_20_+_ 9457363_ 9457400_ 9453925_ 9454012_ 9459567_ 9461889_1.0,1.0	-0.217	Down	0.000554 27	0.02701 4163
PIP5K1C	SE	ENSG00000186111_PIP5K1C_19_-_ 3633434_ 3633518_ 3630180_ 3633167_ 3638881_ 3639014_0.294,0.257	-0.243	Down	0.000560 58	0.02725 6868
C19orf60	SE	ENSG00000006015_C19orf60_19_+_ 18700222_ 18700493_ 18699804_ 18699887_ 18702917_ 18703146_1.0,1.0	-0.228	Down	0.000565 18	0.02743 7058
PLEKHN1	SE	ENSG00000187583_PLEKHN1_1_+_ 908565_ 908706_ 908240_ 908390_ 908879_ 909020_1.0,1.0	-0.286	Down	0.000569 15	0.02756 2587
PDCD2L	SE	ENSG00000126249_PDCD2L_19_+_ 34895553_ 34895720_ 34895288_ 34895443_ 34900065_ 34900415_0.454,1.0	0.273	Up	0.000576 17	0.02774 9389
TMEM175	SE	ENSG00000127419_TMEM175_4_+_ 941496_ 941680_ 926248_ 926328_ 944208_ 944306_0.418,0.601	0.4	Up	0.000586 77	0.02809 2469
LPP	SE	ENSG00000145012_LPP_3_+_187943192_187943315_187871718_187871809_188123899_188124101_0.469,0.761	0.342	Up	0.000586 99	0.02809 2469
DCAF8	SE	ENSG00000132716_DCAF8_1_-_160231074_160231148_160213749_160213824_160231906_160232241_0.878,0.825	-0.205	Down	0.000588 38	0.02811 4847
STK19	SE	ENSG00000204344_STK19_6_+_ 31940397_ 31940534_ 31940078_ 31940288_ 31946679_ 31946775_1.0,1.0	-0.228	Down	0.000599 07	0.02840 2433
ATG9A	SE	ENSG00000198925_ATG9A_2_-_220093155_220093204_220092643_220092775_220093731_220094047_0.425,0.663	0.405	Up	0.000604 24	0.02851 4443
UBR1	SE	ENSG00000159459_UBR1_15_-_ 43339358_ 43339487_ 43335411_ 43335593_ 43346939_ 43347097_0.757,1.0	-0.289	Down	0.000619 6	0.02893 0808
MRPL22	SE	ENSG00000082515_MRPL22_5_+_154330362_154330498_154320776_154320825_154335930_154335996_1.0,0.901	-0.205	Down	0.000635 95	0.02937 3205
PAM	SE	ENSG00000145730_PAM_5_+_102360834_102361038_102355493_102355547_102363885_102363942_0.739,0.527	0.321	Up	0.000660 99	0.03011 8626
BIRC5	SE	ENSG00000089685_BIRC5_17_+_ 76212046_ 76212862_ 76210760_ 76210870_ 76218908_ 76219060_1.0,1.0	-0.365	Down	0.000678 74	0.03078 911
HELB	SE	ENSG00000127311_HELB_12_+_ 66707765_ 66707943_ 66703485_ 66704388_ 66709021_ 66709163_0.305,1.0	0.348	Up	0.000710 02	0.03201 7299
GOPC	SE	ENSG00000047932_GOPC_6_-_117892022_117892118_117888016_117888197_117894629_117894795_1.0,1.0	-0.202	Down	0.000712 32	0.03202 9787

CBR3-AS1	SE	ENSG00000236830_CBR3-AS1_21_-_ 37518553_ 37518653_ 37504064_ 37505372_ 37528514_ 37528615_1.0,1.0	-0.242	Down	0.000717 01	0.03214 1841
PGAP3	SE	ENSG00000161395_PGAP3_17_-_ 37840849_ 37841002_ 37830869_ 37830932_ 37842174_ 37842272_1.0,0.588	0.206	Up	0.000719 27	0.03219 5789
ATP2C1	SE	ENSG00000017260_ATP2C1_3_+_130613574_130613619_130613025_1 30613181_130649259_130649370_0.751,1.0	-0.254	Down	0.000740 16	0.03288 9205
CDC14B	SE	ENSG00000081377_CDC14B_9_-_ 99277930_ 99278074_ 99265846_ 99266071_ 99284787_ 99284885_1.0,1.0	-0.289	Down	0.000747 87	0.03314 3265
SYNE4	SE	ENSG00000181392_SYNE4_19_-_ 36497651_ 36497846_ 36496234_ 36496339_ 36499118_ 36499269_0.0,0.294	0.674	Up	0.000748 06	0.03314 3265
C14orf159	SE	ENSG00000133943_C14orf159_14_+_ 91636346_ 91636530_ 91633568_ 91633722_ 91639632_ 91639783_1.0,1.0	-0.5	Down	0.000762 81	0.03343 4632
SEMA4D	SE	ENSG00000187764_SEMA4D_9_-_ 91996088_ 91996261_ 91995969_ 91996013_ 92001281_ 92001397_1.0,1.0	-0.234	Down	0.000797 81	0.03464 141
RUFY2	SE	ENSG00000204130_RUFY2_10_-_ 70140988_ 70141156_ 70139180_ 70139278_ 70143554_ 70143671_1.0,0.941	-0.209	Down	0.000819 24	0.03507 1797
UBE2V1	SE	ENSG00000244687_UBE2V1_20_-_ 48732021_ 48732158_ 48713208_ 48713357_ 48732235_ 48732491_1.0,1.0	-0.214	Down	0.000823 26	0.03519 4353
PPT2	SE	ENSG00000221988_PPT2_6_+_ 32122806_ 32122960_ 32122363_ 32122554_ 32123464_ 32123560_1.0,1.0	-0.275	Down	0.000834 3	0.03522 1019
GLS	SE	ENSG00000115419_GLS_2_+_191819309_191819386_191818290_1918 18352_191827555_191827896_0.659,0.563	0.389	Up	0.000826 32	0.03522 1019
MOK	SE	ENSG00000080823_MOK_14_- _102732159_102732249_102729882_102729953_102749814_1027499 29_1.0,0.87	-0.215	Down	0.000827 31	0.03522 1019
C5orf38	SE	ENSG00000186493_C5orf38_5_+_ 2753398_ 2753469_ 2752793_ 2752868_ 2755142_ 2755195_0.665,1.0	-0.296	Down	0.000849 23	0.03565 3598
AGBL5	SE	ENSG00000084693_AGBL5_2_+_ 27291915_ 27291962_ 27291499_ 27291612_ 27292440_ 27292574_1.0,0.529	-0.628	Down	0.000860 03	0.03585 9749
CLTCL1	SE	ENSG00000070371_CLTCL1_22_-_ 19175069_ 19175240_ 19170902_ 19171124_ 19175492_ 19175603_1.0,0.0	0.5	Up	0.000862 53	0.03587 8889
CARF	SE	ENSG00000138380_CARF_2_+_203839056_203839219_203836227_203 836461_203841991_203842055_1.0,1.0	-0.326	Down	0.000862 85	0.03587 8889
ANAPC10	SE	ENSG00000164162_ANAPC10_4_- _145985723_145985844_145916607_145916755_146002811_1460029 02_0.762,0.608	0.231	Up	0.000887 73	0.03671 2952
PTK2	SE	ENSG00000169398_PTK2_8_- _141935759_141935848_141900641_141900868_142011223_1420112 57_0.119,0.224	0.233	Up	0.000890 51	0.03672 8206
FGFR2	SE	ENSG00000066468_FGFR2_10_- _123278195_123278343_123276847_123276977_123279492_1232796 83_0.0,0.195	0.394	Up	0.000898 53	0.03686 5658
SMAP1	SE	ENSG00000112305_SMAP1_6_+_ 71508359_ 71508440_ 71483052_ 71483128_ 71546643_ 71546731_1.0,0.596	0.202	Up	0.000927 01	0.03747 1894
FAM193B	SE	ENSG00000146067_FAM193B_5_- _176958282_176958522_176951185_176952206_176959443_1769595 34_1.0,1.0	-0.278	Down	0.000940 24	0.03785 5662
ZNF530	SE	ENSG00000183647_ZNF530_19_+_ 58117053_ 58119195_ 58115644_ 58115774_ 58123870_ 58124090_0.401,1.0	0.299	Up	0.000939 62	0.03785 5662
N4BP2L2	SE	ENSG00000244754_N4BP2L2_13_-_ 33052023_ 33052185_ 33016524_ 33018263_ 33054726_ 33054774_1.0,0.0	0.5	Up	0.000942 07	0.03787 939
PTBP2	SE	ENSG00000117569_PTBP2_1_+_ 97271974_ 97272008_ 97270340_ 97270495_ 97272421_ 97272514_0.898,1.0	-0.548	Down	0.000943 93	0.03790 4239
RBM33	SE	ENSG00000184863_RBM33_7_+_155556502_155556712_155537654_1 55538296_155559160_155559250_1.0,1.0	-0.204	Down	0.000947 78	0.03790 8684
MACROD1	SE	ENSG00000133315_MACROD1_11_-_ 63766309_ 63766344_ 63766031_ 63766159_ 63766426_ 63766694_0.762,1.0	-0.268	Down	0.000958 89	0.03815 2371
TIRAP	SE	ENSG00000150455_TIRAP_11_+_126161319_126161464_126160697_1 26160856_126162371_126162582_0.395,0.355	-0.265	Down	0.000961 47	0.03815 5592

SRSF11	SE	ENSG00000116754_SRSF11_1_+_ 70696239_ 70696301_ 70694104_ 70694238_ 70696777_ 70697253_0.708,0.717	-0.403	Down	0.000970 89	0.03823 0055
GRK5	SE	ENSG00000198873_GRK5_10_+_121201510_121201600_121199242_12 1199280_121203055_121203264_1.0,1.0	-0.262	Down	0.000967 95	0.03823 0055
CENPE	SE	ENSG00000138778_CENPE_4_- _104060945_104061236_104059507_104059606_104061412_1040615 71_1.0,1.0	-0.35	Down	0.000974 59	0.03832 6461
KCNAB2	SE	ENSG00000069424_KCNAB2_1_+_ 6101890_ 6101932_ 6100576_ 6100705_ 6132814_ 6132858_0.434,0.184	0.372	Up	0.000978 09	0.03841 4457
ATG9A	SE	ENSG00000198925_ATG9A_2_- _220093155_220093207_220092643_220092775_220093731_2200940 62_0.522,0.773	0.328	Up	0.000986 63	0.03866 6886
WDR27	SE	ENSG00000184465_WDR27_6_- _170089222_170089404_170088912_170089108_170101646_1701021 44_0.796,1.0	-0.386	Down	0.001000 93	0.03900 9472
RAB28	SE	ENSG00000157869_RAB28_4_-_ 13371494_ 13371589_ 13369347_ 13370274_ 13378168_ 13378246_0.123,0.073	0.237	Up	0.000999 81	0.03900 9472
TEP1	SE	ENSG00000129566_TEP1_14_-_ 20874391_ 20874559_ 20873609_ 20873744_ 20876031_ 20876622_1.0,1.0	-0.273	Down	0.001008 5	0.03920 3944
C11orf54	SE	ENSG00000182919_C11orf54_11_+_ 93475128_ 93475260_ 93474853_ 93474894_ 93480467_ 93480614_0.506,0.0	0.416	Up	0.001011 2	0.03925 8699
OSBPL6	SE	ENSG00000079156_OSBPL6_2_+_179188903_179188996_179170756_1 79171013_179192982_179193105_1.0,0.906	-0.301	Down	0.001013 36	0.03929 2706
CNOT2	SE	ENSG00000111596_CNOT2_12_+_ 70726546_ 70726626_ 70713077_ 70713144_ 70729217_ 70729343_0.745,0.846	-0.265	Down	0.001015 5	0.03932 5587
KLHDC9	SE	ENSG00000162755_KLHDC9_1_+_161069387_161069586_161068455_1 61068852_161069850_161070133_0.832,0.759	0.205	Up	0.001020 15	0.03940 5163
AFMID	SE	ENSG00000183077_AFMID_17_+_ 76201683_ 76201834_ 76201520_ 76201599_ 76202026_ 76202131_1.0,0.657	-0.422	Down	0.001034 36	0.03980 1927
SSBP2	SE	ENSG00000145687_SSBP2_5_-_ 80724403_ 80724502_ 80716106_ 80716352_ 80733248_ 80733649_0.559,1.0	0.22	Up	0.001053 18	0.04022 1859
NT5DC3	SE	ENSG00000111696_NT5DC3_12_- _104179348_104179525_104179112_104179253_104181218_1041813 05_0.423,0.18	-0.266	Down	0.001052 06	0.04022 1859
STK19	SE	ENSG00000204344_STK19_6_+_ 31940397_ 31940696_ 31940128_ 31940288_ 31946679_ 31946775_1.0,1.0	-0.358	Down	0.001052 05	0.04022 1859
PEX7	SE	ENSG00000112357_PEX7_6_+_137191027_137191141_137147456_137 147607_137219279_137219379_0.524,0.216	0.63	Up	0.001056 6	0.04030 1714
PPP1R7	SE	ENSG00000115685_PPP1R7_2_+_242089673_242089962_242089052_2 42089123_242092890_242093019_1.0,1.0	-0.262	Down	0.001077 57	0.04079 4732
AP3S2	SE	ENSG00000157823_AP3S2_15_-_ 90421496_ 90421532_ 90380846_ 90380954_ 90431752_ 90431864_0.284,0.166	0.497	Up	0.001094 22	0.04114 6706
MARCH7	SE	ENSG00000136536_MARCH7_2_+_160572191_160572277_160569017_ 160569172_160585519_160585686_0.0,0.081	0.212	Up	0.001096 69	0.04114 6706
ABHD6	SE	ENSG00000163686_ABHD6_3_+_ 58235604_ 58235669_ 58223232_ 58223643_ 58242288_ 58242432_0.505,0.505	0.382	Up	0.001097 24	0.04114 6706
MRPS15	SE	ENSG00000116898_MRPS15_1_-_ 36926864_ 36926913_ 36923523_ 36923582_ 36929406_ 36929451_0.597,1.0	-0.451	Down	0.001138 17	0.04206 7291
RNF185	SE	ENSG00000138942_RNF185_22_+_ 31591454_ 31591567_ 31588669_ 31588688_ 31592921_ 31593143_0.713,0.734	0.276	Up	0.001134 97	0.04206 7291
PNPLA8	SE	ENSG00000135241_PNPLA8_7_- _108161919_108161965_108154879_108156018_108166472_1081665 68_1.0,0.762	-0.485	Down	0.001147 67	0.04229 1671
RP11-480I12.5	SE	ENSG00000214796_RP11-480I12.5_1_- _202828009_202828230_202820955_202822408_202830575_2028307 36_1.0,1.0	-0.317	Down	0.001169 45	0.04278 3258
NUP214	SE	ENSG00000126883_NUP214_9_+_134064439_134064518_134053697_1 34053797_134070619_134070681_0.489,0.389	0.561	Up	0.001173 57	0.04281 4613

CCDC148	SE	ENSG00000153237_CCDC148_2_-_159196753_159196905_159195501_159195597_159197109_159197192_1.0,1.0	-0.213	Down	0.00117453	0.042814613
NME6	SE	ENSG00000172113_NME6_3_-_48341920_48342124_48339916_48340013_48342768_48342795_1.0,1.0	-0.5	Down	0.0011778	0.042831467
MFGE8	SE	ENSG00000140545_MFGE8_15_-_89442886_89443042_89441915_89442763_89444781_89444966_0.32,0.397	0.425	Up	0.00117695	0.042831467
GOLIM4	SE	ENSG00000173905_GOLIM4_3_-_167758573_167758657_167754623_167754782_167759179_167759262_0.802,0.734	-0.228	Down	0.0011889	0.043108727
MCTP1	SE	ENSG00000175471_MCTP1_5_-_94253600_94253678_94248510_94248681_94259666_94259726_1.0,0.719	-0.408	Down	0.00119881	0.043336704
ALDOA	SE	ENSG00000149925_ALDOA_16_+_30066492_30066648_30064447_30064820_30075049_30075569_0.32,0.0	0.651	Up	0.00120235	0.043352453
SERINC3	SE	ENSG00000132824_SERINC3_20_-_43138531_43138669_43133441_43133532_43142519_43142681_1.0,1.0	-0.5	Down	0.00120864	0.043416728
PVR	SE	ENSG00000073008_PVR_19_+_45162009_45162033_45161029_45161178_45164558_45164590_0.46,1.0	-0.238	Down	0.00122309	0.043538752
TMCC1	SE	ENSG00000172765_TMCC1_3_-_129551616_129551669_129390091_129390107_129599151_129599309_1.0,1.0	-0.312	Down	0.00122664	0.04356661
SLC29A1	SE	ENSG00000112759_SLC29A1_6_+_44193709_44193904_44191350_44191378_44194999_44195079_0.529,0.375	-0.236	Down	0.00123419	0.043732636
NAA16	SE	ENSG00000172766_NAA16_13_+_41936866_41937009_41936261_41936295_41941574_41941788_0.496,1.0	-0.502	Down	0.00126358	0.044360691
ARHGEF10	SE	ENSG00000104728_ARHGEF10_8_+_1828213_1828330_1824736_1824900_1830800_1830915_0.449,0.0	0.461	Up	0.00127144	0.044533897
RIMS1	SE	ENSG00000079841_RIMS1_6_+_72975662_72975752_72974677_72974755_72993749_72993821_1.0,1.0	-0.5	Down	0.00128664	0.044911576
JADE2	SE	ENSG00000043143_JADE2_5_+_133909334_133909452_133901805_133902270_133912457_133912586_0.448,0.748	0.402	Up	0.00132737	0.045755769
AGR2	SE	ENSG00000106541_AGR2_7_-_16851288_16851379_16841281_16841427_16872879_16873057_0.377,0.232	0.58	Up	0.00134193	0.045923128
CD163L1	SE	ENSG00000177675_CD163L1_12_-_7520682_7520793_7509975_7510082_7521528_7521561_1.0,0.796	-0.313	Down	0.00133713	0.045923128
SECISBP2	SE	ENSG00000187742_SECISBP2_9_+_91934566_91934712_91933420_91933527_91940341_91940591_1.0,1.0	-0.351	Down	0.00134039	0.045923128
CBWD2	SE	ENSG00000136682_CBWD2_2_+_114228609_114228666_114222705_114222750_114239753_114239805_0.886,1.0	-0.223	Down	0.00134868	0.045974784
SPIN1	SE	ENSG00000106723_SPIN1_9_+_91063855_91063904_91003344_91003453_91083286_91083520_0.721,0.526	0.377	Up	0.0013521	0.045983493
CXADR	SE	ENSG00000154639_CXADR_21_+_18933019_18933142_18931293_18931449_18937745_18942418_0.895,0.873	-0.35	Down	0.00135401	0.045996954
RP11-529K1.2	SE	ENSG00000261777_RP11-529K1.2_16_-_70375842_70376002_70367685_70367863_70380101_70380650_0.189,0.582	0.615	Up	0.00136743	0.046224553
ZNF620	SE	ENSG00000177842_ZNF620_3_+_40553892_40554006_40552960_40553087_40557350_40557435_0.397,0.355	-0.316	Down	0.00139477	0.046601626
CD163L1	SE	ENSG00000177675_CD163L1_12_-_7520653_7520793_7509975_7510082_7521528_7521566_1.0,0.764	-0.439	Down	0.0013948	0.046601626
PER1	SE	ENSG00000179094_PER1_17_-_8048077_8048311_8046583_8047194_8049275_8049455_1.0,1.0	-0.349	Down	0.00139963	0.046661458
MAGI1	SE	ENSG00000151276_MAGI1_3_-_65433696_65433732_65428466_65428524_65438932_65439015_0.254,0.665	-0.391	Down	0.00140765	0.04687754
REPS1	SE	ENSG00000135597_REPS1_6_-_139247537_139247618_139242173_139242261_139251113_139251235_0.367,0.269	0.295	Up	0.00142463	0.047339289
MACF1	SE	ENSG00000127603_MACF1_1_+_39930766_39930784_39929283_39929358_39934286_39934404_0.683,0.596	-0.299	Down	0.00142675	0.047358094
PLS1	SE	ENSG00000120756_PLS1_3_+_142338294_142338480_142316078_142316190_142383043_142383149_0.0,0.097	0.573	Up	0.00146836	0.048372332

RTFDC1	SE	ENSG00000022277_RTFDC1_20_+_ 55046669_ 55046725_ 55043734_ 55043822_ 55047381_ 55047471_0.0,0.0	0.294	Up	0.001491 05	0.04895 5876
ELP2	SE	ENSG00000134759_ELP2_18_+_ 33721099_ 33721164_ 33718232_ 33718389_ 33734812_ 33734962_1.0,1.0	-0.423	Down	0.001492 58	0.04895 5876
FBF1	SE	ENSG00000188878_FBF1_17_-_ 73931712_ 73931754_ 73929075_ 73929169_ 73933646_ 73933675_0.697,0.365	0.395	Up	0.001498 24	0.04908 879
SLC38A1	SE	ENSG00000111371_SLC38A1_12_-_ 46648596_ 46648719_ 46633461_ 46633676_ 46662308_ 46662780_0.347,0.0	0.268	Up	0.001507 37	0.04933 4854
NAT1	SE	ENSG00000171428_NAT1_8_+_ 18068701_ 18068851_ 18067617_ 18067689_ 18069899_ 18070283_0.325,1.0	-0.662	Down	0.001537 19	0.04989 1357
EML3	A3SS	ENSG00000149499_EML3_11_-_ 62378558_ 62378819_ 62378558_ 62378816_ 62378896_ 62379068_1.0,1.0	-1	Down	4.35E-11	1.56E-07
SUGP1	A3SS	ENSG00000105705_SUGP1_19_-_ 19414532_ 19414852_ 19414532_ 19414721_ 19416657_ 19416885_1.0,1.0	-0.851	Down	7.41E-10	1.33E-06
PILRB	A3SS	ENSG00000121716_PILRB_7_+_ 99954016_ 99954506_ 99954372_ 99954506_ 99952765_ 99952863_1.0,1.0	-0.649	Down	2.29E-08	2.74E-05
DMXL2	A3SS	ENSG00000104093_DMXL2_15_-_ 51768785_ 51768916_ 51768785_ 51768913_ 51770467_ 51770544_1.0,1.0	-0.644	Down	5.46E-08	4.91E-05
NPEPPS	A3SS	ENSG00000141279_NPEPPS_17_+_ 45654410_ 45654526_ 45654446_ 45654526_ 45646782_ 45646860_1.0,1.0	-0.734	Down	7.30E-08	5.25E-05
C5orf45	A3SS	ENSG00000161010_C5orf45_5_-_179264275_179267959_179264275_179264885_179268906_179269064_1.0,1.0	-0.475	Down	5.31E-07	0.00023 9008
SMYD2	A3SS	ENSG00000143499_SMYD2_1_+_214504292_214507651_214507542_214507651_214503510_214503621_1.0,1.0	-0.784	Down	5.28E-07	0.00023 9008
MAPKBP1	A3SS	ENSG00000137802_MAPKBP1_15_+_ 42107456_ 42107997_ 42107821_ 42107997_ 42106747_ 42106937_1.0,1.0	-0.479	Down	4.75E-07	0.00023 9008
CARF	A3SS	ENSG00000138380_CARF_2_+_203789019_203789138_203789079_203789138_203782599_203782766_0.583,1.0	-0.617	Down	8.12E-07	0.00032 4523
AGTRAP	A3SS	ENSG00000177674_AGTRAP_1_+_ 11805986_ 11806280_ 11806044_ 11806280_ 11805859_ 11805894_0.0,0.0	0.529	Up	1.39E-06	0.00050 1864
RBM26	A3SS	ENSG00000139746_RBM26_13_-_ 79928573_ 79928705_ 79928573_ 79928696_ 79929354_ 79929519_1.0,1.0	-0.374	Down	1.71E-06	0.00055 8221
CCNL2	A3SS	ENSG00000221978_CCNL2_1_-_ 1326145_ 1326955_ 1326145_ 1326245_ 1328169_ 1328183_1.0,1.0	-0.422	Down	2.28E-06	0.00068 2766
C16orf93	A3SS	ENSG00000196118_C16orf93_16_-_ 30770974_ 30771130_ 30770974_ 30771045_ 30771604_ 30771989_0.0,0.237	0.881	Up	2.75E-06	0.00076 1887
HSD17B1	A3SS	ENSG00000108786_HSD17B1_17_+_ 40706419_ 40706600_ 40706422_ 40706600_ 40705811_ 40705905_1.0,1.0	-0.528	Down	4.48E-06	0.00115 1632
SLC25A10	A3SS	ENSG00000183048_SLC25A10_17_+_ 79684723_ 79684891_ 79684786_ 79684891_ 79684428_ 79684521_0.0,0.0	0.227	Up	4.85E-06	0.00116 4853
FNBP1	A3SS	ENSG00000187239_FNBP1_9_-_132686122_132686305_132686122_132686218_132687238_132687436_1.0,1.0	-0.447	Down	5.42E-06	0.00121 8324
ZNF473	A3SS	ENSG00000142528_ZNF473_19_+_ 50534148_ 50534348_ 50534270_ 50534348_ 50529149_ 50529379_1.0,1.0	-0.44	Down	6.67E-06	0.00141 2024
PGS1	A3SS	ENSG00000087157_PGS1_17_+_ 76410959_ 76411108_ 76411032_ 76411108_ 76399648_ 76400170_1.0,1.0	-0.347	Down	7.81E-06	0.00156 1927
ZNF584	A3SS	ENSG00000171574_ZNF584_19_+_ 58927159_ 58927307_ 58927185_ 58927307_ 58926890_ 58927013_1.0,0.771	-0.643	Down	1.05E-05	0.00183 0116
UBXN11	A3SS	ENSG00000158062_UBXN11_1_-_ 26627416_ 26627544_ 26627416_ 26627515_ 26628184_ 26628213_0.0,0.0	0.538	Up	1.27E-05	0.00207 8188
TTC18	A3SS	ENSG00000156042_TTC18_10_-_ 75082720_ 75082855_ 75082720_ 75082785_ 75090934_ 75091034_1.0,0.889	-0.382	Down	1.37E-05	0.00214 8384
MASTL	A3SS	ENSG00000120539_MASTL_10_+_ 27462046_ 27462188_ 27462049_ 27462188_ 27458872_ 27460012_0.62,0.746	-0.399	Down	1.51E-05	0.00217 7315
NFKBID	A3SS	ENSG00000167604_NFKBID_19_-_ 36387814_ 36388005_ 36387814_ 36387960_ 36388552_ 36388758_0.0,0.0	0.512	Up	1.85E-05	0.00228 3351

SYBU	A3SS	ENSG00000147642_SYBU_8_-_110654956_110655161_110654956_110655158_110656864_110656945_1.0,1.0	-0.836	Down	1.90E-05	0.002283351
SDHA	A3SS	ENSG00000073578_SDHA_5_+_ 254472_ 254621_ 254507_ 254621_ 240472_ 240591_1.0,1.0	-0.293	Down	1.74E-05	0.002283351
FCF1	A3SS	ENSG00000119616_FCF1_14_+_ 75182523_ 75182802_ 75182653_ 75182802_ 75181574_ 75181646_0.0,0.0	0.214	Up	1.89E-05	0.002283351
XRCC3	A3SS	ENSG00000126215_XRCC3_14_-_104177802_104177998_104177802_104177904_104181760_104181821_1.0,1.0	-0.365	Down	1.87E-05	0.002283351
FKBP7	A3SS	ENSG00000079150_FKBP7_2_-_179334378_179334512_179334378_179334509_179341788_179341940_0.927,1.0	-0.369	Down	2.29E-05	0.002657611
WDR27	A3SS	ENSG00000184465_WDR27_6_-_170068077_170068281_170068077_170068191_170070664_170070789_1.0,1.0	-0.55	Down	2.54E-05	0.002857305
CCDC88A	A3SS	ENSG00000115355_CCDC88A_2_-_ 55555429_ 55555571_ 55555429_ 55555568_ 55559701_ 55559829_1.0,1.0	-0.294	Down	4.04E-05	0.004280811
GMIP	A3SS	ENSG00000089639_GMIP_19_-_ 19746223_ 19746530_ 19746223_ 19746378_ 19747515_ 19747605_1.0,1.0	-0.309	Down	4.96E-05	0.005104898
PRKCSH	A3SS	ENSG00000130175_PRKCSH_19_+_ 11558507_ 11558604_ 11558537_ 11558604_ 11558253_ 11558433_1.0,0.935	-0.245	Down	5.83E-05	0.005674275
ZNF512	A3SS	ENSG00000243943_ZNF512_2_+_ 27820933_ 27821121_ 27820936_ 27821121_ 27806524_ 27806583_1.0,1.0	-0.274	Down	6.45E-05	0.00595625
PLEKHA6	A3SS	ENSG00000143850_PLEKHA6_1_-_204230433_204230636_204230433_204230576_204234069_204234170_0.636,1.0	-0.744	Down	7.34E-05	0.006369705
QKI	A3SS	ENSG00000112531_QKI_6_+_163985698_163991177_163986977_163991177_163984451_163984751_0.786,0.797	-0.329	Down	7.43E-05	0.006369705
ATP11A	A3SS	ENSG00000068650_ATP11A_13_+_113536126_113541482_113536189_113541482_113530089_113530255_1.0,1.0	-0.293	Down	8.15E-05	0.006823016
PXK	A3SS	ENSG00000168297_PXK_3_+_ 58398627_ 58398690_ 58398630_ 58398690_ 58395816_ 58395886_1.0,1.0	-0.266	Down	9.07E-05	0.007418349
PLD3	A3SS	ENSG00000105223_PLD3_19_+_ 40872290_ 40872417_ 40872325_ 40872417_ 40871459_ 40871492_0.347,1.0	-0.622	Down	9.28E-05	0.007423023
ZNF780A	A3SS	ENSG00000197782_ZNF780A_19_-_ 40587725_ 40587824_ 40587725_ 40587821_ 40589017_ 40589144_0.0,0.105	0.264	Up	0.00010605	0.008296985
PTBP2	A3SS	ENSG00000117569_PTBP2_1_+_ 97270340_ 97270495_ 97270355_ 97270495_ 97250614_ 97250810_1.0,0.783	-0.581	Down	0.00011187	0.00854441
ATP11A	A3SS	ENSG00000068650_ATP11A_13_+_113536129_113541482_113536189_113541482_113530089_113530255_1.0,1.0	-0.266	Down	0.00011954	0.008622085
MITF	A3SS	ENSG00000187098_MITF_3_+_ 70000962_ 70001037_ 70000980_ 70001037_ 69998201_ 69998319_0.0,0.0	0.208	Up	0.0001326	0.008837481
YAF2	A3SS	ENSG00000015153_YAF2_12_-_ 42604349_ 42604482_ 42604349_ 42604421_ 42631400_ 42631526_0.0,0.148	0.508	Up	0.00013092	0.008837481
WDR31	A3SS	ENSG00000148225_WDR31_9_-_116093263_116093396_116093263_116093393_116094186_116094330_1.0,1.0	-0.369	Down	0.0001554	0.009812291
BAHD1	A3SS	ENSG00000140320_BAHD1_15_+_ 40754110_ 40754493_ 40754113_ 40754493_ 40750649_ 40752095_0.395,0.495	0.46	Up	0.00018884	0.011717874
CBX7	A3SS	ENSG00000100307_CBX7_22_-_ 39530405_ 39530757_ 39530405_ 39530478_ 39534640_ 39534707_0.454,0.599	0.474	Up	0.00021144	0.01289799
PMS2P5	A3SS	ENSG00000123965_PMS2P5_7_+_ 74312515_ 74312628_ 74312525_ 74312628_ 74312262_ 74312349_1.0,1.0	-0.404	Down	0.00022006	0.012983429
ZNF764	A3SS	ENSG00000169951_ZNF764_16_-_ 30565084_ 30567431_ 30565084_ 30567428_ 30569053_ 30569167_0.164,0.0	0.386	Up	0.00025609	0.013964395
POT1	A3SS	ENSG00000128513_POT1_7_-_124568868_124569053_124568868_124569050_124569847_124569879_0.0,0.595	0.66	Up	0.00028815	0.015280968
ZNF382	A3SS	ENSG00000161298_ZNF382_19_+_ 37100803_ 37100955_ 37100828_ 37100955_ 37098453_ 37098524_0.0,0.521	-0.261	Down	0.00033651	0.016590267

TMEM25	A3SS	ENSG00000149582_TMEM25_11_+_118402489_118402586_118402492_118402586_118401906_118401949_0.495,0.246	0.377	Up	0.00033398	0.016590267
PPFIA2	A3SS	ENSG00000139220_PPFIA2_12_-_ 81675035_ 81675229_ 81675035_ 81675211_ 81688613_ 81688814_0.622,0.717	0.26	Up	0.00038496	0.01872248
CIC	A3SS	ENSG00000079432_CIC_19_+_ 42798086_ 42798241_ 42798089_ 42798241_ 42797743_ 42797988_0.655,0.76	-0.235	Down	0.00040532	0.019194159
PEX1	A3SS	ENSG00000127980_PEX1_7_-_ 92130820_ 92131393_ 92130820_ 92130987_ 92132354_ 92132509_1.0,1.0	-0.207	Down	0.00042177	0.019641809
PSIP1	A3SS	ENSG00000164985_PSIP1_9_-_ 15470633_ 15471309_ 15470633_ 15471229_ 15472629_ 15472748_0.704,0.543	-0.359	Down	0.00050071	0.021976396
DRG2	A3SS	ENSG00000108591_DRG2_17_+_ 18002946_ 18003749_ 18003676_ 18003749_ 18002330_ 18002391_1.0,0.46	0.27	Up	0.00051546	0.022085037
SYNGAP1	A3SS	ENSG00000197283_SYNGAP1_6_+_ 33414351_ 33414563_ 33414357_ 33414563_ 33412220_ 33412394_1.0,1.0	-0.294	Down	0.00058903	0.024146708
CEP57L1	A3SS	ENSG00000183137_CEP57L1_6_+_109480420_109480665_109480471_109480665_109480227_109480305_0.328,0.234	-0.258	Down	0.0006314	0.025532567
ACOT8	A3SS	ENSG00000101473_ACOT8_20_-_ 44482561_ 44482623_ 44482561_ 44482618_ 44483797_ 44483931_0.0,0.326	0.618	Up	0.0007425	0.028428371
ZNF566	A3SS	ENSG00000186017_ZNF566_19_-_ 36963812_ 36963911_ 36963812_ 36963908_ 36964233_ 36964360_0.0,0.246	0.311	Up	0.00072844	0.028428371
DESI2	A3SS	ENSG00000121644_DESI2_1_+_244855180_244855322_244855185_244855322_244849898_244849971_1.0,1.0	-0.289	Down	0.00075569	0.028628728
MSTO1	A3SS	ENSG00000125459_MSTO1_1_+_155581217_155581394_155581339_155581394_155581006_155581082_0.056,0.082	0.205	Up	0.00077717	0.028835537
MAP4K2	A3SS	ENSG00000168067_MAP4K2_11_-_ 64564575_ 64564664_ 64564575_ 64564640_ 64564746_ 64564852_1.0,1.0	-0.27	Down	0.00077458	0.028835537
PLEKHA7	A3SS	ENSG00000166689_PLEKHA7_11_-_ 16812557_ 16812749_ 16812557_ 16812746_ 16816034_ 16816261_0.0,1.0	0.5	Up	0.00081097	0.029186647
MAGIX	A3SS	ENSG00000017621_MAGIX_X_+_ 49022412_ 49022971_ 49022427_ 49022971_ 49021527_ 49021699_0.644,1.0	-0.608	Down	0.00086938	0.029910832
PCGF3	A3SS	ENSG00000185619_PCGF3_4_+_ 726188_ 726287_ 726232_ 726287_ 724758_ 724899_1.0,1.0	-0.209	Down	0.00087264	0.029910832
FOXP1	A3SS	ENSG00000114861_FOXP1_3_-_ 71026793_ 71026873_ 71026793_ 71026870_ 71026978_ 71027180_0.83,0.895	-0.227	Down	0.00097283	0.031304838
CLTCL1	A3SS	ENSG00000070371_CLTCL1_22_-_ 19183776_ 19184167_ 19183776_ 19183926_ 19187244_ 19187352_1.0,1.0	-0.607	Down	0.00102339	0.032308461
STOML1	A3SS	ENSG00000067221_STOML1_15_-_ 74276999_ 74277212_ 74276999_ 74277209_ 74277658_ 74277854_1.0,0.893	-0.326	Down	0.00104832	0.032524899
GPNMB	A3SS	ENSG00000136235_GPNMB_7_+_ 23306099_ 23306234_ 23306135_ 23306234_ 23300074_ 23300392_0.0,0.0	0.231	Up	0.00110842	0.033990085
MIB2	A3SS	ENSG00000197530_MIB2_1_+_ 1560925_ 1562134_ 1562029_ 1562134_ 1560665_ 1560808_1.0,0.627	-0.415	Down	0.00111445	0.033990085
SPPL2B	A3SS	ENSG00000005206_SPPL2B_19_+_ 2339822_ 2339965_ 2339825_ 2339965_ 2339067_ 2339207_0.797,0.688	0.202	Up	0.0011624	0.035155148
GTF2IRD1	A3SS	ENSG00000006704_GTF2IRD1_7_+_ 73969722_ 73969824_ 73969767_ 73969824_ 73969503_ 73969553_1.0,0.602	-0.443	Down	0.0012057	0.035807557
PHF21A	A3SS	ENSG00000135365_PHF21A_11_-_ 46098304_ 46098391_ 46098304_ 46098370_ 46100684_ 46100717_0.465,0.063	-0.252	Down	0.00146089	0.040444252
ARHGAP33	A3SS	ENSG00000004777_ARHGAP33_19_+_ 36277314_ 36277974_ 36277797_ 36277974_ 36276310_ 36276385_1.0,1.0	-0.323	Down	0.0015333	0.041420307
RP11-347C12.2	A3SS	ENSG00000183604_RP11-347C12.2_16_-_ 30288584_ 30288749_ 30288584_ 30288707_ 30288917_ 30289114_1.0,1.0	-0.283	Down	0.00163348	0.041613387
SEPT5	A3SS	ENSG00000184702_SEPT5_22_+_ 19709344_ 19709480_ 19709355_ 19709480_ 19709162_ 19709259_1.0,1.0	-0.222	Down	0.00160079	0.041613387
MIB2	A3SS	ENSG00000197530_MIB2_1_+_ 1558768_ 1559079_ 1558810_ 1559079_ 1551887_ 1551994_0.0,0.658	0.474	Up	0.00160602	0.041613387
IRF7	A3SS	ENSG00000185507_IRF7_11_-_ 614475_ 614534_ 614475_ 614531_ 614796_ 615007_1.0,1.0	-0.23	Down	0.00178502	0.044001848

METTL17	A3SS	ENSG00000165792_METTL17_14_+_ 21460250_ 21460364_ 21460282_ 21460364_ 21458622_ 21458757_0.404,0.494	-0.245	Down	0.001949 88	0.04736 8335
ZNF19	A3SS	ENSG00000157429_ZNF19_16_-_ 71512781_ 71513003_ 71512781_ 71512908_ 71515984_ 71516046_1.0,0.0	0.5	Up	0.002008 09	0.04818 0824
PLXND1	A3SS	ENSG00000004399_PLXND1_3_-_129304794_129304924_129304794_129304891_129305014_129305115_0.708,0.669	0.285	Up	0.002072 04	0.04874 0417
PTPN4	A5SS	ENSG00000088179_PTPN4_2_+_120672754_120674266_120672754_120672818_120689999_120690125_1.0,1.0	-0.925	Down	1.89E-15	4.62E-12
ELMOD3	A5SS	ENSG00000115459_ELMOD3_2_+_ 85582677_ 85582907_ 85582677_ 85582721_ 85584089_ 85584375_0.176,0.0	0.912	Up	4.30E-14	5.26E-11
ELMOD3	A5SS	ENSG00000115459_ELMOD3_2_+_ 85582677_ 85582839_ 85582677_ 85582721_ 85584089_ 85584375_0.213,0.0	0.893	Up	3.11E-13	2.54E-10
ELMOD3	A5SS	ENSG00000115459_ELMOD3_2_+_ 85582677_ 85583019_ 85582677_ 85582721_ 85584089_ 85584375_0.137,0.096	0.883	Up	1.56E-10	9.55E-08
UBE2J2	A5SS	ENSG00000160087_UBE2J2_1_-_ 1203112_ 1203372_ 1203241_ 1203372_ 1201477_ 1201670_1.0,1.0	-0.814	Down	8.07E-09	3.95E-06
MGAT4B	A5SS	ENSG00000161013_MGAT4B_5_-_179225503_179225591_179225512_179225591_179225164_179225277_1.0,1.0	-0.84	Down	1.48E-07	6.02E-05
MRRF	A5SS	ENSG00000148187_MRRF_9_+_125047447_125048225_125047447_125047566_125048317_125048445_1.0,1.0	-0.708	Down	2.58E-07	7.90E-05
HDLBP	A5SS	ENSG00000115677_HDLBP_2_-_242208372_242208710_242208620_242208710_242207891_242207956_0.152,0.152	0.848	Up	2.41E-07	7.90E-05
CCDC84	A5SS	ENSG00000186166_CCDC84_11_+_118881930_118882021_118881930_ 118881993_118882648_118882713_0.0,0.0	0.813	Up	3.85E-07	0.00010 4831
AC007405.6	A5SS	ENSG00000239467_AC007405.6_2_+_171627622_171627937_171627622_171627697_171633886_171633935_1.0,1.0	-0.625	Down	4.86E-07	0.00011 9082
P4HTM	A5SS	ENSG00000178467_P4HTM_3_+_ 49039932_ 49043620_ 49039932_ 49040029_ 49044119_ 49044548_1.0,1.0	-0.607	Down	7.13E-07	0.00015 8677
PNISR	A5SS	ENSG00000132424_PNISR_6_-_ 99851704_ 99852578_ 99852478_ 99852578_ 99850415_ 99850586_1.0,1.0	-0.558	Down	1.03E-06	0.00021 0146
ITPR1	A5SS	ENSG00000150995_ITPR1_3_+_ 4716751_ 4716932_ 4716751_ 4716905_ 4718297_ 4718485_0.0,0.0	0.636	Up	1.22E-06	0.00021 399
ACAA2	A5SS	ENSG00000167315_ACAA2_18_-_ 47340051_ 47340323_ 47340186_ 47340323_ 47329056_ 47329223_0.753,0.487	0.38	Up	1.22E-06	0.00021 399
PTBP3	A5SS	ENSG00000119314_PTBP3_9_-_115060111_115060196_115060120_115060196_115030328_115030475_1.0,0.956	-0.267	Down	1.38E-06	0.00022 581
CDK20	A5SS	ENSG00000156345_CDK20_9_-_ 90585482_ 90585812_ 90585690_ 90585812_ 90584710_ 90584834_1.0,1.0	-0.477	Down	1.77E-06	0.00027 0055
CD46	A5SS	ENSG00000117335_CD46_1_+_207940357_207943707_207940357_207940540_207956636_207956675_1.0,1.0	-0.419	Down	1.99E-06	0.00028 6107
GMIP	A5SS	ENSG00000089639_GMIP_19_-_ 19753343_ 19753428_ 19753345_ 19753428_ 19752784_ 19752860_0.568,0.862	0.285	Up	3.88E-06	0.00050 0181
ZNF276	A5SS	ENSG00000158805_ZNF276_16_+_ 89793686_ 89793765_ 89793686_ 89793733_ 89795642_ 89795726_0.83,1.0	-0.404	Down	3.77E-06	0.00050 0181
NOL8	A5SS	ENSG00000198000_NOL8_9_-_ 95087187_ 95087632_ 95087599_ 95087632_ 95086304_ 95086491_0.084,0.153	0.488	Up	1.54E-05	0.00171 0276
CLPTM1L	A5SS	ENSG00000049656_CLPTM1L_5_-_ 1331913_ 1331998_ 1331917_ 1331998_ 1325865_ 1325931_1.0,1.0	-0.35	Down	2.02E-05	0.00206 5092
ZSCAN25	A5SS	ENSG00000197037_ZSCAN25_7_+_ 99217183_ 99217620_ 99217183_ 99217616_ 99218995_ 99219197_0.163,0.0	0.269	Up	4.24E-05	0.00399 4425
CLN6	A5SS	ENSG00000128973_CLN6_15_-_ 68503893_ 68504201_ 68503986_ 68504201_ 68503600_ 68503656_1.0,1.0	-0.369	Down	5.25E-05	0.00475 8795
RMND1	A5SS	ENSG00000155906_RMND1_6_-_151757554_151757689_151757580_151757689_151754289_151754365_0.0,0.0	0.201	Up	5.53E-05	0.00483 1338
CCNL2	A5SS	ENSG00000221978_CCNL2_1_-_ 1328058_ 1328183_ 1328169_ 1328183_ 1326145_ 1326245_1.0,1.0	-0.266	Down	6.16E-05	0.00486 266

WDR90	A5SS	ENSG00000161996_WDR90_16_+_ 703745_ 705147_ 703745_ 703803_ 705306_ 705468_1.0,1.0	-0.64	Down	5.96E-05	0.00486266
MYO9A	A5SS	ENSG00000066933_MYO9A_15_-_ 72244042_ 72244237_ 72244117_ 72244237_ 72231192_ 72231268_0.722,1.0	-0.53	Down	6.76E-05	0.00486 4673
HDLBP	A5SS	ENSG00000115677_HDLBP_2_-_242208368_242208710_242208620_242208710_242207891_242207956_0.471,0.516	0.506	Up	6.59E-05	0.00486 4673
MSTO1	A5SS	ENSG00000125459_MSTO1_1_+_155583447_155583557_155583447_155583524_155583849_155584726_0.821,0.649	0.233	Up	8.17E-05	0.00540 7656
ZMYND8	A5SS	ENSG00000101040_ZMYND8_20_-_ 45867501_ 45867882_ 45867639_ 45867882_ 45865069_ 45865260_0.091,0.0	0.215	Up	8.59E-05	0.00553 1606
MYB	A5SS	ENSG00000118513_MYB_6_+_135515493_135515598_135515493_135515589_135516885_135517140_1.0,1.0	-0.254	Down	9.95E-05	0.00624 7279
STK16	A5SS	ENSG00000115661_STK16_2_+_220110617_220111598_220110617_220110807_220112136_220112257_1.0,1.0	-0.268	Down	0.000107 32	0.00639 2125
SLC25A19	A5SS	ENSG00000125454_SLC25A19_17_-_ 73284468_ 73284672_ 73284578_ 73284672_ 73282713_ 73282883_1.0,1.0	-0.244	Down	0.000117 81	0.00670 7005
GALE	A5SS	ENSG00000117308_GALE_1_-_ 24122998_ 24123272_ 24123186_ 24123272_ 24122640_ 24122755_1.0,1.0	-0.241	Down	0.000122 97	0.00684 1878
SERF2	A5SS	ENSG00000140264_SERF2_15_+_ 44084565_ 44084809_ 44084565_ 44084776_ 44085172_ 44085281_0.492,0.336	0.46	Up	0.000126 23	0.00686 7108
RAD51AP1	A5SS	ENSG00000111247_RAD51AP1_12_+_ 4652928_ 4653077_ 4652928_ 4653070_ 4655474_ 4655584_0.488,0.192	-0.299	Down	0.000134 01	0.00713 1874
QARS	A5SS	ENSG00000172053_QARS_3_-_ 49141789_ 49141904_ 49141805_ 49141904_ 49141295_ 49141405_1.0,1.0	-0.259	Down	0.000150 09	0.00781 7344
CLK3	A5SS	ENSG00000179335_CLK3_15_+_ 74912349_ 74914557_ 74912349_ 74912566_ 74914834_ 74914901_1.0,1.0	-0.426	Down	0.000183 56	0.00898 7034
SDR39U1	A5SS	ENSG00000100445_SDR39U1_14_-_ 24911303_ 24911466_ 24911383_ 24911466_ 24909988_ 24910132_1.0,0.559	-0.539	Down	0.000234 81	0.01105 4303
MSH5	A5SS	ENSG00000204410_MSH5_6_+_ 31707724_ 31707997_ 31707724_ 31707839_ 31708939_ 31709063_0.0,0.584	0.534	Up	0.000253 42	0.01170 5236
NOL8	A5SS	ENSG00000198000_NOL8_9_-_ 95087587_ 95087632_ 95087599_ 95087632_ 95086304_ 95086491_0.077,0.664	0.534	Up	0.000311 4	0.01367 3823
PLCD1	A5SS	ENSG00000187091_PLCD1_3_-_ 38051394_ 38051766_ 38051621_ 38051766_ 38051143_ 38051302_1.0,1.0	-0.399	Down	0.000312 8	0.01367 3823
BRF1	A5SS	ENSG00000185024_BRF1_14_-_105766782_105781926_105781658_105781926_105752632_105752713_1.0,1.0	-0.45	Down	0.000448 76	0.01771 8689
PACRGL	A5SS	ENSG00000163138_PACRGL_4_+_ 20702081_ 20702410_ 20702081_ 20702370_ 20706088_ 20706156_0.631,0.591	0.295	Up	0.000447 72	0.01771 8689
RP11-296I10.6	A5SS	ENSG00000261556_RP11-296I10.6_16_-_ 70265225_ 70265426_ 70265339_ 70265426_ 70264896_ 70265061_1.0,1.0	-0.427	Down	0.000492 06	0.01882 1468
SNRNP70	A5SS	ENSG00000104852_SNRNP70_19_+_ 49605370_ 49606844_ 49605370_ 49605430_ 49607890_ 49607992_1.0,1.0	-0.447	Down	0.000504 31	0.01899 3156
WDR90	A5SS	ENSG00000161996_WDR90_16_+_ 712672_ 713064_ 712672_ 712844_ 715678_ 715801_0.052,0.279	0.603	Up	0.000525 3	0.01902 0499
RTEL1	A5SS	ENSG00000258366_RTEL1_20_+_ 62326680_ 62327003_ 62326680_ 62326833_ 62327130_ 62327606_1.0,0.474	-0.463	Down	0.000543 89	0.01902 0499
HDLBP	A5SS	ENSG00000115677_HDLBP_2_-_242208615_242208710_242208620_242208710_242207891_242207956_0.659,0.591	0.375	Up	0.000654 81	0.02257 7006
STXBP2	A5SS	ENSG00000076944_STXBP2_19_+_ 7712047_ 7712397_ 7712047_ 7712133_ 7712610_ 7712759_1.0,1.0	-0.224	Down	0.000725 83	0.02401 1284
STOX1	A5SS	ENSG00000165730_STOX1_10_+_ 70644015_ 70646374_ 70644015_ 70644215_ 70652344_ 70652816_0.261,1.0	0.369	Up	0.000777 77	0.02505 0544
TMSB15B	A5SS	ENSG00000158427_TMSB15B_X_+_103217241_103218867_103217241_103217296_103219078_103219195_1.0,0.58	-0.576	Down	0.000800 44	0.02512 1517

RAB15	A5SS	ENSG00000139998_RAB15_14_-_ 65417660_ 65417869_ 65417791_ 65417869_ 65417042_ 65417132_0.045,0.038	0.207	Up	0.000818 75	0.02518 6223
SSBP4	A5SS	ENSG00000130511_SSBP4_19_+_ 18544519_ 18544742_ 18544519_ 18544627_ 18545026_ 18545372_1.0,0.732	-0.503	Down	0.000840 34	0.02539 6805
MUTYH	A5SS	ENSG00000132781_MUTYH_1_-_ 45803857_ 45804328_ 45804178_ 45804328_ 45800062_ 45800183_0.232,1.0	-0.508	Down	0.000882 74	0.02583 8286
SLC39A11	A5SS	ENSG00000133195_SLC39A11_17_-_ 70943869_ 70944014_ 70943890_ 70944014_ 70845772_ 70845943_0.367,0.118	0.313	Up	0.000917 45	0.02642 2656
RBMS2	A5SS	ENSG00000076067_RBMS2_12_+_ 56981337_ 56981448_ 56981337_ 56981443_ 56982077_ 56982158_0.0,0.326	0.595	Up	0.001053 22	0.02915 7551
RPS6KL1	A5SS	ENSG00000198208_RPS6KL1_14_-_ 75375803_ 75376851_ 75376245_ 75376851_ 75375552_ 75375635_0.107,1.0	0.447	Up	0.001235	0.03322 2834
ELMOD3	A5SS	ENSG00000115459_ELMOD3_2_+_ 85598208_ 85598685_ 85598208_ 85598332_ 85604466_ 85604597_0.22,0.0	0.589	Up	0.001253 34	0.03334 9614
FAM86B1	A5SS	ENSG00000186523_FAM86B1_8_-_ 12051385_ 12051591_ 12051483_ 12051591_ 12049287_ 12049350_0.54,0.227	0.617	Up	0.001422 72	0.03705 1247
NECAP2	A5SS	ENSG00000157191_NECAP2_1_+_ 16775587_ 16778510_ 16775587_ 16775696_ 16782312_ 16782388_1.0,0.18	0.41	Up	0.001478 22	0.03750 4445
KAT6B	A5SS	ENSG00000156650_KAT6B_10_+_ 76741544_ 76744999_ 76741544_ 76741686_ 76748776_ 76748870_1.0,1.0	-0.384	Down	0.001552 56	0.03800 6669
KLK4	A5SS	ENSG00000167749_KLK4_19_-_ 51411614_ 51412085_ 51411834_ 51412085_ 51410189_ 51410342_0.657,0.481	-0.207	Down	0.001594 94	0.03824 6239
U2SURP	A5SS	ENSG00000163714_U2SURP_3_+_142740191_142740227_142740191_142740224_142740314_142740397_0.704,0.62	-0.255	Down	0.001581 23	0.03824 6239
CTNND1	A5SS	ENSG00000198561_CTNND1_11_+_ 57529268_ 57529591_ 57529268_ 57529540_ 57561481_ 57561553_1.0,0.921	-0.241	Down	0.001609 22	0.03824 6239
PARD3	A5SS	ENSG00000148498_PARD3_10_-_ 34626202_ 34626354_ 34626205_ 34626354_ 34625126_ 34625171_1.0,0.329	-0.5	Down	0.001695 36	0.03915 3271
RNF146	A5SS	ENSG00000118518_RNF146_6_+_127588027_127588240_127588027_127588070_127601375_127601485_0.184,0.231	-0.208	Down	0.001758 81	0.03968 7137
SGK494	A5SS	ENSG00000167524_SGK494_17_-_ 26938410_ 26938674_ 26938584_ 26938674_ 26938160_ 26938271_1.0,1.0	-0.314	Down	0.001781 23	0.03968 7137
USP32	A5SS	ENSG00000170832_USP32_17_-_ 58296988_ 58297148_ 58297030_ 58297148_ 58291980_ 58292135_0.237,0.363	0.221	Up	0.001858 51	0.04026 226
SDR39U1	A5SS	ENSG00000100445_SDR39U1_14_-_ 24911314_ 24911466_ 24911383_ 24911466_ 24909988_ 24910132_1.0,0.401	-0.428	Down	0.002051 43	0.04366 869
HPS1	A5SS	ENSG00000107521_HPS1_10_-_100193696_100193848_100193739_100193848_100190887_100191048_0.0,0.179	0.279	Up	0.002149 02	0.04535 1676
SCAPER	A5SS	ENSG00000140386_SCAPER_15_-_ 77087581_ 77087781_ 77087620_ 77087781_ 77067195_ 77067458_0.281,0.143	-0.212	Down	0.002385 83	0.04851 0638
ZNF384	A5SS	ENSG00000126746_ZNF384_12_-_ 6798263_ 6798676_ 6798533_ 6798676_ 6797332_ 6797392_1.0,1.0	-0.305	Down	0.002417 61	0.04851 0638
CAPN10	A5SS	ENSG00000142330_CAPN10_2_+_241530231_241530428_241530231_241530417_241531349_241531567_0.65,0.764	0.293	Up	0.002479 11	0.04894 2331
MBD5	A5SS	ENSG00000204406_MBD5_2_+_149240678_149241704_149240678_149241005_149243310_149243519_1.0,1.0	-0.325	Down	0.002461 11	0.04894 2331
NUP54	RI	ENSG00000138750_NUP54_4_-_ 77038816_ 77039347_ 77038816_ 77038895_ 77039227_ 77039347_1.0,1.0	-0.955	Down	2.94E-12	8.94E-09
ADC	RI	ENSG00000142920_ADC_1_+_ 33583502_ 33586131_ 33583502_ 33583717_ 33585644_ 33586131_1.0,1.0	-1	Down	2.72E-10	4.15E-07
RHOT2	RI	ENSG00000140983_RHOT2_16_+_ 718655_ 720175_ 718655_ 718699_ 720122_ 720175_1.0,1.0	-0.743	Down	6.94E-10	5.28E-07
MTO1	RI	ENSG00000135297_MTO1_6_+_ 74189658_ 74190090_ 74189658_ 74189849_ 74190015_ 74190090_0.0,0.0	0.789	Up	5.98E-10	5.28E-07
B4GALNT1	RI	ENSG00000135454_B4GALNT1_12_-_ 58021400_ 58022045_ 58021400_ 58021674_ 58021904_ 58022045_0.0,0.0	1	Up	2.70E-09	1.65E-06
ZNF598	RI	ENSG00000167962_ZNF598_16_-_ 2052521_ 2053729_ 2052521_ 2052733_ 2053616_ 2053729_1.0,1.0	-0.601	Down	9.90E-08	4.31E-05

TMEM147	RI	ENSG00000105677_TMEM147_19_+_ 36037573_ 36038142_ 36037573_ 36037710_ 36038020_ 36038142_0.623,0.513	0.432	Up	2.01E-07	7.65E-05
BEST1	RI	ENSG00000167995_BEST1_11_+_ 61725617_ 61727050_ 61725617_ 61725770_ 61726969_ 61727050_1.0,1.0	-0.785	Down	2.90E-07	9.82E-05
EME2	RI	ENSG00000197774_EME2_16_+_ 1825041_ 1825409_ 1825041_ 1825133_ 1825315_ 1825409_1.0,1.0	-0.656	Down	4.07E-07	0.00012 3849
ABCD4	RI	ENSG00000119688_ABCD4_14_-_ 74759450_ 74759951_ 74759450_ 74759572_ 74759856_ 74759951_0.273,0.18	-0.217	Down	2.51E-06	0.00069 4062
HMBS	RI	ENSG00000256269_HMBS_11_+_118959344_118959841_118959344_1 18959558_118959791_118959841_1.0,1.0	-0.54	Down	2.88E-06	0.00072 9566
EXOSC8	RI	ENSG00000120699_EXOSC8_13_+_ 37577070_ 37578698_ 37577070_ 37577144_ 37578613_ 37578698_1.0,1.0	-0.693	Down	3.17E-06	0.00074 3572
NSUN5P1	RI	ENSG00000223705_NSUN5P1_7_+_ 75042066_ 75044301_ 75042066_ 75042210_ 75044162_ 75044301_1.0,0.0	0.5	Up	3.93E-06	0.00085 4722
CLK1	RI	ENSG00000013441_CLK1_2_-_201724402_201726189_201724402_201724469_201725960_201726189_1.0,0.839	-0.566	Down	5.90E-06	0.00119 7648
ZNF276	RI	ENSG00000158805_ZNF276_16_+_ 89789544_ 89790117_ 89789544_ 89789591_ 89789667_ 89790117_0.0,0.047	0.225	Up	6.93E-06	0.00131 975
CASKIN2	RI	ENSG00000177303_CASKIN2_17_-_ 73499469_ 73499841_ 73499469_ 73499608_ 73499739_ 73499841_0.114,0.0	0.44	Up	8.47E-06	0.00149 9108
RSRC2	RI	ENSG00000111011_RSRC2_12_-_123003385_123005975_123003385_123003598_123005931_123005975_1.0,1.0	-0.871	Down	8.86E-06	0.00149 9108
OTUD5	RI	ENSG00000068308_OTUD5_X_-_ 48791736_ 48792140_ 48791736_ 48791885_ 48791968_ 48792140_1.0,1.0	-0.464	Down	2.24E-05	0.00296 3835
RBM3	RI	ENSG00000102317_RBM3_X_+_ 48433948_ 48434471_ 48433948_ 48434055_ 48434202_ 48434471_1.0,1.0	-0.406	Down	2.38E-05	0.00301 3639
DDX26B	RI	ENSG00000165359_DDX26B_X_+_134703261_134706958_134703261_1 34703356_134706739_134706958_0.019,1.0	0.491	Up	2.72E-05	0.00331 0828
GPT	RI	ENSG00000167701_GPT_8_+_145730153_145730514_145730153_1457 30262_145730380_145730514_0.764,0.289	0.474	Up	2.88E-05	0.00336 7982
MAP4K2	RI	ENSG00000168067_MAP4K2_11_-_ 64564746_ 64565006_ 64564746_ 64564852_ 64564972_ 64565006_0.041,0.137	0.22	Up	3.49E-05	0.00353 5579
PGAP1	RI	ENSG00000197121_PGAP1_2_-_197711726_197712761_197711726_197711924_197712670_197712761_0.386,0.136	-0.261	Down	3.56E-05	0.00353 5579
ROBO3	RI	ENSG00000154134_ROBO3_11_+_124747414_124748027_124747414_ 124747648_124747832_124748027_1.0,1.0	-0.586	Down	3.45E-05	0.00353 5579
NARFL	RI	ENSG00000103245_NARFL_16_-_ 780842_ 782900_ 780842_ 781000_ 782300_ 782900_1.0,1.0	-0.553	Down	4.16E-05	0.00395 6292
CUTA	RI	ENSG00000112514_CUTA_6_-_ 33384873_ 33385087_ 33384873_ 33384919_ 33385023_ 33385087_1.0,1.0	-0.338	Down	4.69E-05	0.00432 5253
WASH4P	RI	ENSG00000234769_WASH4P_16_-_ 66915_ 67427_ 66915_ 67051_ 67290_ 67427_0.424,1.0	-0.712	Down	5.83E-05	0.00471 1769
AP1G2	RI	ENSG00000213983_AP1G2_14_-_ 24035024_ 24035369_ 24035024_ 24035101_ 24035272_ 24035369_0.06,0.3	0.379	Up	6.95E-05	0.00529 2631
SLC10A3	RI	ENSG00000126903_SLC10A3_X_-_153718645_153719002_153718645_153718697_153718932_153719002_1.0,1.0	-0.539	Down	7.24E-05	0.00537 4709
NDUFV1	RI	ENSG00000167792_NDUFV1_11_+_ 67375870_ 67376193_ 67375870_ 67375949_ 67376030_ 67376193_1.0,1.0	-0.234	Down	7.91E-05	0.00565 8202
HCG18	RI	ENSG00000231074_HCG18_6_-_ 30258782_ 30262741_ 30258782_ 30260376_ 30262247_ 30262741_1.0,1.0	-0.484	Down	8.39E-05	0.00580 602
TMEM256-PLSCR3	RI	ENSG00000187838_TMEM256-PLSCR3_17_-_ 7296919_ 7297586_ 7296919_ 7297155_ 7297422_ 7297586_0.0,0.0	0.593	Up	0.000110 18	0.00745 5524
SYTL1	RI	ENSG00000142765_SYTL1_1_+_ 27675888_ 27676256_ 27675888_ 27675989_ 27676142_ 27676256_0.388,0.323	0.557	Up	0.000114 42	0.00747 2626
QKI	RI	ENSG00000112531_QKI_6_+_163984451_163991177_163984451_1639 84751_163986977_163991177_0.746,0.738	-0.337	Down	0.000161 14	0.00994 1709

MSTO1	RI	ENSG00000125459_MSTO1_1_+_155581006_155581394_155581006_155581146_155581339_155581394_1.0,1.0	-0.222	Down	0.00017381	0.010177852
SNX16	RI	ENSG00000104497_SNX16_8_-_82751846_82752317_82751846_82751986_82752073_82752317_1.0,1.0	-0.209	Down	0.00018617	0.010498115
NOL3	RI	ENSG00000140939_NOL3_16_+_67208064_67208847_67208064_67208367_67208523_67208847_0.0,0.0	0.268	Up	0.00026998	0.01417397
LYPD3	RI	ENSG00000124466_LYPD3_19_-_43967277_43967921_43967277_43967439_43967750_43967921_1.0,1.0	-0.436	Down	0.00044091	0.020342193
B4GALNT1	RI	ENSG00000135454_B4GALNT1_12_-_58021400_58022045_58021400_58021641_58021904_58022045_0.0,0.0	0.244	Up	0.00049383	0.021792868
MITD1	RI	ENSG00000158411_MITD1_2_-_99785725_99786073_99785725_99785933_99786012_99786073_1.0,0.641	-0.579	Down	0.00054074	0.023190847
GGA3	RI	ENSG00000125447_GGA3_17_-_73236422_73237138_73236422_73236493_73236892_73237138_0.205,0.341	-0.249	Down	0.00068183	0.025698707
GMPPA	RI	ENSG00000144591_GMPPA_2_+_220370179_220370483_220370179_220370277_220370416_220370483_1.0,1.0	-0.207	Down	0.00074717	0.025698707
ZFC3H1	RI	ENSG00000133858_ZFC3H1_12_-_72050122_72051081_72050122_72050343_72050664_72051081_1.0,1.0	-0.353	Down	0.00075113	0.025698707
SCARB1	RI	ENSG00000073060_SCARB1_12_-_125267228_125271049_125267228_125267357_125270986_125271049_1.0,1.0	-0.342	Down	0.00067127	0.025698707
COMTD1	RI	ENSG00000165644_COMTD1_10_-_76994695_76994936_76994695_76994750_76994817_76994936_1.0,0.643	-0.677	Down	0.00071795	0.025698707
DRG2	RI	ENSG00000108591_DRG2_17_+_18002330_18003749_18002330_18002391_18003676_18003749_1.0,0.207	0.396	Up	0.00071099	0.025698707
SBNO2	RI	ENSG00000064932_SBNO2_19_-_1109133_1109597_1109133_1109210_1109504_1109597_1.0,1.0	-0.286	Down	0.0007396	0.025698707
PRPF39	RI	ENSG00000185246_PRPF39_14_+_45565626_45565961_45565626_45565695_45565798_45565961_1.0,1.0	-0.283	Down	0.00069634	0.025698707
CDK5RAP3	RI	ENSG00000108465_CDK5RAP3_17_+_46048487_46048773_46048487_46048518_46048727_46048773_0.062,0.166	0.334	Up	0.00079578	0.026923852
SNHG14	RI	ENSG00000224078_SNHG14_15_+_25349005_25351441_25349005_25349117_25351310_25351441_1.0,1.0	-0.56	Down	0.00127796	0.038150771
C19orf24	RI	ENSG00000228300_C19orf24_19_+_1276091_1277298_1276091_1276672_1277181_1277298_1.0,1.0	-0.33	Down	0.00147825	0.041599891
USE1	RI	ENSG00000053501_USE1_19_+_17326610_17326879_17326610_17326660_17326800_17326879_0.599,0.199	-0.348	Down	0.00159587	0.043778679
GALT	RI	ENSG00000213930_GALT_9_+_34647085_34647958_34647085_34647255_34647828_34647958_1.0,0.854	-0.227	Down	0.00167546	0.045551509
FAM133B	RI	ENSG00000234545_FAM133B_7_-_92206968_92207496_92206968_92206990_92207463_92207496_0.312,0.476	0.606	Up	0.00189848	0.048990 5
C11orf65	MXE	ENSG00000166323_C11orf65_11_-_108277822_108277876_108302472_108302565_108277489_108277690_108332205	-1	Down	3.95E-10	6.88E-07
AC093838.4	MXE	ENSG00000152117_AC093838.4_2_+_132254782_132254866_132256439_132256526_132250648_132250713_132257776	0.835	Up	4.84E-10	6.88E-07
TBCD	MXE	ENSG00000141556_TBCD_17_+_80851422_80851508_80863811_80863929_80842020_80842078_80869633	-0.93	Down	1.76E-10	6.88E-07
SNX10	MXE	ENSG00000086300_SNX10_7_+_26393676_26393804_26396626_26396747_26386039_26386086_26400594	0.873	Up	7.26E-10	7.75E-07
HNF4G	MXE	ENSG00000164749_HNF4G_8_+_76456045_76456214_76459821_76459916_76402323_76402443_76463622	-0.872	Down	2.72E-09	2.32E-06
IKBKB	MXE	ENSG00000104365_IKBKB_8_+_42129600_42129723_42146151_42146246_42128835_42128987_42147673	-0.799	Down	8.76E-09	6.24E-06
PAQR3	MXE	ENSG00000163291_PAQR3_4_-_79843294_79843575_79843982_79844137_79841687_79841835_79845010	-0.577	Down	1.11E-08	6.79E-06
RNF121	MXE	ENSG00000137522_RNF121_11_+_71673197_71673335_71689131_71689281_71671795_71671937_71693806	0.855	Up	1.37E-08	7.30E-06

EGF	MXE	ENSG00000138798_EGF_4_+_110920834_110921002_110925660_110925778_110915888_110916036_110932357	-0.563	Down	8.86E-08	4.20E-05
TMEM87A	MXE	ENSG00000103978_TMEM87A_15_-_42523389_42523458_42524041_42524113_42520909_42521018_42525410	0.218	Up	9.88E-08	4.22E-05
SFMBT1	MXE	ENSG00000163935_SFMBT1_3_-_52988332_52988427_53003116_53003274_52977368_52977609_53077151	0.35	Up	2.15E-07	8.34E-05
TBC1D1	MXE	ENSG00000065882_TBC1D1_4_+_38053519_38053681_38054726_38054846_38051238_38051519_38055819	-0.641	Down	3.00E-07	0.000106587
FAM86C1	MXE	ENSG00000158483_FAM86C1_11_+_71502784_71502865_71504425_71504527_71500828_71500891_71507062	0.799	Up	3.57E-07	0.000108713
CDKL3	MXE	ENSG00000006837_CDKL3_5_-_133685939_133686118_133695587_133695782_133657481_133657594_133706688	0.538	Up	3.46E-07	0.000108713
CD99L2	MXE	ENSG00000102181_CD99L2_X_-_149984751_149984928_149996778_149998077_149984479_149984551_149999703	0.848	Up	1.00E-06	0.000285628
KLC4	MXE	ENSG00000137171_KLC4_6_+_43039304_43039357_43039589_43039660_43039012_43039112_43039884	-0.622	Down	1.30E-06	0.000339195
SS18	MXE	ENSG00000141380_SS18_18_-_23660268_23660387_23664015_23664139_23658039_23658124_23667464	-0.534	Down	1.50E-06	0.000355586
PICK1	MXE	ENSG00000100151_PICK1_22_+_38466844_38466898_38467688_38467751_38465039_38465129_38468483	0.485	Up	2.24E-06	0.000503036
PGAP3	MXE	ENSG00000161395_PGAP3_17_-_37830869_37830932_37840849_37841002_37827374_37829119_37842174	0.28	Up	7.12E-06	0.001382047
LGMN	MXE	ENSG00000100600_LGMN_14_-_93207406_93207524_93208049_93208204_93198993_93199160_93214833	0.524	Up	8.86E-06	0.001645266
SS18	MXE	ENSG00000141380_SS18_18_-_23658974_23659110_23660268_23660387_23658039_23658124_23667464	0.51	Up	1.04E-05	0.001858621
SS18	MXE	ENSG00000141380_SS18_18_-_23658974_23659089_23660268_23660387_23658039_23658124_23667464	0.498	Up	1.58E-05	0.002591643
TOP3B	MXE	ENSG00000100038_TOP3B_22_-_22322990_22323147_22326248_22326323_22321974_22322088_22326983	-0.375	Down	1.70E-05	0.002680038
ANKRD30A	MXE	ENSG00000148513_ANKRD30A_10_+_37442499_37442590_37478394_37478485_37440987_37441049_37481991	-0.365	Down	1.91E-05	0.002906826
MIS18BP1	MXE	ENSG00000129534_MIS18BP1_14_-_45701935_45702023_45705016_45705147_45700343_45700501_45706850	-0.231	Down	2.63E-05	0.003735758
CERS4	MXE	ENSG00000090661_CERS4_19_+_8275589_8275746_8315927_8316133_8274209_8274378_8319382	0.472	Up	2.94E-05	0.004041851
HDAC11	MXE	ENSG00000163517_HDAC11_3_+_13524963_13525064_13543370_13543433_13522745_13522894_13544383	-0.468	Down	3.30E-05	0.004406354
BBS1	MXE	ENSG00000174483_BBS1_11_+_66281876_66282149_66283010_66283057_66278675_66278710_66283163	-0.224	Down	3.99E-05	0.005004718
OSGEPL1	MXE	ENSG00000128694_OSGEPL1_2_-_190615275_190615382_190617378_190617450_190611385_190611894_190617574	-0.247	Down	5.88E-05	0.006972228
USP13	MXE	ENSG00000058056_USP13_3_+_179399665_179399791_179408028_179408089_179370837_179371181_179418795	-0.25	Down	8.55E-05	0.009363459
RNF115	MXE	ENSG00000121848_RNF115_1_+_145646278_145646469_145648015_145648067_145646114_145646173_145650482	0.665	Up	8.97E-05	0.009577285
CCDC14	MXE	ENSG00000175455_CCDC14_3_-_123665649_123666166_123667537_123667632_123663695_123663837_123667742	-0.235	Down	0.00010665	0.010588157
UBE2J2	MXE	ENSG00000160087_UBE2J2_1_-_1200162_1200210_1201477_1201670_1198725_1198766_1203241	-0.223	Down	0.00012462	0.010639683
PPAPDC1B	MXE	ENSG00000147535_PPAPDC1B_8_-_38125414_38125478_38125888_38125925_38124784_38124909_38126399	-0.203	Down	0.00012376	0.010639683
TTC23	MXE	ENSG00000103852_TTC23_15_-_99785593_99785715_99789826_99790004_99768737_99768937_99791359	-0.689	Down	0.00011892	0.010639683
ARNTL2	MXE	ENSG00000029153_ARNTL2_12_+_27523061_27523163_27529278_27529320_27521194_27521345_27533179	-0.274	Down	0.00014085	0.011563592

TAB3	MXE	ENSG00000157625_TAB3_X_-_ 30861082_ 30861166_ 30864667_ 30864761_ 30852167_ 30852269_ 30870894	-0.259	Down	0.000147 9	0.01185 4621
PRR5	MXE	ENSG00000186654_PRR5_22_+_ 45110470_ 45110551_ 45121123_ 45121172_ 45098371_ 45098488_ 45122456	0.282	Up	0.000149 95	0.01185 4621
RANBP9	MXE	ENSG00000010017_RANBP9_6_-_ 13644776_ 13644961_ 13652890_ 13652913_ 13641430_ 13641539_ 13657340	0.294	Up	0.000166 36	0.01224 4845
ZBTB8OS	MXE	ENSG00000176261_ZBTB8OS_1_-_ 33099245_ 33099328_ 33099551_ 33099673_ 33093108_ 33093145_ 33116029	0.205	Up	0.000180 42	0.01283 7124
MARCH8	MXE	ENSG00000165406_MARCH8_10_-_ 45959686_ 45959775_ 45984814_ 45984865_ 45956678_ 45956859_ 46028557	-0.331	Down	0.000179 38	0.01283 7124
TBC1D19	MXE	ENSG00000109680_TBC1D19_4_+_ 26641762_ 26641809_ 26661218_ 26661329_ 26640392_ 26640456_ 26667954	0.317	Up	0.000197 91	0.01385 0415
DBR1	MXE	ENSG00000138231_DBR1_3_-_137882619_137882700_137885922_137886147_137882190_137882336_137888948	-0.299	Down	0.000203 21	0.01399 1929
HDAC8	MXE	ENSG00000147099_HDAC8_X_-_ 71787738_ 71787880_ 71788603_ 71788734_ 71715005_ 71715118_ 71791906	-0.274	Down	0.000211 12	0.01421 9938
TRDMT1	MXE	ENSG00000107614_TRDMT1_10_-_ 17203481_ 17203547_ 17210839_ 17210916_ 17202303_ 17202373_ 17216549	0.426	Up	0.000256 39	0.01644 909
DENND2C	MXE	ENSG00000175984_DENND2C_1_-_115164515_115164686_115165607_115165720_115161006_115161103_115166127	0.364	Up	0.000258 16	0.01644 909
PUS7	MXE	ENSG00000091127_PUS7_7_-_105111134_105111295_105112578_105112640_105108783_105108910_105121498	-0.229	Down	0.000305 85	0.01877 7486
MGLL	MXE	ENSG00000074416_MGLL_3_-_127413817_127414033_127429418_127429508_127410959_127411166_127439895	-0.46	Down	0.000350 38	0.02077 4724
C20orf96	MXE	ENSG00000196476_C20orf96_20_-_ 256608_ 256727_ 257433_ 257520_ 251503_ 251908_ 257684	0.248	Up	0.000369 22	0.02159 1902
PTPN20B	MXE	ENSG00000183675_PTPN20B_10_-_ 48754797_ 48755132_ 48774224_ 48774376_ 48751806_ 48752022_ 48792686	0.33	Up	0.000422 48	0.02337 1924
UBE2F	MXE	ENSG00000184182_UBE2F_2_+_238881733_238881867_238925207_238925275_238875721_238875774_238933982	-0.226	Down	0.000438 58	0.02340 3865
ZNF415	MXE	ENSG00000170954_ZNF415_19_-_ 53625656_ 53625865_ 53625914_ 53625996_ 53619565_ 53619686_ 53636108	-0.258	Down	0.000438 49	0.02340 3865
TMEM164	MXE	ENSG00000157600_TMEM164_X_+_109246728_109247392_109310574_109310624_109246322_109246384_109352307	-0.286	Down	0.000471 97	0.02457 1047
ASAP1	MXE	ENSG00000153317_ASAP1_8_-_131249167_131249240_131370262_131370389_131226801_131226947_131414130	-0.249	Down	0.000533 09	0.02690 1602
IST1	MXE	ENSG00000182149_IST1_16_+_ 71957190_ 71957283_ 71958675_ 71958720_ 71956376_ 71956583_ 71961516	0.24	Up	0.000564 52	0.02738 5756
ZFAND2B	MXE	ENSG00000158552_ZFAND2B_2_+_220072608_220072760_220072977_220073070_220072369_220072501_220073147	-0.35	Down	0.000579 47	0.02779 5101
SLC30A6	MXE	ENSG00000152683_SLC30A6_2_+_ 32431954_ 32432002_ 32434561_ 32434630_ 32429658_ 32429761_ 32445281	-0.248	Down	0.000642 98	0.02983 553
SRSF11	MXE	ENSG00000116754_SRSF11_1_+_ 70696777_ 70696886_ 70697541_ 70697658_ 70694104_ 70694238_ 70697950	0.339	Up	0.000705 28	0.03203 0422
OVGP1	MXE	ENSG00000085465_OVGP1_1_-_111963897_111964083_111964186_111964295_111962231_111962348_111965548	0.279	Up	0.000733 68	0.03262 6054
TNRC6A	MXE	ENSG00000090905_TNRC6A_16_+_ 24741573_ 24741621_ 24788253_ 24788679_ 24741033_ 24741167_ 24800552	0.295	Up	0.000732 1	0.03262 6054
SUN1	MXE	ENSG00000164828_SUN1_7_+_ 888054_ 888252_ 889559_ 889670_ 882977_ 883157_ 891020	0.237	Up	0.000756 66	0.03330 0692
BOK	MXE	ENSG00000176720_BOK_2_+_242501762_242501891_242509539_242509703_242498135_242498408_242511711	0.21	Up	0.000876 45	0.03563 4117
BORA	MXE	ENSG00000136122_BORA_13_+_ 73303063_ 73303231_ 73305418_ 73305525_ 73302060_ 73302145_ 73309097	-0.401	Down	0.001088 46	0.04076 0108

GUK1	MXE	ENSG00000143774_GUK1_1_+_228333713_228333768_228334542_228334639_228333211_228333325_228335315	0.291	Up	0.00111033	0.041217334
ADAM15	MXE	ENSG00000143537_ADAM15_1_+_155033893_155033965_155034379_155034593_155033238_155033308_155034720	-0.433	Down	0.00126144	0.0449702
ICA1L	MXE	ENSG00000163596_ICA1L_2_-_203653552_203653810_203661612_203661687_203650640_203650730_203676468	0.243	Up	0.00124726	0.0449702
DAG1	MXE	ENSG00000173402_DAG1_3_+_ 49508397_ 49508482_ 49530255_ 49530406_ 49507564_ 49507866_ 49547851	0.253	Up	0.0012641	0.0449702
XPNPEP1	MXE	ENSG00000108039_XPNPEP1_10_-_111652769_111652833_111667448_111667573_111651479_111651584_111674768	0.206	Up	0.00127955	0.045143644
ZNF467	MXE	ENSG00000181444_ZNF467_7_-_149466178_149466289_149467528_149467645_149461451_149463328_149468087	0.239	Up	0.00135433	0.046252954
SLC3A2	MXE	ENSG00000168003_SLC3A2_11_+_ 62649976_ 62650090_ 62650138_ 62650279_ 62649170_ 62649538_ 62650379	-0.285	Down	0.00138134	0.046432492
TMEM241	MXE	ENSG00000134490_TMEM241_18_-_ 20936557_ 20936627_ 20950179_ 20950225_ 20889643_ 20889708_ 20951385	0.365	Up	0.00137078	0.046432492

Supplementary Table 12.3: mRNA expression level of alternatively spliced genes following JMJD6 siRNA knockdown compared to non-targeting control siRNA.

Gene	Event Type	mRNA expression level (FPKM)		log2 fold change	p value	q value	significant
		Control siRNA	JMJD6 siRNA				
AASS	SE	4.71675	5.6038	0.25	0.30	0.82	no
ABCD4	RI	10.9504	8.67052	-0.34	0.29	0.81	no
ABHD2	SE	208.86	242.89	0.22	0.56	0.93	no
ABHD6	SE	8.70414	7.79742	-0.16	0.56	0.93	no
AC007405.6	A5SS	2.93556	3.84786	0.39	0.48	0.90	no
AC093838.4	MXE	3.80299	3.4731	-0.13	0.72	0.97	no
AC104667.3	SE	1.74211	1.33038	-0.39	0.64	0.95	no
ACIN1	SE	46.625	34.2067	-0.45	0.16	0.70	no
ACOT8	A3SS	6.79276	10.8335	0.67	0.08	0.53	no
ACSL1	SE	104.607	101.469	-0.04	0.81	0.98	no
ADC	RI	0.255328	0	NA	1.00	1.00	no
AFMID	SE	24.1841	24.5963	0.02	0.93	0.99	no
AFMID	SE	24.1841	24.5963	0.02	0.93	0.99	no
AFMID	SE	24.1841	24.5963	0.02	0.93	0.99	no
AFMID	SE	24.1841	24.5963	0.02	0.93	0.99	no
AGBL5	SE	22.3701	23.6535	0.08	0.79	0.98	no
AGR2	SE	12.5259	15.7974	0.33	0.26	0.79	no
AGTRAP	A3SS	98.2074	116.687	0.25	0.20	0.74	no
AHI1	SE	10.2687	12.2033	0.25	0.53	0.92	no
AKAP13	SE	19.0718	23.3399	0.29	0.54	0.92	no
ALDOA	SE	832.054	708.151	-0.23	0.21	0.75	no
ALDOA	SE	832.054	708.151	-0.23	0.21	0.75	no
ANAPC10	SE	10.0579	5.65255	-0.83	0.44	0.89	no
ANKMY1	SE	4.48723	3.7893	-0.24	0.72	0.97	no
ANKMY2	SE	6.00607	7.00062	0.22	0.39	0.86	no
ANKRD30A	MXE	3.5092	2.23827	-0.65	0.05	0.46	no
ANKS6	SE	1.54435	1.67219	0.11	0.83	0.98	no
AP1G1	SE	51.3626	55.9157	0.12	0.62	0.95	no
AP1G1	SE	51.3626	55.9157	0.12	0.62	0.95	no

ARHGAP12	SE	13.2971	17.5777	0.40	0.04	0.42	no
ARHGAP33	A3SS	4.84957	2.43935	-0.99	0.08	0.55	no
ARHGAP44	SE	8.68787	8.88176	0.03	0.90	0.99	no
ARHGAP44	SE	8.68787	8.88176	0.03	0.90	0.99	no
ARHGEF10	SE	3.39515	3.26476	-0.06	0.88	0.99	no
ARHGEF39	SE	7.80051	6.07011	-0.36	0.28	0.81	no
ARNTL2	SE	16.7455	12.9917	-0.37	0.13	0.65	no
ARNTL2	MXE	16.7455	12.9917	-0.37	0.13	0.65	no
ASAH2B	SE	15.5157	15.1939	-0.03	0.92	0.99	no
ASAH2B	SE	15.5157	15.1939	-0.03	0.92	0.99	no
ASAP1	SE	24.8825	18.739	-0.41	0.15	0.67	no
ASAP1	MXE	24.8825	18.739	-0.41	0.15	0.67	no
ASPM	SE	9.11541	10.8211	0.25	0.21	0.75	no
ATG2A	SE	7.53745	10.878	0.53	0.01	0.22	no
ATG2A	SE	7.53745	10.878	0.53	0.01	0.22	no
ATP11A	A3SS	0	0	0.00	1.00	1.00	no
ATP11A	A3SS	12.6956	15.3053	0.27	0.56	0.93	no
ATP11A	SE	0	0	0.00	1.00	1.00	no
ATP11A	SE	12.6956	15.3053	0.27	0.56	0.93	no
ATP11A	A3SS	0	0	0.00	1.00	1.00	no
ATP11A	A3SS	12.6956	15.3053	0.27	0.56	0.93	no
ATP2C1	SE	53.27	65.1864	0.29	0.24	0.78	no
ATP2C1	SE	53.27	65.1864	0.29	0.24	0.78	no
ATXN3	SE	15.7873	24.4099	0.63	0.01	0.17	no
B4GALNT1	RI	10.0978	9.1777	-0.14	0.64	0.95	no
B4GALNT1	RI	10.0978	9.1777	-0.14	0.64	0.95	no
B4GALNT1	SE	10.0978	9.1777	-0.14	0.64	0.95	no
B4GALNT4	SE	14.5948	9.02868	-0.69	0.08	0.53	no
BAD	SE	20.263	32.262	0.67	0.13	0.64	no
BAHD1	A3SS	5.19938	6.05465	0.22	0.34	0.85	no
BANP	SE	18.2514	15.569	-0.23	0.37	0.85	no
BANP	SE	18.2514	15.569	-0.23	0.37	0.85	no
BAZ2B	SE	7.27988	9.40323	0.37	0.45	0.89	no
BCAS3	SE	12.5662	24.5203	0.96	0.00	0.09	no
BCL2L12	SE	15.4712	19.1719	0.31	0.57	0.93	no
BCL6	SE	8.76322	8.62736	-0.02	0.94	0.99	no
BDP1	SE	16.7427	16.6093	-0.01	0.96	0.99	no
BEST1	RI	1.12623	3.31818	1.56	0.18	0.71	no
BIN1	SE	34.1038	27.4207	-0.31	0.15	0.68	no
BIRC5	SE	95.361	106.478	0.16	0.54	0.92	no
BOK	MXE	6.27738	8.03547	0.36	0.14	0.66	no
BOK	SE	6.27738	8.03547	0.36	0.14	0.66	no
BORA	MXE	3.75746	1.80801	-1.06	0.17	0.70	no
BRCA2	SE	9.98455	8.44833	-0.24	0.70	0.96	no
BRF1	A5SS	14.6918	11.9093	-0.30	0.52	0.92	no
BTN2A1	SE	10.3203	9.18998	-0.17	0.50	0.91	no
C11orf54	SE	22.2895	22.3012	0.00	1.00	1.00	no
C11orf65	SE	1.88343	3.74088	0.99	0.45	0.89	no
C11orf65	MXE	1.88343	3.74088	0.99	0.45	0.89	no
C14orf159	SE	3.93865	3.71922	-0.08	0.87	0.99	no
C16orf93	A3SS	2.10458	1.2784	-0.72	0.46	0.90	no
C19orf24	RI	139.521	117.551	-0.25	0.24	0.77	no
C19orf60	SE	6.74417	8.54418	0.34	0.68	0.96	no
C20orf96	MXE	9.85539	6.94575	-0.50	0.06	0.48	no
C3orf18	SE	2.01857	3.57567	0.82	0.17	0.70	no
C4orf29	SE	15.1728	12.2647	-0.31	0.46	0.89	no
C4orf36	SE	2.25316	2.60205	0.21	0.84	0.98	no
C5orf38	SE	7.13743	8.00924	0.17	0.73	0.97	no
C6orf52	SE	1.65291	2.23224	0.43	0.66	0.95	no
C9orf3	SE	4.0439	3.87731	-0.06	0.88	0.99	no

CAMTA1	SE	217.236	176.708	-0.30	0.14	0.67	no
CARF	SE	4.14513	5.76892	0.48	0.48	0.90	no
CARF	A3SS	4.14513	5.76892	0.48	0.48	0.90	no
CASKIN2	RI	5.23121	4.85401	-0.11	0.86	0.99	no
CBR3-AS1	SE	1.32227	1.57519	0.25	0.73	0.97	no
CBWD2	SE	33.3127	31.1896	-0.10	0.66	0.95	no
CBX7	A3SS	3.21588	4.24986	0.40	0.39	0.86	no
CCDC14	MXE	12.3093	14.5414	0.24	0.56	0.93	no
CCDC148	SE	2.42832	2.03318	-0.26	0.61	0.95	no
CCDC15	SE	5.78012	6.31299	0.13	0.65	0.95	no
CCDC171	SE	3.03865	2.34667	-0.37	0.42	0.88	no
CCDC43	SE	51.0106	52.3839	0.04	0.85	0.98	no
CCDC84	A5SS	3.65826	4.77225	0.38	0.76	0.97	no
CCDC88A	A3SS	7.29211	8.2717	0.18	0.46	0.89	no
CCNL2	A3SS	25.8051	28.6817	0.15	0.52	0.92	no
CCNL2	A5SS	25.8051	28.6817	0.15	0.52	0.92	no
CD46	A5SS	129.358	151.183	0.22	0.50	0.91	no
CD99L2	MXE	4.95654	5.76006	0.22	0.47	0.90	no
CDC14B	SE	2.76618	1.51915	-0.86	0.14	0.66	no
CDK20	SE	10.5031	8.31413	-0.34	0.17	0.70	no
CDK20	A5SS	10.5031	8.31413	-0.34	0.17	0.70	no
CENPE	SE	8.07675	8.09151	0.00	0.99	1.00	no
CENPK	SE	21.7903	18.6389	-0.23	0.36	0.85	no
CEP57L1	A3SS	7.94996	6.96483	-0.19	0.47	0.90	no
CEP57L1	SE	7.94996	6.96483	-0.19	0.47	0.90	no
CEP57L1	SE	7.94996	6.96483	-0.19	0.47	0.90	no
CERS4	MXE	12.309	14.1843	0.20	0.43	0.88	no
CHCHD4	SE	43.0702	38.976	-0.14	0.47	0.90	no
CHMP4C	SE	4.50146	4.46049	-0.01	0.98	1.00	no
CIC	A3SS	10.6981	15.5753	0.54	0.14	0.66	no
CLHC1	SE	3.99015	2.63202	-0.60	0.53	0.92	no
CLK1	RI	17.9065	19.7561	0.14	0.53	0.92	no
CLK3	A5SS	33.3694	29.4834	-0.18	0.57	0.93	no
CLPTM1L	A5SS	238.476	274.702	0.20	0.37	0.85	no
CLTCL1	SE	1.3457	1.84929	0.46	0.48	0.90	no
CLTCL1	A3SS	1.3457	1.84929	0.46	0.48	0.90	no
CMC2	SE	97.2579	101.37	0.06	0.90	0.99	no
CMC2	SE	97.2579	101.37	0.06	0.90	0.99	no
CMC2	SE	97.2579	101.37	0.06	0.90	0.99	no
CNOT2	SE	77.7404	58.7748	-0.40	0.31	0.82	no
COBL	SE	11.3292	7.56125	-0.58	0.04	0.39	no
COL4A5	SE	15.7889	18.842	0.26	0.36	0.85	no
COMTD1	RI	20.5664	20.1376	-0.03	0.92	0.99	no
CTC1	SE	28.1343	27.2606	-0.05	0.93	0.99	no
CUTA	RI	94.2181	112.945	0.26	0.37	0.85	no
CXADR	SE	22.5291	19.7687	-0.19	0.53	0.92	no
CXorf38	SE	18.6166	14.5181	-0.36	0.12	0.64	no
DAG1	MXE	57.2809	58.8871	0.04	0.82	0.98	no
DBF4B	SE	6.59538	8.13602	0.30	0.34	0.84	no
DBR1	MXE	15.6041	14.4961	-0.11	0.62	0.95	no
DCLRE1C	SE	10.8523	6.16397	-0.82	0.10	0.59	no
DDX26B	RI	2.73679	4.07606	0.57	0.06	0.49	no
DDX55	SE	12.2916	11.3742	-0.11	0.82	0.98	no
DENND2C	MXE	6.16306	7.89558	0.36	0.13	0.65	no
DESI2	A3SS	43.8724	24.0017	-0.87	0.00	0.01	yes
DET1	SE	0	0	0.00	1.00	1.00	no
DIP2A	SE	6.0569	6.44943	0.09	0.72	0.97	no
DIP2A	SE	6.0569	6.44943	0.09	0.72	0.97	no
DLGAP4	SE	24.0901	26.2852	0.13	0.84	0.98	no
DMTF1	SE	12.8579	10.532	-0.29	0.34	0.84	no

DMXL2	A3SS	6.08537	7.68855	0.34	0.17	0.71	no
DNAH14	SE	39.6868	35.5598	-0.16	0.58	0.94	no
DNASE1L1	SE	12.2669	22.435	0.87	0.20	0.74	no
DOPEY1	SE	11.4601	7.84767	-0.55	0.55	0.93	no
DPH7	SE	6.26558	5.20446	-0.27	0.40	0.87	no
DPM1	SE	98.8748	75.0177	-0.40	0.37	0.85	no
DPY19L2P1	SE	1.40017	1.98394	0.50	0.26	0.79	no
DRG2	A3SS	22.9346	26.3972	0.20	0.45	0.89	no
DRG2	RI	22.9346	26.3972	0.20	0.45	0.89	no
DSN1	SE	20.5127	17.297	-0.25	0.24	0.78	no
DZANK1	SE	0.999571	1.02287	0.03	1.00	1.00	no
ECHDC2	SE	11.1926	14.1062	0.33	0.32	0.83	no
EEF1D	SE	151.436	127.142	-0.25	0.32	0.83	no
EGF	MXE	12.5317	14.6657	0.23	0.39	0.86	no
EGF	SE	12.5317	14.6657	0.23	0.39	0.86	no
EGF	SE	12.5317	14.6657	0.23	0.39	0.86	no
ELMOD3	A5SS	5.23495	8.69409	0.73	0.27	0.80	no
ELMOD3	A5SS	5.23495	8.69409	0.73	0.27	0.80	no
ELMOD3	A5SS	5.23495	8.69409	0.73	0.27	0.80	no
ELMOD3	A5SS	5.23495	8.69409	0.73	0.27	0.80	no
ELP2	SE	54.2802	44.6354	-0.28	0.37	0.85	no
EME2	RI	4.05027	4.69512	0.21	0.86	0.98	no
EML3	A3SS	7.04556	9.79932	0.48	0.20	0.73	no
ENDOV	SE	2.86558	1.71298	-0.74	0.25	0.79	no
ENOX2	SE	11.2779	16.5642	0.55	0.03	0.35	no
ERBB2IP	SE	50.2159	56.3211	0.17	0.39	0.86	no
ESPL1	SE	13.8234	11.9945	-0.20	0.39	0.86	no
EXO5	SE	6.70147	7.09097	0.08	0.79	0.98	no
EXO5	SE	6.70147	7.09097	0.08	0.79	0.98	no
EXOSC8	RI	47.8671	31.6344	-0.60	0.09	0.56	no
EXTL2	SE	8.19924	8.43907	0.04	0.86	0.98	no
FAAH2	SE	8.5958	4.58958	-0.91	0.10	0.58	no
FAM133B	RI	3.07799	4.15426	0.43	0.43	0.88	no
FAM160A1	SE	11.586	14.054	0.28	0.35	0.85	no
FAM173A	SE	24.5648	25.613	0.06	0.91	0.99	no
FAM193B	SE	11.6763	17.9986	0.62	0.15	0.68	no
FAM195A	SE	44.2487	37.1921	-0.25	0.25	0.78	no
FAM222B	SE	22.3342	30.8278	0.46	0.23	0.77	no
FAM86A	SE	13.5858	10.4734	-0.38	0.64	0.95	no
FAM86B1	A5SS	1.11191	2.61702	1.23	0.03	0.37	no
FAM86C1	MXE	4.65572	4.9701	0.09	0.80	0.98	no
FAM86C2P	SE	1.12078	0.571392	-0.97	1.00	1.00	no
FCF1	A3SS	17.4991	14.4773	-0.27	0.33	0.84	no
FER	SE	6.44574	7.2211	0.16	0.73	0.97	no
FGFR2	SE	1.46927	2.71997	0.89	0.04	0.43	no
FHOD3	SE	1.47216	1.92411	0.39	0.69	0.96	no
FKBP7	A3SS	6.74856	7.51671	0.16	0.68	0.96	no
FNBP1	A3SS	12.8287	7.18274	-0.84	0.03	0.36	no
FOXM1	SE	102.249	62.8092	-0.70	0.06	0.48	no
FOXP1	A3SS	14.2924	16.9137	0.24	0.31	0.82	no
FUK	SE	8.31195	4.47264	-0.89	0.04	0.40	no
GAA	SE	22.8276	24.0142	0.07	0.80	0.98	no
GAB1	SE	6.04928	5.69193	-0.09	0.85	0.98	no
GALE	A5SS	13.6987	10.0697	-0.44	0.08	0.55	no
GBA	SE	102.81	139.611	0.44	0.04	0.40	no
GGA3	SE	19.2423	16.9523	-0.18	0.70	0.96	no
GGA3	RI	19.2423	16.9523	-0.18	0.70	0.96	no
GGCT	SE	406.775	368.324	-0.14	0.60	0.94	no
GLS	SE	26.1972	48.012	0.87	0.03	0.38	no
GMIP	SE	5.43856	5.78634	0.09	0.75	0.97	no

GMIP	A5SS	5.43856	5.78634	0.09	0.75	0.97	no
GMIP	A3SS	5.43856	5.78634	0.09	0.75	0.97	no
GMPPA	RI	27.7284	27.2545	-0.02	0.91	0.99	no
GNB1	SE	381.789	399.975	0.07	0.82	0.98	no
GOLGA2	SE	10.6973	9.34274	-0.20	0.73	0.97	no
GOLIM4	SE	25.2667	26.2565	0.06	0.77	0.97	no
GORAB	SE	5.52927	5.93174	0.10	0.71	0.97	no
GPNMB	A3SS	18.5359	21.9765	0.25	0.32	0.83	no
GPR98	SE	3.30525	5.78481	0.81	0.19	0.73	no
GPT	RI	0.403824	1.73929	2.11	0.09	0.56	no
GRK5	SE	1.62381	2.82755	0.80	0.05	0.45	no
GTDC1	SE	10.7027	14.9921	0.49	0.16	0.69	no
GTF2IRD1	A3SS	18.214	19.7742	0.12	0.76	0.97	no
GUK1	MXE	329.782	298.824	-0.14	0.46	0.90	no
HDAC11	MXE	4.98096	10.2091	1.04	0.03	0.34	no
HDAC8	MXE	16.5138	17.9133	0.12	0.64	0.95	no
HDLBP	A5SS	383.461	412.285	0.10	0.74	0.97	no
HDLBP	SE	383.461	412.285	0.10	0.74	0.97	no
HDLBP	A5SS	383.461	412.285	0.10	0.74	0.97	no
HDLBP	A5SS	383.461	412.285	0.10	0.74	0.97	no
HDX	SE	5.44256	5.0944	-0.10	0.77	0.97	no
HELB	SE	4.95996	3.8028	-0.38	0.14	0.66	no
HERC2P3	SE	11.4943	10.7073	-0.10	0.75	0.97	no
HERC2P3	SE	11.4943	10.7073	-0.10	0.75	0.97	no
HERC3	SE	70.8088	72.1824	0.03	0.90	0.99	no
HIST1H2BJ	SE	503.76	319.536	-0.66	0.00	0.04	yes
HMBS	RI	84.7645	61.1709	-0.47	0.07	0.51	no
HMGN1	SE	261.464	213.833	-0.29	0.29	0.81	no
HNF4G	MXE	1.39722	1.89836	0.44	0.49	0.91	no
HNRNPDL	SE	92.9038	47.5749	-0.97	0.00	0.01	yes
HPS1	A5SS	13.1502	14.8478	0.18	0.54	0.92	no
HSD17B1	A3SS	1.784	2.08991	0.23	0.88	0.99	no
ICA1L	MXE	6.91096	8.36845	0.28	0.42	0.88	no
IFT122	SE	10.8559	9.10485	-0.25	0.48	0.90	no
IKBKB	MXE	7.62018	5.01691	-0.60	0.11	0.61	no
IKBKG	SE	8.1193	8.83903	0.12	0.89	0.99	no
IL15RA	SE	1.3969	1.29608	-0.11	1.00	1.00	no
IL15RA	SE	1.3969	1.29608	-0.11	1.00	1.00	no
ILF3	SE	215.141	157.156	-0.45	0.09	0.57	no
IQCH	SE	2.41581	2.22394	-0.12	0.89	0.99	no
IRAK4	SE	12.6567	14.3743	0.18	0.46	0.89	no
IRF3	SE	22.4482	15.0055	-0.58	0.24	0.78	no
IRF3	SE	22.4482	15.0055	-0.58	0.24	0.78	no
IRF3	SE	22.4482	15.0055	-0.58	0.24	0.78	no
IRF7	A3SS	5.09736	4.30495	-0.24	0.46	0.90	no
ITPR1	A5SS	3.72894	3.5337	-0.08	0.86	0.98	no
JADE2	SE	8.89683	6.40132	-0.47	0.08	0.55	no
KANSL2	SE	32.0581	43.1158	0.43	0.12	0.61	no
KAT6B	A5SS	9.99903	11.7986	0.24	0.22	0.76	no
KCNAB2	SE	7.72408	9.80737	0.34	0.41	0.87	no
KCNG1	SE	1.40049	2.59244	0.89	0.09	0.56	no
KIAA1191	SE	76.2189	60.3316	-0.34	0.14	0.65	no
KIAA1958	SE	8.53828	7.77729	-0.13	0.76	0.97	no
KIF9	SE	15.6849	11.8602	-0.40	0.45	0.89	no
KLC4	MXE	2.31082	3.72369	0.69	0.31	0.82	no
KLHDC10	SE	26.8001	29.317	0.13	0.70	0.96	no
KLHDC9	SE	6.69499	6.47064	-0.05	0.90	0.99	no
KLK4	SE	97.4664	96.246	-0.02	0.93	0.99	no
KLK4	A5SS	97.4664	96.246	-0.02	0.93	0.99	no
L3MBTL3	SE	8.20912	5.50213	-0.58	0.12	0.63	no

LEF1	SE	19.5718	13.8115	-0.50	0.07	0.53	no
LEF1	SE	19.5718	13.8115	-0.50	0.07	0.53	no
LETMD1	SE	19.3236	24.9884	0.37	0.15	0.69	no
LGMN	MXE	27.1435	26.0198	-0.06	0.82	0.98	no
LIMCH1	SE	120.163	148.272	0.30	0.25	0.78	no
LIMCH1	SE	120.163	148.272	0.30	0.25	0.78	no
LIMCH1	SE	120.163	148.272	0.30	0.25	0.78	no
LIMK2	SE	9.48231	9.84379	0.05	0.86	0.99	no
LIN7A	SE	4.17644	4.73439	0.18	0.59	0.94	no
LIN9	SE	14.7665	14.2739	-0.05	0.81	0.98	no
LPCAT4	SE	3.55463	2.77828	-0.36	0.40	0.87	no
LPHN1	SE	37.2896	39.4958	0.08	0.80	0.98	no
LPP	SE	65.4074	76.0136	0.22	0.58	0.94	no
LPXN	SE	4.65798	6.15184	0.40	0.20	0.74	no
LRP5	SE	28.7732	21.9058	-0.39	0.06	0.48	no
LSM14B	SE	29.6989	25.791	-0.20	0.35	0.85	no
LYPD3	RI	1.38091	1.03246	-0.42	1.00	1.00	no
MACROD1	SE	7.39604	13.8671	0.91	0.51	0.91	no
MAGI1	SE	14.0266	12.2186	-0.20	0.36	0.85	no
MAGIX	A3SS	2.30249	1.55785	-0.56	0.38	0.86	no
MAP2	SE	13.0094	12.0307	-0.11	0.68	0.96	no
MAP2K5	SE	8.97422	8.52363	-0.07	0.78	0.98	no
MAP4K2	RI	34.5996	40.7583	0.24	0.40	0.87	no
MAP4K2	A3SS	34.5996	40.7583	0.24	0.40	0.87	no
MAPK7	SE	10.7264	8.98161	-0.26	0.49	0.91	no
MAPKBP1	SE	5.16759	6.1749	0.26	0.58	0.94	no
MAPKBP1	A3SS	5.16759	6.1749	0.26	0.58	0.94	no
MAPT	SE	3.47631	3.54211	0.03	0.96	0.99	no
Mar-07	SE	70.7222	57.088	-0.31	0.27	0.80	no
Mar-08	MXE	19.2481	22.1573	0.20	0.44	0.89	no
MASTL	A3SS	30.8289	23.3367	-0.40	0.29	0.81	no
MB	SE	11.8666	15.2931	0.37	0.24	0.77	no
MBD5	A5SS	12.0197	5.48461	-1.13	0.26	0.80	no
MCTP1	SE	9.63205	9.5528	-0.01	0.99	1.00	no
METTL17	A3SS	19.6604	13.9437	-0.50	0.05	0.46	no
MFGE8	SE	6.24596	6.55296	0.07	0.82	0.98	no
MFGE8	SE	0	0	0.00	1.00	1.00	no
MGAT4B	A5SS	93.8679	93.1119	-0.01	0.98	1.00	no
MGLL	MXE	2.13187	4.54246	1.09	0.08	0.55	no
MIB2	A3SS	7.79405	13.4265	0.78	0.01	0.23	no
MIB2	A3SS	7.79405	13.4265	0.78	0.01	0.23	no
MIB2	SE	7.79405	13.4265	0.78	0.01	0.23	no
MIS18BP1	MXE	8.55561	9.00826	0.07	0.82	0.98	no
MITD1	RI	14.1699	11.5895	-0.29	0.81	0.98	no
MITF	A3SS	7.94364	7.16152	-0.15	0.60	0.94	no
MKL1	SE	6.07039	5.28597	-0.20	0.65	0.95	no
MKS1	SE	10.2275	11.7529	0.20	0.45	0.89	no
MKS1	SE	10.2275	11.7529	0.20	0.45	0.89	no
MLPH	SE	7.95102	10.281	0.37	0.29	0.81	no
MLPH	SE	7.95102	10.281	0.37	0.29	0.81	no
MOK	SE	6.96943	7.57269	0.12	0.85	0.98	no
MPDU1	SE	219.755	188.245	-0.22	0.55	0.93	no
MPDU1	SE	219.755	188.245	-0.22	0.55	0.93	no
MPDZ	SE	8.92075	15.409	0.79	0.06	0.49	no
MRPL22	SE	50.1893	32.043	-0.65	0.02	0.30	no
MRPS15	SE	131.319	103.325	-0.35	0.07	0.50	no
MRRF	SE	31.5962	28.5786	-0.14	0.76	0.97	no
MRRF	A5SS	31.5962	28.5786	-0.14	0.76	0.97	no
MSTO1	RI	55.3638	48.7012	-0.18	0.78	0.98	no
MSTO1	A5SS	55.3638	48.7012	-0.18	0.78	0.98	no

MSTO1	A3SS	55.3638	48.7012	-0.18	0.78	0.98	no
MTL5	SE	17.8305	16.0816	-0.15	0.66	0.96	no
MTMR14	SE	26.8379	29.1807	0.12	0.65	0.95	no
MTO1	RI	25.7677	22.993	-0.16	0.52	0.92	no
MTRF1	SE	6.19738	4.83561	-0.36	0.30	0.82	no
MUTYH	A5SS	10.507	7.22882	-0.54	0.23	0.76	no
MYB	A5SS	4.19006	2.83238	-0.56	0.04	0.41	no
MYO5A	SE	7.72726	7.3114	-0.08	0.78	0.98	no
MYO6	SE	89.8789	84.2696	-0.09	0.69	0.96	no
MYO9A	A5SS	6.60831	4.15008	-0.67	0.25	0.79	no
MYO9A	SE	6.60831	4.15008	-0.67	0.25	0.79	no
NAA16	SE	13.3673	12.4672	-0.10	0.72	0.97	no
NAPB	SE	3.54527	4.6994	0.41	0.13	0.65	no
NARFL	RI	22.6173	17.3912	-0.38	0.25	0.78	no
NAT1	SE	12.653	18.032	0.51	0.04	0.39	no
NCOA1	SE	37.0507	44.0489	0.25	0.20	0.74	no
NDUFV1	RI	107.255	107.468	0.00	0.99	1.00	no
NECAP2	A5SS	3.96169	7.13598	0.85	0.05	0.45	no
NEDD1	SE	25.0867	17.7503	-0.50	0.05	0.46	no
NEK1	SE	10.3179	11.5628	0.16	0.56	0.93	no
NEK7	SE	73.6011	81.4634	0.15	0.42	0.88	no
NFKBID	A3SS	4.02485	1.40778	-1.52	0.05	0.44	no
NLE1	SE	14.9152	10.6811	-0.48	0.07	0.52	no
NME6	SE	9.95956	5.56263	-0.84	0.04	0.41	no
NOL3	RI	10.1558	8.86408	-0.20	0.60	0.94	no
NOL8	A5SS	10.6169	15.4958	0.55	0.09	0.57	no
NOL8	A5SS	10.6169	15.4958	0.55	0.09	0.57	no
NPEPPS	A3SS	133.558	121.881	-0.13	0.66	0.95	no
NT5DC3	SE	6.90978	4.20111	-0.72	0.03	0.36	no
NUP214	SE	54.1678	54.0069	0.00	0.99	1.00	no
NUP54	RI	56.4422	37.0117	-0.61	0.00	0.07	no
OBSCN	SE	2.7493	5.06513	0.88	0.17	0.71	no
OCIAD1	SE	205.569	193.011	-0.09	0.61	0.95	no
OGG1	SE	33.936	27.9495	-0.28	0.71	0.97	no
OSBPL5	SE	21.739	25.5056	0.23	0.41	0.87	no
OSBPL5	SE	21.739	25.5056	0.23	0.41	0.87	no
OSBPL6	SE	2.32069	1.91111	-0.28	0.50	0.91	no
OSGEPL1	MXE	7.6573	8.51886	0.15	0.55	0.93	no
OTUD5	RI	21.5184	27.8724	0.37	0.08	0.55	no
OVGP1	MXE	4.95419	6.05538	0.29	0.46	0.89	no
PACRGL	SE	15.531	13.0874	-0.25	0.33	0.84	no
PACRGL	A5SS	15.531	13.0874	-0.25	0.33	0.84	no
PAM	SE	6.39287	9.23406	0.53	0.06	0.48	no
PAM	SE	6.39287	9.23406	0.53	0.06	0.48	no
PAQR3	MXE	26.397	25.8015	-0.03	0.90	0.99	no
PAQR3	SE	26.397	25.8015	-0.03	0.90	0.99	no
PAQR3	SE	26.397	25.8015	-0.03	0.90	0.99	no
PARD3	A5SS	2.92009	3.66147	0.33	0.41	0.87	no
PARD3	SE	2.92009	3.66147	0.33	0.41	0.87	no
PARP11	SE	11.695	15.2616	0.38	0.33	0.84	no
PCCA	SE	17.4771	20.7781	0.25	0.54	0.92	no
PCGF3	A3SS	28.1651	29.6855	0.08	0.75	0.97	no
PCNT	SE	8.09912	5.25961	-0.62	0.29	0.81	no
PDDC1	SE	30.2008	32.809	0.12	0.73	0.97	no
PEX1	A3SS	10.4801	9.94368	-0.08	0.85	0.98	no
PEX10	SE	36.4993	35.8411	-0.03	0.95	0.99	no
PEX11A	SE	5.23495	4.71964	-0.15	0.69	0.96	no
PEX7	SE	16.3577	15.1479	-0.11	0.62	0.95	no
PGAP1	RI	5.7927	6.29141	0.12	0.67	0.96	no
PGAP2	SE	30.1973	25.31	-0.25	0.68	0.96	no

PGAP3	MXE	3.23046	5.05877	0.65	0.30	0.82	no
PGAP3	SE	3.23046	5.05877	0.65	0.30	0.82	no
PGC	SE	6.78692	6.49633	-0.06	0.83	0.98	no
PGS1	A3SS	9.4648	11.6889	0.30	0.30	0.82	no
PHF21A	A3SS	14.4165	13.9383	-0.05	0.84	0.98	no
PHF3	SE	11.2025	12.626	0.17	0.54	0.92	no
PHF3	SE	11.2025	12.626	0.17	0.54	0.92	no
PHYKPL	SE	11.3498	12.9478	0.19	0.73	0.97	no
PICALM	SE	136.057	138.411	0.02	0.89	0.99	no
PICK1	MXE	24.9175	23.8443	-0.06	0.84	0.98	no
PIGO	SE	44.7685	35.1284	-0.35	0.20	0.74	no
PIGO	SE	44.7685	35.1284	-0.35	0.20	0.74	no
PIP5K1C	SE	10.9472	18.3413	0.74	0.03	0.37	no
PKIG	SE	16.746	15.0735	-0.15	0.78	0.98	no
PLA2G7	SE	1.36407	1.07841	-0.34	1.00	1.00	no
PLCB4	SE	6.07196	6.84867	0.17	0.54	0.92	no
PLCD1	A5SS	1.99148	3.88517	0.96	0.04	0.42	no
PLD3	A3SS	38.4304	49.6514	0.37	0.20	0.73	no
PLEKHA6	A3SS	1.47241	1.31629	-0.16	1.00	1.00	no
PLEKHA7	A3SS	9.59308	5.86518	-0.71	0.05	0.46	no
PLEKHN1	SE	2.21024	1.25665	-0.81	0.10	0.58	no
PLS1	SE	43.6938	48.3536	0.15	0.45	0.89	no
PLXND1	A3SS	17.4692	14.9244	-0.23	0.54	0.92	no
PMS2P5	A3SS	3.34029	2.1547	-0.63	0.25	0.78	no
PNISR	SE	15.6691	18.0153	0.20	0.63	0.95	no
PNISR	A5SS	15.6691	18.0153	0.20	0.63	0.95	no
POLK	SE	25.1589	16.3577	-0.62	0.14	0.66	no
PORCN	SE	7.1428	8.81858	0.30	0.38	0.85	no
POT1	A3SS	32.8046	36.3658	0.15	0.61	0.95	no
PPAPDC1B	MXE	87.638	102.59	0.23	0.58	0.94	no
PPFIA2	A3SS	50.0252	66.6211	0.41	0.26	0.79	no
PPM1M	SE	2.77174	4.50663	0.70	0.08	0.55	no
PPP1R7	SE	38.1654	40.5794	0.09	0.75	0.97	no
PPP2R3C	SE	24.8602	29.289	0.24	0.68	0.96	no
PPP6R3	SE	100.173	95.2097	-0.07	0.69	0.96	no
PRIMPOL	SE	7.66627	5.16711	-0.57	0.41	0.87	no
PRKCSH	A3SS	134.5	119.536	-0.17	0.44	0.89	no
PRKD2	SE	17.9956	18.926	0.07	0.80	0.98	no
PRKRIP1	SE	12.216	13.0106	0.09	0.77	0.97	no
PRPF39	SE	9.05352	10.4393	0.21	0.72	0.97	no
PRPF39	RI	9.05352	10.4393	0.21	0.72	0.97	no
PRR3	SE	5.7528	4.11366	-0.48	0.28	0.81	no
PSIP1	A3SS	34.2767	35.3257	0.04	0.87	0.99	no
PTBP2	A3SS	9.67807	9.59379	-0.01	0.96	0.99	no
PTBP2	SE	9.67807	9.59379	-0.01	0.96	0.99	no
PTBP3	A5SS	47.8313	44.1557	-0.12	0.59	0.94	no
PTK2	SE	51.927	47.3107	-0.13	0.62	0.95	no
PTPN20B	MXE	0.683687	0.598834	-0.19	1.00	1.00	no
PTPN4	A5SS	11.2255	13.6352	0.28	0.64	0.95	no
PTPN4	SE	11.2255	13.6352	0.28	0.64	0.95	no
PUS7	MXE	24.0648	25.3724	0.08	0.80	0.98	no
PXDN	SE	4.83312	14.0961	1.54	0.00	0.03	yes
PXK	A3SS	13.4821	13.3449	-0.01	0.95	0.99	no
PXN	SE	50.5561	48.1383	-0.07	0.78	0.97	no
QARS	A5SS	52.6615	52.3587	-0.01	0.98	1.00	no
QKI	RI	79.8827	66.0013	-0.28	0.35	0.85	no
QKI	A3SS	79.8827	66.0013	-0.28	0.35	0.85	no
RAB15	A5SS	6.67906	7.80763	0.23	0.74	0.97	no
RAB17	SE	19.0317	15.7511	-0.27	0.36	0.85	no
RAB28	SE	26.5209	18.5366	-0.52	0.02	0.28	no

RAB8B	SE	21.3801	23.2338	0.12	0.60	0.94	no
RAD51AP1	A5SS	18.4224	24.5198	0.41	0.07	0.51	no
RALGAPB	SE	21.7504	23.8614	0.13	0.52	0.92	no
RANBP9	MXE	46.7932	46.9791	0.01	0.98	1.00	no
RBBP8NL	SE	1.66228	0.868634	-0.94	0.03	0.39	no
RBCK1	SE	42.4882	43.0195	0.02	0.93	0.99	no
RBM26	A3SS	19.6273	16.2766	-0.27	0.17	0.70	no
RBM3	RI	118.215	80.2703	-0.56	0.00	0.12	no
RBM33	SE	17.0881	16.3588	-0.06	0.87	0.99	no
RBMS2	A5SS	5.5849	4.70293	-0.25	0.48	0.90	no
REPS1	SE	11.6714	9.14137	-0.35	0.32	0.83	no
RERE	SE	21.7121	19.3709	-0.16	0.72	0.97	no
RHBDD1	SE	41.2971	50.6722	0.30	0.35	0.85	no
RHOT2	RI	50.109	43.56	-0.20	0.44	0.88	no
RIMS1	SE	2.5522	1.92482	-0.41	0.14	0.66	no
RMND1	A5SS	9.57968	7.37385	-0.38	0.24	0.78	no
RNF115	MXE	14.56	9.65649	-0.59	0.12	0.63	no
RNF121	MXE	34.8383	32.7903	-0.09	0.71	0.97	no
RNF146	A5SS	11.5215	17.6094	0.61	0.01	0.17	no
RNF185	SE	2.97282	4.68592	0.66	0.06	0.48	no
ROBO3	RI	0.917798	1.70507	0.89	0.15	0.67	no
RP11-296I10.6	A5SS	1.22789	1.23775	0.01	1.00	1.00	no
RP11-33B1.1	SE	1.76015	1.84774	0.07	0.90	0.99	no
RP11-480I12.5	SE	1.70359	2.36778	0.47	0.54	0.92	no
RP11-529K1.2	SE	0.448701	0.259856	-0.79	1.00	1.00	no
RPS6KL1	A5SS	3.1204	4.98132	0.67	0.17	0.70	no
RSRC2	RI	118.544	86.5897	-0.45	0.09	0.55	no
RSRC2	SE	118.544	86.5897	-0.45	0.09	0.55	no
RUFY2	SE	10.7367	11.3952	0.09	0.85	0.98	no
SAC3D1	SE	14.7588	18.565	0.33	0.22	0.76	no
SAC3D1	SE	14.7588	18.565	0.33	0.22	0.76	no
SBNO2	RI	38.9356	56.2525	0.53	0.20	0.74	no
SCAPER	A5SS	8.37896	9.41883	0.17	0.66	0.95	no
SCARB1	RI	92.4204	70.5623	-0.39	0.11	0.60	no
SCRN3	SE	37.7638	40.0399	0.08	0.74	0.97	no
SCYL3	SE	8.10831	9.85481	0.28	0.47	0.90	no
SDHA	A3SS	62.1071	65.719	0.08	0.69	0.96	no
SDR39U1	SE	25.986	46.1454	0.83	0.01	0.14	no
SDR39U1	A5SS	25.986	46.1454	0.83	0.01	0.14	no
SDR39U1	SE	25.986	46.1454	0.83	0.01	0.14	no
SDR39U1	A5SS	25.986	46.1454	0.83	0.01	0.14	no
SECISBP2	SE	7.26276	5.19585	-0.48	0.15	0.67	no
SEMA4D	SE	8.91406	12.3273	0.47	0.15	0.68	no
SENP1	SE	27.632	20.8035	-0.41	0.25	0.78	no
SENP6	SE	44.5823	38.4748	-0.21	0.42	0.88	no
Sep-09	SE	87.8741	87.1879	-0.01	0.96	0.99	no
SERINC3	SE	92.7085	114.927	0.31	0.12	0.64	no
SERTAD3	SE	9.16291	9.81657	0.10	0.74	0.97	no
SGK1	SE	3.55832	7.61488	1.10	0.00	0.13	no
SGSM2	SE	5.92142	3.83839	-0.63	0.38	0.86	no
SLC10A3	RI	35.2765	48.3962	0.46	0.02	0.33	no
SLC1A3	SE	5.80252	7.55379	0.38	0.32	0.83	no
SLC25A19	A5SS	36.5801	29.2566	-0.32	0.17	0.71	no
SLC26A1	SE	7.26513	7.54705	0.05	0.90	0.99	no
SLC29A1	SE	32.7636	24.1396	-0.44	0.02	0.34	no
SLC2A8	SE	11.0171	13.0381	0.24	0.36	0.85	no
SLC30A6	SE	33.5147	34.5511	0.04	0.82	0.98	no
SLC30A6	MXE	33.5147	34.5511	0.04	0.82	0.98	no
SLC35B3	SE	13.5541	15.0445	0.15	0.56	0.93	no
SLC37A3	SE	43.2205	50.477	0.22	0.25	0.78	no

SLC37A3	SE	43.2205	50.477	0.22	0.25	0.78	no
SLC38A1	SE	169.41	169.214	0.00	0.99	1.00	no
SLC39A11	A5SS	7.68875	14.2493	0.89	0.00	0.09	no
SLC3A2	MXE	181.763	209.184	0.20	0.38	0.85	no
SLC41A2	SE	8.3797	13.2394	0.66	0.08	0.54	no
SLC43A1	SE	35.125	52.8085	0.59	0.02	0.29	no
SLC45A4	SE	7.09503	7.45309	0.07	0.84	0.98	no
SLC4A7	SE	41.9817	27.6367	-0.60	0.00	0.06	no
SLC9A8	SE	7.55777	6.75185	-0.16	0.57	0.93	no
SLC9A8	SE	7.55777	6.75185	-0.16	0.57	0.93	no
SMAP1	SE	7.92887	7.38831	-0.10	0.80	0.98	no
SMYD2	A3SS	7.05432	5.41621	-0.38	0.22	0.76	no
SNAP47	SE	25.5508	29.8666	0.23	0.56	0.93	no
SNHG14	RI	1.08849	0.628395	-0.79	1.00	1.00	no
SNRNP70	A5SS	123.96	155.962	0.33	0.14	0.66	no
SNX10	SE	18.9027	14.1926	-0.41	0.06	0.49	no
SNX10	SE	18.9027	14.1926	-0.41	0.06	0.49	no
SNX10	MXE	18.9027	14.1926	-0.41	0.06	0.49	no
SNX16	RI	4.25353	5.1449	0.27	0.40	0.87	no
SOS2	SE	9.58055	10.8612	0.18	0.42	0.88	no
SPG11	SE	17.0576	23.6197	0.47	0.27	0.80	no
SPIN1	SE	72.861	69.5842	-0.07	0.73	0.97	no
SPOP	SE	53.3605	51.7696	-0.04	0.81	0.98	no
SPRED2	SE	22.8278	22.1324	-0.04	0.83	0.98	no
SRFBP1	SE	19.4119	16.4227	-0.24	0.32	0.83	no
SRSF11	SE	71.8466	67.5983	-0.09	0.73	0.97	no
SRSF11	MXE	71.8466	67.5983	-0.09	0.73	0.97	no
SS18	MXE	69.9697	65.7612	-0.09	0.62	0.95	no
SS18	MXE	69.9697	65.7612	-0.09	0.62	0.95	no
SS18	MXE	69.9697	65.7612	-0.09	0.62	0.95	no
SSBP2	SE	12.2161	12.5461	0.04	0.90	0.99	no
SSBP4	A5SS	18.899	19.5015	0.05	0.91	0.99	no
STAP2	SE	49.3071	31.9605	-0.63	0.02	0.28	no
STAU1	SE	64.8466	72.4984	0.16	0.37	0.85	no
STK16	A5SS	16.5117	20.7205	0.33	0.68	0.96	no
STOML1	A3SS	6.04632	9.91556	0.71	0.02	0.34	no
STOX1	A5SS	1.08148	0.988056	-0.13	1.00	1.00	no
SUGP1	A3SS	20.8663	14.2338	-0.55	0.17	0.71	no
SYBU	A3SS	6.4931	5.77268	-0.17	0.56	0.93	no
SYNGAP1	A3SS	4.77327	7.3873	0.63	0.42	0.88	no
SYTL1	RI	3.6428	6.75412	0.89	0.05	0.45	no
TAB3	MXE	30.3678	28.2786	-0.10	0.60	0.94	no
TACC2	SE	21.6637	20.4537	-0.08	0.78	0.97	no
TBC1D1	MXE	20.882	16.2208	-0.36	0.23	0.77	no
TBC1D1	SE	20.882	16.2208	-0.36	0.23	0.77	no
TBC1D19	MXE	6.17759	7.20128	0.22	0.44	0.89	no
TBCD	MXE	65.4323	69.6832	0.09	0.73	0.97	no
TBCD	SE	65.4323	69.6832	0.09	0.73	0.97	no
TCTN1	SE	25.886	25.2654	-0.04	0.91	0.99	no
TEAD2	SE	1.21611	1.0327	-0.24	1.00	1.00	no
TEP1	SE	4.07857	6.71522	0.72	0.20	0.73	no
TGFBR2	SE	2.07533	1.37246	-0.60	0.04	0.43	no
TIRAP	SE	12.2703	9.03174	-0.44	0.21	0.75	no
TM2D1	SE	36.3678	34.4552	-0.08	0.75	0.97	no
TM2D3	SE	51.9064	61.5108	0.24	0.26	0.79	no
TM9SF4	SE	26.1218	27.6295	0.08	0.75	0.97	no
TMCC1	SE	22.4499	25.2813	0.17	0.59	0.94	no
TMEM129	SE	13.0377	18.124	0.48	0.04	0.42	no
TMEM147	RI	138.159	150.865	0.13	0.50	0.91	no
TMEM164	MXE	15.8188	12.1635	-0.38	0.10	0.58	no

TMEM175	SE	31.6896	65.9391	1.06	0.01	0.19	no
TMEM206	SE	16.6468	13.6194	-0.29	0.19	0.73	no
TMEM241	SE	51.4983	41.5245	-0.31	0.26	0.79	no
TMEM241	MXE	51.4983	41.5245	-0.31	0.26	0.79	no
TMEM53	SE	9.27678	5.99666	-0.63	0.32	0.83	no
TMEM87A	MXE	62.4721	33.4231	-0.90	0.00	0.07	no
TMSB15B	A5SS	3.7779	3.84887	0.03	0.96	0.99	no
TNRC6A	MXE	42.6179	36.6176	-0.22	0.53	0.92	no
TOP1MT	SE	18.5083	10.0379	-0.88	0.01	0.14	no
TOP3B	MXE	7.45533	7.87407	0.08	0.83	0.98	no
TPCN1	SE	9.963	11.1089	0.16	0.58	0.94	no
TRAF3	SE	16.4679	14.9789	-0.14	0.57	0.93	no
TRAPPC6A	SE	11.7815	17.118	0.54	0.38	0.86	no
TRDMT1	MXE	4.29298	3.67378	-0.22	0.60	0.94	no
TSGA10	SE	6.78335	9.54247	0.49	0.63	0.95	no
TTC18	A3SS	2.11445	2.09904	-0.01	0.99	1.00	no
TTC23	MXE	8.00881	8.52812	0.09	0.79	0.98	no
TTC6	SE	8.48558	6.46556	-0.39	0.66	0.96	no
TTLL11	SE	4.95257	5.79793	0.23	0.50	0.91	no
TUG1	SE	0.787067	0.733828	-0.10	1.00	1.00	no
TXN	SE	84.114	90.2932	0.10	0.60	0.94	no
TYSND1	SE	11.8626	11.9952	0.02	0.94	0.99	no
U2SURP	A5SS	34.4096	31.8851	-0.11	0.64	0.95	no
UBA1	SE	142.823	149.937	0.07	0.69	0.96	no
UBE2J2	MXE	87.7445	72.8178	-0.27	0.16	0.69	no
UBE2J2	A5SS	87.7445	72.8178	-0.27	0.16	0.69	no
UBR1	SE	25.5826	30.3242	0.25	0.31	0.82	no
UBXN11	A3SS	6.80275	6.77842	-0.01	0.99	1.00	no
UBXN8	SE	22.9079	14.6118	-0.65	0.03	0.36	no
UFM1	SE	42.8404	45.225	0.08	0.69	0.96	no
UNC119	SE	27.3577	32.3458	0.24	0.91	0.99	no
USE1	RI	18.2844	13.3816	-0.45	0.11	0.61	no
USP13	MXE	29.7408	22.1133	-0.43	0.06	0.49	no
USP32	A5SS	47.0365	49.146	0.06	0.80	0.98	no
WASF1	SE	17.0857	22.1393	0.37	0.08	0.55	no
WASF3	SE	23.3144	12.0289	-0.95	0.00	0.01	yes
WASH4P	RI	1.75983	1.07835	-0.71	0.16	0.69	no
WDR27	A3SS	5.03959	4.18771	-0.27	0.46	0.89	no
WDR27	SE	5.03959	4.18771	-0.27	0.46	0.89	no
WDR31	A3SS	2.71158	3.72063	0.46	0.17	0.70	no
WDR31	SE	2.71158	3.72063	0.46	0.17	0.70	no
WDR62	SE	6.20685	4.40599	-0.49	0.07	0.51	no
WDR90	A5SS	10.0923	12.9299	0.36	0.35	0.85	no
WDR90	A5SS	10.0923	12.9299	0.36	0.35	0.85	no
WIBG	SE	45.7102	39.2702	-0.22	0.34	0.84	no
WNK1	SE	95.631	102.737	0.10	0.76	0.97	no
WNK2	SE	14.3598	15.5048	0.11	0.81	0.98	no
WNK2	SE	14.3598	15.5048	0.11	0.81	0.98	no
WRN	SE	4.57267	5.00461	0.13	0.58	0.94	no
XIAP	SE	26.3639	25.8072	-0.03	0.92	0.99	no
XPNPEP1	MXE	29.7209	32.9836	0.15	0.53	0.92	no
XRCC3	A3SS	18.0572	13.8209	-0.39	0.68	0.96	no
YAF2	A3SS	28.3123	21.6668	-0.39	0.27	0.80	no
YAF2	SE	28.3123	21.6668	-0.39	0.27	0.80	no
ZBTB8OS	MXE	18.5193	25.0709	0.44	0.25	0.79	no
ZBTB8OS	SE	18.5193	25.0709	0.44	0.25	0.79	no
ZC3HC1	SE	11.9951	11.4098	-0.07	0.79	0.98	no
ZFAND2B	MXE	7.67883	11.3936	0.57	0.06	0.48	no
ZFC3H1	RI	9.471	12.6906	0.42	0.31	0.83	no
ZHX3	SE	27.0214	21.2709	-0.35	0.42	0.88	no

ZHX3	SE	27.0214	21.2709	-0.35	0.42	0.88	no
ZIK1	SE	4.59986	3.3908	-0.44	0.27	0.80	no
ZMYND8	A5SS	10.388	8.25826	-0.33	0.37	0.85	no
ZNF195	SE	19.5181	19.0163	-0.04	0.89	0.99	no
ZNF276	A5SS	11.9928	16.2885	0.44	0.40	0.87	no
ZNF276	RI	11.9928	16.2885	0.44	0.40	0.87	no
ZNF382	A3SS	4.89895	4.65847	-0.07	0.91	0.99	no
ZNF384	A5SS	28.2025	30.6944	0.12	0.65	0.95	no
ZNF397	SE	5.73235	7.09267	0.31	0.47	0.90	no
ZNF415	MXE	10.7307	12.8994	0.27	0.43	0.88	no
ZNF44	SE	10.0361	10.097	0.01	0.97	1.00	no
ZNF445	SE	5.18193	5.71707	0.14	0.51	0.91	no
ZNF467	MXE	3.65036	4.09855	0.17	0.66	0.95	no
ZNF473	A3SS	7.59824	4.90576	-0.63	0.05	0.46	no
ZNF530	SE	2.41644	2.6098	0.11	0.81	0.98	no
ZNF562	SE	46.8138	40.9575	-0.19	0.51	0.91	no
ZNF562	SE	46.8138	40.9575	-0.19	0.51	0.91	no
ZNF562	SE	46.8138	40.9575	-0.19	0.51	0.91	no
ZNF566	A3SS	14.3403	9.81594	-0.55	0.04	0.40	no
ZNF573	SE	3.0362	3.84877	0.34	0.41	0.87	no
ZNF584	A3SS	11.4828	8.0918	-0.50	0.08	0.54	no
ZNF598	RI	22.8531	17.4095	-0.39	0.11	0.61	no
ZNF606	SE	5.38348	7.72714	0.52	0.04	0.42	no
ZNF620	SE	4.33092	4.50644	0.06	0.86	0.98	no
ZNF639	SE	48.6351	34.8441	-0.48	0.05	0.47	no
ZNF75A	SE	17.7986	17.7931	0.00	1.00	1.00	no
ZNF786	SE	3.49609	4.04545	0.21	0.42	0.88	no
ZNF827	SE	8.69835	11.3111	0.38	0.10	0.59	no
ZNF83	SE	19.827	21.4177	0.11	0.71	0.97	no
ZNF845	SE	21.6354	19.7416	-0.13	0.74	0.97	no
ZNF92	SE	12.4105	9.81533	-0.34	0.11	0.60	no
ZSCAN25	A5SS	6.81236	8.71737	0.36	0.13	0.65	no

13

References

1. Bray, F., J. Ferlay, I. Soerjomataram, et al., *Global cancer statistics 2018: GLOBOCAN estimates of incidence and mortality worldwide for 36 cancers in 185 countries.* CA Cancer J Clin, 2018. **68**(6): p. 394-424.
2. CRUK. *Prostate cancer mortality statistics*. [cited 2020; Available from: https://www.cancerresearchuk.org/health-professional/cancer-statistics/statistics-by-cancer-type/prostate-cancer#heading-One.
3. Huggins, C., R.E. Stevens, Jr, and C.V. Hodges, *Studies on prostatic cancer: Ii. the effects of castration on advanced carcinoma of the prostate gland.* Archives of Surgery, 1941. **43**(2): p. 209-223.
4. Watson, P.A., V.K. Arora, and C.L. Sawyers, *Emerging mechanisms of resistance to androgen receptor inhibitors in prostate cancer.* Nat Rev Cancer, 2015. **15**(12): p. 701-11.
5. Paschalis, A., A. Sharp, J.C. Welti, et al., *Alternative splicing in prostate cancer.* Nat Rev Clin Oncol, 2018.
6. McCrea, E., T.M. Sissung, D.K. Price, C.H. Chau, and W.D. Figg, *Androgen receptor variation affects prostate cancer progression and drug resistance.* Pharmacol Res, 2016. **114**: p. 152-162.
7. Agoulnik, I.U. and N.L. Weigel, *Coactivator selective regulation of androgen receptor activity.* Steroids, 2009. **74**(8): p. 669-74.
8. Karantanos, T., P.G. Corn, and T.C. Thompson, *Prostate cancer progression after androgen deprivation therapy: mechanisms of castrate resistance and novel therapeutic approaches.* Oncogene, 2013. **32**: p. 5501.
9. Chang, C.S., J. Kokontis, and S.T. Liao, *Molecular cloning of human and rat complementary DNA encoding androgen receptors.* Science, 1988. **240**(4850): p. 324-6.
10. van Laar, J.H., J. Bolt-de Vries, M.M. Voorhorst-Ogink, and A.O. Brinkmann, *The human androgen receptor is a 110 kDa protein.* Mol Cell Endocrinol, 1989. **63**(1-2): p. 39-44.

11. Shaffer, P.L., A. Jivan, D.E. Dollins, F. Claessens, and D.T. Gewirth, *Structural basis of androgen receptor binding to selective androgen response elements.* Proc Natl Acad Sci U S A, 2004. **101**(14): p. 4758-63.
12. Davey, R.A. and M. Grossmann, *Androgen Receptor Structure, Function and Biology: From Bench to Bedside.* Clin Biochem Rev, 2016. **37**(1): p. 3-15.
13. Azad, A.A., A. Zoubeidi, M.E. Gleave, and K.N. Chi, *Targeting heat shock proteins in metastatic castration-resistant prostate cancer.* Nat Rev Urol, 2015. **12**(1): p. 26-36.
14. Cutress, M.L., H.C. Whitaker, I.G. Mills, M. Stewart, and D.E. Neal, *Structural basis for the nuclear import of the human androgen receptor.* J Cell Sci, 2008. **121**(Pt 7): p. 957-68.
15. Guo, Z. and Y. Qiu, *A New Trick of an Old Molecule: Androgen Receptor Splice Variants Taking the Stage?!* Int J Biol Sci, 2011. **7**(6): p. 815-22.
16. Hellerstedt, B.A. and K.J. Pienta, *The current state of hormonal therapy for prostate cancer.* CA Cancer J Clin, 2002. **52**(3): p. 154-79.
17. Mohler, J.L., E.S. Antonarakis, A.J. Armstrong, et al., *Prostate Cancer, Version 2.2019, NCCN Clinical Practice Guidelines in Oncology.* J Natl Compr Canc Netw, 2019. **17**(5): p. 479-505.
18. Scher, H.I. and C.L. Sawyers, *Biology of Progressive, Castration-Resistant Prostate Cancer: Directed Therapies Targeting the Androgen-Receptor Signaling Axis.* Journal of Clinical Oncology, 2005. **23**(32): p. 8253-8261.
19. de Bono, J.S., C.J. Logothetis, A. Molina, et al., *Abiraterone and increased survival in metastatic prostate cancer.* N Engl J Med, 2011. **364**(21): p. 1995-2005.
20. Scher, H.I., K. Fizazi, F. Saad, et al., *Increased survival with enzalutamide in prostate cancer after chemotherapy.* N Engl J Med, 2012. **367**(13): p. 1187-97.
21. Petrylak, D.P., C.M. Tangen, M.H. Hussain, et al., *Docetaxel and estramustine compared with mitoxantrone and prednisone for advanced refractory prostate cancer.* N Engl J Med, 2004. **351**(15): p. 1513-20.
22. Machiels, J.P., F. Mazzeo, M. Clausse, et al., *Prospective randomized study comparing docetaxel, estramustine, and prednisone with docetaxel and prednisone in metastatic hormone-refractory prostate cancer.* J Clin Oncol, 2008. **26**(32): p. 5261-8.
23. Mateo, J., S. Carreira, S. Sandhu, et al., *DNA-Repair Defects and Olaparib in Metastatic Prostate Cancer.* N Engl J Med, 2015. **373**(18): p. 1697-708.
24. James, N.D., J.S. de Bono, M.R. Spears, et al., *Abiraterone for Prostate Cancer Not Previously Treated with Hormone Therapy.* New England Journal of Medicine, 2017. **377**(4): p. 338-351.
25. Fizazi, K., N. Tran, L. Fein, et al., *Abiraterone plus Prednisone in Metastatic, Castration-Sensitive Prostate Cancer.* N Engl J Med, 2017. **377**(4): p. 352-360.
26. Marques, R.B., S. Erkens-Schulze, C.M. de Ridder, et al., *Androgen receptor modifications in prostate cancer cells upon long-termandrogen ablation and antiandrogen treatment.* Int J Cancer, 2005. **117**(2): p. 221-9.
27. Dehm, S.M., L.J. Schmidt, H.V. Heemers, R.L. Vessella, and D.J. Tindall, *Splicing of a novel androgen receptor exon generates a constitutively active androgen receptor that mediates prostate cancer therapy resistance.* Cancer Res, 2008. **68**(13): p. 5469-77.
28. Lu, C. and J. Luo, *Decoding the androgen receptor splice variants.* Transl Androl Urol, 2013. **2**(3): p. 178-86.

29. Hu, R., T.A. Dunn, S. Wei, et al., *Ligand-independent androgen receptor variants derived from splicing of cryptic exons signify hormone-refractory prostate cancer.* Cancer Res, 2009. **69**(1): p. 16-22.
30. Matera, A.G. and Z. Wang, *A day in the life of the spliceosome.* Nat Rev Mol Cell Biol, 2014. **15**(2): p. 108-21.
31. Nilsen, T.W. and B.R. Graveley, *Expansion of the eukaryotic proteome by alternative splicing.* Nature, 2010. **463**(7280): p. 457-63.
32. Wahl, M.C., C.L. Will, and R. Lührmann, *The spliceosome: design principles of a dynamic RNP machine.* Cell, 2009. **136**(4): p. 701-18.
33. Lerner, M.R., J.A. Boyle, S.M. Mount, S.L. Wolin, and J.A. Steitz, *Are snRNPs involved in splicing?* Nature, 1980. **283**(5743): p. 220-4.
34. Will, C.L. and R. Lührmann, *Spliceosome structure and function.* Cold Spring Harb Perspect Biol, 2011. **3**(7).
35. Matera, A.G., R.M. Terns, and M.P. Terns, *Non-coding RNAs: lessons from the small nuclear and small nucleolar RNAs.* Nature Reviews Molecular Cell Biology, 2007. **8**(3): p. 209-220.
36. Sleeman, J.E. and A.I. Lamond, *Newly assembled snRNPs associate with coiled bodies before speckles, suggesting a nuclear snRNP maturation pathway.* Curr Biol, 1999. **9**(19): p. 1065-74.
37. Staknis, D. and R. Reed, *SR proteins promote the first specific recognition of Pre-mRNA and are present together with the U1 small nuclear ribonucleoprotein particle in a general splicing enhancer complex.* Mol Cell Biol, 1994. **14**(11): p. 7670-82.
38. Valcárcel, J., R.K. Gaur, R. Singh, and M.R. Green, *Interaction of U2AF65 RS region with pre-mRNA branch point and promotion of base pairing with U2 snRNA [corrected].* Science, 1996. **273**(5282): p. 1706-9.
39. De Conti, L., M. Baralle, and E. Buratti, *Exon and intron definition in pre-mRNA splicing.* Wiley Interdiscip Rev RNA, 2013. **4**(1): p. 49-60.
40. Yang, F., X.Y. Wang, Z.M. Zhang, et al., *Splicing proofreading at 5' splice sites by ATPase Prp28p.* Nucleic Acids Res, 2013. **41**(8): p. 4660-70.
41. Hoskins, A.A., L.J. Friedman, S.S. Gallagher, et al., *Ordered and dynamic assembly of single spliceosomes.* Science, 2011. **331**(6022): p. 1289-95.
42. Daguenet, E., G. Dujardin, and J. Valcarcel, *The pathogenicity of splicing defects: mechanistic insights into pre-mRNA processing inform novel therapeutic approaches.* EMBO Rep, 2015. **16**(12): p. 1640-55.
43. Wang, Z. and C.B. Burge, *Splicing regulation: From a parts list of regulatory elements to an integrated splicing code.* Rna, 2008. **14**(5): p. 802-13.
44. Fu, X.D. and M. Ares, *Context-dependent control of alternative splicing by RNA-binding proteins.* Nat Rev Genet, 2014. **15**(10): p. 689-701.
45. Ule, J., G. Stefani, A. Mele, et al., *An RNA map predicting Nova-dependent splicing regulation.* Nature, 2006. **444**(7119): p. 580-6.
46. Lee, J.A., Z.Z. Tang, and D.L. Black, *An inducible change in Fox-1/A2BP1 splicing modulates the alternative splicing of downstream neuronal target exons.* Genes Dev, 2009. **23**(19): p. 2284-93.
47. Ip, J.Y., D. Schmidt, Q. Pan, et al., *Global impact of RNA polymerase II elongation inhibition on alternative splicing regulation.* Genome Res, 2011. **21**(3): p. 390-401.
48. Weigand, J.E., J.N. Boeckel, P. Gellert, and S. Dimmeler, *Hypoxia-Induced Alternative Splicing in Endothelial Cells.* PLoS One, 2012. **7**(8).

49. Hang, X., P. Li, Z. Li, et al., *Transcription and splicing regulation in human umbilical vein endothelial cells under hypoxic stress conditions by exon array.* BMC Genomics, 2009. **10**: p. 126.
50. Yamamoto, K., M.T. Furukawa, K. Fukumura, et al., *Control of the heat stress-induced alternative splicing of a subset of genes by hnRNP K.* Genes Cells, 2016. **21**(9): p. 1006-14.
51. Keller, M., Y. Hu, A. Mesihovic, et al., *Alternative splicing in tomato pollen in response to heat stress.* DNA Res, 2017. **24**(2): p. 205-17.
52. Busa, R., R. Geremia, and C. Sette, *Genotoxic stress causes the accumulation of the splicing regulator Sam68 in nuclear foci of transcriptionally active chromatin.* Nucleic Acids Res, 2010. **38**(9): p. 3005-18.
53. Kornblihtt, A.R., I.E. Schor, M. Alló, et al., *Alternative splicing: a pivotal step between eukaryotic transcription and translation.* Nature Reviews Molecular Cell Biology, 2013. **14**: p. 153.
54. Wang, Y., X. Xiao, J. Zhang, et al., *A complex network of factors with overlapping affinities represses splicing through intronic elements.* Nat Struct Mol Biol, 2013. **20**(1): p. 36-45.
55. Wang, Y., M. Ma, X. Xiao, and Z. Wang, *Intronic splicing enhancers, cognate splicing factors and context-dependent regulation rules.* Nat Struct Mol Biol, 2012. **19**(10): p. 1044-52.
56. Tropp, B.E., *Principles of molecular biology. Ch.14*. 2014, Jones & Bartlett Learning.
57. Wang, E.T., R. Sandberg, S. Luo, et al., *Alternative Isoform Regulation in Human Tissue Transcriptomes.* Nature, 2008. **456**(7221): p. 470-6.
58. Scotti, M.M. and M.S. Swanson, *RNA mis-splicing in disease.* Nat Rev Genet, 2016. **17**(1): p. 19-32.
59. Iñiguez, L.P. and G. Hernández, *The Evolutionary Relationship between Alternative Splicing and Gene Duplication.* Front Genet, 2017. **8**.
60. Cuajungco, M.P., M. Leyne, J. Mull, et al., *Tissue-specific reduction in splicing efficiency of IKBKAP due to the major mutation associated with familial dysautonomia.* Am J Hum Genet, 2003. **72**(3): p. 749-58.
61. Ibrahim, E.C., M.M. Hims, N. Shomron, et al., *Weak definition of IKBKAP exon 20 leads to aberrant splicing in familial dysautonomia.* Hum Mutat, 2007. **28**(1): p. 41-53.
62. Harbour, J.W., E.D.O. Roberson, H. Anbunathan, et al., *Recurrent mutations at codon 625 of the splicing factor SF3B1 in uveal melanoma.* Nat Genet, 2013. **45**(2): p. 133-5.
63. Biankin, A.V., N. Waddell, K.S. Kassahn, et al., *Pancreatic cancer genomes reveal aberrations in axon guidance pathway genes.* Nature, 2012. **491**(7424): p. 399-405.
64. Imielinski, M., A.H. Berger, P.S. Hammerman, et al., *Mapping the hallmarks of lung adenocarcinoma with massively parallel sequencing.* Cell, 2012. **150**(6): p. 1107-20.
65. Stephens, P.J., P.S. Tarpey, H. Davies, et al., *The landscape of cancer genes and mutational processes in breast cancer.* Nature, 2012. **486**(7403): p. 400-4.
66. Armenia, A.M., SA; Liu, D; Gao, J; Kundra, R; Reznik, Ed; Chatila, W.K; Chakravarty, DG; Han, C; Coleman, L; Montgomery, B; Pritchard, C; Morrissey, C; Barbieri, C.E; Beltran, H; Sboner, A; Zafeiriou, Z; Miranda, S; Bielski, CM; Penson, AV; Tolonen, C; Huang, F.W; Robinson, D; Wu, Y.M; Lonigro, R; Garraway, L.A; Demichelis, F; Kantoff, P.W; Taplin M,E; Abida, W; Taylor B.S; Scher, H,I; Nelson, P.S; de Bono, JS, Rubin, M.A; Sawyers, C.L; Chinnaiyan, A.M; PCF/SU2C International Prostate Cancer Dream Team, Schultz,

N; Van Allen, E.M, *The long tail of oncogenic drivers in prostate cancer.* Nature Genetics, 2017.
67. Dvinge, H., E. Kim, O. Abdel-Wahab, and R.K. Bradley, *RNA splicing factors as oncoproteins and tumour suppressors.* Nat Rev Cancer, 2016. **16**(7): p. 413-30.
68. DeBoever, C., E.M. Ghia, P.J. Shepard, et al., *Transcriptome sequencing reveals potential mechanism of cryptic 3' splice site selection in SF3B1-mutated cancers.* PLoS Comput Biol, 2015. **11**(3): p. e1004105.
69. Je, E.M., N.J. Yoo, Y.J. Kim, M.S. Kim, and S.H. Lee, *Mutational analysis of splicing machinery genes SF3B1, U2AF1 and SRSF2 in myelodysplasia and other common tumors.* Int J Cancer, 2013. **133**(1): p. 260-5.
70. Busa, R., M.P. Paronetto, D. Farini, et al., *The RNA-binding protein Sam68 contributes to proliferation and survival of human prostate cancer cells.* Oncogene, 2007. **26**(30): p. 4372-82.
71. Bielli, P., R. Busa, M.P. Paronetto, and C. Sette, *The RNA-binding protein Sam68 is a multifunctional player in human cancer.* Endocr Relat Cancer, 2011. **18**(4): p. R91-r102.
72. Dhillon, A.S., S. Hagan, O. Rath, and W. Kolch, *MAP kinase signalling pathways in cancer.* Oncogene, 2007. **26**(22): p. 3279-90.
73. Paronetto, M.P., M. Cappellari, R. Busa, et al., *Alternative splicing of the cyclin D1 proto-oncogene is regulated by the RNA-binding protein Sam68.* Cancer Res, 2010. **70**(1): p. 229-39.
74. Li, Y., N. Donmez, C. Sahinalp, et al., *SRRM4 Drives Neuroendocrine Transdifferentiation of Prostate Adenocarcinoma Under Androgen Receptor Pathway Inhibition.* European Urology. **71**(1): p. 68-78.
75. Schoenherr, C.J. and D.J. Anderson, *The neuron-restrictive silencer factor (NRSF): a coordinate repressor of multiple neuron-specific genes.* Science, 1995. **267**(5202): p. 1360-3.
76. Beltran, H., S. Tomlins, A. Aparicio, et al., *Aggressive Variants of Castration Resistant Prostate Cancer.* Clin Cancer Res, 2014. **20**(11): p. 2846-50.
77. Koh, C.M., C.J. Bieberich, C.V. Dang, et al., *MYC and Prostate Cancer.* Genes Cancer, 2010. **1**(6): p. 617-28.
78. Hsu, T.Y., L.M. Simon, N.J. Neill, et al., *The spliceosome is a therapeutic vulnerability in MYC-driven cancer.* Nature, 2015. **525**(7569): p. 384-8.
79. Ushigome, M., T. Ubagai, H. Fukuda, et al., *Up-regulation of hnRNP A1 gene in sporadic human colorectal cancers.* Int J Oncol, 2005. **26**(3): p. 635-40.
80. Cui, H., F. Wu, Y. Sun, G. Fan, and Q. Wang, *Up-regulation and subcellular localization of hnRNP A2/B1 in the development of hepatocellular carcinoma.* BMC Cancer, 2010. **10**: p. 356.
81. Zhou, J., L. Nong, M. Wloch, et al., *Expression of early lung cancer detection marker: hnRNP-A2/B1 and its relation to microsatellite alteration in non-small cell lung cancer.* Lung Cancer, 2001. **34**(3): p. 341-50.
82. Savage K , I., J. Gorski J , M. Barros E , et al., *Identification of a BRCA1-mRNA Splicing Complex Required for Efficient DNA Repair and Maintenance of Genomic Stability.* Mol Cell, 2014. **54**(3): p. 445-59.
83. Black, A.R., J.D. Black, and J. Azizkhan-Clifford, *Sp1 and kruppel-like factor family of transcription factors in cell growth regulation and cancer.* J Cell Physiol, 2001. **188**(2): p. 143-60.

84. Narla, G., A. DiFeo, S. Yao, et al., *Targeted inhibition of the KLF6 splice variant, KLF6 SV1, suppresses prostate cancer cell growth and spread.* Cancer Res, 2005. **65**(13): p. 5761-8.
85. Liu, X.M., A. Gomez-Pinillos, C. Loder, et al., *KLF6 Loss of Function in Human Prostate Cancer Progression Is Implicated in Resistance to Androgen Deprivation.* Am J Pathol, 2012. **181**(3): p. 1007-16.
86. Turner, N. and R. Grose, *Fibroblast growth factor signalling: from development to cancer.* Nat Rev Cancer, 2010. **10**(2): p. 116-29.
87. Carstens, R.P., J.V. Eaton, H.R. Krigman, P.J. Walther, and M.A. Garcia-Blanco, *Alternative splicing of fibroblast growth factor receptor 2 (FGF-R2) in human prostate cancer.* Oncogene, 1997. **15**(25): p. 3059-65.
88. Kwabi-Addo, B., M. Ozen, and M. Ittmann, *The role of fibroblast growth factors and their receptors in prostate cancer.* Endocr Relat Cancer, 2004. **11**(4): p. 709-24.
89. Antonarakis, E.S., C. Lu, H. Wang, et al., *AR-V7 and resistance to enzalutamide and abiraterone in prostate cancer.* N Engl J Med, 2014. **371**(11): p. 1028-38.
90. Efstathiou, E., M. Titus, S. Wen, et al., *Molecular characterization of enzalutamide-treated bone metastatic castration-resistant prostate cancer.* Eur Urol, 2015. **67**(1): p. 53-60.
91. Antonarakis, E.S., C. Lu, B. Luber, et al., *Clinical Significance of Androgen Receptor Splice Variant-7 mRNA Detection in Circulating Tumor Cells of Men With Metastatic Castration-Resistant Prostate Cancer Treated With First- and Second-Line Abiraterone and Enzalutamide.* J Clin Oncol, 2017. **35**(19): p. 2149-2156.
92. Antonarakis, E., A. Armstrong, S. Dehm, and J. Luo, *Androgen receptor variant-driven prostate cancer: clinical implications and therapeutic targeting.* Prostate Cancer Prostatic Dis, 2016. **19**(3): p. 231-41.
93. Kohli, M., Y. Ho, D.W. Hillman, et al., *Androgen Receptor Variant AR-V9 Is Coexpressed with AR-V7 in Prostate Cancer Metastases and Predicts Abiraterone Resistance.* Clin Cancer Res, 2017. **23**(16): p. 4704-4715.
94. Hu, R., C. Lu, E.A. Mostaghel, et al., *Distinct transcriptional programs mediated by the ligand-dependent full-length androgen receptor and its splice variants in castration-resistant prostate cancer.* Cancer Res, 2012. **72**(14): p. 3457-62.
95. Guo, Z., X. Yang, F. Sun, et al., *A novel androgen receptor splice variant is up-regulated during prostate cancer progression and promotes androgen depletion-resistant growth.* Cancer Res, 2009. **69**(6): p. 2305-13.
96. Luo, J., G. Attard, S.P. Balk, et al., *Role of Androgen Receptor Variants in Prostate Cancer: Report from the 2017 Mission Androgen Receptor Variants Meeting.* Eur Urol, 2018. **73**(5): p. 715-723.
97. Liu, L.L., N. Xie, S. Sun, et al., *Mechanisms of the androgen receptor splicing in prostate cancer cells.* Oncogene, 2014. **33**(24): p. 3140-50.
98. Henzler, C., Y. Li, R. Yang, et al., *Truncation and constitutive activation of the androgen receptor by diverse genomic rearrangements in prostate cancer.* Nat Commun, 2016. **7**: p. 13668.
99. Nadiminty, N., R. Tummala, C. Liu, et al., *NF-kappaB2/p52:c-Myc:hnRNPA1 Pathway Regulates Expression of Androgen Receptor Splice Variants and Enzalutamide Sensitivity in Prostate Cancer.* Mol Cancer Ther, 2015. **14**(8): p. 1884-95.

100. Teply, B.A., H. Wang, B. Luber, et al., *Bipolar androgen therapy in men with metastatic castration-resistant prostate cancer after progression on enzalutamide: an open-label, phase 2, multicohort study.* Lancet Oncol, 2018. **19**(1): p. 76-86.
101. Schweizer, M.T., E.S. Antonarakis, H. Wang, et al., *Effect of bipolar androgen therapy for asymptomatic men with castration-resistant prostate cancer: results from a pilot clinical study.* Sci Transl Med, 2015. **7**(269): p. 269ra2.
102. Courtney, K.D., R.B. Corcoran, and J.A. Engelman, *The PI3K pathway as drug target in human cancer.* J Clin Oncol, 2010. **28**(6): p. 1075-83.
103. Robinson, D., E.M. Van Allen, Y.M. Wu, et al., *Integrative clinical genomics of advanced prostate cancer.* Cell, 2015. **161**(5): p. 1215-1228.
104. Pourmand, G., A.A. Ziaee, A.R. Abedi, et al., *Role of PTEN gene in progression of prostate cancer.* Urol J, 2007. **4**(2): p. 95-100.
105. Ferraldeschi, R., D. Nava Rodrigues, R. Riisnaes, et al., *PTEN protein loss and clinical outcome from castration-resistant prostate cancer treated with abiraterone acetate.* Eur Urol, 2015. **67**(4): p. 795-802.
106. Wang, S., J. Gao, Q. Lei, et al., *Prostate-specific deletion of the murine Pten tumor suppressor gene leads to metastatic prostate cancer.* Cancer Cell, 2003. **4**(3): p. 209-21.
107. Stiles, B., M. Groszer, S. Wang, J. Jiao, and H. Wu, *PTENless means more.* Dev Biol, 2004. **273**(2): p. 175-84.
108. Chen, Z., L.C. Trotman, D. Shaffer, et al., *Crucial role of p53-dependent cellular senescence in suppression of Pten-deficient tumorigenesis.* Nature, 2005. **436**(7051): p. 725-30.
109. Blaustein, M., F. Pelisch, T. Tanos, et al., *Concerted regulation of nuclear and cytoplasmic activities of SR proteins by AKT.* Nat Struct Mol Biol, 2005. **12**(12): p. 1037-44.
110. Patel, N.A., S. Kaneko, H.S. Apostolatos, et al., *Molecular and genetic studies imply Akt-mediated signaling promotes protein kinase CbetaII alternative splicing via phosphorylation of serine/arginine-rich splicing factor SRp40.* J Biol Chem, 2005. **280**(14): p. 14302-9.
111. National Center for Biotechnology Information (NCBI)[Internet]. Bethesda (MD): National Library of Medicine (US), N.C.f.B.I.
112. Gurel, B., T. Iwata, C.M. Koh, et al., *Nuclear MYC protein overexpression is an early alteration in human prostate carcinogenesis.* Mod Pathol, 2008. **21**(9): p. 1156-67.
113. Visakorpi, T., A.H. Kallioniemi, A.C. Syvänen, et al., *Genetic changes in primary and recurrent prostate cancer by comparative genomic hybridization.* Cancer Res, 1995. **55**(2): p. 342-7.
114. Ellwood-Yen, K., T.G. Graeber, J. Wongvipat, et al., *Myc-driven murine prostate cancer shares molecular features with human prostate tumors.* Cancer Cell, 2003. **4**(3): p. 223-38.
115. Nowak, D.G., H. Cho, T. Herzka, et al., *MYC Drives Pten/Trp53-Deficient Proliferation and Metastasis due to IL6 Secretion and AKT Suppression via PHLPP2.* Cancer Discov, 2015. **5**(6): p. 636-51.
116. Hubbard, G.K., L.N. Mutton, M. Khalili, et al., *Combined MYC Activation and Pten Loss Are Sufficient to Create Genomic Instability and Lethal Metastatic Prostate Cancer.* Cancer Res, 2016. **76**(2): p. 283-92.

117. Phillips, J.W., Y. Pan, B.L. Tsai, et al., *Pathway-guided analysis identifies Myc-dependent alternative pre-mRNA splicing in aggressive prostate cancers.* Proceedings of the National Academy of Sciences, 2020. **117**(10): p. 5269.
118. Zhang, D. and D.G. Tang, *"Splice" a way towards neuroendocrine prostate cancer.* EBioMedicine, 2018. **35**: p. 12-13.
119. Zhang, D., Q. Hu, X. Liu, et al., *Intron retention is a hallmark and spliceosome represents a therapeutic vulnerability in aggressive prostate cancer.* Nature Communications, 2020. **11**(1): p. 2089.
120. Bai, S., S. Cao, L. Jin, et al., *A positive role of c-Myc in regulating androgen receptor and its splice variants in prostate cancer.* Oncogene, 2019. **38**(25): p. 4977-4989.
121. Jung, S.J., S. Oh, G.T. Lee, et al., *Clinical Significance of Wnt/β-Catenin Signalling and Androgen Receptor Expression in Prostate Cancer.* World J Mens Health, 2013. **31**(1): p. 36-46.
122. Huang, S.P., W.C. Ting, L.M. Chen, et al., *Association analysis of Wnt pathway genes on prostate-specific antigen recurrence after radical prostatectomy.* Ann Surg Oncol, 2010. **17**(1): p. 312-22.
123. Clevers, H., *Wnt/beta-catenin signaling in development and disease.* Cell, 2006. **127**(3): p. 469-80.
124. Choi, H.J., H. Park, H.W. Lee, and Y.G. Kwon, *The Wnt pathway and the roles for its antagonists, DKKS, in angiogenesis.* IUBMB Life, 2012. **64**(9): p. 724-31.
125. Beltran, H., R. Yelensky, G.M. Frampton, et al., *Targeted Next-generation Sequencing of Advanced Prostate Cancer Identifies Potential Therapeutic Targets and Disease Heterogeneity.* Eur Urol, 2013. **63**(5): p. 920-6.
126. Isaacsson Velho, P., W. Fu, H. Wang, et al., *Wnt-pathway Activating Mutations Are Associated with Resistance to First-line Abiraterone and Enzalutamide in Castration-resistant Prostate Cancer.* Eur Urol, 2020. **77**(1): p. 14-21.
127. Terry, S., X. Yang, M.W. Chen, F. Vacherot, and R. Buttyan, *Multifaceted interaction between the androgen and Wnt signaling pathways and the implication for prostate cancer.* J Cell Biochem, 2006. **99**(2): p. 402-10.
128. Lee, E., S. Ha, and S.K. Logan, *Divergent Androgen Receptor and Beta-Catenin Signaling in Prostate Cancer Cells.* PLoS One, 2015. **10**(10): p. e0141589.
129. Gonçalves, V., P. Matos, and P. Jordan, *The beta-catenin/TCF4 pathway modifies alternative splicing through modulation of SRp20 expression.* Rna, 2008. **14**(12): p. 2538-49.
130. Pak, S., S. Park, Y. Kim, et al., *The small molecule WNT/β-catenin inhibitor CWP232291 blocks the growth of castration-resistant prostate cancer by activating the endoplasmic reticulum stress pathway.* Journal of Experimental & Clinical Cancer Research, 2019. **38**(1): p. 342.
131. Zhang, W. and H.T. Liu, *MAPK signal pathways in the regulation of cell proliferation in mammalian cells.* Cell Research, 2002. **12**(1): p. 9-18.
132. Li, S., K.W. Fong, G. Gritsina, et al., *Activation of MAPK Signaling by CXCR7 Leads to Enzalutamide Resistance in Prostate Cancer.* Cancer Res, 2019. **79**(10): p. 2580-2592.
133. Chen, C., S. Zhao, A. Karnad, and J.W. Freeman, *The biology and role of CD44 in cancer progression: therapeutic implications.* Journal of Hematology & Oncology, 2018. **11**(1): p. 64.
134. Weg-Remers, S., H. Ponta, P. Herrlich, and H. König, *Regulation of alternative pre-mRNA splicing by the ERK MAP-kinase pathway.* Embo j, 2001. **20**(15): p. 4194-203.

135. Tomlins, S.A., A. Bjartell, A.M. Chinnaiyan, et al., *ETS gene fusions in prostate cancer: from discovery to daily clinical practice.* Eur Urol, 2009. **56**(2): p. 275-86.
136. Tomlins, S.A., D.R. Rhodes, S. Perner, et al., *Recurrent fusion of TMPRSS2 and ETS transcription factor genes in prostate cancer.* Science, 2005. **310**(5748): p. 644-8.
137. Tomlins, S.A., B. Laxman, S. Varambally, et al., *Role of the TMPRSS2-ERG gene fusion in prostate cancer.* Neoplasia, 2008. **10**(2): p. 177-88.
138. Wang, J., Y. Cai, W. Yu, et al., *Pleiotropic biological activities of alternatively spliced TMPRSS2/ERG fusion gene transcripts.* Cancer Res, 2008. **68**(20): p. 8516-24.
139. Klezovitch, O., M. Risk, I. Coleman, et al., *A causal role for ERG in neoplastic transformation of prostate epithelium.* Proc Natl Acad Sci U S A, 2008. **105**(6): p. 2105-10.
140. Nguyen, L.T., M.S. Tretiakova, M.R. Silvis, et al., *ERG Activates the YAP1 Transcriptional Program and Induces the Development of Age-Related Prostate Tumors.* Cancer Cell, 2015. **27**(6): p. 797-808.
141. Carver, B.S., J. Tran, A. Gopalan, et al., *Aberrant ERG expression cooperates with loss of PTEN to promote cancer progression in the prostate.* Nat Genet, 2009. **41**(5): p. 619-24.
142. King, J.C., J. Xu, J. Wongvipat, et al., *Cooperativity of TMPRSS2-ERG with PI3-kinase pathway activation in prostate oncogenesis.* Nat Genet, 2009. **41**(5): p. 524-6.
143. Esgueva, R., S. Perner, J.L. C, et al., *Prevalence of TMPRSS2-ERG and SLC45A3-ERG gene fusions in a large prostatectomy cohort.* Mod Pathol, 2010. **23**(4): p. 539-46.
144. Maher, C.A., N. Palanisamy, J.C. Brenner, et al., *Chimeric transcript discovery by paired-end transcriptome sequencing.* Proc Natl Acad Sci U S A, 2009. **106**(30): p. 12353-8.
145. Pflueger, D., D.S. Rickman, A. Sboner, et al., *N-myc downstream regulated gene 1 (NDRG1) is fused to ERG in prostate cancer.* Neoplasia, 2009. **11**(8): p. 804-11.
146. Hu, Y., A. Dobi, T. Sreenath, et al., *Delineation of TMPRSS2-ERG splice variants in prostate cancer.* Clin Cancer Res, 2008. **14**(15): p. 4719-25.
147. Rastogi, A., S.H. Tan, A.A. Mohamed, et al., *Functional antagonism of TMPRSS2-ERG splice variants in prostate cancer.* Genes Cancer, 2014. **5**(7-8): p. 273-84.
148. Parimi, V., R. Goyal, K. Poropatich, and X.J. Yang, *Neuroendocrine differentiation of prostate cancer: a review.* Am J Clin Exp Urol, 2014. **2**(4): p. 273-85.
149. Small, E.J., J. Huang, J. Youngren, et al., *Characterization of neuroendocrine prostate cancer (NEPC) in patients with metastatic castration resistant prostate cancer (mCRPC) resistant to abiraterone (Abi) or enzalutamide (Enz): Preliminary results from the SU2C/PCF/AACR West Coast Prostate Cancer Dream Team (WCDT).* Journal of Clinical Oncology, 2015. **33**(15_suppl): p. 5003-5003.
150. Lapuk, A.V., S.V. Volik, Y. Wang, and C.C. Collins, *The role of mRNA splicing in prostate cancer.* Asian J Androl, 2014. **16**(4): p. 515-21.
151. Mu, P., Z. Zhang, M. Benelli, et al., *SOX2 promotes lineage plasticity and antiandrogen resistance in TP53- and RB1-deficient prostate cancer.* Science, 2017. **355**(6320): p. 84-8.
152. Zhou, Z., A. Flesken-Nikitin, D.C. Corney, et al., *Synergy of p53 and Rb deficiency in a conditional mouse model for metastatic prostate cancer.* Cancer Res, 2006. **66**(16): p. 7889-98.

153. Bass, A.J., H. Watanabe, C.H. Mermel, et al., *SOX2 is an amplified lineage-survival oncogene in lung and esophageal squamous cell carcinomas.* Nat Genet, 2009. **41**(11): p. 1238-42.
154. Abou Faycal, C., S. Gazzeri, and B. Eymin, *A VEGF-A/SOX2/SRSF2 network controls VEGFR1 pre-mRNA alternative splicing in lung carcinoma cells.* Scientific Reports, 2019. **9**(1): p. 336.
155. Tung, C.-L., P.-H. Hou, Y.-L. Kao, et al., *SOX2 modulates alternative splicing in transitional cell carcinoma.* Biochemical and Biophysical Research Communications, 2010. **393**(3): p. 420-425.
156. Kelsey, R., *SRRM4 drives NEPC progression.* Nature Reviews Urology, 2016. **13**(7): p. 371-371.
157. Lee, A.R., Y. Gan, Y. Tang, and X. Dong, *A novel mechanism of SRRM4 in promoting neuroendocrine prostate cancer development via a pluripotency gene network.* EBioMedicine, 2018. **35**: p. 167-177.
158. Kinney, S.R., M.T. Moser, M. Pascual, et al., *Opposing roles of Dnmt1 in early- and late-stage murine prostate cancer.* Mol Cell Biol, 2010. **30**(17): p. 4159-74.
159. Zhang, Q., L. Chen, B.T. Helfand, et al., *TGF-β regulates DNA methyltransferase expression in prostate cancer, correlates with aggressive capabilities, and predicts disease recurrence.* PLoS One, 2011. **6**(9): p. e25168.
160. Hsu, C.H., K.L. Peng, M.L. Kang, et al., *TET1 suppresses cancer invasion by activating the tissue inhibitors of metalloproteinases.* Cell Rep, 2012. **2**(3): p. 568-79.
161. Nickerson, M.L., S. Das, K.M. Im, et al., *TET2 binds the androgen receptor and loss is associated with prostate cancer.* Oncogene, 2017. **36**(15): p. 2172-2183.
162. Lev Maor, G., A. Yearim, and G. Ast, *The alternative role of DNA methylation in splicing regulation.* Trends Genet, 2015. **31**(5): p. 274-80.
163. Anastasiadou, C., A. Malousi, N. Maglaveras, and S. Kouidou, *Human epigenome data reveal increased CpG methylation in alternatively spliced sites and putative exonic splicing enhancers.* DNA Cell Biol, 2011. **30**(5): p. 267-75.
164. Wang, G., D. Zhao, D.J. Spring, and R.A. DePinho, *Genetics and biology of prostate cancer.* Genes Dev, 2018. **32**(17-18): p. 1105-1140.
165. Shain, A.H. and J.R. Pollack, *The spectrum of SWI/SNF mutations, ubiquitous in human cancers.* PLoS One, 2013. **8**(1): p. e55119.
166. Roberts, C.W.M. and S.H. Orkin, *The SWI/SNF complex — chromatin and cancer.* Nature Reviews Cancer, 2004. **4**(2): p. 133-142.
167. Link, K.A., S. Balasubramaniam, A. Sharma, et al., *Targeting the BAF57 SWI/SNF subunit in prostate cancer: a novel platform to control androgen receptor activity.* Cancer Res, 2008. **68**(12): p. 4551-8.
168. Chen, K., H. Xiao, J. Zeng, et al., *Alternative Splicing of EZH2 pre-mRNA by SF3B3 Contributes to the Tumorigenic Potential of Renal Cancer.* Clin Cancer Res, 2017. **23**(13): p. 3428-3441.
169. Zibetti, C., A. Adamo, C. Binda, et al., *Alternative splicing of the histone demethylase LSD1/KDM1 contributes to the modulation of neurite morphogenesis in the mammalian nervous system.* J Neurosci, 2010. **30**(7): p. 2521-32.
170. Coleman, D.J., D.A. Sampson, A. Sehrawat, et al., *Alternative splicing of LSD1+8a in neuroendocrine prostate cancer is mediated by SRRM4.* Neoplasia, 2020. **22**(6): p. 253-262.

171. Zraly, C.B. and A.K. Dingwall, *The chromatin remodeling and mRNA splicing functions of the Brahma (SWI/SNF) complex are mediated by the SNR1/SNF5 regulatory subunit.* Nucleic Acids Res, 2012. **40**(13): p. 5975-87.
172. Vivas-Mejia, P.E., C. Rodriguez-Aguayo, H.D. Han, et al., *Silencing Survivin Splice Variant 2B Leads to Antitumor Activity in Taxane-Resistant Ovarian Cancer.* Clin Cancer Res, 2011. **17**(11): p. 3716-26.
173. Sotillo, E., D.M. Barrett, K.L. Black, et al., *Convergence of Acquired Mutations and Alternative Splicing of CD19 Enables Resistance to CART-19 Immunotherapy.* Cancer Discov, 2015. **5**(12): p. 1282-95.
174. Poulikakos, P.I., Y. Persaud, M. Janakiraman, et al., *RAF inhibitor resistance is mediated by dimerization of aberrantly spliced BRAF(V600E).* Nature, 2011. **480**(7377): p. 387-90.
175. Wang, Y., A.J. Bernhardy, C. Cruz, et al., *The BRCA1-Delta11q Alternative Splice Isoform Bypasses Germline Mutations and Promotes Therapeutic Resistance to PARP Inhibition and Cisplatin.* Cancer Res, 2016. **76**(9): p. 2778-90.
176. Litton, J., H.S. Rugo, J. Ettl, et al., *Abstract GS6-07: EMBRACA: A phase 3 trial comparing talazoparib, an oral PARP inhibitor, to physician's choice of therapy in patients with advanced breast cancer and a germline BRCA mutation.* Cancer Research, 2018. **78**(4 Supplement): p. GS6-07.
177. Gelmon, K.A., M. Tischkowitz, H. Mackay, et al., *Olaparib in patients with recurrent high-grade serous or poorly differentiated ovarian carcinoma or triple-negative breast cancer: a phase 2, multicentre, open-label, non-randomised study.* Lancet Oncol, 2011. **12**(9): p. 852-61.
178. Willems, A.J., S.J. Dawson, H. Samaratunga, et al., *Loss of heterozygosity at the BRCA2 locus detected by multiplex ligation-dependent probe amplification is common in prostate cancers from men with a germline BRCA2 mutation.* Clin Cancer Res, 2008. **14**(10): p. 2953-61.
179. Liu, C., W. Lou, Y. Zhu, et al., *Niclosamide inhibits androgen receptor variants expression and overcomes enzalutamide resistance in castration-resistant prostate cancer.* Clin Cancer Res, 2014. **20**(12): p. 3198-3210.
180. Liu, C., C. Armstrong, Y. Zhu, W. Lou, and A.C. Gao, *Niclosamide enhances abiraterone treatment via inhibition of androgen receptor variants in castration resistant prostate cancer.* Oncotarget, 2016. **7**(22): p. 32210-20.
181. Li, Y., S.C. Chan, L.J. Brand, et al., *Androgen receptor splice variants mediate enzalutamide resistance in castration-resistant prostate cancer cell lines.* Cancer Res, 2013. **73**(2): p. 483-9.
182. Yin, Y., R. Li, K. Xu, et al., *Androgen Receptor Variants Mediate DNA Repair after Prostate Cancer Irradiation.* Cancer Res, 2017. **77**(18): p. 4745-4754.
183. Watson, P.A., Y.F. Chen, M.D. Balbas, et al., *Constitutively active androgen receptor splice variants expressed in castration-resistant prostate cancer require full-length androgen receptor.* Proc Natl Acad Sci U S A, 2010. **107**(39): p. 16759-65.
184. Hornberg, E., E.B. Ylitalo, S. Crnalic, et al., *Expression of androgen receptor splice variants in prostate cancer bone metastases is associated with castration-resistance and short survival.* PLoS One, 2011. **6**(4): p. e19059.
185. Scher, H.I., D. Lu, N.A. Schreiber, et al., *Association of AR-V7 on Circulating Tumor Cells as a Treatment-Specific Biomarker With Outcomes and Survival in Castration-Resistant Prostate Cancer.* JAMA Oncol, 2016. **2**(11): p. 1441-1449.

186. Scher, H.I., R.P. Graf, N.A. Schreiber, et al., *Nuclear-specific AR-V7 Protein Localization is Necessary to Guide Treatment Selection in Metastatic Castration-resistant Prostate Cancer.* Eur Urol, 2017. **71**(6): p. 874-882.
187. Bernemann, C., T.J. Schnoeller, M. Luedeke, et al., *Expression of AR-V7 in Circulating Tumour Cells Does Not Preclude Response to Next Generation Androgen Deprivation Therapy in Patients with Castration Resistant Prostate Cancer.* Eur Urol, 2017. **71**(1): p. 1-3.
188. To, S.Q., E.M. Kwan, H.C. Fettke, et al., *Expression of Androgen Receptor Splice Variant 7 or 9 in Whole Blood Does Not Predict Response to Androgen-Axis–targeting Agents in Metastatic Castration-resistant Prostate Cancer.* European Urology.
189. Welti, J., D.N. Rodrigues, A. Sharp, et al., *Analytical Validation and Clinical Qualification of a New Immunohistochemical Assay for Androgen Receptor Splice Variant-7 Protein Expression in Metastatic Castration-resistant Prostate Cancer.* Eur Urol, 2016. **70**(4): p. 599-608.
190. Lee, S.C.W., *Therapeutic Targeting of Splicing in Cancer.* 2016. **22**(9): p. 976-86.
191. Bonnal, S., L. Vigevani, and J. Valcarcel, *The spliceosome as a target of novel antitumour drugs.* Nat Rev Drug Discov, 2012. **11**(11): p. 847-59.
192. Kaida, D., H. Motoyoshi, E. Tashiro, et al., *Spliceostatin A targets SF3b and inhibits both splicing and nuclear retention of pre-mRNA.* Nat Chem Biol, 2007. **3**(9): p. 576-83.
193. Kotake, Y., K. Sagane, T. Owa, et al., *Splicing factor SF3b as a target of the antitumor natural product pladienolide.* Nat Chem Biol, 2007. **3**(9): p. 570-5.
194. Furumai, R., K. Uchida, Y. Komi, et al., *Spliceostatin A blocks angiogenesis by inhibiting global gene expression including VEGF.* Cancer Sci, 2010. **101**(11): p. 2483-9.
195. Sakai, T., T. Sameshima, M. Matsufuji, et al., *Pladienolides, new substances from culture of Streptomyces platensis Mer-11107. I. Taxonomy, fermentation, isolation and screening.* J Antibiot (Tokyo), 2004. **57**(3): p. 173-9.
196. Mizui, Y., T. Sakai, M. Iwata, et al., *Pladienolides, new substances from culture of Streptomyces platensis Mer-11107. III. In vitro and in vivo antitumor activities.* J Antibiot (Tokyo), 2004. **57**(3): p. 188-96.
197. Iwata, M., Y. Ozawa, T. Uenaka, et al., *E7107, a new 7-urethane derivative of pladienolide D, displays curative effect against several human tumor xenografts.* Cancer Research, 2004. **64**(7 Supplement): p. 691.
198. Sakai, Y., T. Yoshida, K. Ochiai, et al., *GEX1 compounds, novel antitumor antibiotics related to herboxidiene, produced by Streptomyces sp. I. Taxonomy, production, isolation, physicochemical properties and biological activities.* J Antibiot (Tokyo), 2002. **55**(10): p. 855-62.
199. Nakajima, H., Y. Hori, H. Terano, et al., *New antitumor substances, FR901463, FR901464 and FR901465. II. Activities against experimental tumors in mice and mechanism of action.* J Antibiot (Tokyo), 1996. **49**(12): p. 1204-11.
200. Albert, B.J., A. Sivaramakrishnan, T. Naka, N.L. Czaicki, and K. Koide, *Total syntheses, fragmentation studies, and antitumor/antiproliferative activities of FR901464 and its low picomolar analogue.* J Am Chem Soc, 2007. **129**(9): p. 2648-59.
201. Seiler, M., A. Yoshimi, R. Darman, et al., *H3B-8800, an orally available small-molecule splicing modulator, induces lethality in spliceosome-mutant cancers.* Nat Med, 2018. **24**(4): p. 497-504.
202. Muraki, M., B. Ohkawara, T. Hosoya, et al., *Manipulation of alternative splicing by a newly developed inhibitor of Clks.* J Biol Chem, 2004. **279**(23): p. 24246-54.

203. Fukuhara, T., T. Hosoya, S. Shimizu, et al., *Utilization of host SR protein kinases and RNA-splicing machinery during viral replication.* Proc Natl Acad Sci U S A, 2006. **103**(30): p. 11329-33.
204. Araki, S., R. Dairiki, Y. Nakayama, et al., *Inhibitors of CLK Protein Kinases Suppress Cell Growth and Induce Apoptosis by Modulating Pre-mRNA Splicing.* PLoS One, 2015. **10**(1).
205. Vaishampayan, U.N., V. Narayan, D. Wise, et al., *A phase Ib open-label, dose escalation and expansion study to investigate the safety, pharmacokinetics, pharmacodynamics and clinical activity of GSK525762 in combination with abiraterone or enzalutamide in metastatic castrate-resistant prostate cancer.* Journal of Clinical Oncology, 2018. **36**(6_suppl): p. TPS391-TPS391.
206. Tsujikawa L., N.K., Calosing C., Attwell S., Gilham D., Sharma N., Tobin J., Haager M., Jahagirdar R., Lakhotia S., et al. , *Preclinical development and clinical validation of a whole blood pharmacodynamic marker assay for the BET bromodomain inhibitor ZEN-3694 in metastatic castration-resistant prostate cancer (mCRPC) patients.* Proceedings of the AACR Annual Meeting 2017; Washington, DC, USA, 2017.
207. Asangani, I.A., K. Wilder-Romans, V.L. Dommeti, et al., *BET Bromodomain Inhibitors Enhance Efficacy and Disrupt Resistance to AR Antagonists in the Treatment of Prostate Cancer.* Mol Cancer Res, 2016. **14**(4): p. 324-31.
208. O'Brien, K., A.J. Matlin, A.M. Lowell, and M.J. Moore, *The biflavonoid isoginkgetin is a general inhibitor of Pre-mRNA splicing.* J Biol Chem, 2008. **283**(48): p. 33147-54.
209. Pilch, B., E. Allemand, M. Facompré, et al., *Specific Inhibition of Serine- and Arginine-rich Splicing Factors Phosphorylation, Spliceosome Assembly, and Splicing by the Antitumor Drug NB-506.* Cancer Research, 2001. **61**(18): p. 6876.
210. Eskens, F.A., F.J. Ramos, H. Burger, et al., *Phase I pharmacokinetic and pharmacodynamic study of the first-in-class spliceosome inhibitor E7107 in patients with advanced solid tumors.* Clin Cancer Res, 2013. **19**(22): p. 6296-304.
211. Hong, D.S., R. Kurzrock, A. Naing, et al., *A phase I, open-label, single-arm, dose-escalation study of E7107, a precursor messenger ribonucleic acid (pre-mRNA) splicesome inhibitor administered intravenously on days 1 and 8 every 21 days to patients with solid tumors.* Invest New Drugs, 2014. **32**(3): p. 436-44.
212. Fan, L., F. Zhang, S. Xu, et al., *Histone demethylase JMJD1A promotes alternative splicing of AR variant 7 (AR-V7) in prostate cancer cells.* Proc Natl Acad Sci U S A, 2018. **115**(20): p. E4584-e4593.
213. Duan, L., Z. Chen, J. Lu, et al., *Histone lysine demethylase KDM4B regulates the alternative splicing of the androgen receptor in response to androgen deprivation.* Nucleic Acids Res, 2019. **47**(22): p. 11623-11636.
214. Prasad, J., K. Colwill, T. Pawson, and J.L. Manley, *The Protein Kinase Clk/Sty Directly Modulates SR Protein Activity: Both Hyper- and Hypophosphorylation Inhibit Splicing.* Mol Cell Biol, 1999. **19**(10): p. 6991-7000.
215. Welti, J., A. Sharp, W. Yuan, et al., *Targeting bromodomain and extra-terminal (BET) family proteins in castration resistant prostate cancer (CRPC).* Clin Cancer Res, 2018.
216. Aukema, K.G., K.K. Chohan, G.L. Plourde, K.B. Reimer, and S.D. Rader, *Small molecule inhibitors of yeast pre-mRNA splicing.* ACS Chem Biol, 2009. **4**(9): p. 759-68.
217. Chae, Y.K., K. Ranganath, P.S. Hammerman, et al., *Inhibition of the fibroblast growth factor receptor (FGFR) pathway: the current landscape and barriers to clinical application.* Oncotarget, 2017. **8**(9): p. 16052-74.

218. Bai, A., K. Meetze, N.Y. Vo, et al., *GP369, an FGFR2-IIIb-specific antibody, exhibits potent antitumor activity against human cancers driven by activated FGFR2 signaling.* Cancer Res, 2010. **70**(19): p. 7630-9.
219. Cirak, S., V. Arechavala-Gomeza, M. Guglieri, et al., *Exon skipping and dystrophin restoration in patients with Duchenne muscular dystrophy after systemic phosphorodiamidate morpholino oligomer treatment: an open-label, phase 2, dose-escalation study.* Lancet, 2011. **378**(9791): p. 595-605.
220. Zanetta, C., M. Nizzardo, C. Simone, et al., *Molecular therapeutic strategies for spinal muscular atrophies: current and future clinical trials.* Clin Ther, 2014. **36**(1): p. 128-40.
221. Smith Lindsay, D., F. Leme de Calais, M. Raponi, et al., *Novel splice-switching oligonucleotide promotes BRCA1 aberrant splicing and susceptibility to PARP inhibitor action.* International Journal of Cancer, 2017. **140**(7): p. 1564-1570.
222. Bianchini, D., A. Omlin, C. Pezaro, et al., *First-in-human Phase I study of EZN-4176, a locked nucleic acid antisense oligonucleotide to exon 4 of the androgen receptor mRNA in patients with castration-resistant prostate cancer.* Br J Cancer, 2013. **109**(10): p. 2579-86.
223. Minamiguchi, K., M. Seki, H. Aoyagi, et al., *TAS3681: New class of androgen receptor antagonist with androgen receptor downregulating activity.* Journal of Clinical Oncology, 2015. **33**(7_suppl): p. 266-266.
224. Bevan, C.L., S. Hoare, F. Claessens, D.M. Heery, and M.G. Parker, *The AF1 and AF2 domains of the androgen receptor interact with distinct regions of SRC1.* Mol Cell Biol, 1999. **19**(12): p. 8383-92.
225. Myung, J.K., C.A. Banuelos, J.G. Fernandez, et al., *An androgen receptor N-terminal domain antagonist for treating prostate cancer.* J Clin Invest, 2013. **123**(7): p. 2948-60.
226. Nappi, L., A.H. Aguda, N.A. Nakouzi, et al., *Ivermectin inhibits HSP27 and potentiates efficacy of oncogene targeting in tumor models.* J Clin Invest, 2020. **130**(2): p. 699-714.
227. Juarez, M., A. Schcolnik-Cabrera, and A. Dueñas-Gonzalez, *The multitargeted drug ivermectin: from an antiparasitic agent to a repositioned cancer drug.* Am J Cancer Res, 2018. **8**(2): p. 317-331.
228. Ferraldeschi, R., J. Welti, M.V. Powers, et al., *Second-Generation HSP90 Inhibitor Onalespib Blocks mRNA Splicing of Androgen Receptor Variant 7 in Prostate Cancer Cells.* Cancer Res, 2016. **76**(9): p. 2731-42.
229. Miller, T.C., B. Simon, V. Rybin, et al., *A bromodomain-DNA interaction facilitates acetylation-dependent bivalent nucleosome recognition by the BET protein BRDT.* Nat Commun, 2016. **7**: p. 13855.
230. Stewart, H.J., G.A. Horne, S. Bastow, and T.J. Chevassut, *BRD4 associates with p53 in DNMT3A-mutated leukemia cells and is implicated in apoptosis by the bromodomain inhibitor JQ1.* Cancer Med, 2013. **2**(6): p. 826-35.
231. Dawson, M.A., R.K. Prinjha, A. Dittmann, et al., *Inhibition of BET recruitment to chromatin as an effective treatment for MLL-fusion leukaemia.* Nature, 2011. **478**(7370): p. 529-33.
232. Delmore, J.E., G.C. Issa, M.E. Lemieux, et al., *BET bromodomain inhibition as a therapeutic strategy to target c-Myc.* Cell, 2011. **146**(6): p. 904-17.
233. Dhalluin, C., J.E. Carlson, L. Zeng, et al., *Structure and ligand of a histone acetyltransferase bromodomain.* Nature, 1999. **399**(6735): p. 491-6.

234. Sachchidanand, L. Resnick-Silverman, S. Yan, et al., *Target structure-based discovery of small molecules that block human p53 and CREB binding protein association.* Chem Biol, 2006. **13**(1): p. 81-90.
235. Filippakopoulos, P., J. Qi, S. Picaud, et al., *Selective inhibition of BET bromodomains.* Nature, 2010. **468**(7327): p. 1067-73.
236. Nicodeme, E., K.L. Jeffrey, U. Schaefer, et al., *Suppression of inflammation by a synthetic histone mimic.* Nature, 2010. **468**(7327): p. 1119-23.
237. Gosmini, R., V.L. Nguyen, J. Toum, et al., *The discovery of I-BET726 (GSK1324726A), a potent tetrahydroquinoline ApoA1 up-regulator and selective BET bromodomain inhibitor.* J Med Chem, 2014. **57**(19): p. 8111-31.
238. Berthon, C., E. Raffoux, X. Thomas, et al., *Bromodomain inhibitor OTX015 in patients with acute leukaemia: a dose-escalation, phase 1 study.* Lancet Haematol, 2016. **3**(4): p. e186-95.
239. Lewin, J., J.C. Soria, A. Stathis, et al., *Phase Ib Trial With Birabresib, a Small-Molecule Inhibitor of Bromodomain and Extraterminal Proteins, in Patients With Selected Advanced Solid Tumors.* J Clin Oncol, 2018. **36**(30): p. 3007-3014.
240. Picaud, S., C. Wells, I. Felletar, et al., *RVX-208, an inhibitor of BET transcriptional regulators with selectivity for the second bromodomain.* Proc Natl Acad Sci U S A, 2013. **110**(49): p. 19754-9.
241. Zhou, X., L.X. Fan, D.J. Peters, et al., *Therapeutic targeting of BET bromodomain protein, Brd4, delays cyst growth in ADPKD.* Hum Mol Genet, 2015. **24**(14): p. 3982-93.
242. Mertz, J.A., A.R. Conery, B.M. Bryant, et al., *Targeting MYC dependence in cancer by inhibiting BET bromodomains.* Proc Natl Acad Sci U S A, 2011. **108**(40): p. 16669-74.
243. Bandopadhayay, P., G. Bergthold, B. Nguyen, et al., *BET bromodomain inhibition of MYC-amplified medulloblastoma.* Clin Cancer Res, 2014. **20**(4): p. 912-25.
244. Coleman, D.J., L. Gao, J. Schwartzman, et al., *Maintenance of MYC expression promotes de novo resistance to BET bromodomain inhibition in castration-resistant prostate cancer.* Scientific Reports, 2019. **9**(1): p. 3823.
245. Rathert, P., M. Roth, T. Neumann, et al., *Transcriptional plasticity promotes primary and acquired resistance to BET inhibition.* Nature, 2015. **525**(7570): p. 543-547.
246. Amorim, S., A. Stathis, M. Gleeson, et al., *Bromodomain inhibitor OTX015 in patients with lymphoma or multiple myeloma: a dose-escalation, open-label, pharmacokinetic, phase 1 study.* Lancet Haematol, 2016. **3**(4): p. e196-204.
247. Stathis, A., E. Zucca, M. Bekradda, et al., *Clinical Response of Carcinomas Harboring the BRD4-NUT Oncoprotein to the Targeted Bromodomain Inhibitor OTX015/MK-8628.* Cancer Discov, 2016. **6**(5): p. 492-500.
248. Hottinger, A.F., M. Sanson, E. Moyal, et al., *Dose optimization of MK-8628 (OTX015), a small molecule inhibitor of bromodomain and extra-terminal (BET) proteins, in patients (pts) with recurrent glioblastoma (GB).* Journal of Clinical Oncology, 2016. **34**(15_suppl): p. e14123-e14123.
249. Abramson, J.S., K.A. Blum, I.W. Flinn, et al., *BET Inhibitor CPI-0610 Is Well Tolerated and Induces Responses in Diffuse Large B-Cell Lymphoma and Follicular Lymphoma: Preliminary Analysis of an Ongoing Phase 1 Study.* Blood, 2015. **126**(23): p. 1491-1491.
250. O'Dwyer, P.J., S.A. Piha-Paul, C. French, et al., *Abstract CT014: GSK525762, a selective bromodomain (BRD) and extra terminal protein (BET) inhibitor: results from part 1 of*

a phase I/II open-label single-agent study in patients with NUT midline carcinoma (NMC) and other cancers. Cancer Research, 2016. **76**(14 Supplement): p. CT014.
251. Shapiro, G.I., A. Dowlati, P.M. LoRusso, et al., *Abstract A49: Clinically efficacy of the BET bromodomain inhibitor TEN-010 in an open-label substudy with patients with documented NUT-midline carcinoma (NMC).* Molecular Cancer Therapeutics, 2015. **14**(12 Supplement 2): p. A49.
252. Postel-Vinay, S., K. Herbschleb, C. Massard, et al., *First-in-human phase I study of the bromodomain and extraterminal motif inhibitor BAY 1238097: emerging pharmacokinetic/pharmacodynamic relationship and early termination due to unexpected toxicity.* Eur J Cancer, 2019. **109**: p. 103-110.
253. Wang, F., H. Liu, W.P. Blanton, et al., *Brd2 disruption in mice causes severe obesity without Type 2 diabetes.* Biochem J, 2009. **425**(1): p. 71-83.
254. Korb, E., M. Herre, I. Zucker-Scharff, R.B. Darnell, and C.D. Allis, *BET protein Brd4 activates transcription in neurons and BET inhibitor Jq1 blocks memory in mice.* Nat Neurosci, 2015. **18**(10): p. 1464-73.
255. Sullivan, J.M., A. Badimon, U. Schaefer, et al., *Autism-like syndrome is induced by pharmacological suppression of BET proteins in young mice.* J Exp Med, 2015. **212**(11): p. 1771-81.
256. Seyhan, A.A., *Lost in translation: the valley of death across preclinical and clinical divide – identification of problems and overcoming obstacles.* Translational Medicine Communications, 2019. **4**(1): p. 18.
257. Risbridger, G.P., R. Toivanen, and R.A. Taylor, *Preclinical Models of Prostate Cancer: Patient-Derived Xenografts, Organoids, and Other Explant Models.* Cold Spring Harb Perspect Med, 2018. **8**(8).
258. Lin, A., C.J. Giuliano, A. Palladino, et al., *Off-target toxicity is a common mechanism of action of cancer drugs undergoing clinical trials.* Sci Transl Med, 2019. **11**(509).
259. ClinicalTrials.gov [Internet]. Bethesda (MD): National Library of Medicine (US). 2000 Feb 29 - . Identifier: NCT00932126, T.I.T.F.S.U.E.D.O.
260. ClinicalTrials.gov [Internet]. Bethesda (MD): National Library of Medicine (US). 2000 Feb 29 - . Identifier: NCT02606123, S.a.A.-T.S.o.O.E.-.
261. 2001., O.W.B.i.r.a.V.a.v.W.
262. Slamon, D.J., B. Leyland-Jones, S. Shak, et al., *Use of chemotherapy plus a monoclonal antibody against HER2 for metastatic breast cancer that overexpresses HER2.* N Engl J Med, 2001. **344**(11): p. 783-92.
263. Imperiale, T.F., D.F. Ransohoff, and S.H. Itzkowitz, *Multitarget stool DNA testing for colorectal-cancer screening.* N Engl J Med, 2014. **371**(2): p. 187-8.
264. https://www.gov.uk/government/publications/prostate-cancer-risk-management-programme-psa-test-benefits-and-risks/prostate-cancer-risk-management-programme-pcrmp-benefits-and-risks-of-psa-testing, P.H.E.P.c.r.m.p.P.b.a.r.o.P.t.I.G.U.A.f.
265. De Angelis, G., H.G. Rittenhouse, S.D. Mikolajczyk, L. Blair Shamel, and A. Semjonow, *Twenty Years of PSA: From Prostate Antigen to Tumor Marker.* Rev Urol, 2007. **9**(3): p. 113-23.
266. Catalona, W.J., J.P. Richie, F.R. Ahmann, et al., *Comparison of digital rectal examination and serum prostate specific antigen in the early detection of prostate cancer: results of a multicenter clinical trial of 6,630 men.* J Urol, 1994. **151**(5): p. 1283-90.

267. Conteduca, V., C. Oromendia, K.W. Eng, et al., *Clinical features of neuroendocrine prostate cancer.* Eur J Cancer, 2019. **121**: p. 7-18.
268. Graham, L.S., B. Montgomery, H.H. Cheng, et al., *Mismatch repair deficiency in metastatic prostate cancer: Response to PD-1 blockade and standard therapies.* PLoS One, 2020. **15**(5): p. e0233260.
269. de Bono, J.S., H.I. Scher, R.B. Montgomery, et al., *Circulating tumor cells predict survival benefit from treatment in metastatic castration-resistant prostate cancer.* Clin Cancer Res, 2008. **14**(19): p. 6302-9.
270. Turpin, A., E. Girard, C. Baillet, et al., *Imaging for Metastasis in Prostate Cancer: A Review of the Literature.* Front Oncol, 2020. **10**: p. 55.
271. Afshar-Oromieh, A., C.M. Zechmann, A. Malcher, et al., *Comparison of PET imaging with a (68)Ga-labelled PSMA ligand and (18)F-choline-based PET/CT for the diagnosis of recurrent prostate cancer.* Eur J Nucl Med Mol Imaging, 2014. **41**(1): p. 11-20.
272. Eiber, M., W.P. Fendler, S.P. Rowe, et al., *Prostate-Specific Membrane Antigen Ligands for Imaging and Therapy.* J Nucl Med, 2017. **58**(Suppl 2): p. 67s-76s.
273. Rahbar, K., M. Schmidt, A. Heinzel, et al., *Response and Tolerability of a Single Dose of 177Lu-PSMA-617 in Patients with Metastatic Castration-Resistant Prostate Cancer: A Multicenter Retrospective Analysis.* J Nucl Med, 2016. **57**(9): p. 1334-8.
274. Ahmadzadehfar, H., S. Wegen, A. Yordanova, et al., *Overall survival and response pattern of castration-resistant metastatic prostate cancer to multiple cycles of radioligand therapy using [(177)Lu]Lu-PSMA-617.* Eur J Nucl Med Mol Imaging, 2017. **44**(9): p. 1448-1454.
275. Rahbar, K., H. Ahmadzadehfar, C. Kratochwil, et al., *German Multicenter Study Investigating 177Lu-PSMA-617 Radioligand Therapy in Advanced Prostate Cancer Patients.* J Nucl Med, 2017. **58**(1): p. 85-90.
276. Paschalis, A., B. Sheehan, R. Riisnaes, et al., *Prostate-specific Membrane Antigen Heterogeneity and DNA Repair Defects in Prostate Cancer.* Eur Urol, 2019. **76**(4): p. 469-478.
277. Pervaiz, M., P. Mishra, and S. Gunther, *Bromodomain Drug Discovery - the Past, the Present, and the Future.* Chem Rec, 2018. **18**(12): p. 1808-1817.
278. Lockwood, W.W., K. Zejnullahu, J.E. Bradner, and H. Varmus, *Sensitivity of human lung adenocarcinoma cell lines to targeted inhibition of BET epigenetic signaling proteins.* Proc Natl Acad Sci U S A, 2012. **109**(47): p. 19408-13.
279. Wu, S.Y., A.Y. Lee, H.T. Lai, H. Zhang, and C.M. Chiang, *Phospho switch triggers Brd4 chromatin binding and activator recruitment for gene-specific targeting.* Mol Cell, 2013. **49**(5): p. 843-57.
280. Weinstein, J.N., E.A. Collisson, G.B. Mills, et al., *The Cancer Genome Atlas Pan-Cancer analysis project.* Nat Genet, 2013. **45**(10): p. 1113-20.
281. Heim, A., C. Grimm, U. Müller, et al., *Jumonji domain containing protein 6 (Jmjd6) modulates splicing and specifically interacts with arginine-serine-rich (RS) domains of SR- and SR-like proteins.* Nucleic Acids Res, 2014. **42**(12): p. 7833-50.
282. Mantri, M., T. Krojer, E.A. Bagg, et al., *Crystal structure of the 2-oxoglutarate- and Fe(II)-dependent lysyl hydroxylase JMJD6.* J Mol Biol, 2010. **401**(2): p. 211-22.
283. Winer, J., C.K. Jung, I. Shackel, and P.M. Williams, *Development and validation of real-time quantitative reverse transcriptase-polymerase chain reaction for monitoring gene expression in cardiac myocytes in vitro.* Anal Biochem, 1999. **270**(1): p. 41-9.

284. Sharp, A., I. Coleman, W. Yuan, et al., *Androgen receptor splice variant-7 expression emerges with castration resistance in prostate cancer.* J Clin Invest, 2019. **129**(1): p. 192-208.
285. McCarty, K.S., Jr., E. Szabo, J.L. Flowers, et al., *Use of a monoclonal anti-estrogen receptor antibody in the immunohistochemical evaluation of human tumors.* Cancer Res, 1986. **46**(8 Suppl): p. 4244s-4248s.
286. Detre, S., G. Saclani Jotti, and M. Dowsett, *A "quickscore" method for immunohistochemical semiquantitation: validation for oestrogen receptor in breast carcinomas.* J Clin Pathol, 1995. **48**(9): p. 876-8.
287. Wilkins, S.E., M.S. Islam, J.M. Gannon, et al., *JMJD5 is a human arginyl C-3 hydroxylase.* Nature Communications, 2018. **9**(1): p. 1180.
288. Webby, C.J., A. Wolf, N. Gromak, et al., *Jmjd6 catalyses lysyl-hydroxylation of U2AF65, a protein associated with RNA splicing.* Science, 2009. **325**(5936): p. 90-3.
289. Islam, M.S., M.A. McDonough, R. Chowdhury, et al., *Biochemical and structural investigations clarify the substrate selectivity of the 2-oxoglutarate oxygenase JMJD6.* J Biol Chem, 2019. **294**(30): p. 11637-11652.
290. Trapnell, C., A. Roberts, L. Goff, et al., *Differential gene and transcript expression analysis of RNA-seq experiments with TopHat and Cufflinks.* Nat Protoc, 2012. **7**(3): p. 562-78.
291. Kumar, A., I. Coleman, C. Morrissey, et al., *Substantial interindividual and limited intraindividual genomic diversity among tumors from men with metastatic prostate cancer.* Nature Medicine, 2016. **22**: p. 369.
292. Wang, G., S.J. Jones, M.A. Marra, and M.D. Sadar, *Identification of genes targeted by the androgen and PKA signaling pathways in prostate cancer cells.* Oncogene, 2006. **25**(55): p. 7311-23.
293. Liberzon, A., C. Birger, H. Thorvaldsdottir, et al., *The Molecular Signatures Database (MSigDB) hallmark gene set collection.* Cell Syst, 2015. **1**(6): p. 417-425.
294. Kim, D. and S.L. Salzberg, *TopHat-Fusion: an algorithm for discovery of novel fusion transcripts.* Genome Biol, 2011. **12**(8): p. R72.
295. Shen, S., J.W. Park, J. Huang, et al., *MATS: a Bayesian framework for flexible detection of differential alternative splicing from RNA-Seq data.* Nucleic Acids Res, 2012. **40**(8): p. e61.
296. Subramanian, A., P. Tamayo, V.K. Mootha, et al., *Gene set enrichment analysis: A knowledge-based approach for interpreting genome-wide expression profiles.* Proceedings of the National Academy of Sciences, 2005. **102**(43): p. 15545.
297. Visakorpi, T., E. Hyytinen, P. Koivisto, et al., *In vivo amplification of the androgen receptor gene and progression of human prostate cancer.* Nat Genet, 1995. **9**(4): p. 401-6.
298. Monaghan, A.E. and I.J. McEwan, *A sting in the tail: the N-terminal domain of the androgen receptor as a drug target.* Asian J Androl, 2016. **18**(5): p. 687-94.
299. Zhao, X.-Y., P.J. Malloy, A.V. Krishnan, et al., *Glucocorticoids can promote androgen-independent growth of prostate cancer cells through a mutated androgen receptor.* Nature Medicine, 2000. **6**(6): p. 703-706.
300. Lallous, N., S.V. Volik, S. Awrey, et al., *Functional analysis of androgen receptor mutations that confer anti-androgen resistance identified in circulating cell-free DNA from prostate cancer patients.* Genome Biol, 2016. **17**: p. 10.

301. Li, J., C. Yen, D. Liaw, et al., *PTEN, a Putative Protein Tyrosine Phosphatase Gene Mutated in Human Brain, Breast, and Prostate Cancer.* Science, 1997. **275**(5308): p. 1943.
302. Ebersole, J.L., M.J. Novak, L. Orraca, et al., *Hypoxia-inducible transcription factors, HIF1A and HIF2A, increase in aging mucosal tissues.* Immunology, 2018.
303. Fraga, A., R. Ribeiro, P. Principe, C. Lopes, and R. Medeiros, *Hypoxia and Prostate Cancer Aggressiveness: A Tale With Many Endings.* Clin Genitourin Cancer, 2015. **13**(4): p. 295-301.
304. Doll, R. and A.B. Hill, *Smoking and carcinoma of the lung; preliminary report.* Br Med J, 1950. **2**(4682): p. 739-48.
305. Wynder, E.L. and E.A. Graham, *Tobacco smoking as a possible etiologic factor in bronchiogenic carcinoma; a study of 684 proved cases.* J Am Med Assoc, 1950. **143**(4): p. 329-36.
306. van Bokhoven, A., M. Varella-Garcia, C. Korch, et al., *Molecular characterization of human prostate carcinoma cell lines.* Prostate, 2003. **57**(3): p. 205-25.
307. Yu, Z., S. Chen, A.G. Sowalsky, et al., *Rapid induction of androgen receptor splice variants by androgen deprivation in prostate cancer.* Clin Cancer Res, 2014. **20**(6): p. 1590-600.
308. Bottger, A., M.S. Islam, R. Chowdhury, C.J. Schofield, and A. Wolf, *The oxygenase Jmjd6--a case study in conflicting assignments.* Biochem J, 2015. **468**(2): p. 191-202.
309. Kwok, J., M. O'Shea, D.A. Hume, and A. Lengeling, *Jmjd6, a JmjC Dioxygenase with Many Interaction Partners and Pleiotropic Functions.* Front Genet, 2017. **8**.
310. Chen, R. and N. Forsyth, *Editorial: The Development of New Classes of Hypoxia Mimetic Agents for Clinical Use.* Frontiers in Cell and Developmental Biology, 2019. **7**: p. 120.
311. Reyes-Gutierrez, P., J.W. Carrasquillo-Rodriguez, and A.N. Imbalzano, *Promotion of adipogenesis by JMJD6 requires the AT hook-like domain and is independent of its catalytic function.* PLoS One, 2019. **14**(8): p. e0216015.
312. Hannus, M., M. Beitzinger, J.C. Engelmann, et al., *siPools: highly complex but accurately defined siRNA pools eliminate off-target effects.* Nucleic Acids Res, 2014. **42**(12): p. 8049-61.
313. Jackson, A.L., J. Burchard, D. Leake, et al., *Position-specific chemical modification of siRNAs reduces "off-target" transcript silencing.* Rna, 2006. **12**(7): p. 1197-205.
314. Liu, W., Q. Ma, K. Wong, et al., *Brd4 and JMJD6-associated Anti-pause Enhancers in Regulation of Transcriptional Pause Release.* Cell, 2013. **155**(7): p. 1581-95.
315. Liu, X., W. Si, X. Liu, et al., *JMJD6 promotes melanoma carcinogenesis through regulation of the alternative splicing of PAK1, a key MAPK signaling component.* Mol Cancer, 2017. **16**(1): p. 175.
316. Boeckel, J.N., V. Guarani, M. Koyanagi, et al., *Jumonji domain-containing protein 6 (Jmjd6) is required for angiogenic sprouting and regulates splicing of VEGF-receptor 1.* Proc Natl Acad Sci U S A, 2011. **108**(8): p. 3276-81.
317. Barman-Aksozen, J., C. Beguin, A.M. Dogar, X. Schneider-Yin, and E.I. Minder, *Iron availability modulates aberrant splicing of ferrochelatase through the iron- and 2-oxoglutarate dependent dioxygenase Jmjd6 and U2AF(65.).* Blood Cells Mol Dis, 2013. **51**(3): p. 151-61.
318. Yi, J., H.F. Shen, J.S. Qiu, et al., *JMJD6 and U2AF65 co-regulate alternative splicing in both JMJD6 enzymatic activity dependent and independent manner.* Nucleic Acids Res, 2017. **45**(6): p. 3503-3518.

319. Han, G., J. Li, Y. Wang, et al., *The hydroxylation activity of Jmjd6 is required for its homo-oligomerization.* J Cell Biochem, 2012. **113**(5): p. 1663-70.
320. Kwok, J., M. O'Shea, D.A. Hume, and A. Lengeling, *Jmjd6, a JmjC Dioxygenase with Many Interaction Partners and Pleiotropic Functions.* Front Genet, 2017. **8**: p. 32.
321. Sims, D., I. Sudbery, N.E. Ilott, A. Heger, and C.P. Ponting, *Sequencing depth and coverage: key considerations in genomic analyses.* Nature Reviews Genetics, 2014. **15**(2): p. 121-132.
322. Mantri, M., C.J. Webby, N.D. Loik, et al., *Self-hydroxylation of the splicing factor lysyl hydroxylase, JMJD6.* MedChemComm, 2012. **3**(1): p. 80-85.
323. Wang, F., L. He, P. Huangyang, et al., *JMJD6 promotes colon carcinogenesis through negative regulation of p53 by hydroxylation.* PLoS Biol, 2014. **12**(3): p. e1001819.
324. Poulard, C., J. Rambaud, N. Hussein, L. Corbo, and M. Le Romancer, *JMJD6 regulates ERalpha methylation on arginine.* PLoS One, 2014. **9**(2): p. e87982.
325. Chang, B., Y. Chen, Y. Zhao, and R.K. Bruick, *JMJD6 is a histone arginine demethylase.* Science, 2007. **318**(5849): p. 444-7.
326. Mahon, P.C., K. Hirota, and G.L. Semenza, *FIH-1: a novel protein that interacts with HIF-1alpha and VHL to mediate repression of HIF-1 transcriptional activity.* Genes Dev, 2001. **15**(20): p. 2675-86.
327. Bulusu, K.C., J.E. Tym, E.A. Coker, A.C. Schierz, and B. Al-Lazikani, *canSAR: updated cancer research and drug discovery knowledgebase.* Nucleic Acids Res, 2014. **42**(Database issue): p. D1040-7.
328. Tym, J.E., C. Mitsopoulos, E.A. Coker, et al., *canSAR: an updated cancer research and drug discovery knowledgebase.* Nucleic Acids Res, 2016. **44**(D1): p. D938-43.
329. Berman, H.M., J. Westbrook, Z. Feng, et al., *The Protein Data Bank.* Nucleic Acids Res, 2000. **28**(1): p. 235-42.
330. Yeh, T.L., T.M. Leissing, M.I. Abboud, et al., *Molecular and cellular mechanisms of HIF prolyl hydroxylase inhibitors in clinical trials.* Chem Sci, 2017. **8**(11): p. 7651-7668.
331. Leung, I.K., T.J. Krojer, G.T. Kochan, et al., *Structural and mechanistic studies on gamma-butyrobetaine hydroxylase.* Chem Biol, 2010. **17**(12): p. 1316-24.
332. Bonnici, J., A. Tumber, A. Kawamura, and C.J. Schofield, *Inhibitors of both the N-methyl lysyl- and arginyl-demethylase activities of the JmjC oxygenases.* Philos Trans R Soc Lond B Biol Sci, 2018. **373**(1748).
333. Rose, N.R., M.A. McDonough, O.N. King, A. Kawamura, and C.J. Schofield, *Inhibition of 2-oxoglutarate dependent oxygenases.* Chem Soc Rev, 2011. **40**(8): p. 4364-97.
334. Thalhammer, A., J. Mecinović, C. Loenarz, et al., *Inhibition of the histone demethylase JMJD2E by 3-substituted pyridine 2,4-dicarboxylates.* Organic & Biomolecular Chemistry, 2011. **9**(1): p. 127-135.
335. Majmundar, A.J., W.J. Wong, and M.C. Simon, *Hypoxia-inducible factors and the response to hypoxic stress.* Mol Cell, 2010. **40**(2): p. 294-309.
336. Miller, T.E., B.B. Liau, L.C. Wallace, et al., *Transcription elongation factors represent in vivo cancer dependencies in glioblastoma.* Nature, 2017. **547**(7663): p. 355-359.
337. Tschank, G., M. Raghunath, V. Günzler, and H.M. Hanauske-Abel, *Pyridinedicarboxylates, the first mechanism-derived inhibitors for prolyl 4-hydroxylase, selectively suppress cellular hydroxyprolyl biosynthesis. Decrease in interstitial collagen and Clq secretion in cell culture.* Biochem J, 1987. **248**(3): p. 625-33.

338. Kristensen, L.H., A.L. Nielsen, C. Helgstrand, et al., *Studies of H3K4me3 demethylation by KDM5B/Jarid1B/PLU1 reveals strong substrate recognition in vitro and identifies 2,4-pyridine-dicarboxylic acid as an in vitro and in cell inhibitor.* Febs j, 2012. **279**(11): p. 1905-14.
339. Zheng, H., Y. Tie, Z. Fang, et al., *Jumonji domain-containing 6 (JMJD6) identified as a potential therapeutic target in ovarian cancer.* Signal Transduct Target Ther, 2019. **4**: p. 24.
340. Fadok, V.A., D.L. Bratton, D.M. Rose, et al., *A receptor for phosphatidylserine-specific clearance of apoptotic cells.* Nature, 2000. **405**(6782): p. 85-90.
341. Wolf, A., C. Schmitz, and A. Böttger, *Changing story of the receptor for phosphatidylserine-dependent clearance of apoptotic cells.* EMBO reports, 2007. **8**(5): p. 465-469.
342. Cikala, M., O. Alexandrova, C.N. David, et al., *The phosphatidylserine receptor from Hydra is a nuclear protein with potential Fe(II) dependent oxygenase activity.* BMC Cell Biol, 2004. **5**: p. 26.
343. Loenarz, C. and C.J. Schofield, *Expanding chemical biology of 2-oxoglutarate oxygenases.* Nat Chem Biol, 2008. **4**(3): p. 152-6.
344. *UniProt: a worldwide hub of protein knowledge.* Nucleic Acids Res, 2019. **47**(D1): p. D506-d515.
345. Wolf, A., M. Mantri, A. Heim, et al., *The polyserine domain of the lysyl-5 hydroxylase Jmjd6 mediates subnuclear localization.* Biochem J, 2013. **453**(3): p. 357-70.
346. Hahn, P., I. Wegener, A. Burrells, et al., *Analysis of Jmjd6 cellular localization and testing for its involvement in histone demethylation.* PLoS One, 2010. **5**(10): p. e13769.
347. Hong, X., J. Zang, J. White, et al., *Interaction of JMJD6 with single-stranded RNA.* Proc Natl Acad Sci U S A, 2010. **107**(33): p. 14568-72.
348. Böse, J., A.D. Gruber, L. Helming, et al., *The phosphatidylserine receptor has essential functions during embryogenesis but not in apoptotic cell removal.* J Biol, 2004. **3**(4): p. 15.
349. Kunisaki, Y., S. Masuko, M. Noda, et al., *Defective fetal liver erythropoiesis and T lymphopoiesis in mice lacking the phosphatidylserine receptor.* Blood, 2004. **103**(9): p. 3362-4.
350. Schneider, J.E., J. Bose, S.D. Bamforth, et al., *Identification of cardiac malformations in mice lacking Ptdsr using a novel high-throughput magnetic resonance imaging technique.* BMC Dev Biol, 2004. **4**: p. 16.
351. Bose, J., A.D. Gruber, L. Helming, et al., *The phosphatidylserine receptor has essential functions during embryogenesis but not in apoptotic cell removal.* J Biol, 2004. **3**(4): p. 15.
352. Yanagihara, T., F. Sanematsu, T. Sato, et al., *Intronic regulation of Aire expression by Jmjd6 for self-tolerance induction in the thymus.* Nat Commun, 2015. **6**: p. 8820.
353. Krieser, R.J., F.E. Moore, D. Dresnek, et al., *The Drosophila homolog of the putative phosphatidylserine receptor functions to inhibit apoptosis.* Development, 2007. **134**(13): p. 2407-14.
354. Migliori, V., J. Muller, S. Phalke, et al., *Symmetric dimethylation of H3R2 is a newly identified histone mark that supports euchromatin maintenance.* Nat Struct Mol Biol, 2012. **19**(2): p. 136-44.

355. Yuan, C.C., A.G. Matthews, Y. Jin, et al., *Histone H3R2 symmetric dimethylation and histone H3K4 trimethylation are tightly correlated in eukaryotic genomes.* Cell Rep, 2012. **1**(2): p. 83-90.
356. Unoki, M., A. Masuda, N. Dohmae, et al., *Lysyl 5-hydroxylation, a novel histone modification, by Jumonji domain containing 6 (JMJD6).* J Biol Chem, 2013. **288**(9): p. 6053-62.
357. Liu, X., W.L. Kraus, and X. Bai, *Ready, pause, go: regulation of RNA polymerase II pausing and release by cellular signaling pathways.* Trends Biochem Sci, 2015. **40**(9): p. 516-25.
358. Adelman, K. and J.T. Lis, *Promoter-proximal pausing of RNA polymerase II: emerging roles in metazoans.* Nat Rev Genet, 2012. **13**(10): p. 720-31.
359. Yamada, T., Y. Yamaguchi, N. Inukai, et al., *P-TEFb-mediated phosphorylation of hSpt5 C-terminal repeats is critical for processive transcription elongation.* Mol Cell, 2006. **21**(2): p. 227-37.
360. Parra, M., B.W. Booth, R. Weiszmann, et al., *An important class of intron retention events in human erythroblasts is regulated by cryptic exons proposed to function as splicing decoys.* Rna, 2018. **24**(9): p. 1255-1265.
361. Calarco, J.A., *'Cryptic' exons reveal some of their secrets.* Elife, 2013. **2**: p. e00476.
362. Alahari, S., M. Post, and I. Caniggia, *Jumonji Domain Containing Protein 6: A Novel Oxygen Sensor in the Human Placenta.* Endocrinology, 2015. **156**(8): p. 3012-25.
363. Aprelikova, O., K. Chen, L.H. El Touny, et al., *The epigenetic modifier JMJD6 is amplified in mammary tumors and cooperates with c-Myc to enhance cellular transformation, tumor progression, and metastasis.* Clin Epigenetics, 2016. **8**: p. 38.
364. Zhang, J., S.S. Ni, W.L. Zhao, X.C. Dong, and J.L. Wang, *High expression of JMJD6 predicts unfavorable survival in lung adenocarcinoma.* Tumour Biol, 2013. **34**(4): p. 2397-401.
365. Lee, Y.F., L.D. Miller, X.B. Chan, et al., *JMJD6 is a driver of cellular proliferation and motility and a marker of poor prognosis in breast cancer.* Breast Cancer Res, 2012. **14**(3): p. R85.
366. Reed, S.M. and D.E. Quelle, *p53 Acetylation: Regulation and Consequences.* Cancers (Basel), 2014. **7**(1): p. 30-69.
367. Peng, Y. and C.M. Croce, *The role of MicroRNAs in human cancer.* Signal Transduct Target Ther, 2016. **1**: p. 15004.
368. Jao, T.M., M.H. Tsai, H.Y. Lio, et al., *Protocadherin 10 suppresses tumorigenesis and metastasis in colorectal cancer and its genetic loss predicts adverse prognosis.* Int J Cancer, 2014. **135**(11): p. 2593-603.
369. Biswas, A., A. Shettar, G. Mukherjee, P. Kondaiah, and K.V. Desai, *JMJD6 induces HOTAIR, an oncogenic lincRNA, by physically interacting with its proximal promoter.* Biochem J, 2018. **475**(1): p. 355-371.
370. Zhang, Z., Y. Yang, and X. Zhang, *MiR-770 inhibits tumorigenesis and EMT by targeting JMJD6 and regulating WNT/beta-catenin pathway in non-small cell lung cancer.* Life Sci, 2017. **188**: p. 163-171.
371. Wilson, C. and A.J. Krieg, *KDM4B: A Nail for Every Hammer?* Genes (Basel), 2019. **10**(2).
372. Yamane, K., C. Toumazou, Y. Tsukada, et al., *JHDM2A, a JmjC-containing H3K9 demethylase, facilitates transcription activation by androgen receptor.* Cell, 2006. **125**(3): p. 483-95.

373. Walport, L.J., R.J. Hopkinson, R. Chowdhury, et al., *Arginine demethylation is catalysed by a subset of JmjC histone lysine demethylases.* Nat Commun, 2016. **7**: p. 11974.
374. *DepMap at Broad Institute. Cancer Dependency Map. DepMap https://depmap.org/portal/ (2018).*
375. Cerami, E., J. Gao, U. Dogrusoz, et al., *The cBio cancer genomics portal: an open platform for exploring multidimensional cancer genomics data.* Cancer Discov, 2012. **2**(5): p. 401-4.
376. Eidelman, E., J. Twum-Ampofo, J. Ansari, and M.M. Siddiqui, *The Metabolic Phenotype of Prostate Cancer.* Front Oncol, 2017. **7**: p. 131.
377. Wang, Q., R.A. Hardie, A.J. Hoy, et al., *Targeting ASCT2-mediated glutamine uptake blocks prostate cancer growth and tumour development.* J Pathol, 2015. **236**(3): p. 278-89.
378. Shafi, A.A., V. Putluri, J.M. Arnold, et al., *Differential regulation of metabolic pathways by androgen receptor (AR) and its constitutively active splice variant, AR-V7, in prostate cancer cells.* Oncotarget, 2015. **6**(31): p. 31997-2012.
379. Zhou, X., X. Yang, X. Sun, et al., *Effect of PTEN loss on metabolic reprogramming in prostate cancer cells.* Oncol Lett, 2019. **17**(3): p. 2856-2866.
380. Wise, D.R., R.J. DeBerardinis, A. Mancuso, et al., *Myc regulates a transcriptional program that stimulates mitochondrial glutaminolysis and leads to glutamine addiction.* Proceedings of the National Academy of Sciences, 2008. **105**(48): p. 18782.
381. Goetzman, E.S. and E.V. Prochownik, *The Role for Myc in Coordinating Glycolysis, Oxidative Phosphorylation, Glutaminolysis, and Fatty Acid Metabolism in Normal and Neoplastic Tissues.* Front Endocrinol (Lausanne), 2018. **9**: p. 129.
382. Reynolds, M.R., A.N. Lane, B. Robertson, et al., *Control of glutamine metabolism by the tumor suppressor Rb.* Oncogene, 2014. **33**(5): p. 556-66.
383. Harami-Papp, H., L.S. Pongor, G. Munkácsy, et al., *TP53 mutation hits energy metabolism and increases glycolysis in breast cancer.* Oncotarget, 2016. **7**(41): p. 67183-67195.
384. Eriksson, M., G. Ambroise, A.T. Ouchida, et al., *Effect of Mutant p53 Proteins on Glycolysis and Mitochondrial Metabolism.* Mol Cell Biol, 2017. **37**(24).
385. Eales, K.L., K.E.R. Hollinshead, and D.A. Tennant, *Hypoxia and metabolic adaptation of cancer cells.* Oncogenesis, 2016. **5**(1): p. e190-e190.
386. Marchiq, I. and J. Pouysségur, *Hypoxia, cancer metabolism and the therapeutic benefit of targeting lactate/H+ symporters.* Journal of Molecular Medicine, 2016. **94**(2): p. 155-171.
387. Wise, D.R., P.S. Ward, J.E. Shay, et al., *Hypoxia promotes isocitrate dehydrogenase-dependent carboxylation of α-ketoglutarate to citrate to support cell growth and viability.* Proc Natl Acad Sci U S A, 2011. **108**(49): p. 19611-6.
388. Hayashi, Y., A. Yokota, H. Harada, and G. Huang, *Hypoxia/pseudohypoxia-mediated activation of hypoxia-inducible factor-1α in cancer.* Cancer Science, 2019. **110**(5): p. 1510-1517.
389. Maxwell, P.H., M.S. Wiesener, G.W. Chang, et al., *The tumour suppressor protein VHL targets hypoxia-inducible factors for oxygen-dependent proteolysis.* Nature, 1999. **399**(6733): p. 271-5.
390. Zundel, W., C. Schindler, D. Haas-Kogan, et al., *Loss of PTEN facilitates HIF-1-mediated gene expression.* Genes Dev, 2000. **14**(4): p. 391-6.

391. Selak, M.A., S.M. Armour, E.D. MacKenzie, et al., *Succinate links TCA cycle dysfunction to oncogenesis by inhibiting HIF-alpha prolyl hydroxylase.* Cancer Cell, 2005. **7**(1): p. 77-85.
392. Pasini, B. and C.A. Stratakis, *SDH mutations in tumorigenesis and inherited endocrine tumours: lesson from the phaeochromocytoma-paraganglioma syndromes.* J Intern Med, 2009. **266**(1): p. 19-42.

14

Appendix

Appendix A: Bioinformatic QC results from RNA sequencing; LNCaP vs LNCaP95

Samples	PF ALIGNED BASES	RIBOSOMAL BASES	CODING BASES	UTR BASES	INTRONIC BASES	INTERGENIC BASES	IGNORED READS	CORRECT STRAND READS	INCORRECT STRAND READS
LNCaP95_DMSO_48_1	9654006202	64636566	5780911427	3022424130	301473076	484561898	0	81579888	204769
LNCaP95_DMSO_48_2	9639361971	67614652	5823933466	2992031045	287996856	467786861	0	81674651	205009
LNCaP95_DMSO_8_1	12147625223	77571838	7827860640	3516382465	247805180	478006163	0	105202897	182045
LNCaP95_DMSO_8_2	12773240627	69045418	8247568899	3666025131	274023587	516579048	0	110466573	195309
LNCaP_DMSO_48_1	11955814332	101273508	7822917981	3171954542	305257377	554412640	0	100223263	229541
LNCaP_DMSO_48_2	8505674144	68298624	5550256168	2267408367	236563216	383148348	0	71373090	171948
LNCaP_DMSO_8_1	10488509048	69047236	6698262145	2866264106	242892990	612043268	0	87207367	174690
LNCaP_DMSO_8_2	10926236485	70508100	7052069809	2934080483	251835339	617743482	0	90962403	182152

Samples	RIBOSOMAL BASES	CODING BASES	UTR BASES	INTRONIC BASES	INTERGENIC BASES	mRNA BASES	USABLE BASES	CORRECT STRAND READS	MEDIAN CV COVERAGE	MEDIAN 5' BIAS	MEDIAN 3' BIAS	MEDIAN 5' TO 3' BIAS
LNCaP95_DMSO_48_1	0.67%	59.88%	31.31%	3.12%	5.02%	91.19%	91.18%	99.75%	56.78%	7.99%	17.55%	59.11%
LNCaP95_DMSO_48_2	0.70%	60.42%	31.04%	2.99%	4.85%	91.46%	91.45%	99.75%	55.63%	10.15%	17.54%	71.18%
LNCaP95_DMSO_8_1	0.64%	64.44%	28.95%	2.04%	3.94%	93.39%	93.38%	99.83%	58.25%	8.65%	16.00%	63.84%
LNCaP95_DMSO_8_2	0.54%	64.57%	28.70%	2.15%	4.04%	93.27%	93.27%	99.82%	58.62%	8.55%	15.86%	67.56%
LNCaP_DMSO_48_1	0.85%	65.43%	26.53%	2.55%	4.64%	91.96%	91.96%	99.77%	59.68%	7.08%	17.23%	54.33%
LNCaP_DMSO_48_2	0.80%	65.25%	26.66%	2.78%	4.50%	91.91%	91.91%	99.76%	59.52%	7.14%	16.91%	52.19%
LNCaP_DMSO_8_1	0.66%	63.86%	27.33%	2.32%	5.84%	91.19%	91.19%	99.80%	60.19%	5.95%	17.13%	52.66%
LNCaP_DMSO_8_2	0.65%	64.54%	26.85%	2.30%	5.65%	91.40%	91.39%	99.80%	60.39%	7.01%	16.42%	59.80%

Appendix A: Bioinformatic QC results from RNA sequencing analyses comparing spliceosome-related gene expression levels between LNCaP and LNCaP95 prostate cancer cells.

Appendix B: Bioinformatic QC results from RNA sequencing; iBET-151 vs Vehicle

Samples	PF ALIGNED BASES	RIBOSOMAL BASES	CODING BASES	UTR BASES	INTRONIC BASES	INTERGENIC BASES	IGNORED READS	CORRECT STRAND READS	INCORRECT STRAND READS
LNCaP95_2uM_48_1	10410874590	88332176	6453724531	3133458143	251128594	484232364	0	88814230	202149
LNCaP95_2uM_48_2	12192788281	116376038	7006897503	4096002930	340261521	633251748	0	102963288	233011
LNCaP95_2uM_8_1	10585056260	56533134	7225919834	2717979645	184856533	399767960	0	91982730	157842
LNCaP95_2uM_8_2	8020438874	48220026	5357510381	2122163800	144141673	348403678	0	69215214	114995
LNCaP95_500nM_48_1	11918164127	111240996	7336810997	3572805303	298191110	599118095	0	101028720	227223
LNCaP95_500nM_48_2	14660300381	124374632	8907407072	4527055633	378870153	722594458	0	124509738	284023
LNCaP95_500nM_8_1	11397316636	71379528	7584058489	3095175064	203779433	442925063	0	98903495	162326
LNCaP95_500nM_8_2	12184413006	77553052	7980168304	3418429375	222282047	485981221	0	105579309	174229

Samples	RIBOSOMAL BASES	CODING BASES	UTR BASES	INTRONIC BASES	INTERGENIC BASES	mRNA BASES	USABLE BASES	CORRECT STRAND READS	MEDIAN CV COVERAGE	MEDIAN 5' BIAS	MEDIAN 3' BIAS	MEDIAN 5' TO 3' BIAS
LNCaP95_2uM_48_1	0.85%	61.99%	30.10%	2.41%	4.65%	92.09%	92.08%	99.77%	56.23%	11.34%	16.39%	80.25%
LNCaP95_2uM_48_2	0.95%	57.47%	33.59%	2.79%	5.19%	91.06%	91.06%	99.77%	55.18%	7.20%	19.87%	48.07%
LNCaP95_2uM_8_1	0.53%	68.27%	25.68%	1.75%	3.78%	93.94%	93.94%	99.83%	57.03%	13.77%	14.70%	93.27%
LNCaP95_2uM_8_2	0.60%	66.80%	26.46%	1.80%	4.34%	93.26%	93.25%	99.83%	59.47%	10.15%	14.71%	74.73%
LNCaP95_500nM_48_1	0.93%	61.56%	29.98%	2.50%	5.03%	91.54%	91.53%	99.78%	58.31%	9.17%	16.18%	71.86%
LNCaP95_500nM_48_2	0.85%	60.76%	30.88%	2.58%	4.93%	91.64%	91.63%	99.77%	56.94%	8.95%	16.55%	68.35%
LNCaP95_500nM_8_1	0.63%	66.54%	27.16%	1.79%	3.89%	93.70%	93.70%	99.84%	60.08%	8.53%	15.04%	67.28%
LNCaP95_500nM_8_2	0.64%	65.49%	28.06%	1.82%	3.99%	93.55%	93.55%	99.84%	58.06%	8.49%	16.11%	60.52%

Appendix B: Bioinformatic QC results from RNA sequencing analyses comparing spliceosome-related gene expression levels between LNCaP95 prostate cancer cells treated with either I-BET151 or DMSO.

Appendix C: Experimental sample QC prior to RNA sequencing; JMJD6 siRNA vs Control siRNA

LNCaP95	AR		
Sample	Technical Replicate 1	Technical Replicate 2	Average
Control siRNA 1	1.04	0.95	0.99
Control siRNA 2	1.16	1.06	1.11
JMJD6 siRNA 1	1.07	0.99	1.03
JMJD6 siRNA 2	0.91	1.00	0.96

LNCaP95	AR-V7		
Sample	Technical Replicate 1	Technical Replicate 2	Average
Control siRNA 1	1.02	1.00	1.01
Control siRNA 2	0.99	1.06	1.02
JMJD6 siRNA 1	0.42	0.56	0.49
JMJD6 siRNA 2	0.49	0.53	0.51

LNCaP95	JMJD6		
Sample	Technical Replicate 1	Technical Replicate 2	Average
Control siRNA 1	1.07	0.83	0.95
Control siRNA 2	1.05	0.85	0.95
JMJD6 siRNA 1	0.05	0.05	0.05
JMJD6 siRNA 2	0.04	0.04	0.04

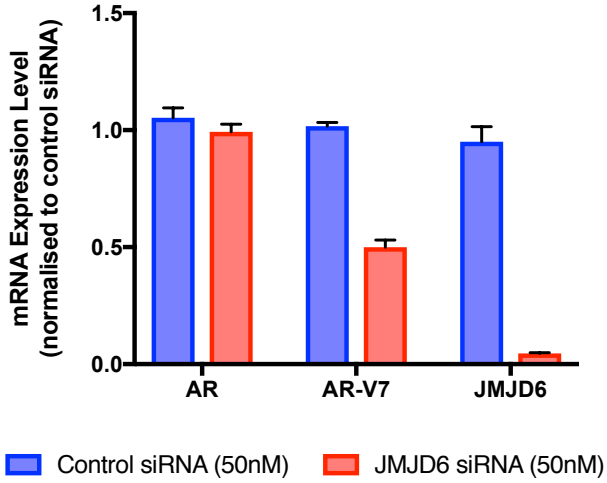

Appendix C: qPCR results obtained from samples prior to RNA sequencing. Prior to RNA sequencing, qPCR analyses were performed on LNCaP95 prostate cancer cell whole cell lysates following treatment with either JMJD6 siRNA (50 nM) or non-targeting control siRNA (50 nM) to ensure adequate transfection of siRNA. qPCR raw data shown (tables) alongside bar chart of average expression levels. Demonstrates that in the samples used for RNA sequencing, JMJD6 mRNA expression levels were significantly knocked down (highlighted in blue). Furthermore, in keeping with previous results, AR-V7 was also downregulated in these samples (highlighted in orange).

Appendix D: Bioinformatic QC results from RNA sequencing; JMJD6 siRNA vs Control siRNA

Samples	PF ALIGNED BASES	RIBOSOMAL BASES	CODING BASES	UTR BASES	INTRONIC BASES	INTERGENIC BASES	IGNORED READS	CORRECT STRAND READS	INCORRECT STRAND READS
Control siRNA 1	1893909213	24339681	1105165379	695303207	29633225	39468451	0	12312039	46793
Control siRNA 2	2039990975	26805007	1096227050	842523528	30759504	43676591	0	13336162	47752
JMJD6 siRNA 1	830836516	13552827	472430797	313470879	13573467	17808972	0	5478944	28613
JMJD6 siRNA 2	1391888865	19401031	764008488	554770416	23533837	30175649	0	9154456	56096

Samples	RIBOSOMAL BASES	CODING BASES	UTR BASES	INTRONIC BASES	INTERGENIC BASES	mRNA BASES	USABLE BASES	CORRECT STRAND READS	MEDIAN CV COVERAGE	MEDIAN 5' BIAS	MEDIAN 3' BIAS	MEDIAN 5' TO 3' BIAS
Control siRNA 1	1.3%	58.4%	36.7%	1.6%	2.1%	95.1%	95.1%	99.6%	86.4%	6.7%	10.0%	67.0%
Control siRNA 2	1.3%	53.7%	41.3%	1.5%	2.1%	95.0%	95.0%	99.6%	89.8%	5.5%	11.8%	47.0%
JMJD6 siRNA 1	1.6%	56.9%	37.7%	1.6%	2.1%	94.6%	94.6%	99.5%	87.3%	6.1%	10.7%	71.0%
JMJD6 siRNA 2	1.4%	54.9%	39.9%	1.7%	2.2%	94.7%	94.7%	99.4%	88.7%	6.3%	10.8%	63.3%

Appendix D: Bioinformatic QC results from RNA sequencing analyses comparing spliceosome-related gene expression levels between LNCaP95 prostate cancer cells treated with either JMJD6 siRNA or non-targeting control siRNA.